Testosterone metabolism in the human endometrium: A combination of metabolic (mass spectrometry) and enzyme expression (RT-PCR).

Taylor, Angela Elizabeth

Testosterone metabolism in the human endometrium: A combination of metabolic (mass spectrometry) and enzyme expression (RT-PCR)

Angela Elizabeth Taylor MChem

Submitted to the University of Wales in fulfilment of the requirements for the Degree of Doctor of Philosophy

Swansea University

2009

ProQuest LLC.
789 East Eisenhower Parkway
P.O. Box 1346
Ann Arbor, MI 48106 – 1346

Abstract

Localised steroid metabolism is important in proliferative disorders of the endometrium. The metabolism of testosterone, an important precursor in endometrial disorders, was investigated by mass spectrometry and RT-PCR (real-time polymerase chain reaction), allowing determination of steroid metabolites and expression of steroid converting enzymes; aromatase, 17β-HSD1, 2, 4, 5, 7, 8, (hydroxysteroid dehydrogenase) and 5AR1, 2 (alpha reductase). Samples were derived from cell lines (Ishikawa, HEC-1A, HEC-1B, RL95-2, COV434), and biopsies; fertile, endometriosis, poly-cystic ovary syndrome (PCOS), endometrial hyperplasia, unexplained infertility, endometrial polyp.

Optimum mass spectrometry techniques, determined using steroid standards, were LC/MS for androgens and LC/MS/MS for oestrogens, following dansyl-chloride derivatisation. GC/MS was less sensitive.

The route of testosterone metabolism varied in the cell lines and clinical biopsies, the major metabolite was correlated with high expression of 5AR1 or 17β-HSD2, 4 and 8. If DHT (dihydrotestosterone) was produced high basal expression of 5AR1 was observed and if androstenedione was produced high basal expression of HSD2, 4 or 8 was observed. A mixture of DHT and androstenedione was correlated with expression of 5AR1 and 17β-HSD2, 4 or HSD8.

Changes in enzyme expression were correlated with changes in steroid concentration after testosterone treatment, as follows:

1. Increased 5AR1 expression was correlated with increased DHT concentration in Ishikawa, HEC-1B, COV434, PCOS, endometriosis, stromal hyperplasia and ovarian cyst biopsies.
2. Increased expression of 5AR2 was correlated with increased androsterone concentration in fertile and unexplained infertility biopsies.
3. Increased 17β-HSD5 expression was correlated with increased testosterone concentration in HEC-1A cells.
4. Increased aromatase expression was correlated to increased oestradiol and oestrone concentrations in a hyperplasia biopsy.

Analysis of a range of enzymes and steroids produced testosterone metabolism maps of the endometrium (and associated disorders) highlighting steroids which could contribute to endometrial disorders and viable enzyme target(s) for inhibition (5AR1, 17β-HSD2, 4, 8).

DECLARATION

This work has not previously been accepted in substance for any degree and is not being concurrently submitted in candidature for any degree.

Signed .... (candidate)

Date .....19/9/2009.....

STATEMENT 1

This thesis is the result of my own investigations, except where otherwise stated. Where correction services have been used, the extent and nature of the correction is clearly marked in a footnote(s).

Other sources are acknowledged by footnotes giving explicit references. A bibliography is appended.

Signed ..... (candidate)

Date .....19/9/2009.....

STATEMENT 2

I hereby give consent for my thesis, if accepted, to be available for photocopying and for inter-library loan, and for the title and summary to be made available to outside organisations.

Signed ..... . (candidate)

Date .....19/9/2009.....

Contents

Chapter Three
Experimental methods

Chapter Four

Optimisation of analytical procedures for the detection and extraction of steroids

Tables

Table of figures

Abbreviations

5-AR- 5 alpha reductase
a-alpha (α)
AR-androgen receptor
b- beta (β)
DC- Dansyl-chloride
DHEA- Dehydroepiandrosterone
DHT- Dihydrotestosterone
E1- Oestrone.
E2- 17β-oestradiol
E3- Oestriol
EI- Electron Ionisation
ESI- Electrospray ionisation
ER-Oestrogen receptor
FCS-Foetal calf serum also (foetal bovine serum)
GC/MS- Gas Chromatography Mass Spectrometry
GC MSD- Agilent Instrument
GC/MS MD800- Fisons Instrument
HPLC- High Performance Liquid Chromatography
HSD- Hydroxy steroid dehydrogenase a number of different isoforms
IS- Internal Standard
LC- Liquid chromatography
LOD- Limit of detection
MS/MS- Tandem mass spectrometry
m/z- Mass-to-charge ratio
PR- Progesterone receptor
OH- Hydroxyl
RIA-Radioimmunoassays
RNA-Ribonucleic acid
RSD-Relative standard deviation
RT-PCR- Real time reverse transcription polymerase chain reaction
SIM-Selected ion monitoring
SPE- Solid phase extraction
TMS- Trimethylsiyl

Acknowledgements

I would firstly like to say a massive thank-you to my supervisors Professor Gareth Brenton and Professor John White for their constant guidance, encouragement and enthusiasm throughout this project.

I also thank my colleagues at the Institute of Mass Spectrometry, Institue of Life Sciences, Reproductive Biology Group, Chemistry Department and the EPSRC National Mass Spectrometry Service Centre at Swansea University. I would like to especially thank Dr Deyarina Gonzalez and Dr Edward Dudley who have been invaluable to me regarding their teaching in the labs and assistance with data management.

I would like to thank all the patients and staff at Singleton Hospital, who provided the endometrial biopsies.

I would also like to thank the Engineering and Physical Sciences Research Council (EPSRC) for funding this project.

And finally I would like to thank my family and my fiancé Rhys for supporting my ambitions as an eternal student!

Chapter One

Steroid Metabolism in the Human Endometrium

1.0 Introduction

This chapter describes steroid structure, metabolism and the roles of specific steroid converting enzymes in the normal endometrium and endometrial disorders. The techniques required to establish steroid profiles and steroid converting enzyme expression are also described.

Steroids are metabolised in a number of tissues in the human body including the liver, endometrium, brain and breast. Significant steroid metabolism takes place in the liver, where the majority of cholesterol is produced which goes on to form the wide variety of other steroids described in figure 1.1. The biosynthetic pathways are similar in all these organs, however rates of production, important enzymes involved and concentrations of each steroid can vary significantly. The role of each steroid in each tissue is varied, for example, oestrogens in the bone protects against progression of osteoporosis[1] but have been linked to progression of cancer in the endometrium.[2]

When steroid metabolism is displaced from a normal pattern a number of steroid related disorders can occur. Examples of steroid related disorders are;

1. Breast cancer. Localised production of androgens and oestrogens has been described in breast cancer development.[3]
2. Addison's Disease. Decreased secretion of the adrenal glucocorticoids and mineralocorticoids causes a number of conditions due to low blood sugar and ultra-filtration problems.[4]
3. Endometrial cancer. Localised synthesis of oestrogens is thought to be important in endometrial cancer development.[5]

1.1 Structure of steroids

Steroids have a four ring system comprising three cyclohexane rings and one cyclopentane ring.[6] Differences in biological activity are due to differing constituent groups and their stereochemistry on the basic ring structure. Steroids are separated into five major groups based on their structure and function (Table1.0).

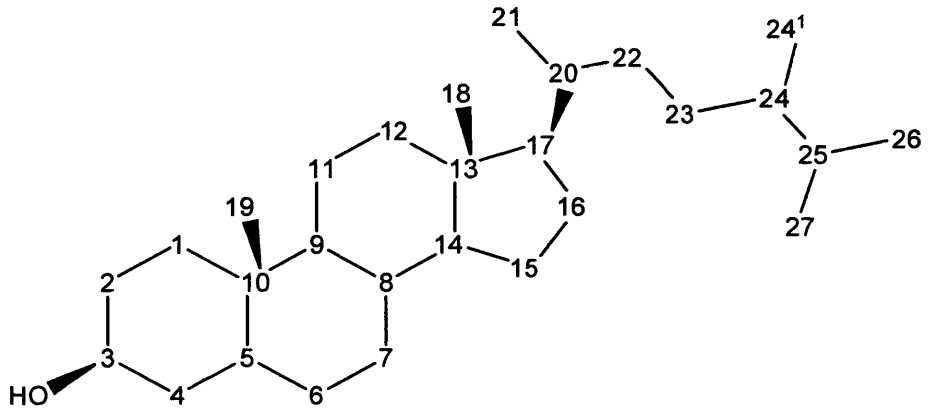

Fig 1.0: Numbering of the steroid skeleton.

Table1.0. Steroid grouping, structure, origin and biological function in females.

Group name	Typical structure	Tissue of origin	Major biological function in females
Androgen	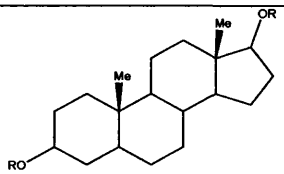 C_{19}	Ovaries Adrenal glands	Precursor of oestrogens in gonadal sites such as the ovaries and extragondal sites such as the brain, bone, and adipose tissue
Oestrogen	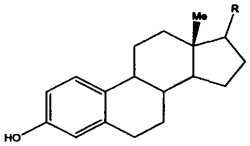 C_{18}	Placenta Ovaries Andrenal cortex Adipose tissue Breast Endometrium	Designate female characteristics Regulation of menstrual cycle Cognitive function Bone minerlisation
Progestin	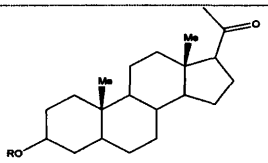 C_{21}	Ovaries	Important for implantation and maintenance of pregnancy Regulation of menstrual cycle
Mineralocorticoid	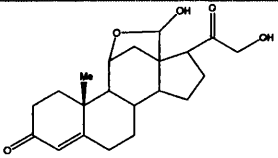	Adrenal cortex	Affect the mineral content of the blood through ultra-filtration in the kidneys (re-absorption of sodium and loss of potassium)
Glucocorticoid	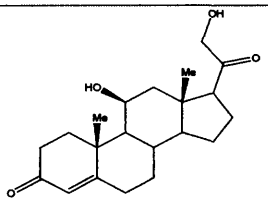	Adrenal cortex	Affect blood sugar levels and stimulate gluconeogenesis in the liver, also involved in resistance to infection (T-cell control) and anti-inflammatory effects

R= functional group such as alkyl or aryl side chains or hydrogen.

1.2 Steroid Metabolism

Steroids can be arranged into a bio-pathway based on their metabolism in the body. A number of different enzymes are involved in steroid metabolism, expression and activity of individual enzymes within a tissue leads to flux through specific routes of the bio-pathway. The metabolism routes, rates, and products can vary due to differences in biological phenotype and steroid converting enzyme expression. Steroid profiles produced experimentally can indicate metabolism routes, combined with steroid converting enzyme expression data this can provide novel information concerning normal and altered steroid metabolism in specific tissues, which could aid development of specific enzyme antagonists.

Cholesterol is the precursor of steroid metabolism in the human body. It can be metabolised through a number of key rate limiting enzymes to produce all the steroids defined in figure 1.1. The initial step is the conversion of cholesterol to pregnenolone which occurs in the adrenal glands or gonads through the P450scc enzyme, after this the bio-pathway branches to produce mineralocorticoids or glucocorticoids or androgens and oestrogens. This occurs in a number of organs and tissues throughout the human body such as the adrenal glands, liver, ovaries, and adipose tissue. Active steroids can also be metabolised from their inactive sulphated analogues (usually present at high concentration in the plasma) through the action of steroid sulphatase, common circulatory steroid sulphates are dehydroepiandrosterone-sulphate (DHEAS) and oestrone (E1) sulphate. The route and production of specific steroids may be important for progression of androgen and oestrogen responsive conditions; the degree of importance is dependent on the condition.[7]

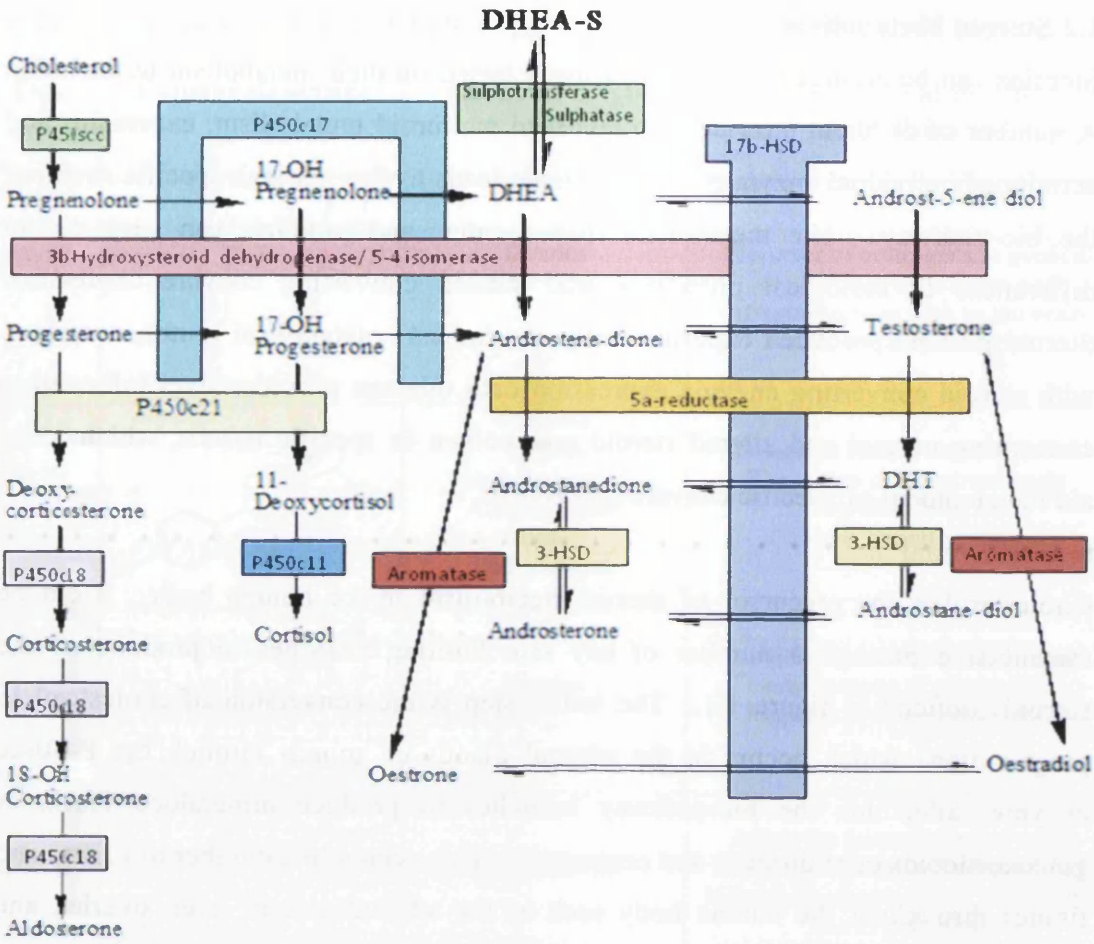

Fig 1.1: Metabolism of Cholesterol. The left hand side of the diagram illustrates the bio-pathways for the production of the mineralocorticoid aldosterone and the glucorticoid cortisol. The right hand side of the diagram illustrates the reversible metabolism of the androgens, androsterone, androstanediol and the non-reversible metabolism of the oestrogens, oestradiol and oestrone. a = alpha b = beta, OH= hydroxyl. Steroid converting enzymes are coloured. Aromatase is the rate limiting enzyme in oestrogen bio-synthesis (red). HSD= hydroxysteroid dehydrogenase these are either oxidative or reductive enzymes, which have a number of different isoforms. P450s are a group of enzymes which act at specific points in the carbon skeleton.

1.2.1 Important steroids in the bio-pathway

There are specific steroids in the bio-pathway that are described as the most potent or biologically active in their group. The metabolism of these steroids can have a significant effect on a number of biological functions, for example, DHT (dihydrotestosterone) is described as the most potent androgen, and is implicated in development of prostate cancer.[8] Oestradiol (E2) is described as the most potent oestrogen and is highlighted as a key steroid in endometrial cancer development.[2] Cortisol is the most potent glucocorticoid, it is secreted from the adrenal glands in

response to stress, an increase cortisol concentration affects a number of biological functions such as gluconeogenesis in the liver and insulin binding in muscles and adipose tissue.[9] Aldosterone is the most potent mineralocorticoid, its major function is involved in maintenance of blood sodium and potassium levels in the kidney, high levels of aldosterone have been recorded in patients with heart failure and myocardial fibrosis, suggesting a role in these conditions.[10] Accumulation or depletion of these steroids may lead to progression of endocrine disorders.

Testosterone is another important steroid present in females, it is a major circulatory androgen and is a precursor to oestrogens synthesis in a number of tissues including in the normal and proliferative endometrium.[11] DHEAS is also an important precursor for androgen biosynthesis through steroid sulphatase. Expression of steroid sulphatase and the concentration of plasma DHEAS has been linked to tumour growth and progression through conversion to androgens and oestrogens in steroid responsive cancers such as adrenal tumours.[12]

1.3 Steroid converting enzymes

There are a number of enzymes involved in steroid metabolism represented by the coloured boxes in figure 1.1. These all act on specific steroid substrates to oxidise, reduce, hydroxylate, aromatise, or sulphate the steroid precursor. The expression levels of each enzyme can affect the steroid concentration in that tissue (precursor to product ratio). Described here are enzymes involved in the androgenic and oestrogenic metabolism, which could be implicated in hormone responsive endometrial disorders. Investigations into these enzymes could lead to more specific treatments for steroid dependent conditions through steroid bio-pathway intervention.

1.3.1 Cholesterol lyase P450scc

P450scc is a member of the cytochrome P450 superfamily, P450s are involved in a number of biological functions such as oxidation, reduction, aromatisation, and hydroxylation. P450scc is important as it catalyses the initial step in steroid bio-synthesis. The P450scc enzyme cleaves between C20 and C22 of the cholesterol side chain to produce a ketone group, this is the rate limiting step in the wider steroidogenesis pathway.[13] P450scc action is dependent on the inclusion of the cofactor NADPH.

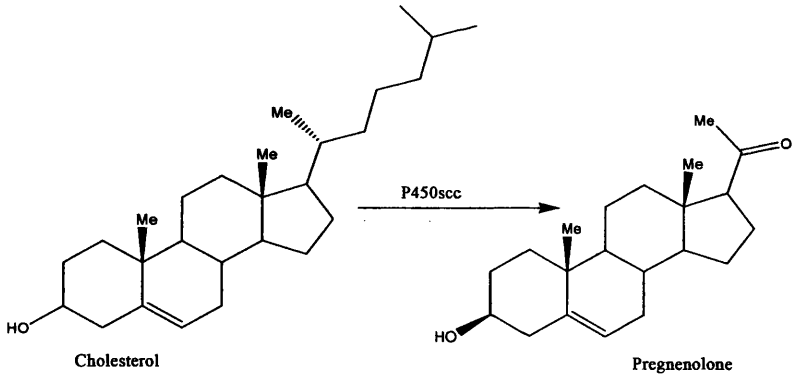

Fig 1.2: Illustration of the conversion of cholesterol to pregnenolone via the P450scc enzyme.

1.3.2 The aromatase enzyme

P450 aromatase is a member of the P450 superfamily. P450 aromatase comprises of 2 proteins, the first is NADPH-cytochrome P450 reductase and the second is cytochrome P450 aromatase, which contains a heme molecule and a steroid binding site.[14] P450 aromatase acts on position 3 of the steroid skeleton and converts the keto group into a hydroxyl group, and converts the 4-ene in the cyclo-hexane ring into a benzene (tricyclo-hexene) structure (aromatisation).[15] Aromatase converts androgens to oestrogen (testosterone to oestradiol and androstenedione to oestrone) which is the rate limiting step in oestrogen synthesis.[16] Expression of aromatase has been studied in many steroid responsive tissues such as the breast and endometrium and it has been linked to the progression of a number of disorders such as breast cancer and endometriosis.[17] To combat excess aromatase expression a number of aromatase inhibitors have been developed such as anastrozole.[18]

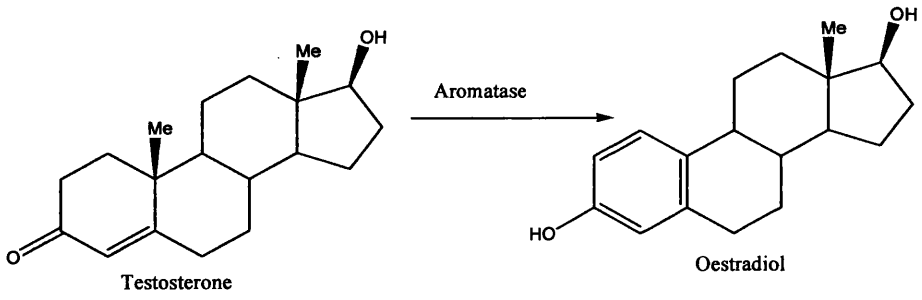

Fig 1.3: Illustration of the aromatase conversion reaction. Testosterone aromatisation to oestradiol.

1.3.3 The 5 α-Reductases (5AR)

5ARs are from the 3-oxo-5-alpha-steroid 4-dehydrogenase 2 protein superfamily,[19] which are dependent on the inclusion of the cofactor NADPH.[20] The five α-reductases act between position 4 and 5 of the steroid skeleton to reduce the double bond to a single bond. There are two isoforms of 5AR, described as 5AR1 and 5AR2 which both metabolise testosterone to DHT and/or androstenedione to androstane-dione. These isoforms however have different affinities for their substrates.

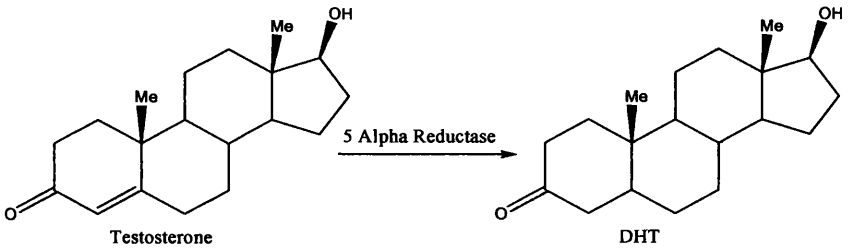

Fig 1.4: Illustration of a 5-α reductase conversion of C4-ene group in steroid skeleton to the saturated compound. Testosterone to DHT.

1.3.4 The hydroxysteroid dehydrogenases (HSD)

There are two types of HSDs involved in androgenic steroid conversions under investigation in these experiments these are 17β-HSD and 3β-HSD which act primarily at position 17 or 3 of the steroid skeleton to convert between a keto and an alcohol group (or the reverse). They are all short-chain dehydrogenases/reducatses except HSD5 which is an all aldo-keto reductase and can act in a reductive or oxidative manner through the inclusion of NADP(H) or NAD(H) depending on the reaction.[21]

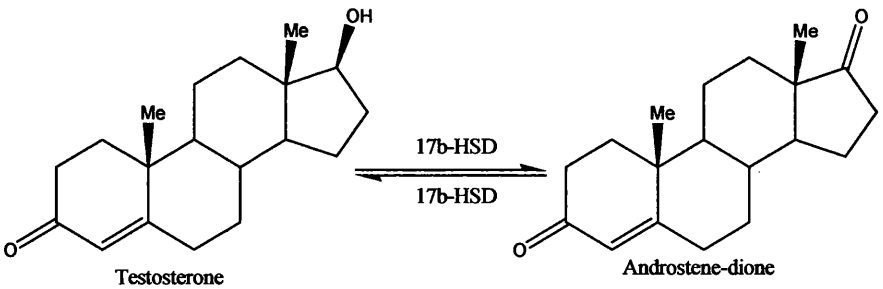

Fig 1.5: Illustration of a 17β-HSD reaction conversion of a hydroxyl to a ketone group at position 17. The oxidative reaction is the conversion of testosterone to androstenedione and the reductive reaction is the conversion of androstenedione to testosterone.

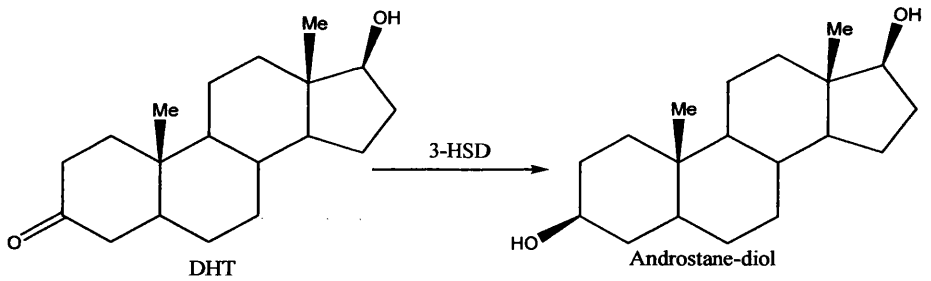

Fig 1.6: Illustration of a 3β-HSD reductive conversion at the 3 keto group to a 3 hydroxyl group.

To date fifteen isoforms of 17β-HSD have been identified which have varying tissue and cellular distribution.[22] The expressions of a number of these isoforms are investigated in this thesis. The major reactions of each isoform is described below each HSD may act on multiple substrates.[23]

17β-HSD1- along with 17β-HSD2 this is the most widely studied 17β-HSD. 17β-HSD1 converts oestrone to oestradiol.[24] Specific inhibition of this isoform is being developed for the treatment of endometriosis.

17β-HSD2- this isoform converts oestradiol to oestrone, testosterone to androstenedione, DHT to androstane-dione, androstanediol to androsterone, and 20α-progesterone to progesterone and is involved in the oxidation of retinols.

17β-HSD3- is involved in testosterone metabolism, exclusively in the testes. Specific inhibition of 17β-HSD3 is being developed for treatment of prostate cancer.[25]

17β-HSD4- this isoform converts testosterone to androstenedione, oestradiol to oestrone, and is involved in peroxisomal fatty acid metabolism.

17β-HSD5- converts androstenedione to testosterone, androstane-dione to DHT, androsterone to androstanediol and oestrone to oestradiol. 17β-HSD5 is a multifunctional enzyme which can also convert at the 3α- or 20α steroid position, for example converting progesterone to 20α hydroxy-progesterone.[26]

17β-HSD6- this isoform converts androstanediol to DHT at position 3, but is still classed as a 17β-HSD.

17β-HSD7- converts oestrone to oestradiol, DHT to androstanediol and is involved in cholesterol biosynthesis.

17β-HSD8- converts DHT to androstane-dione, oestradiol to oestrone and testosterone to androstenedione, and is involved in fatty acid metabolism.

17β-HSD9- converts at the 3 and 17 positions of the steroid skeleton, identified in the rat, no analogue has been positively identified in humans.

17β-HSD10- this isoform is similar to 17β-HSD4. It has been found in the human brain and has been linked to Alzheimer's disease.[27]

17β-HSD11-15 are more recently discovered and less widely explored.

1.3.5 Steroid sulphatase and steroid sulphotransferase

Steroid sulphatase is from the animal sulphatase superfamily, which acts through inclusion of the co-factor calcium. Steroid sulphatase hydrolyses inactive steroid sulphates into their biologically active analogues. Steroid sulphatase converts the hydroxyl or phenol group at position 3 into a sulphated analogue, (steroid sulphotransferase does the reverse of this reaction).

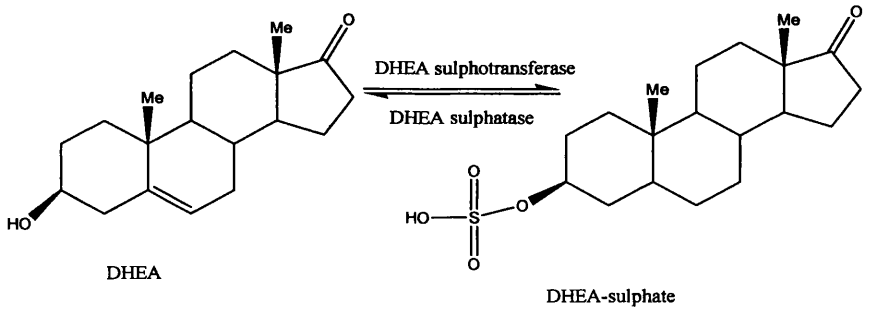

Fig 1.7: Illustration of the steroid sulphatase/sulphotransferase conversion reaction. Conversion of DHEA to DHEA-sulphate (DHEAS) by the steroid sulphatase (DHEA sulphatase), and the reverse by the steroid sulphotransferase (DHEA sulphotransferase).

The sulphated analogues of steroids such as the abundant circulatory steroids oestrone sulphate and DHEAS act as the primary precursors for localised oestrogen synthesis in breast cancer patients.[28] The production of oestrogens in breast cancer patients through the oestrogen sulphatase pathway has been defined as being 40-500 times higher than the aromatase pathway.[2] In endometrial cancers production of oestrogens through oestrogen sulphatase is an important pathway, however localised production of oestrogens through androgens and the aromatase enzyme is also significantly.[29] Steroid sulphatase has also been linked to benign endometrial conditions, Purohit and co-workers investigated the role of steroid sulphatase in relation to bio-accumulation of oestrogens in women with endometriosis, they found that the more severe the condition the higher the sulphatase activity,[30] again

suggesting a number of routes for steroid production may contribute to steroid related disorders.

Steroid sulphotransferase is an enzymes which add a sulphate group to steroid hydroxyl groups to form the inactive steroid sulphates. They are members of the SULT (cytosolic sulphotransferase) superfamily,[31] the co-factors required for these conversions must supply the sulphate group, for example in the conversion of DHEA to DHEAS, 3'-phosphoadenosine-5'-phosphosulphate (PAP) is the cofactor supplying the sulphate group.[32] Steroid sulphotransferase acts at position 3 to form the sulphated steroid analogues (as shown in figure 1.7).

1.4 Steroid metabolism

The quantity of any steroid in a specific tissue or within the body depends on four factors.

1. Secretion. The secretion rate from issuing tissue, such as the ovary, adrenal glands or adipose tissue.

2. Uptake. The ability of the tissue to uptake the steroid. Steroids are lipophillic molecules which readily diffuse through cell membranes. The binding of a steroid to its specific receptor determines the retention of that steroid within the cell. When steroid-receptor binding occurs the receptor changes configuration and through regulation of receptor interacting factors can influence expression of target genes. Expression of these genes can be involved in normal cell cycle processes or can be involved in progression of steroid related disorders. There are a number of steroid receptors such as the androgen, oestrogen, progesterone, mineralocorticoid and glucocorticoid receptors (AR, ER, PR, MR and GR). The ER and PR receptors have two isoforms known as α and β, the expression of which is dependent on tissue type under investigation. ERα for example is the main isoform expressed in the endometrium.[33] ER expression has been directly linked to expression of some growth factors important in endometrial cancer proliferation.[34]

3. Metabolism. The rate of metabolism of the steroid in the tissue under investigation through conversion to other steroids or steroid analogues is related to the expression and activity of specific steroid converting enzymes. A steroid within a tissue can be converted into a number of metabolites, all of which may have significant biological effects.

4. Inactivation/Excretion. Circulatory steroids are primarily inactivated by liver sulphotransferases to their inactive sulphated analogues. Steroids are subsequently removed from the body via the urine or faeces,[35] to excrete steroids in the urine they must first be metabolised into hydrophilic compounds this is achieved by a number of enzymes within the kidneys which reduce, oxidise, hydroxyalte or conjugate the steroids.[36]

1.5 The human endometrium

The endometrium is the inner lining of the uterus illustrated in figure 1.8. Steroids are important in the normal functioning endometrium, and progression of some endometrial disorders. The normal cycling endometrium is a dynamic tissue subject to monthly changes in multiple steroid concentrations as well as changes in steroid receptor status, gene and enzyme expression. These changes are associated with the endometrial phases, the proliferative phase (follicular), the secretory phase (luteal) and the menstrual phase. The endometrium undergoes depletion and repletion during these phases, making it a unique tissue. The steroids generating these changes are the ovarian steroids oestradiol and progesterone which cause the morphology of the endometrium to change throughout the cycle. Oestradiol controls the proliferative phase by stimulating the endometrial glands stromal cells and epithelial cells to proliferate. Oestradiol concentrations increase throughout the proliferative phase and the endometrial lining thickens. Directly following the highest oestradiol concentration LH (luteinising hormone) and FSH (follicle stimulating hormone) are produced by the pituitary gland, these hormones are responsible for ovulation and induction of progesterone secretion in the ovarian follicle. In the secretory phase oestradiol concentrations reduce and progesterone concentrations increase inducing endometrial glands to secrete glycogen. If implantation does not occur the corpus luteum (present in the ovary) degenerates, the levels of oestradiol and progesterone decreases and the menstrual phase begins.[37] These changes in morphology make the endometrium a difficult organ to study, as the day of the cycle a biopsy is taken can result in a large variation in steroid concentration or enzyme expression levels.

Any dysfunction or change in global, ovarian or localised steroid metabolism can result in development of endometrial disorders. The production of excess oestrogens for example without progestins (unopposed oestrogen) has been shown to promote

growth factors such as insulin-like growth factor and vascular endothelial growth factor which are implicated in development and progression of endometrial cancer.[38]

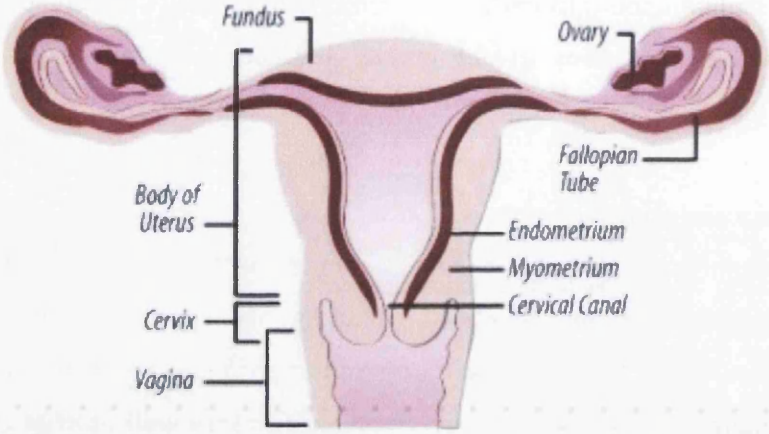

Fig 1.8: Diagram of the Uterus. The endometrium is the inner lining of the uterus labelled above. Diagram from the US National Institute of Health.[39]

1.5.1 Structure of endometrium

The uterine wall compromises of a number of layers of different cell types. These are the perimetrium, myometrium, endometrial stromal and endometrial epithelial layers (figure 1.9). The perimetrium is the outer layer of the uterus, the myometrium is a thick muscular layer containing arteries which supply blood to the endometrium. The endometrium itself consists of two cell types, stromal and epithelial.

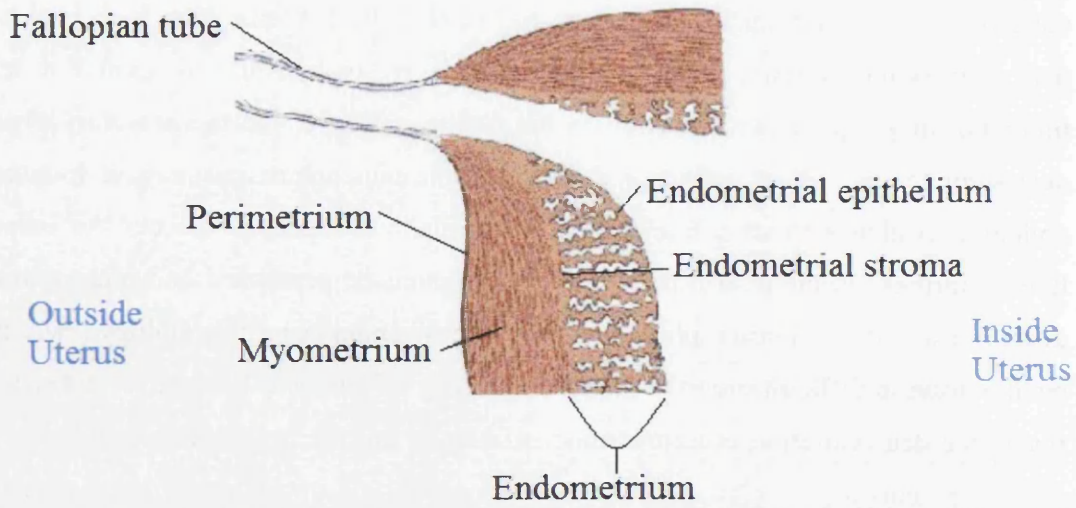

Fig 1.9: Structure of the uterine wall. The uterus has four distinct sections the perimetrium, myometrium, endometrial stroma and endometrial epithelium.

1.5.2 The role of stromal cells

Stromal cells make up the connective tissue in the endometrium. Stromal cells are found in a number of tissues, and act as a support to surface epithelial cells. Endometrial stromal cells (fibroblasts) have been shown to regulate growth and differentiation in endometrial epithelial cells via a paracrine relationship. Throughout the menstrual cycle oestradiol or progesterone bind to receptors expressed in the stromal cells, which can cause responses in the surrounding epithelial cells such as promotion of cell development or differentiation.[40]

1.5.3 The role of epithelial cells

Epithelial cells cover the surface of an organ, such as the lungs, gastro-intestinal tract and the endometrium. The epithelium itself can contain glands and has a number of functions such as secretion (through glands formation) and absorption (of nutrients in the intestine). There are a number of types of epithelial cells, the cell type is determined by its shape and how deep the cell layers are, for example squamous cells are surface (flat) cells and adenomatous cells are glandular.[41]

1.6 Current steroid metabolism investigations

Studies which highlight important steroids and steroid converting enzymes involved in progression of a number of endometrial disorders such as endometriosis, endometrial hyperplasia, and endometrial cancer have been completed.

The major volume of articles investigating steroid metabolism in the endometrium and its disorders are concerned with either measuring the concentration of a specific steroid or the expression of a specific enzyme such as aromatase. In endometrial cancer investigations, for example Berstein and colleagues recorded oestradiol concentrations in endometria from normal and cancerous patients.[42] Endometriosis is the most widely investigated benign endometrial disorder many studies focussing on the expression of aromatase or 17β-HSD1 and 17β-HSD2.[43] Oestradiol has also been recorded at high concentrations at the site of endometriosis and at endometrial cancer precursor lesions sites,[44] while the circulatory oestrogen concentration remains normal. These studies have lead to the conclusion that localised steroid synthesis is responsible for the increased tissue steroid concentrations, however the wider pathways have not been fully explored. Identification of steroid bio-pathways

in these pathologies permits identification of important metabolism routes and enzymes allowing future development of specific 'targeted' treatments.

The presence (or absence) of a specific enzymes alone does not itself provide proof of steroid metabolism, to confirm steroid metabolism is occurring a technique which combines enzyme expression with steroid identification is required. Conclusions drawn from analysis of a single steroid are restricted, information concerning the wider bio-pathway is often more informative, Rauh recently described the increased clinical value of determination a steroid profile in comparison to measurement of a single steroid in a number of endocrine conditions.[45] Single enzyme or steroid studies highlight important, but small parts of steroid metabolism our study aims to discover the wider picture of steroid metabolism by production of both steroid and enzyme expression profiles following steroid treatments of endometrial cell lines and biopsies from benign endometrial conditions.

1.6.1 Endometrial cancer and endometrial established cell line pathologies

Localised oestrogen metabolism and aromatase expression are described as the key steps in the progression of endometrial cancer. In a healthy endometrium there is very little aromatase expression. The roles of the hydroxysteroid dehydrogenases, 5-α reductases, sulphatase, sulphotransferase and other steroid converting enzymes could also be important in endometrial cancer progression,[2] however localised steroid metabolism information in combination with RNA expression data from multiple steroid converting enzymes has to our knowledge not been undertaken.

An investigation into steroid metabolism in established endometrial cell lines has been undertaken in this study. Epithelial cancer cell lines are excellent models which permit investigation into altered steroid metabolism in endometrial cancers.[11] The use of specific cell lines which are known to metabolise steroids permits development of robust methods for determination of steroid metabolism routes. Cell lines are employed in these experiments as model systems as they have homogeneous cell types and can be studied over long time periods (in comparison to primary biopsies).[46] They were also studied to overcome the problems associated with experimental variation between patients and to optimise and assess the methods required for determination of steroid profiles and steroid converting enzyme

expression (which can be later applied to primary cell biopsies). The endometrial cell lines investigated were the endometrial cell lines, Ishikawa, HEC-1A, HEC-1B, and RL95-2.

The endometrial cell lines Ishikawa, HEC-1A and HEC-1B are all representative of endometrioid (type one) cancers. Type one endometrial cancer is hormone dependent, which progresses if there are increased levels of oestrogens without increased concentrations of progesterone (unopposed oestrogen).[47] Development of type one endometrial cancers can occur due to a number of gene abnormalities the major cause of endometrial cancer is PTEN inactivation (a tumour suppressor gene approximately 55% of cancers[48]), although microsatellite instability (~20%) and mutations in other genes are also implicated p53 (~5-10%), β-catenin (~25-38%), K-ras (~13-26%).[49] Type one cancers have superficial invasion into the myometrium, are more common in younger women and have good patient prognosis if detected early. RL95-2 is derived from a uterine adenosquamous carcinoma (a tumour from both glandular and squamous cells). Once optimised these methods and results were applied to and compared with steroid metabolism and enzyme expression in a number of endometrial biopsies from fertile and benign conditions.

1.6.2 Benign endometrial disorders

There are a number of benign endometrial disorders whose development may be related to an alteration in global or local steroid metabolism. It is vital to elucidate the steroid bio-pathways in these conditions to determine important steroids and steroid converting enzymes, before effective treatments can be developed.

1. Poly Cystic Ovary Syndrome (PCOS). The US Department of Health and Human Services estimates that PCOS affects 1 in 10 women of child bearing age.[50] Women with PCOS are defined as having two of the following three symptoms;

   i) high levels of the circulatory androgens testosterone and androstenedione (hyperandrogenism),
   ii) oligo or annovulation and,
   iii) polycystic ovaries present on ultrasound.

After treatment for PCOS (ovulation medication, ovarian drilling or surgical removal) these women are often sub-fertile and at increased risk of developing further endometrial disorders such as endometrial hyperplasia and endometrial

cancer.[51] Altered endometrial steroid converting enzyme expression- a possible cause was identified by Bacallao and co-workers who recorded changes in expression of the steroid converting enzymes 17β-HSD1 and 17β-HSD2; (17β-HSD1 expression increased and expression of 17β-HSD2 was decreased in the endometria of women with PCOS compared to normal females).[52]

2. Endometriosis. Endometriosis is defined as the presence of endometrial tissue outside the uterus it affects from 2 to 22% of women, there is a huge variation in symptoms and severity of the condition, from non-symptomatic to chronic pelvic pain and infertility.[53] Endometriosis is mostly found in women of reproductive age, before puberty and after menopause the incidence of endometriosis decreases suggesting a link between ovarian steroid hormones and progression of the disease. Endometriosis lesion sites have been described as aromatase positive with reduced 17β-HSD2 expression,[54] suggesting bio-accumulation of oestradiol, however most studies are limited to RNA expression information for these enzymes only, without complimentary steroid metabolism information. Aromatase inhibitors such as anastrozole have been used to treat endometriosis with impressive results (patient's conditions improve within 9 months),[55] suggesting an important role for oestrogens and aromatase in disease progression. There are four stages of endometriosis stage one (minimal) is represented by a few endometriotic implants and can be asymptomatic. In stage two (mild) there are more and deeper endometrial implants possibly spreading to the ovaries, at stage three (moderate) the number of endometrial implants has increased and they are deeper and can affect a number of reproductive areas. At stage four (severe) deep endometrial implants are observed throughout the pelvic area which can be coupled with chronic pain and infertility.[56] The metabolism of steroids and expression of specific steroid converting enzymes may not be identical at each stage of endometriosis.

3. Endometrial hyperplasia. Endometrial hyperplasia is excessive non-invasive proliferation (cell growth) in the endometrium.[57] Endometrial hyperplasia is related to hormonal in-balances in the endometrium (unopposed oestrogen) and the first course of treatment is often a progestin to combat the unopposed oestrogen. There are two types of hyperplasia the first is atypical which is recognised by changes (enlargements) in endometrial glands, stomal cells and epithelial cells. Atypical hyperplasia is divided into four groups based on the likelihood of progression to endometrial cancer. Simple hyperplasia has a ~1% chance of progression to

endometrial cancer, complex hyperplasia a ~3% chance, simple hyperplasia with aptypia a ~8% chance and complex hyperplasia with atypia a ~29% chance[58] if left untreated. The second type of endometrial hyperplasia (non-atypical) does not progress to endometrial cancer and is not dependent on oestrogens or progestins.

4. Secondary infertility. The patient has already carried at least one child to term but cannot conceive again. There can be a number of causes of secondary infertility in females such as changes in ovulation, formation of endometrial fibroids or progression of tubal disease due to infections such as Chlamydia. Fetal bone fragments from the previous child can also cause secondary infertility.[59] It is also possible that some of these women are infertile due to altered steroid metabolism in their endometrial, although to our knowledge no investigations have been conducted.

5. Unexplained infertility. The tests currently available to these couples do not define the reason for their infertility (15% of population who take the tests).[60] A number of reasons can be hypothesised, such as the inability of the ovum to implant in the endometrium itself, even after *in-vitro* fertilisation successful pregnancy does not always occur. Unexplained infertility in some patients could be due to altered endometrial steroid metabolism.

A wider investigation into steroid metabolism in the endometria of women with benign endometrial conditions could further elucidate any altered steroid metabolism following steroid treatments, highlighting possible therapeutic targets. Similarities between benign endometrial conditions, if observed can also be highlighted by these methods.

Fertile patients in this study have none of the endometrial disorders under investigation. They were in hospital due to hysterectomy for exploratory investigations or sterilisation, and have a normal cycling endometrium. A 'control' fertile biopsy is difficult to obtain as the endometrium is a dynamic organ, also the numbers of women entering hospital without any underlying endometrial condition was low. All biopsies were obtained on the same day of the cycle to try and minimise variation between biopsies, and biopsies were cultured for a number of days where the media was changed sequentially this should remove any residual steroids. Biopsies from patients with tubal disorders were also collected, tubal disease can occur due to previous infections such as Chlamydia,[61] or as a result of

inflammation caused by past surgery.[62] In the endometria of these patients it is expected that normal steroid bio-synthesis should occur if this is confirmed experimentally they can be included in the fertile group.

All endometrial cell lines were epithelial cells, and the majority of biopsy samples were stromal cells. In the endometrium there is evidence of stromal cells directly affecting epithelial cells, causing alterations in epithelial cell function. For example Pierro and colleagues used a co-culture technique and were able to demonstrate that epithelial cell proliferation was induced through oestradiol action in the stromal cells.[63] It is the altered steroid metabolism in epithelial cells which leads to progression and maintenance of epithelial endometrial cancers. This demonstrates epithelial/stromal cell interactions are important in the normal endometrium and in endometrial disorders such as hyperplasia and endometrial cancer. Determination of altered steroid metabolism in epithelial and stromal cells separately should first be completed, following this the co-culture of epithelial and stromal cells would further elucidate the interactions between the two cell types in the endometrium.

1.7 Detection of steroids

For positive determination of steroid bio-pathways analytical techniques must first be validated and optimised. This includes techniques to remove steroids from the cells and cell media under investigation, and analysis methods to positively identify specific steroids. RNA extraction procedures and quantitative real-time, reverse transcription polymerase chain reaction (QRT-PCR) was required to ascertain expression levels of specific steroid converting enzymes.

1.7.1 Steroid extraction techniques

As steroids are lipophillic compounds they should readily move from an aqueous to an organic environment. This property allows for simple liquid-liquid extractions, addition of an organic solvent to a cell pellet causes the cell membranes to rupture and the steroids to be extracted into the organic phase (although some purification may be required).[64] With more complex matrices such as plasma or serum there may be problems with phase separation causing more sophisticated methods of extraction to be developed, such as solid phase extraction, where specific stationary phases have been developed to retain steroids while interfering compounds are removed.

Free steroids can be separated from the sulphated and glucuronide analogues using a variety of techniques. Alousi and colleagues investigated different separation methods to achieve this, they compared three separation methods- a Lipidex-5000 column, Sep-PakC18 cartridges and a Sephadex LH-20 column.[65] They found that for optimum recovery a methanol/water elution system is needed, and four to six Sep-Pak cartridges were ideal for removal of non-steroidal contaminants.

After effective, efficient extraction of steroids positive identification was required. To achieve this a sensitive, reproducible, accurate technique was essential. Steroid metabolism has been studied in endometrial cells, by a number of methods such as electrochemical detection,[66] radioimmunoassay (RIA)[67] and fluorescence detection.[68] RIA is widely used for identification of steroids, and is applied to detect low concentrations of steroids (below parts per million levels) and is a relatively cheap and simple technique.[69] RIA's are specific and sensitive, however a single assay is required for each steroid under investigation, and therefore calculation of steroid profiles by this method is time intensive. Cross-reactivity of steroids which are structurally similar such as DHT and testosterone can be problematic in these assays leading to false positives.[70] Another widely used technique for the identification of steroids is mass spectrometry, which is employed for the rapid, specific, sensitive detection of steroids.[71] Mass spectrometers can be linked to chromatographic separation techniques (such as liquid or gas chromatography) to determine a steroid profile in a single experiment. Mass spectrometers identify steroids by their molecular weight or molecular structure (after fragmentation). Quantitation of a steroid(s) within a sample can be achieved by calibration against appropriate standards,[72] for these reasons mass spectrometry was the chosen analytical method in these investigations.

There were two major techniques which can be linked to mass spectrometers to separate a steroid mixture into specific steroid fractions, these were liquid chromatography and gas chromatography. Mass Spectrometry in combination with either of these chromatographic separation procedures can be used to establish a qualitative and quantitative profile of steroids within a sample. Positive identification of a compound was achieved through the four parameters described

below, in combination these four parameters permit confident assignment of steroids present in a sample.

1. Matching retention time. A direct comparison between the retention times of a steroid standard to the same steroid present within a sample. To give unambiguous results using this method requires high resolution over a wide range of standards, (no co-elution of steroids of the same mass)

2. Identical molecular weight. The molecular weight is usually measured to its nominal mass and sometimes depending on the mass spectrometer to its accurate mass. Accurate mass permits determination of the elemental composition of the compound. The molecular species seen in the spectra depends on the technique, for example, the $[M+H]^+$ species is present in CI (chemical ionisation) and ESI (electrospray ionisation) and the $[M^{\bullet+}]$ in EI (electron ionisation). This alone may not be sufficient for positive steroid identification due to many steroids producing the same molecular protonated species, for example, DHEA and testosterone.

3. Identical unique fragmentation patterns by MS/MS. Fragmentation patterns were obtained using the ion trap, which assisted in determination of molecular structure. This can be somewhat limited in steroid analysis due to similar fragmentation patterns from the same steroidal groups after the molecular ion, however unique ions for some steroids may be observed aiding structure elucidation.

4. Library searches. Databases were utilised to compare mass spectra obtained experimentally to mass spectra (and fragmentation patterns) of steroid standards.

1.7.2 Chromatography

There are two chromatography systems investigated in these experiments to determine the optimum separation of steroids, these are liquid chromatography and gas chromatography, which separated steroids via different methods as described below;

1. Liquid chromatography (LC) permits separation of a mixture of liquid analytes into separate analyte fractions. This is achieved with the use of a column packed with a stationary phase which retains the analytes. Typical stationary phases which act to retain steroids are C_{18} and phenyl-hexyl, which in combination can separate mixtures of corticosteroids, androgens and

progestins.[73] Steroids are retained on the column stationary phase at differing degrees based on their polarity, increasing the polarity of the mobile phase elutes the steroids sequentially. Typical mobile phases used in steroid analysis via LC/MS have one aqueous and one organic mobile phase such as water/methanol[74] or water/acetonitrile.[75] The development of high-pressure liquid chromatography (HPLC) in the late 1960's has overcome problems associated with mobile phase flow rates which led to poor efficiency, and now liquid chromatography is comparable to gas chromatography in performance.[76]

2. Gas chromatography (GC) permits separation of liquid analytes which are vaporised in the GC injector. These (now gaseous) steroids travel through the heated column and arrive at the mass spectrometer at different times due to differences in interactions with the column. GC has been widely used in steroid chemistry, usually after chemical derivatisation of the steroids to increase the volatility and stability of the steroid which produces optimum sensitivity and chromatographic resolution. Typical derivatisation procedures involve addition of a trimethyl-silyl group which adds to any hydroxy group present on the steroid skeleton.[77] Steroid specific gas chromatography columns have been produced that retain the steroids at high temperatures, producing excellent chromatographic resolution, examples are the widely used (5%-phenyl)-methylpolysiloxane columns such as the DB5[78] and the more specialised dimethylpolysiloxane stationary phase columns.[79]

1.7.3 Mass Spectrometry

After chromatographic separation the steroids sequentially enter the ionisation source of the mass spectrometer. The general operating principles of mass spectrometry are similar, the four step procedure is outlined below;

1. Ionisation. The ionisation source vaporises (if needed) and ionises the sample to produce gaseous ions. There are many types of ionisation source including, electron ionisation (EI), chemical ionisation (CI), electrospray ionisation (ESI), and atmospheric pressure chemical ionisation (APCI).

2. Fragmentation. Where there is excess internal energy (i.e. more energy than is required to ionise the molecule), the energy can be transferred into vibrational

energy levels of the molecule, this can cause molecular bonds to break and so fragmentation occurs. Controlled fragmentation, for example, collision induced dissociation (CID) in an ion trap allows structural information about a given molecule to be obtained.

3. Separation. A mass analyser separates ions accurately according to the m/z ratios of the ions, mass separation is achieved using magnetic or an electrical field or a combination of both.

4. Detection. Ions are detected by a variety of detection devices, the choice being dependent on the instrument design, a signal proportional to the ion signal (or count) is passed to a data system which processes this raw data into mass spectra and ion chromatograms.

1.7.4 Ionisation methods in mass spectrometry

Electron Ionisation (EI)

High energy electrons are created from a tungsten or rhenium filament, these high energy electrons (70eV) are 'fired' at the sample which causes a molecular ion [$M^{\bullet+}$] (a radical cation) to form. EI spectra characteristically show considerable fragmentation due to excess internal energy, and the molecular ion signal can be small or absent. The excessive fragmentation of steroids in EI mode is regarded as an impediment in using EI mass spectra for structural elucidation, therefore this ionisation method is generally not used in steroids analysis. EI has however been applied to distinguish between isomers of the same steroid based on the differences in their energy levels, for example Mák and co-workers distinguished between the two isomers 11α and 11β- estran.[80] EI was the ionisation source employed in all GC/MS applications in these experiments.

Chemical Ionisation (CI)

This technique is much softer than EI producing ions representative of the molecule i.e. $[M+H]^+$ or $[M+$ adduct ion$]^+$. The CI source is identical to that of EI (electrons from a filament), however a reagent gas such as ammonia or methane is added at higher pressure than the sample gas into the ionisation chamber. The source volume is usually more gas tight for CI operation (than EI) with the use of small entrance holes. Electrons ionise the reagent gas forming an excess of reagent gas ions- if ammonia is the reagent gas the following reaction occur in the source;

$NH_3 + e \rightarrow NH_3^{+\cdot}$

$NH_3^{+\cdot} + NH_3 \rightarrow NH_4^+ + NH_2^{\cdot}$

$NH_4^+ + M \rightarrow NH_3 + [M+H]^+ + [M+ \text{adduct ion}]$

Positively charged reagent ions NH_4^+ react with sample molecules (M) and the analyte becomes protonated. The reagent psuedo-molecular ion is identified as the adduct, or quasi-molecular ion, the structure of which is dependent on the reagent gas and the sample present.[81] CI steroid analysis has been conducted using a number of different reagent gasses such as methane, isobutane, and ammonia, producing spectra that provide information concerning molecular weight[82] which may not be possible with EI.

Electrospray Ionisation (ESI)

ESI permits direct coupling of a liquid chromatography system to a mass spectrometer. $[M+H]^+$ ions are generally produced in ESI spectra, although sodium adducts are commonly seen, and if a reagent such as ammonium acetate is added, $[M+NH_4]^+$ ions. A fine capillary with a drawn needle tip (~10μm tip diameter) sprays the liquid which becomes a gaseous ionised species before entering the mass spectrometer. The needle tip is metallised and has a high voltage applied typically 1-3 kV. The high electric field strength causes the liquid to form a Taylor cone, which extends to a tip (or filament) from which a spray of ionised droplets is emitted.[83] The droplets then move towards the mass spectrometer due to potential (and pressure) gradients. A gas counter current is applied to the tip which desolvates the droplets, a typical desolvation gas used is dry nitrogen. ESI has been developed to include micro and nano-spray techniques. ESI was the source employed in all liquid chromatography mass spectrometry (LC/MS) experiments in these investigations using the LCQ DECA mass spectrometer.

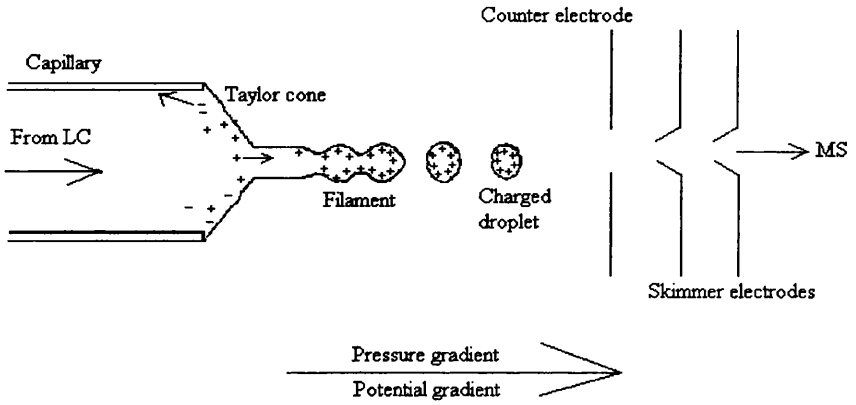

Fig 1.10: Illustration of the electrospray ionization process at the capillary tip. LC = liquid chromatography MS= mass spectrometry.

There are two main theories about the mechanism by which the analyte becomes ionised. In both theories a solvated ion is ejected from the electrospray needle tip and the ions are eventually focused and sampled by the mass spectrometer.

The Ion Evaporation Theory. As the droplet moves through the system it loses solvent and charge until only a single ion remains surrounded by a solvent shell. Nitrogen gas acts to remove the remaining solvent leaving a protonated analyte molecule. This model is relevant if the molecule under investigation is relatively small (up to a 1000Da), this theory is the probable ionisation mode for steroids.[84]

The Charge-Residue Theory. The droplets loses solvent until they reach the Rayleigh limit, where Coloumbic (repulsive) forces between the ions are greater than surface tension forces, which causes the droplet to explode into smaller droplets, these explosions continue until there is little or no solvent remaining. Then nitrogen acts to remove any remaining solvent until only the ionised analyte remains.[85] This theory is accepted to be accurate for larger molecules such as globular proteins.

ESI is an ideal technique for steroid analysis due to the likelihood of the molecular ion being formed. ESI has been widely applied in the detection of steroids and can be switched from positive mode for detection of androgens to negative mode for

oestrogen detection, producing a full androgen and oestrogen profile on one instrument.[86]

1.7.5 Mass Analysers in mass spectrometry

Magnetic Sector

A magnetic separator mass analyser separates ions due to their mass to charge (m/z) ratio using a magnetic field. The ions are deflected in a circular path with the magnetic field strength, B. The deflection of an ion depends on mass (m), charge (z) and magnetic field strength (B). It can be expressed in the equation below, where R is the radius of the arc of deflection and V is the accelerating voltage,

$$\frac{m}{z} = \frac{B^2 R^2}{2V} \qquad \text{(equ 1.0)}$$

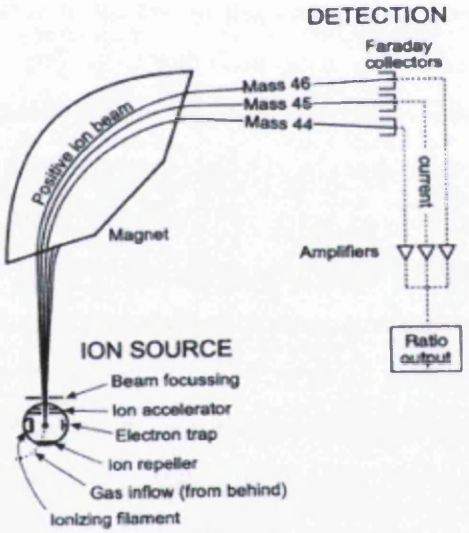

Fig 1.11: Diagram of magnetic separator, courtesy of the US Geological Survey.[87]

Ions with a heavier mass are deflected less than ions of lighter mass (assuming identical charges). An electric field is also involved in this instrument to compensate and correct for energy spread, the electric field is applied orthogonally to the ion path. The magnetic field can be varied resulting in detection of different mass-to-charge (m/z) ions. This technique can be used for both accurate mass studies and full scan studies.

Quadrupole mass analysers

A quadrupole mass analyser uses oscillating electric fields to separate ions. It has four parallel rods with each opposite pair being linked together. Voltages are applied across the pairs of rods which have a direct current (dc) component, U, and a radio frequency (rf) component, V. The voltages U and V are varied so the ratio of U:V is constant focusing ions of different m/z ratio ions through the quadrupole. When only the rf voltage, V, is applied the device transmits all masses and acts as a simple ion transmission device. The quadrupole allows for continuous monitoring of ions and so can be directly linked to a continuous source, such as gas or liquid chromatography system.

Multiple quadrupoles can be aligned in an MS/MS configuration to obtain fragmentation data. Three quadrupoles can be set up in series, the central of which only operates in rf mode acting as a gas collision cell. The other two act to separate ions due to m/z ratios they have rf and dc fields applied either scanning the full mass range or set at a given m/z value. The rf only (central) quadrupole acts as a collision cell with the introduction of an inert collision gas such as helium or nitrogen. Fragment scans, product ion scans precursor and neutral loss scans can then be completed to obtain more information about the sample under investigation. Triple quadrupole mass spectrometers using precursor ion scans are used in steroid analysis to identify chemically altered designer steroids used illegally in sport as steroids with similar structures have similar dissociation patterns. [88] Neutral loss scans have been employed in the analysis of sulphated steroid metabolites in urine, the neutral loss of the sulphate group was monitored to detect the steroids such as oestradiol sulphate and dehydroepiandrosterone sulphate.[89]

The quadrupole ion trap

The ion trap is a folded quadrupole mass analyser that has a curved central electrode (a ring), and two end cap electrodes above and below the ring (figure 1.12). Ions are trapped within this system with the aid of a small pressure of helium to stabilise the ions in the trap. Ions are then mass selectively expelled from the trap by variation of the applied voltages, the technique is highly sensitive, with unit mass resolution. It can be used in MS/MS and MS^n mode producing detailed fragmentation patterns and assisting in chemical structure elucidation. The ion trap is a robust interface with a

wide dynamic range,[90] (10^4) it has been employed for steroid analysis in numerous investigations,[91,92] for this reason an ion trap was employed in these experiments for steroid analysis.

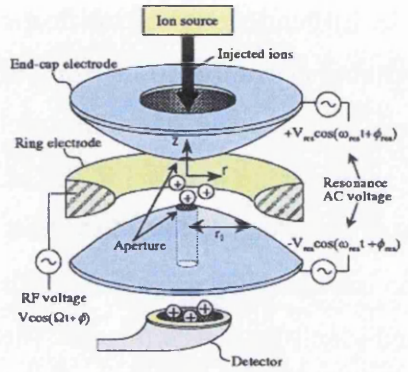

Fig 1.12: Diagram of Quadrupole Ion Trap system, reproduced from University of Heidelberg on-line resources.[93]

There are other types of mass analyser such as time-of-flight, fourier transform ion cyclotron resonance (FTICR) and orbitrap, as these were not used in these investigations they are not described.

1.7.6 Detection of ions in mass spectrometry

Initially photographic plates were used to detect ions produced by the mass spectrometer, ions of the same m/z ratio reach the plate at the same point. The intensity of the spot or line (or its darkness) is associated to the abundance of that ion in the sample (calculated by comparison to a standard). This technique is not very sensitive and lacks dynamic range and is no longer applied in practice. Development of a number of sensitive detectors has been achieved including the faraday cup, electron (and photon) multipliers tubes and microchannel plates. These all detect and amplify (by up to 10^8) the incoming ion flux and transfer them into electrical signals which are passed to a data system.

1.8 Real-time reverse transcription polymerase chain reaction (RT-PCR) for the detection of RNA relating to steroid converting enzyme expression

To calculate the amount of RNA related to specific steroid converting enzyme expression a technique called QRT-PCR was employed. This procedure permits calculation of differences (and similarities) in RNA relating to steroid converting

enzyme expression between the endometrial pathologies as well as temporal changes in steroid converting enzyme expression after steroid treatments.

1.9 Analysis methods

Mass spectrometry permits identification and quantification of multiple steroids and was applied in these experiments in combination with chromatography (LC or GC) to obtain and quantify steroid profiles and identify steroid metabolites. Real time (reverse-transcription) polymerase chain reaction RT-PCR permits specific, sensitive determination of expression of multiple enzymes involved in steroid biosynthesis. In combination these two techniques produced a novel model of steroid metabolism in the endometrium and allowed identification of possible therapeutic targets.

1.10 Project Aims

Production of a robust method for detection of a mixture of steroid standards, through optimised and validated gas and liquid chromatography (GC and LC) and mass spectrometry.

Development of cell culture for maximum growth to obtain enough cellular material for time related steroid treatments, and to assess expression of RNA relating to steroid converting enzymes.

Optimisation and validation of steroid extraction methods from cells and cell media.

Determination of testosterone metabolism pathways in cell lines, fertile biopsies and biopsies from a number of benign endometrial pathologies.

Determination of basal and temporal changes (after testosterone treatment) of enzyme expression in fertile biopsies, endometrial cancer cell lines and benign endometrial pathologies.

The combination of mass spectrometry steroid metabolism profiles with enzyme expression profiles to provide novel information concerning testosterone metabolism in a number of endometrial pathologies.

1.11 References Chapter One

[1] Simpson ER. J. Steroid Biochem and Mol Biology **86** (2003) 225-230

[2] Utsunomiya H, Ito K, Suzuki T, Kitamura T, Kanedko C, Nakata T, Niikura H, Okanura K, Yaegashi N, Sasano H. Clinical Cancer Research **10** (2004) 5850-5856

[3] Suzuki R, Miki Y, Nakamura Y, Moriya T, Ito K, Ojuchi N, Sasano H. Endocrine Related Cancer **12** (2005) 701-720

[4] Online medical Dictionary (1997) accessed online 23rd November 2008 http://cancerweb.ncl.ac.uk/cgibin/omd?action=Search+OMD&query=Addison%27s+Disease

[5] Key T J, Pike M C. Br J Cancer **57** (1988) 205-212

[6] Rowland M, Biology Published by Nelson, Uni Of Bath Science (1992) 16-19

[7] Boivin RP, Luu-The V, Lachance FL, Poirier D. J Med Chem **43** (2000) 4465-4478

[8] Carruba G, Granata OM, Farruggio R, Cannella S, Bue AL, Leake RE, Pavone-Macaluso M, Castagnetta LAM. Steroids **61** (1996) 41-46

[9] Norton JA, Bollinger RR, Chang AE, Lowry SF, Mulvihill SJ, Pass HI, Thompson RW. Surgery Basic Science and Clinical Evidence Pub Springer (2001) 73-75

[10] Ulmschneider S. Müller-Vieira U, mitrenga M, Hartmann RW, Oberwinkler MS, Klein CD, Bureik M, Bernhardt R, Antes I Lengauer T. J Med Chem **48** (2005) 1796-1805

[11] Bukulmez O, Hardy DB, Carr BR, Auchus RJ, Toloubeydokhti T, Word RA, Mendelson CR. J Clin Endocrinol Metab **93** (2008) 3471-3477

[12] Kříž L, Bičíová M, Mohapl M, Hill M, Černý I, Hampl R. J Steroids Biochem Mol Biol **109** (2008) 31-39

[13]Thiboutot D, Jabara S, McAllister JM, Sivarajah A, Gilliland K, Cong Z, Clawson G. J Invest dermatol **120** (2003) 905-914

[14] Carreau S, Bourguiba S, Lambard S, Silandre D, Delalande C. Reproductive Biology. Review Paper **4** (2004) 23-34

[15] Simpson E R, Mahendroo M S, Means G D, Kilgore M W, Hinshelwood M M, Graham-Lorence S, Amarneh B, Ito Y, Fisher C R, Micheal M D, Mendelson C R, Bulun S E. Endo Rev **15** (1994) 342-355

[16] Hu Y, Ghosh S, Amleh A, Yue W, Lu Y, Katz A Li R. Oncogene **24** (2005) 8343-8348

[17] Simpson ER, Davis SR. Endocrinology **142** (2001) 4589-4594

[18] Meresman G, Bilotas M, Abello V, Buqet R, Tesone M, Sueldo C. Fertility and Sterility **84** (2005) 459-463

[19]Mouse Genome Information accessed online 5th December 2008 http://www.informatics.jax.org/javawi2/servlet/WIFetch?page=pirsfDetail&key=4001227

[20] Taylor ME, Wang M, Bhattacharyya AK, Chiang N, Tai H-H, Collins DC. Steroids **62** (1997) 373-378

[21] Steckelbroeck S, Jin Y, Gopishetty S, Oyesanmi B, Penning TM. J Bio Chem **279** (2004) 10784-10795

[22] Day JM, Tutill HJ, Purohit A, Reed MJ. Endo-related Cancer **15** (2008) 665-692

[23] Moeller G, Adamski J. Mol Cell Endo **248** (2006) 47-55

[24] Pelletier G, Luu-The V, Li S, Ren L Labrie F. J of Mole Endo **33** (2004) 459-465

[25] Spires TE, Fink BE, KickEK, You D, Rizzo CA, Takenaka I, Lawernce RM, Ruan Z, Salvati ME, Vite GD, Weinmann R, Attar RM, Gottardis MM, Lorenzi V. The Prostate **65** (2005) 159-170

[26] Penning TM, Burczynski ME, Jez JM, Hung CF, Lin HK, Ma H, Moore M, Palackal N, Ratnam K. Biochem J **351** (2000) 67-77

[27] Yang S-Y, He X-Y, Miller D. Mol Genetic and Metabolism **92** (2007) 36-42

[28] Suzuki T, Miki Y, Akahira J-I, Moriya T, Ohuchi N, Sasano H. Endocrine Journal **55** (2008) 455-463

[29] Foster PA, Woo LLW, Potter BVL, Reed MJ, Purohit A. Endocrinology **149** (2008) 4035-4042

[30] Purohit A, Fusi L, Brosens J, Woo LWL, PotterBVL, Reed MJ. Hum Reprod **23** (2008) 290-297

[31] Glatt H. Current Toxicology Series. Enzyme Systems that Metabolise Drugs and other Xenobiotics. Sulphotransferases chapter (2002) Wiley and Sons Ltd.

[32] Rehse PH, Zhou M, Lin S-X. Biochem J. **364** (2002) 165-171

[33] Enmark E and Gustafsson J-A. J Internal Medicine **246** (1999) 133-138

[34] Driggers PH, Segars JH. Trends in Endocrinology and Metab **13** (2002) 422-427

[35] Gower DB. Steroid Hormones, (1979) Publisher Croom Helm London, chapter 5 268-368.

[36] Steimer T. Reproductive Health, Steroid Hormone Metabolism, University of Geneva accessed online 9th December 2008
http://www.gfmer.ch/Books/Reproductive_health/Steroid_hormone_metabolism.html
[37] Lobo RA, Mishell DR, Paulson RJ, Shoupe D. Infertility, Contraception and Reproductive Endocrinology (1997) Publisher Blackwell Science Fourth Edition.
[38] Matsumoto M, Yamaguchi Y, Seino Y, Hatakeyama A, Takei H, Niikura H, Ito K, Suzuki T, Sasano H, Yaegashi N, Hayashi S-I. Endocrine Related Cancer **15** (2008) 451-463
[39] Diagram from the National Uterine Fibroids Foundation accessed online 20th December 2008
http://www.nuff.org/health_theuterus.htm
[40] Arnold JA, Kaufman DG, Seppälä M, Lessey BA. Human reproduction **16** (2001) 836-845
[41] Cancer research UK accessed online 4th December 2008
http://www.cancerhelp.org.uk/help/default.asp?page=98#epith
[42] Berstein LM, Tchernobrovkina AE, Gamajunova VB, Kovalevskij AJ, Vasilyev DA, Chepik OF, Turkevitch EA, Tsyrlina EV, Maximov SJ, Ashrafian LA, Thijssen JHH. J Cancer Res Clin Oncol **129** (2003) 245-249
[43] Velasco I, Rudeda J, Acién P. Mol Human Reproduction **12** (2006) 377-381
[44] Lukanova A, Kaaks R. Cancer Epidemiology, biomarkers and prevention Review **14** (2005) 98-102
[45] Rauh M. Molecular and Cellular Endocrinology **301** (2009) 272-281
[46] Way DL, Grosso DS, Davis JR, Surwit EA, Christian CD. In Vitro **19** (1983) 147-153
[47] Sherman ME. Theories of endometrial carcinogenesis: a multidisciplinary approach. Modern Pathology **13** (2000) 295-308
[48] Hecht JL, Mutter GL. J Clinical Endocrinology **24** (2008) 4783-4791
[49] Doll A, Abal M, Rigau M, Monge M, Gonzalez M, Demajo S, Colás E, Llauradó M, Alazzouzi H, Planagumá J, Lohmann MA, Garcia J, Castellvi S, Ramon y Cajal J, Gil-Moreno A, Xercavins J, Alameda F, Reventós J. Steroid Biochem and Mol Biol **108** (2008) 221-229
[50] US Department of Health and Human Services accessed online 16th October 2008
http://www.4woman.gov/FAQ/pcos.htm
[51] Giudice LC, Best Practise and Research Clinical Endocrin and Met **20** (2006) 235-244
[52] Bacallao K, Leon L, Gabler F, Soto E, Romero C, Valladares L, Vega M. J steroid Biochem Mol Biol **110** (2008) 163-169
[53] Johnson N, Farquhar CM. BMJ (2006) Clinical Evidence, Endometriosis (Women's health) accessed online 4th December 2008
http://clinicalevidence.bmj.com/ceweb/conditions/woh/0802/0802_background.jsp
[54] Kitawaki J, Kado N, Ishihara H, Koshiba H, Kitaoka Y, Honjo H. J Steroid Biochem and Mol Biol **83** (2003) 149-155
[55] Takayama K, Zeitoun K, Gunby RT, Sasano H, Carr BR, Bulun SE. Fertility and Sterility **69** (1998) 709-713
[56] The Merck Manuals. Online medical library-Gynaecology and Obstetrics, Endometriosis. Accessed online 16th December 2008 http://www.merck.com/mmpe/sec18/ch247/ch247a.html#CACEJEHC
[57] Horn L-C, Meinel A, Handzel R, Einenkel J. Pathology **11** (2007) 297-311
[58] Zaino RJ, Kauderer J, Liu Trimble C, Silverberg SG, Curtin JP, Lim PC, Gallup DG. Cancer **106** (2006) 804-811
[59] Elsford K, Claman P. Fertility and Sterility **79** (2003) 1028-1030
[60] Guzik DS, Sullivan MW, Adamson GD, Ceders MI, Falk RJ, Peterson EP, Steinkampf MP. Fertility and Sterility **70** (1998) 207-213
[61] Malik A, Jain S, Rizvi M, Shukla I, Hakim S. Fertility and Sterility **91** (2009) 91-95
[62] Cheong YC, Li TC. Current Obstetrics and Gynaecology **15** (2005) 306-313
[63] Pierro E, Minici F, Alesiani O, Miceli F, Proto C, Screpanti I, Mancuso S, Lanzone A. Biology of Reproduction **64** (2001) 831-838
[64] Xu CL, Chu XG, Peng CF, Jin ZY, Wany LY. J Pharma Biomed Anal **41** (2006) 616-621
[65] al-Alousi LM, Anderson RA. Steroids **67** (2002) 269-275
[66] Mishra A, Joy KP. General and Comparative Endocrinology **145** (2006) 84-91
[67] Raeside JI, Christie H L, renaud RL, Waelchli RO, Betteridge KJ. Bol of Reproduction **71** (2004) 1120-1127
[68] Delvoux B, Husen B, Aldenhoff Y, Koole L, Dunselman G, Thole H, Groothuis P. J of Steroid Biochem and Mol Biol **104** (2007) 246-251
[69] Today's Chemist at work, ACS Publictaions, M. Cooke, G. C. Clarke, L. Goeyens, W Baeyens. **9**, No.7 15,16,19 (2000)

[70] Nieschlag E, Behre HM. Testosterone: Action, deficiency, substitution Cambridge Uni Press (2004) 653-657
[71] Brooks CJW. Phil Trans. R Soc Lond A **293** (1979) 53-67
[72] Ahmadkhaniha R, Shafiee A, Rastkari N, Kobarfard F. Anal Chem Acta **631** (2009) 80-86
[73] Agilent technologies accessed online 7th December 2008
https://www.chem.agilent.com/Library/chromatograms/(PI136)_029065.jpg
[74] Chang Y-C, Li C-M, Li L-A, Jong S-B, Liao P-C, Chang L W. The Analyst **128** (2003) 363-368
[75] Zhao M, Baker S D, Yan X, Zhao Y, W W Wright, B R Zirkin J P Jarow Steroids **69** (2004)721-726
[76] Chromatography online accessed online 9th December 2008
http://chromatographyonline.findpharma.com/lcgc/article/articleDetail.jsp?id=159255
[77] Nagaoka M, Numazawa M. Steroids **70** (2005) 831-839
[78] Leyssens L, Royackers E. GC/MS Varian Application Note number 33
[79] Sellers K. Restek Chromatography Products Online resources. accessed online 9th December 2008
http://www.restek.com/aoi_forensics_A005.asp
[80] Mák M, Francsics-Czinege E, Tuba Z. Steroids **69** (2004) 831-840
[81] deHoffmann E, Stroobant V Mass Spectrometry Principals and Applications, Second Edition, (2003) 14-25
[82] Lin YY. Lipids **15** (1980) 756-763
[83] Gaskell S J. J of Mass Spectrom. **32** (1997) 677-688
[84] Mass Spectrometry Principals and Applications, E deHoffmann and V Stroobant, Second Edition, (2003) 33-36
[85] Griffiths WJ, Jonsson AP, Liu S, Rai DK, Wang Y. Biochem J, **355** (2001) 545-561
[86] Cheng C, Tsai H-R Anal Chimica Acta **623** (2008) 168-177
[87] Diagram of magnetic separator downloaded from US Geological Survey accessed on-line 25th November 2008. http://en.wikipedia.org/wiki/Mass_spectrometry
[88] Thevis M, Geyer H, Mareck U, Schänzer W. J Mass Spectrometry **40** (2005) 955-962
[89] Lafaye A, Junot C, Ramounet-Le Gall B, Fritsch E, Tabet J-C. JMS **39** (2004) 655-664
[90] Wong PSH, Cooks RG. Ion Trap Mass Spectrometry Current Separations.com accessed online 9th December 2008 http://www.currentseparations.com/issues/16-3/cs16-3c.pdf
[91] Griffiths WJ, Wang Y, Karu K, Samuel E, McDonnell S, Hornshaw M, Shackleton C. Clinical Chem **54** (2008) 1317-1324
[92] Choi MH, Kim JN, Chung BC. Clinical Chem **49** (2003) 322-325
[93] Diagram of quadrupole ion trap accessed online 4th December 2008
http://www.rzuser.uni-heidelberg.de/~bl5/ency/pics/q_trap01.jpg

Chapter Two

Materials and Instrumentation

2.0 General laboratory chemicals

Table 2.1: Chemicals required for derivatisation, extraction and analysis of steroids.

Name	Description	Manufacturer
Triethylamine	99%	Alfa Aesar, Heysham, UK.
Anhydrous sodium sulphate	laboratory grade	Fischer Scientific, Loughborough, UK
Sulphuric acid	Concentrated 98.07%	Phillic Harris, Novora Group Ltd, Ashby de La Zouch, UK
Dansyl chloride	>99% purity (derivatisation grade)	Fluka Sigma Aldrich, Poole, UK
BSFTA + TMCS Bis(trimethylsilyl)trifluoroacetamide trimethylchlorosilane	99:1 (derivatisation grade)	Supleco at Sigma Aldrich.
Formic acid	90% purity	BDH Ltd, Lutterworth, UK
Acetic acid glacial	>99% purity HPLC grade	Fischer Scientific
Trifluoroacetic acid	99% spectrophotometric grade	Sigma Aldrich, UK
Sodium carbonate	>98%	Sigma Aldrich, UK
Potassium hydroxide	Pellets	Sigma Aldrich, UK

2.1 Gases

Nitrogen (oxygen free nitrogen) was used as a desolvation/nebuliser gas in the electrospray ionisation source.

Helium gas was used to de-gas the mobile phases prior to LC/MS analysis,

Helium was also used as the carrier gas in the GC system.

All gases were obtained from BOC (Guildford, UK).

2.2 Solvents

Table 2.2: Table of solvents employed

Name	Description	Manufacturer
Methanol	HPLC grade	Thermo Fisher Scientific, Loughborough, UK
Ethanol	Laboratory grade	Fisher Scientific.
Hexane	Laboratory grade	Fisher Scientific.
Ethyl acetate	Laboratory grade	Fisher Scientific.
2-Butanol	Laboratory grade	BDH Ltd, Poole, UK
De-ionised water	Milli-Q water	Milli-Q purification system (Millipore, USA)
Acetonitrile	Laboratory grade	Fischer Scientific.
Dichloromethane (DCM)	Laboratory grade	Fisher Scientific.
Isooctane	99% purity	Sigma Aldrich.
Methyl *tert*-butyl ether (MTBE)	>99% purity	Sigma Aldrich.
Acetone	Laboratory grade	Fischer Scientific.

2.3 Steroid standards

Table 2.3: Steroid standards.

Name	IUPAC name	Description	Manufacturer
Cholesterol	3β-hydroxycholest-5-ene (3β-cholest-5-en-3-ol)	99% purity	Sigma Aldrich.
Androgens			
Testosterone	17β-hydroxyandrost-4-en-3-one	>98% purity,	Sigma Aldrich.
17-Methyl testosterone	17β-hydroxy-17-methyl-androst-4-en-3-one	analytical standard	Sigma Aldrich.
Dehydroepiandrosterone (DHEA)	3β-hydroxyandrost-5-en-17-one	98% purity	Sigma Aldrich.
Dehydroepiandrosterone 3-sulphate sodium salt dehydrate DHEA-S	17β(sulfooxy)androst-5-en-17-one	>99% purity	Sigma Aldrich.
Dihydrotestosterone 4-androstene17β-ol-3-one (DHT)	17β-hydroxy-5α-androstan-3-one		Sigma Aldrich.
Androsterone	3α-hydroxy-5α-androstan-17-one	>99% purity	Sigma Aldrich.
5α-androstane3β-17α-diol	5α-androst-3β, 17α-diol		Steraloids Inc (Newport, Rhode Island, USA),
4-Androstene-3,17-dione (Androstenedione)	Androst-4-en-3, 17-dione	98% purity	Sigma Aldrich.
Oestrogens			
Oestradiol (E2)	Estra-1,3,5(10)-trien-3,17β-diol	analytical standard	Sigma Aldrich.
Oestrone (E1)	3-hydroxyestra-1,3,5(10)-trien-17-one	99% purity	Sigma Aldrich.
Oestriol	Estra-1,3,5(10)-trien-3,16α,17β-triol	99% purity	Sigma Aldrich.
Progestins			
Progesterone (4-Pregnene-3,20-dione)	Pregn-4-en-3,20-dione	99% purity	Sigma Aldrich.
Pregnenolone5-pregnen-3β-ol-20-one (Pregnenlone)	3β-hydroxypreg-5-en-20-one	98% purity,	Sigma Aldrich.

2.4 Cell culture

Established cell lines (see table 2.5)

Sterile cell culture flaks, slides, dishes and pipettes. Cell star tissue culture flasks Greiner Bio One, Frichenhausen, Germany.

Table 2.4: Cell culture chemicals

Name	Description
Dulbecco's Modified Eagle Medium (DMEM)	Media used for all cell lines unless stated
Basal Medium Eagle (BME)	Media for HEC-1B cell line
Foetal Calf Serum (FCS)	Normal and charcoal stripped to remove inferring substances.
L- Glutamine	200nM (100X solution)
Antimycotic antibiotic	10,000 units/mL penicillin G sodium, 10,000 µg/mL streptomycin sulphate 25µg/mL amphotericin B and funizone in 0.85% saline
Sodium Pyruvate	100nM
Sodium Bicarbonate	7.5% solution
Glucose	Sigma Aldrich, UK
Penicillin/streptomycin	10,000 units/mL penicillin G sodium and 10,000µg/mL streptomycin sulphate in 0.85% saline.
L-asparagine monohydrate	>99% Sigma Aldrich, UK
Non-essential amino acids	100X solution
Insulin	
HEPES (4-(2-hydroxyethyl)-1-piperazineethanesulfonic acid)	Standard cell culture material
Hank's Balanced Salt Solution (HBSS +$CaCl_2$ +$MgCl_2$)	1X solution
HBSS (-$CaCl_2$-$MgCl_2$)	1X solution
Trypsin-EDTA (ethylenediaminetetraacetic acid)	0.25% solution
Dimethylsulphoxide (DMSO)	For freezing media

All cell culture chemicals were purchased from Invitrogen cell Culture Company /GIBCO Paisley, UK. All chemicals are specific for use in cell culture.

Table 2.5: Growth conditions and descriptions of five human cell lines.

Name of cell line	Description	Receptor Status	Origin	Media constituents
Ishikawa	Human endometrial cancer	PR + AR + ER +	Imperial College London, UK,	DMEM, 10% FCS, 1.0mM sodium pyruvate, 1.5g/L sodiu bicarbonate, 5ml antimycotic antibiotic, 2mM glutamine.
HEC-1B	Human endometrial adenocarcinoma	PR - AR + ER -	Imperial College London, UK	BME (Eagles media), 1.5g/L sodium bicarbonate,0.1mM no essential amino acids, 1.0mM sodium pyruvate, 10% FCS, 5m antimycotic antibiotic, 2mM L glutamine.
HEC-1A	Human endometrial adenocarcinoma	PR + AR + ER +	Imperial College London, UK	DMEM, 10% FCS, 1.0mM sodium pyruvate, 1.5g/L sodiu bicarbonate, 5ml antimycotic antibiotic, 2mM glutamine. OR DMEM-F12, 10% FCS, 5ml sodium pyruvate, 5ml antimycotic antibiotic, 1.5mM glutamine.
RL95_2	Human uterine epithelial	PR (very low) AR + ER -	Imperial College London, UK	DMEM hans F12, 10% FCS, 5mL HEPES, 1.5g/L sodium bicarbonate (100X), 250µl insulin.
COV434	Human immortalised granulosa	PR (not known) AR (not known) ER +	Imperial College, London, UK	DMEM media 10% FCS, 50µg/mL penicillin/streptomyci 3mmol/L glutamine, 1mmol/L asparagine.

2.4.1 Biopsy samples

Biopsy samples were obtained from the endometria of patients with;

- normal fertility,
- tubal disorders,
- endometriosis,
- PCOS (polycystic ovary syndrome),
- unexplained infertility,
- endometrial hyperplasia,

-ovarian cyst,

-endometrial polyp.

All biopsies were cultured in DMEM-F12, 10% FCS, 5ml sodium pyruvate, 5ml antimycotic antibiotic, 1.5mM glutamine. Biopsy samples were provided by Singleton Hospital Obstetrics and Gynaecology department by Dr L Joels and her surgical team (ethical approval has been obtained).

2.5 Real time Reverse Transcription-Polymerase Chain Reaction materials (RT-PCR)

RNAeasy (Qiagen, Crawley, UK) RNA extraction kit,

RNA-cDNA Ambion reteroscript kit (Ambion, Warrington, UK),

RT-PCR (AB gene, Epsom, UK) RT-PCR SYBR green protocol kit.

Sense and antisense primers for the detection of a number of steroid converting enzymes were all purchased from Sigma Genosys, (Cambridge, UK). Primers were selected for their efficiency, cross binding between primers was low, calculated using Beacon primer design software. The primer sequences and other primer information are outlined in table 2.6.

Table 2.6: Primer sequences for a number of steroid conversion enzymes.

Gene /Steroid converting enzyme name	Melt temperature Tm (°C)	Annealing temperature Ta (°C)	Calculated Sense sequence	Calculated Anti-sense sequence
GADPH	90.0	55	5'-GTCCACTGGCG TCTTCAC	5'-CTTCAGGCTGTTGTC ATACTTC
Aromatase	87.0	53	5'-TGCACAGGTTG GAGGAGGTG	5'-TCAAGAAGAGCGT GTTAGAGGTG
WT1	89.0	55	5'-CTATTCGCAA TCAGGGTTACAG	5'-CATGCTTGAATGA GTGGTTGG
17β-HSD1	89.0	54.7	5'-TTCCACCGCTT CTACCAATACC	5'-CCTCCGCCACCT CCTCAG
17β-HSD2	89.2	54.6	5'-TCGTTAGCCAG CAAGACTTC	5'-TGAGCAAGGCAGA TCCACAAG
17β-HSD4	86.5	52.8	5'-GGATCACGG ATGACTCAGACAG	5'-AGCCACCATTCT CCTCACAAC
17β-HSD5	82.6	49.1	5'-TCCGCCATA TAGATTCTGCTC	5'-TCTCTTCACACT GCCATCTG
17β-HSD7	86.0	52.7	5'-AGGAACATGAG CAAGGCAGAAG	5'-GACAATGGTGAC CTCAGCAGTG
17β-HSD8	88.4	54.2	5'-GATCCGCTGT AACTCTGTCCTC	5'-CGACCACATCTG CCACATCC
5AR1	84.8	51.4	5'-TCTGATGCGA GGAGGAAAGC	5'-ATACACTGCACAA TGGCTCAAG
5AR2	89.6	55.1	5'-CACTTTGGTCG CCCTTGGG	5'-AGGCTCTCCGTGTG CTTCC

For optimal performance the region spanned by the primers was between 75 and 150 base pairs in length as SYBR was used in the PCR reaction.

2.6 Steroid extractions

Solid Phase Extraction (SPE) 100mg C_{18} cartridges. Varian, Yarnton, UK.

2.7 Chromatography columns

Table 2.7: Type of columns used in liquid and gas chromatography experiments.

Name	Description	Manufacturer
Liquid Chromatography		
C_{18} column	15cm x 300μM internal diameter	Dionex, Camberley, UK.
C_{18} column	25cm x 300μM internal diameter	Dionex.
C_{18} column	Prepared and packed in lab 15cm	
Luna phenyl-hexyl	15cm x 1000mm	Phenomenex, Macclesfield, UK
Hypersil BDS Phenyl	15cm x 1000mm	Hypersil (Thermo scientific)
Gas Chromatography		
HP-1	Dimethylpolysiloxane	Agilent (previously Hewlet Packard), Stockport, UK.
Supelco SLB-5ms	Silphenylene polymer filled column	Supleco, Dorset, UK.

2.8 Instrumentation

2.8.1 HPLC linked to the mass spectrometer

Dionex/LC Packings HPLC (Packing's Ultimate HPLC pump and Famos injection system). Auto sampler unit and Ultimate gradient pumping system.

Quadrupole ion trap mass spectrometer (linked to LC) LCQ DECA XP plus (ion trap mass spectrometer) Thermo Finnigan Ltd, Hemel Hempstead, UK.

2.8.2 Typical conditions for full scan mass spectrometry (LCQ DECA)

The HPLC was linked to the mass spectrometer and run in capillary mode at a flow rate of 4μL/minute using the CAP300 calibrator cartridge for androgen and progestin analysis. The LC system was also run at a flow rate of 40μL/minute using the MIC1000 calibrator cartridge for analysis of dansyl chloride (DC) oestrogen derivatives. The LCQ was used in these experiments with an ESI source in positive

mode. The gradient systems pump parameters and injection programmes (i.e. loop size, additives, solvents) were optimised as described in chapter four.

2.8.3 GC/MS linked to the mass spectrometer

There are two GC/MS systems analysed in these experiments the Fisons GC MD800 and an Agilent GC MSD.

2.8.4 Typical conditions for full scan mass spectrometry (GC/MS MD800)

The GC/MS was run in with an EI source in positive mode. The GC oven can be operated to give a gradient system that ranges in temperature of over 400°C. Oven and injector temperature and column type were analysed and optimised for steroid separation as outlined in chapters three and four.

2.8.5 Typical conditions for full scan mass spectrometry GC MSD

The GC MSD has two ionisation sources available CI and EI. The EI source was employed for all steroid investigations in these experiments. The GC MSD has 2 injection ports which offer seven injection procedures, these are hot and cold split and splitless, solvent vent, solvent vent-stop flow and on column injections. The GC oven again had a range of 400°C. Again this technique was optimised for steroid analysis as described in chapter four.

2.8.6 Laboratory equipment

Table 2.8: Laboratory equipment

Laboratory equipment	Version	Supplier
RT-PCR machine 1	Icycler with iQ, (version 3.1)	Bio-rad laboratories Inc, California, USA
RT-PCR machine 2	Mycycler with iQ5 (version 2.0)	Bio-rad laboratories Inc.
PCR machine	Used for reverse transcription processes	Bio-rad laboratories Inc.
Nano-drop	ND100 Spectrophotometer	Labtech International Ltd, Lewes, UK
Vortex	Vortex Genie *2* mixer	Scientific Industries Bohemia, NY, USA
Cell incubator	Auto flow CO_2 jacketed cell incubator	NU-AIRE Caerphilly, UK
Centrifuge1 RT-PCR	Heraeus Labofuge 400	Kendro, Hanau, Germany
Centrifuge 2 cell culture	Sanyo MSE Centaur 2	MSE, London, UK
Cell culture air filter sterile fume hoods	Mars Scanlaf cell culture hoods	Scanlaf Lynge, Denmark
PCR fume hoods	Labconco Purifier PCR enclosure	Labconco, Kansas, USA
Water bath	20-90°C	Grant Instruments Ltd, Cambridge, UK.
Freezers Excel	-16 to -32°C (frost free)	Bosch, UK
Air displacement pipettes	1000, 100, and 10µL	HTL *LabMate* Warsaw, Poland
Eppendorf pipettes and tips	1000, 100 and 10µL	Eppendorf UK Ltd, Cambridge, UK
Glass scintillation vials	20mL	ThermoFisher Scientific Waltham, MA, USA

2.9 Software

Beacon primer design software (version 3.0)

Bioworks RT-PCR data browsers,

-iCycler iQ optical system software (version 3.1)

-iQ5 optical system software (version 2.0)

Chromeleon (LC)

Xcalibur (version1.3) (LC/MS)

Mass Lynx (version 4.0) (GC/MS) MD800 and mass lab software

Microsoft office suite 2003 and 2007.

Chem Station Agilent Productivity (Revision E.01.00, 2007) Agilent 5975C.

Minitab 15 statistics software (2007).

Chapter Three

Experimental methods

Methods for cell culture and steroid converting enzyme (RNA) expression analysis through real time (reverse transcription) polymerase chain reaction (RT-PCR).

Methods for positive identification of steroids via gas and liquid chromatography mass spectrometry.

Methods of steroid extraction procedures via solid phase extractions (SPE).

3.0 Introduction

This chapter describes the experimental methods required for optimum cell growth through cell culture in order to obtain sufficient RNA for reverse transcription and real-time polymerase chain reaction (RT-PCR). Also described are the methods required for detection of steroid standards by gas and liquid chromatography mass spectrometry which were optimised in chapter four and applied to biological samples.

Extractions of steroids from simple and complex liquids and cells are described in this chapter using a number of extraction techniques to determine the most efficient method in terms of the range and concentration of steroids that can be extracted.

3.1 Cell culture methods and reverse transcription (real-time) polymerase chain reaction (RT-PCR) methodologies

Cells were grown and maintained until there was sufficient cellular material available for steroid treatments, extractions and RT-PCR. Cell culture was conducted in a controlled environment that was representative of the human body, at body temperature 37°C, and with the correct amount of carbon dioxide and oxygen gasses as well as the appropriate nutrients provided for growth.

Growing of established cell lines has been extensively optimised to achieve maximum cellular growth through changes in media conditions. Established cell lines were used in these experiments due to their immortality and robustness,[1] and because they are excellent models of cancerous tissue. The Ishikawa cell line for example is a model for type 1 human endometrial cancer.[2]

3.2 Cell culture methodologies; growth and maintenance of cell lines through cell culture methodologies

Both analysis methods (mass spectrometry and real time PCR) require the same initial cell culture steps.

A variety of established cell lines and endometrial biopsies were cultured. The cell lines were chosen as they are less variable than clinical samples, the endometrial cancer cell lines Ishikawa, HEC-1B, HEC-1A and RL95-2 were investigated to

provide understanding of the metabolic processes occurring in the endometrium and as model systems to optimise steroid treatments and extraction methods. The cell line COV434 was chosen as it highly expresses the steroid converting enzyme aromatase, and acts as a positive control in respect to the primers used in RT-PCR.

3.2.1 General cell culture methodologies

The cells were stored under liquid nitrogen until required, after which they were warmed in a 37°C water bath. Each cell line may require different media constituents for optimum growth these are outlined in chapter 2.4. All cell culture media and media additives such as sodium pyruvate, foetal calf serum (FCS), and trypsin EDTA (chapter 2.4) were warmed to 37°C before addition to the cells. The cells were centrifuged to form a pellet and the freezing media removed. The cells then added to a $10cm^3$ sterile plastic cell culture vessel with 10mL of media (plus nutrients) and placed in a 37°C incubator, half the media was changed the following day and thereafter periodically until the cells were 80% confluent. Following this the cells can be subjected to a number of experimental conditions or split into other vessels to produce more cells.

After steroid(s) treatment the cell media was removed (for analysis) and the cells were washed with 5ml of the salt solution HBSS $(-CaCl_2 -MgCl_2)^+$ to remove any remaining media. The cells were treated with 2mL of trypsin EDTA, causing them to detach from the culture dishes (assuming $10cm^3$ cell culture flasks, volumes increase with larger culture vessels). Media was then added to the flasks to neutralise the trypsin and the cells were removed into a centrifuge tube which was spun at 1500 rpm for 5 minutes to form a pellet. The pellet was either re-suspended into more culture vessels or manipulated via steroid or RNA extractions. RNA was extracted using the QIAGEN RNeasy mini kit according to the manufacturer's instructions. Steroids can be extracted from cells and cell media via a number of methods (optimised in chapter 4), the extracted steroids from the cells or cell media were subjected to analysis by LC/MS, LC/MS/MS or GC/MS.

3.3 Procedures relating to culturing of endometrial biopsies

Biopsies were obtained from Singleton Hospital (Swansea NHS Trust) and the blood removed. The tissue was washed a number of times with HBSS and finely minced

using two scalpels, after which 200μL of collagenase and 200μL of DNase type 1 was added. The cells were then placed in the incubator for one hour and were re-suspended every 15 minutes. They were then centrifuged at 400xg for 4 minutes, following this the pellet was re-suspended in media and incubated at 37°C, 24 hours later the stromal cells (attached to dish) and epithelial cells (in suspension) were separated by decanting the media into another cell culture vessel. The epithelial cells were placed in separate cell culture vessels where over time they become attached. The media was again changed periodically as with established cell lines. Stromal cells can be grown and split into larger vessels through the same methods as established cell lines outlined in chapter 3.2. Manipulations or steroid treatments of the biopsies can then proceed followed by RNA and steroid extractions.

3.4 RT-PCR methodologies: RNA extraction, reverse transcription and real-time PCR

RT-PCR was employed to establish expression levels of specific enzymes relating to steroid metabolism these were the steroid converting enzymes; aromatase, 5AR1, 5AR2, 17β-HSD1, 17β-HSD2, 17β-HSD4, 17β-HSD5, 17β-HSD7 and 17β-HSD8. Expression of GADPH (glyceraldehyde-3-phosphate-dehydrogenase) was also recorded in each experiment, and steroid converting enzyme expression was calculated relative to GADPH expression which corrected for any experimental errors. This produced steroid converting enzyme expression values normalised to GADPH for each steroid converting enzyme.

The biopsies or cell lines were grown until confluent and then removed by trypsin-EDTA as a pellet. From these pellets RNA was extracted using the Quigen RNAeasy kit (Qiagen, Crawley, UK following the manufacturer's instructions) and the RNA concentration measured using the Nanodrop ND100 Spectrophotometer. The RNA was diluted into a 10μL solution of 100ng/μL and converted to cDNA using the RETROscript reverse transcription for RT-PCR kit, according to the manufacturer's instructions. The cDNA was then diluted to produce a calibration series of concentrations 20ng/μL, 10ng/μL, 1ng/μL, 0.1ng/μL and 0.01ng/μL (assuming full conversion). A unique genetic sequence for each enzyme was determined and primers were designed which only bind to these specific sequences (described in chapter 3.4.1). 10μL SYBR green supermix, 2.5μL sense and 2.5μL

anti-sense primers (for each enzyme) and 5μL of each cDNA dilution was pipetted into wells on a 96 well real time PCR plate and subjected to QRT-PCR. The fluorescent marker (SYBR green) fluoresces when bound to double strand DNA. The icycler RT-PCR instrument then undergoes a number of cyclic temperature fluctuations which causes double strand DNA (dsDNA) to be produced and denatured until enough dsDNA was present to produce a detectable signal. Through a number of calculations it was then possible to calculate the relative amounts of cDNA present which is related to the concentrations of RNA for specific steroid converting enzymes in the original cells.

Relative expression levels of each steroid converting enzyme in each cell line (and biopsy pathology) were determined. To complete this 100ng/μL of RNA from each of the five cell lines (under basal conditions) was converted to cDNA, combined together and diluted to produce a standard curve. Onto this curve expression of each enzyme under basal conditions was applied, which allowed comparison between different cell lines with significantly different gene expression.

3.4.1 Primer design for specific gene expression detection in cells and biopsies

Primers were designed to bind to specific genetic base sequences of DNA unique to the steroid converting enzyme of interest. The genomic sequence of the gene was calculated from a number of sources including the National Centre for Biotechnology and Information (NCBI, http://www.ncbi.nlm.nih.gov/ database). Sense (forward) and anti-sense (reverse) primers were designed to bind directly to a unique amino-acid sequence of the steroid converting enzyme of interest. These primers were designed using Beacon primer design programme (version 3.0), which calculates primer efficiency and produces efficient primers. Beacon software can be programmed to produce primers that have amplicon lengths of between 75 and 120 base pairs, which produce efficient primer interactions and amplification of the RNA of interest. Primer efficiency was defined by the software as being >85%.

3.5 Mass Spectrometry: Methodology for identification, and detection of a variety of steroid standards using LC/MS, LC/MS/MS and GC/MS

A number of steroid standards were initially analysed by direct infusion into the mass spectrometer in positive mode using an ESI source for LC/MS and LC/MS/MS and

an EI source for GC/MS. This was completed to obtain individual mass spectra and fragmentation patterns (where available) for each steroid. A variety of androgens, oestrogens and progestins were chosen for initial analysis, as they were representative of steroids which could be synthesised in the female body (chapter 1, figure 1.1).

Table 3.1: Structure, molecular weight and nomenclature of nine steroids standards which were studied and considered to be relevant in this study of endometrial tissues.

Name	Molecular weight	Molecular formula	Structure
Testosterone	288	$C_{19}H_{28}O_2$	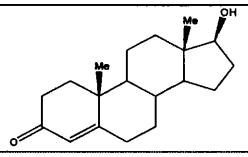
Dihydrotestosterone (DHT)	290	$C_{19}H_{30}O_2$	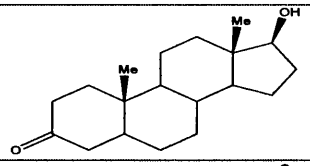
4-Androstene-3,17-dione	286	$C_{19}H_{26}O_2$	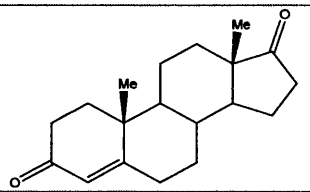
Dehydroepiandrosterone (DHEA)	288	$C_{19}H_{28}O_2$	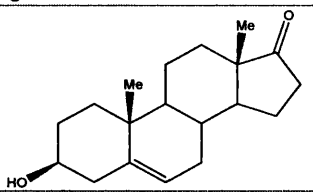
Androsterone	290	$C_{19}H_{30}O_2$	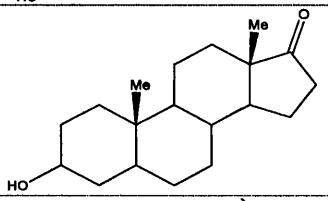
Pregnen-3-ol-20-one	316	$C_{21}H_{32}O_2$	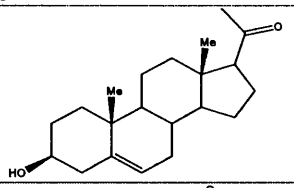
Progesterone	314	$C_{21}H_{30}O_2$	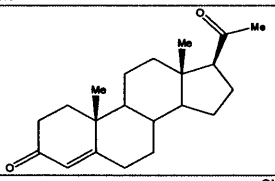
Oestradiol (E2)	272	$C_{18}H_{24}O_2$	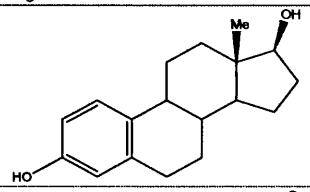
Oestrone (E1)	270	$C_{18}H_{22}O_2$	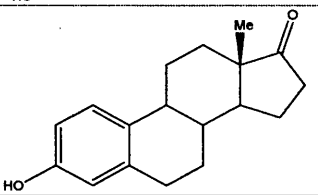

3.6 General set-up of LCQ DECA mass spectrometer

There have been many different liquid chromatography methods developed (column types, solvents) for the detection of steroids from a number of matricies, such as blood, urine, hair,[3] tissues, and cells.[4] The main solvent gradient systems utilised were acetonitrile/water[5,6] and methanol/water,[7,8] chosen because of the solubility of steroids in organic solvents. The main liquid chromatography columns used for androgen and progestin analysis are C_{18} reversed phase columns,[9] however there are many other columns used for LC/MS analysis of steroids such as the 5μ-ultrasphere ODS[10] and the spherisorb column.[11] A number of C_{18} columns were used in these experiments; two Dionex columns, a 25cm x 5μ x 100Å and a 15cm x 3μ x 100 Å also a number of columns were packed under high pressure in the laboratory using a C_{18} slurry.

The steroid standards were initially analysed individually by direct infusion into the mass spectrometer to obtain mass spectra and fragmentation (MS/MS) data. The steroids were dissolved in methanol at concentrations of approx 3μM and infused directly into the LCQ DECA mass spectrometer, in positive mode using an electrospray ionisation source. The major ions such as the $[M+H]^+$ and $[M-H_2O+H]^+$ were then fragmented using collision energies of between 30 and 45eV to obtain MS/MS data allowing any unique fragments of each steroid standard to be identified. The standard operating parameters for the LCQ DECA are described in table 3.2 (below).

Table 3.2: Standard operating parameters for LCQ DECA full scan analysis of steroid standards, using an ESI source in positive mode.

Parameter	Value
General	
Run time	30-120 minutes
Scan events	1.0
Scan event details	Full MS Scan (*m/z* 50-500)
Mobile phases	Methanol Water (each 0.1% acidic additive)
ESI source	
Spray voltage	3.51 kV
Spray current (typ.)	0.58μA
Sheath gas flow rate	29.3
Capillary voltage	15.2 V
Capillary temperature	200 °C
Vacuum	
Ion gauge	2.5×10^{-5} Torr
Ion Optics	
Multipole 1 offset	-5.93 V
Lens voltage	-15.96 V
Multipole 2 offset	-9.59 V
Multipole Rf Amp	400 Vp-p, sp
Entrance lens voltage	-58.7 V
Coarse Trap DC Offset	-10.10 V
Main RF	
Main Rf detected	-0.01 V
RF Detector temperature	38.87 °C
Main RF modulation	0.03 V
Main RF Amplifier	8.26 Vp-p
RF generator temperature	34.1°C
Ion detection system	
Dynode voltage	-14.94 kV
Multiplier voltage	-1125 V

3.7 Additives for improved resolution in liquid chromatography mass spectrometry

Additives were incorporated into the solvents in liquid chromatography systems to improve the resolution of peaks in the chromatograms. The optimum additive for each steroid should produce a high intensity well resolved peak with no peak tailing.[12]

The acidic mobile phase additive required for optimum resolution of steroids was investigated. A mixture of steroids (each 2μM) were injected into the mass spectrometer via a 15cm C_{18} column. The effect of various liquid additives was systematically investigated, these were the acidic additives trifluoroacetic acid, formic acid, acetic acid and propionic acid, which are appropriate for positive mode. Each additive was incorporated into the mobile phase at a concentration of 0.1% (0.1% in methanol and 0.1% in water), a 50/50 methanol/water 0.1% additive solution was also used to prepare the steroid mixtures themselves.

3.8 Procedure for statistical analyses from calibration graphs in both GC/MS and LC/MS using standard reference materials

Experiments with standard reference materials were essential for quantitation of a known steroid in a biological sample, this was conducted via calibration methods. An internal standard is commonly used to improve quantitation statistics, these are usually structurally similar compounds such as deuterated steroids or a steroid derivative.

When completing a calibration series at least six concentrations of each steroid were prepared spanning the concentration range around which the experimental data was estimated to lie within. These results were plotted as a calibration graph of signal (in this case peak area) against concentration (when using an internal standard a ratio of sample peak area/internal standard peak area was used on the y-axis). The internal standard used in these experiments was methyl-testosterone (a testosterone derivative), which was added at the same concentration to each sample (the internal standard was added at a concentration of ~40% of the calibration range). Although this was not ideal (a deuterated analogue of each steroid would be the ideal) methyl-testosterone was useful as it eluted mid-way through the chromatographic run and

was not present in the biological samples. In the absence of deuterated standards methyl-testosterone has been shown to be a good alternative internal standard for steroid analysis.[13] Previous studies have also used other (un-involved) steroids as internal standards, for example Cheng and co-workers used progesterone as the internal standard when studying oestrogens in negative ionisation mode LC/MS.[14]

Linear regression from calibration graphs permitted calculation of the limit of detection and quantitation of each steroid using each instrument. The R^2 value is the coefficient of the linear position of the calibration line, which should be 0.98 or higher for the results to be analytically significant. Regression calculations and accurate quantitative results can only be obtained over the linear region. The same method for quantitative calibration was used in LC/MS and GC/MS.

3.8.1 Calculation of R^2 and limit of detection (LOD)

If a linear relationship was observed between concentration and instrument response (peak area or peak area ratio), the limit of detection can be calculated using the equations below as described by Miller and Miller.[15]

First the standard error of the data series ($S_{y/x}$) was calculated using,

$$S_{y/x} = \left\{ \frac{\sum_i (y_i - \hat{y}_i)^2}{n-2} \right\}^{\frac{1}{2}} \qquad (3.1)$$

where $S_{y/x}$ is the standard error, n is the number of data points and $y_i - \hat{y}_i$ are the y residuals which are related to points on the regression line (calculated using the regression function in Excel 2007).

The limit of detection (LOD) was then calculated as three times the standard error divided by the slope of the linear regression line.

$$\text{L.O.D (concentration)} = \frac{3 \times S_{y/x}}{b} \qquad (3.2)$$

Nine steroid standards were studied to determine the limits of detection for each in each mass spectrometry system (GC/MS and LC/MS). A description of these steroids and their structure is found in table 3.1.

3.8.2 Statistical analysis methods for quantitative calibration by LC/MS

For each steroid standard a minimum of six dilutions (and a blank) were produced ranging from 2μM-10nM. A C_{18} column was prepared by a number of washing steps from 100% water to 100% methanol and subsequently for 20 minutes at the starting gradient. Each dilution for each steroid (plus internal standard) was passed through the column in triplicate (to provide statistical improvement) into the mass spectrometer using methanol/water gradient system (0.1% acetic acid). The results were compiled and calculations concerning R^2 and limit of detection were completed.

3.9 Gas chromatography mass spectrometry for detection of steroids

GC/MS can provide unrivalled chromatographic performance for certain classes of compounds. Steroid analysis by GC/MS is widely utilised, however the majority of procedures involve a derivatisation step. There are limited examples of steroid analysis using GC/MS without derivatisation, due to increased sensitivity and stability upon derivatisation. Derivatisation has been undertaken, in many steroid applications, for example, Leyssens and co-workers used a TMS derivatisation procedure while investigating the illegal use of steroids within the cattle industry.[16]

There were two gas chromatography mass spectrometry systems used in these experiments these were the Fisons GC/MS MD800 and the Agilent 5975C GC/MSD ChemStation linked to a Gerstel auto-sampler. Initial experiments were undertaken prior to derivatisation.

3.9.1 Gas chromatography GC/MS MD800 set-up

Non-derivatised standard steroids of a concentration of 100ng/μL in methanol were prepared, these were then subjected to analysis using the GC/MS MD800 with an electron ionisation (EI) source in positive mode. A range of temperature gradient programmes and settings of the GC were optimised to obtain an intense and well resolved peak for each steroid. Retention times and standard mass spectra for each steroid were obtained. Two columns were used for these investigations a HP-1 dimethylpolysiloxane column and a more specific steroid column a Supelco SLB-5ms silphenylene polymer column. The GC/MS MD800 standard parameters for steroid analysis prior to derivatisation are defined in table 3.3.

Table 3.3: Standard operating parameters for GC/MS MD800 full scan analysis of steroid standards using an EI source in positive mode.

Parameter	Value
General	
Run time	10-20 minutes
Scan events	1.0
Scan event details	Full MS Scan (*m/z* 50-500)
Temperature range (GC oven)	20-300°C
Ionisation mode	Positive
EI source	
Source temperature	200°C
Source current	975 μA
e^- Energy	70 eV
Ion Optics	
Repeller	4.6
Interface temperature	300°C
Detector	
Detector	300
Analyser Pressure	-4 (Vac)
Filament current	4.2 A
Trap current	158 μA

3.9.2 Gas chromatography Agilent GC MSD set-up

The Agilent GC MSD with ChemStation was also used in these experiments. This was a newer instrument than the GC/MS MD800 with a greater variety of injection and auto-sampler systems. These improvements included the capacity of online derivatisation, cooled sample trays and a number of different injection methods such as hot and cold spilt, splitless and on-column injections. Again the steroid standards (100ng/μL) were individually infused into the GC/MSD and a full scan mass spectrum obtained for each. The technique was optimised for detection, and later separation of each of the steroids described in table 3:1.

Table 3.4: Standard operating parameters for GC MSD full scan analysis of steroid standards using an EI source in positive mode.

Parameter	Value
General	
Run time	10-20 minutes
Scan events	1.0
Scan event details	Full MS Scan (*m/z* 50-500)
Temperature range (GC oven)	20-300°C
Ionisation mode	Positive
EI source	
Source temperature	200°C
e^- energy	70 eV
Ion Optics	
Repeller	28.28
Interface temperature	300°C
Detector	
Analyser Pressure	7.67×10^{-6} mbar

3.9.3 Statistical analyses from GC/MS calibration graphs using standard reference materials

The methodology for GC/MS quantitation was similar to that for LC/MS. The samples were made up in methanol and a calibration graph constructed using six different concentrations 20-1μM plus internal standard (and a blank) spanning the region around which the experimental data was expected to lie within. These samples (1μL) were analysed in triplicate. The R^2 value and limit of detection were calculated for each as outlined in chapter 3.8.1.

3.10 Derivatisation of steroids for analysis by GC/MS and LC/MS

Derivatisation agents react with certain functional group(s) to make a substituted molecule which has an improved signal in the mass spectrometer. Derivatisation was applied to;

1. increase (or decrease) volatility of a compound,
2. increase a compound's ionisation efficiency,
3. avoid thermal decomposition of a compound,
4. improve sensitivity and/or,
5. improve chromatographic separation.

In steroid analysis the hydroxyl groups are generally the site of derivatisation. Two derivatisation procedures were investigated utilising the well known reagents, TMS[17] and dansyl chloride.[18]

3.10.1 Trimethyl-silyl (TMS) derivatisation procedure

TMS derivatisation occurs at any hydroxyl groups in the steroid skeleton, through addition of a trimethyl-silyl group (figure 3.1). Some of the steroids within the expected profiles do not have hydroxyl groups, these should not undergo derivatisation, also if multiple hydroxyl groups are present di- or tri-derivatised steroids should be produced.

TMS derivatisation is probably the most widely used derivatisation procedure for GC/MS analysis. The mass shift for a steroid with a hydroxyl group which undergoes TMS derivatisation is +73 mass units for each TMS molecule incorporated into the derivatisation end product. The TMS derivatisation procedure proceeds as follows; the dry steroid extract was obtained and reacted with 30μL of a BSTFA/TMS mixture (Bis(trimethylsilyl)trifluoroacetamide/trimethylchlorosilane) (BSTFA + 1% TMS). The solution was heated at 70°C for 60 minutes and dried under nitrogen before being reconstituted for analysis.[19,20] This procedure was investigated using the steroids testosterone, pregnenolone, oestradiol and oestrone. Solutions of these steroids were prepared at concentrations of 10μM in methanol and dried before derivatisation. The derivatised steroids were reconstituted in methanol and analysed on the GC/MS MD800 using the optimised operating system.

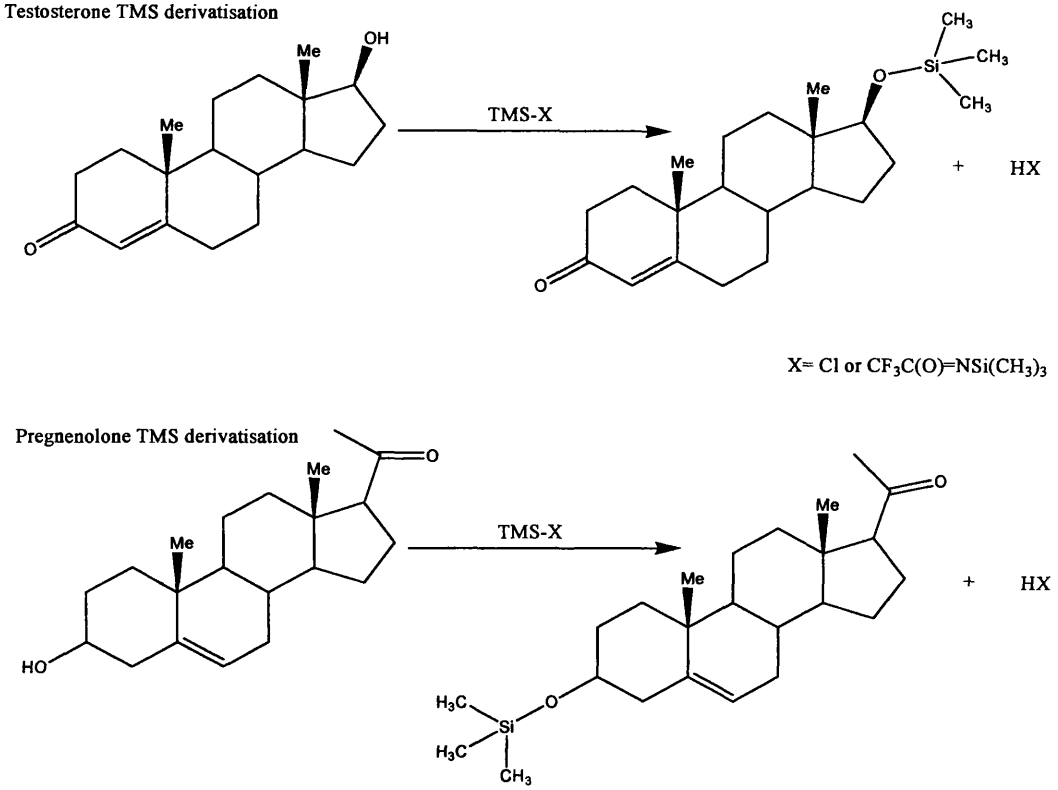

Fig 3.1: Diagram illustrating the TMS derivatisation reactions for testosterone and pregnenolone both products produce a mass shift of +73.

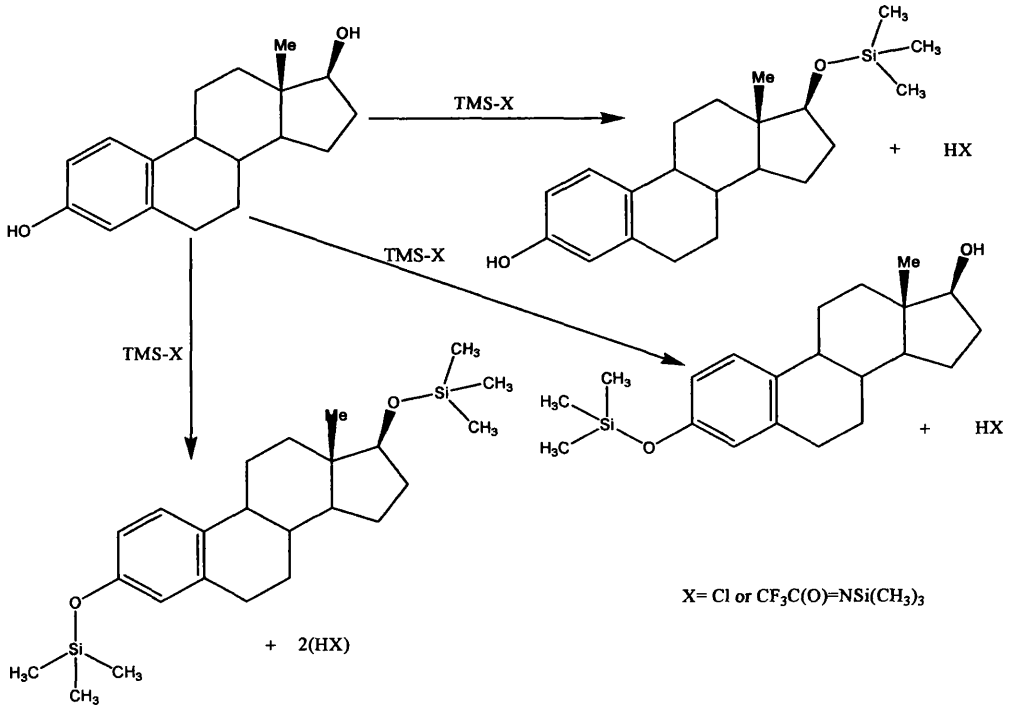

Fig 3.2: Diagram illustrating the TMS derivatisation of oestradiol, two products produce a mass shift of +73, these are mono-derivatised compounds. One product (bottom) has a mass shift of +146 this was the di-derivatised compound.

3.10.2 Dansyl chloride derivatisation procedure

Dansyl chloride derivatisation is another widely used procedure which adds a highly ionisable group to the steroid skeleton. Dansyl chloride derivatises the phenolic hydroxyl group of the steroid skeleton which are unique to oestrogens. Androgens and progestins do not have the required group and should not undergo any derivatisation. Following dansyl chloride derivatisation oestrogens can be readily analysed in positive mode LC/MS.[21] Dansyl chloride derivatisation has also been applied in GC/MS analysis of urinary amphetamines.[22]

To complete dansyl-chloride derivatisation the steroid extract was dissolved in 100µL of 0.1M Na_2CO_3 buffer (pH 10.5) and 100µL of 1.0mg/mL of dansyl chloride in acetone was added. The mixture was vortexed and heated for 3 minutes at 60°C, after which the acetone was evaporated and MTBE (methyl *tert*-butyl ether) was used as an extraction solvent. MTBE was used (at least twice) to extract the steroids from the aqueous into the organic layer, the organic layers were then removed and combined. The organic layer was evaporated to dryness before being reconstituted for LC/MS and GC/MS analysis.[23,24] The mass shift for dansyl-chloride derivatisation was +234. This procedure was investigated using the oestrogens oestrone and oestradiol. The androgen testosterone and progestin pregnenolone were also analysed to ascertain if any derivatisation occurs at their hydroxyl groups.

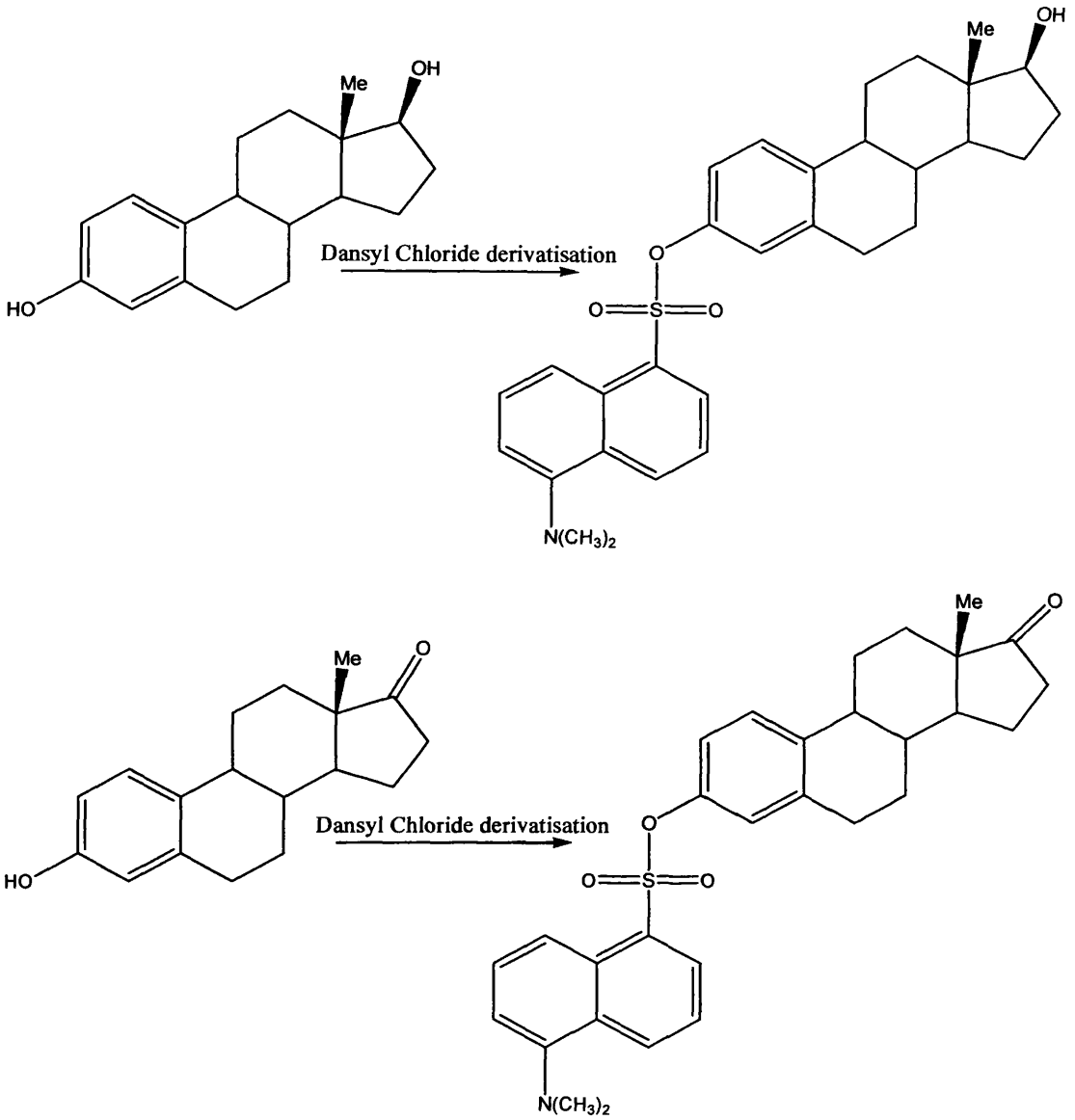

Fig 3.3: Diagram illustrating the dansyl-chloride derivatisation of oestradiol and oestrone. Top diagram illustrates the derivatisation of oestradiol by dansyl chloride. Oestradiol-DC has a mass shift of +234 from the neutral steroid of mass 272 to make a reaction end product of mass 505. Bottom diagram illustrates the derivatisation of oestrone by dansyl chloride. Oestrone-DC has a mass shift of +234 from the neutral steroid of mass 272 to make a reaction end product of mass 503.

3.11 Separation of a mixture of steroids by GC/MS and LC/MS

A mixture of steroids was impossible to analyse using mass spectrometry alone due to their isobaric nature (similar molecular weights and fragmentation patterns), therefore prior chromatographic separation was an essential requirement. There were two separation techniques investigated here, high-performance liquid chromatography (HPLC or LC) and gas chromatography (GC), described previously.

Both GC and HPLC systems can be directly linked to the mass spectrometer thereby combining chemical separation with mass analysis. When optimised these techniques permit excellent detection, resolution and separation of a mixture of steroids.

Separation of a mixture of steroids by chromatography allows another method for identification of steroids-retention time. Positive identification of a steroid in real sample will have identical mass spectra, fragmentation data and a corresponding retention time to that of the steroid standard. Both GC/MS and LC/MS standard steroid separation techniques were optimised, (reported in chapter four, part 1), these techniques were later applied to biological samples. Confidence in the results was further improved by validation of the mass spectrometry methods providing information about the reproducibility of the technique in terms of retention time and instrument response (peak area) (determined in chapter 4.4).

The steroids standards were combined for optimisation of separation procedures. This was completed using LC/MS by changing the mixture of organic and aqueous mobile phases to sequentially elute steroids from an analytical column. Optimisation of the separation of steroid standards was completed using GC/MS by changing the temperature of the column which causes the steroids to sequentially enter the mass spectrometer.

3.12 Steroid extractions

A wide range of steroid extraction procedures from a number of different matrices have been developed. These range from simple liquid-liquid extractions to multiple stage solid phase extractions depending on the matrix from which the steroids are extracted and the type of steroid under investigation.[25] An experiment to determine the solubility of steroids in different mixtures of methanol and water was described also described were a series of simple extraction techniques which were further developed and optimised in chapter four, part 2.

3.12.1 Solubility of steroids in methanol and water

Techniques such as LC/MS and GC/MS require the steroid solutions to be prepared in solvents and results may differ due to the solubility of that steroid in each solvent.

Therefore the solubility of a steroid in the solvent of interest was important, if a steroid was insoluble in that solvent then the experiment cannot proceed, also if the steroid crystallises in the solution the concentration of dissolved steroid will be reduced. In these experiments methanol and water were used as the primary solvents, an experiment was designed to determine the optimum procedure for steroid analysis using these solvents.

1μM solutions of testosterone and pregnenolone were dissolved in methanol, this was then split into three samples and evaporated to dryness under nitrogen. The samples were then dissolved in water, methanol and 50/50 methanol/water, respectively. Following this the solutions were filtered to remove any particulates, transferred to a clean glass 2mL vial and evaporated to dryness. The samples were then dissolved into a 50/50 methanol/water (0.1% acetic acid) solution and analysed by LC/MS (outlined in figure 3.4). The peak areas (proportional to concentration) of each steroid was directly compared for each sample (methanol, methanol/water 50/50 and water) and so the solubility of the steroids in each of the three conditions was calculated. This provides valuable information concerning the solubility of each steroid in water and so in the cell culture media which was mainly water.

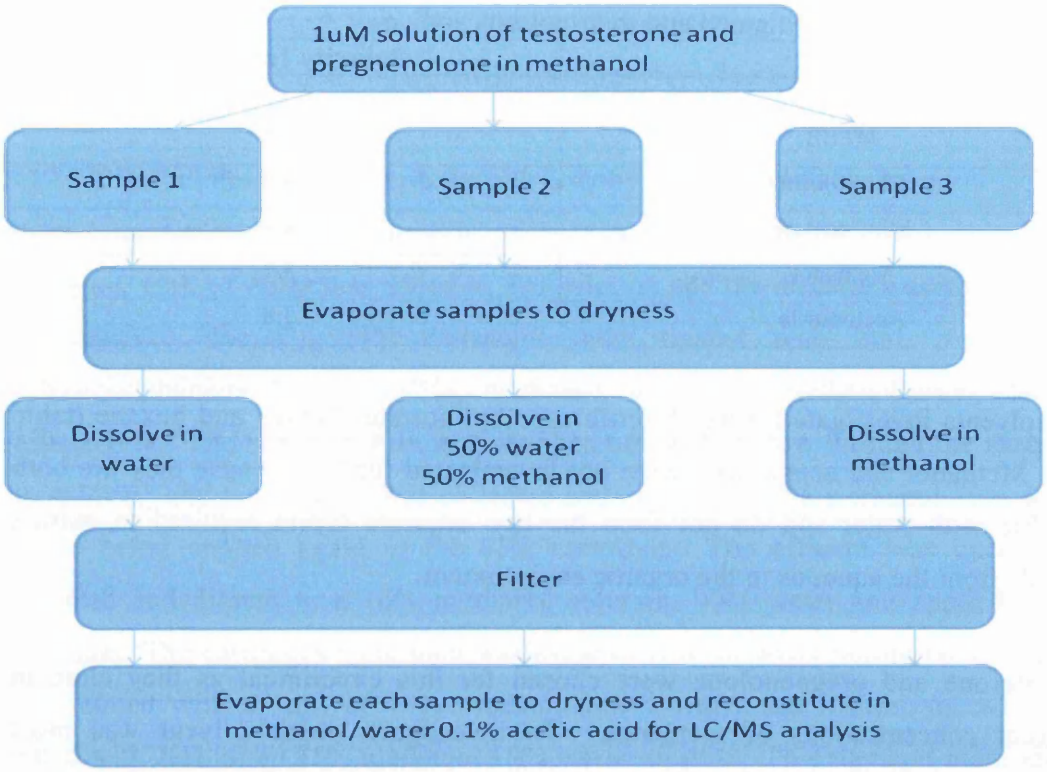

Fig 3.4: Flow chart illustrating the method for determination of the solubility of testosterone and pregnenolone in methanol, water and a 50/50 mixture of methanol and water.

3.12.2 Simple liquid-liquid extractions of steroids

Steroids are extracted from simple matrices such as water by organic/aqueous liquid-liquid extractions using an organic solvent. A difference in the polarity between the two phases causes the steroids in an aqueous environment to readily move to the organic environment.

3.12.3 Determination of the ideal solvent for liquid-liquid extraction of steroid standards

The optimum solvent(s) for steroid extractions were calculated by investigating a number of solvents of differing polarities. Solvents are given a polarity index (PI) value of between 0 and 10, 10 being the most polar and 0 being non-polar. Water is polar and has a PI of 9.5, hexane is non-polar with a PI of 0. The larger the difference in polarity between the two phases the more readily the steroids move from the aqueous to the organic environment.

Table 3.5: Solvents investigated and their polarity indices.

Solvent	Polarity Index (PI)
Hexane	0
MTBE	2.2
Chloroform	4.0
Ethyl acetate	4.4
Methanol	5.1
Acetonitrile	5.8

The solvents investigated were chloroform, ethyl acetate, MTBE and hexane (table 3.5). Methanol and acetonitrile were not investigated further because they are both miscible with water and do not form the two separate layers required to extract steroids from the aqueous to the organic environment.

Testosterone and pregnenolone were chosen for this experiment as they elute in different concentrations of methanol. To investigate which solvent was most effective for steroid extractions 1mg of testosterone and 1mg of pregnenolone were dissolved in 40mL of water. This solution was extracted by a number of simple liquid-liquid extractions. 200μL aliquots of the steroid solution were decanted and 500μL of the solvent under investigation was added and vortexed after which the organic layer was removed, and the extraction repeated. The organic layers were combined and evaporated to dryness, these were then reconstituted in 50/50 methanol/water (0.1% acetic acid) and analysed by LC/MS.

3.13 Solid Phase Extractions (SPE) of steroids

Solid phase extractions using C_{18} solid phase extraction cartridges 100mg (Varian, Yarnton, UK) were investigated. The Varian solid phase extraction cartridges used in these experiments were essentially mini LC reverse-phase C_{18} columns. Steroids were retained on the C_{18} columns due to non-polar and Van Der Waals interactions.[26] Steroids were subsequently eluted from the column with an organic solvent such as methanol.[27,28,29] Optimisation and validation of these SPE methods is defined further in chapter 4, part 2.

SPE is essential for steroid removal from aqueous based complex liquids such as plasma, urine or cell media as it removes interfering substances such as proteins and

FCS which hinder simple liquid-liquid extractions. SPE also overcomes any phase separation problems producing a steroid fraction with a high percentage recovery.

3.13.1 Trial method for solid phase extractions with steroid standards

Steroid solutions of a concentration of 1μM were made up in a 1mL solution of methanol, 1mL of water was added to this solution and the mixture was vortexed for 5 minutes. The C_{18} SPE cartridges were treated with 2mL volumes of dichloromethane/methanol (50/50), methanol, water and methanol/water (50/50), respectively. The steroid solutions were then allowed to flow through the cartridge (0.5ml/min) and the effluent was collected and diluted to 30% methanol 70% water, before being applied again to the SPE cartridge. The effluent was once again collected and diluted to a 10% methanol solution, 90% water and applied to the cartridge. The cartridges were then washed with 2mL of water before polar steroids were eluted with a 2mL of 40% methanol, 60% water and neutral steroids were eluted with 2mL of an 85% methanol 15% water solution. This standard method was efficient for simple liquids such as water, however it was adapted for complex matrices such as cells and cell media.

3.13.2 Solid phase extractions of steroids from established cell lines

The method for SPE of steroids from cells proceeds as follows. Cell pellets were collected for analysis with all cell media removed, and they were suspended in 5mL of ethanol, and heated for 5 minutes at 64°C, the solution was next centrifuged and diluted to a 50% ethanol solution by addition of 5mL of water. The C_{18} Varian cartridge was treated with 2mL of dichloromethane/methanol (50/50), 2mL methanol and 2mL of ethanol/water (50/50) respectively. The cell solution was then passed through the cartridge at a rate of 0.5mL/min. The effluent was collected and diluted to a 30% ethanol solution by addition of water and re-applied to the cartridge. The effluent was again collected diluted to a 10% ethanol solution and again allowed to flow through the cartridge. After a 2mL water wash the steroids were eluted with 2mL of 40% methanol solution followed by 2mL of 85% methanol solution prior to being evaporated to dryness and reconstituted for mass spectrometric analysis.

3.13.3 Solid phase extractions from cell media

SPE of steroids from cell media proceeds as follows. The SPE cartridges were prepared by washing with 2mL dichloromethane/methanol (50/50), 2mL methanol and 2mL of water. 10mL of media was separated from the cells and heated with 2mL of 2M triethylamine sulphate at 64°C for 5 minutes, the media solution was then passed through the SPE cartridge (0.5mL/min) and the effluent discarded. The cartridge was washed with 2mL of water before the steroids were eluted with a 40% methanol (60% water) solution followed by an 85% methanol (15% water) solution. These solutions were then evaporated under nitrogen and reconstituted in 200µL of methanol/water 50/50 0.1% acetic acid ready for LC/MS analysis or 200µL of 100% methanol for GC/MS analysis. This procedure was adapted and optimised through changes in elution solvents to achieve efficient steroid extraction.

To optimise steroid extraction from C_{18} SPE cartridges, the 85% methanol wash step was investigated using the elution solvents methanol, 2-butanol and ethyl-acetate as outlined in the flow chart below (figure 3.5). The steroids investigated were DHEA, androsterone, DHT, oestrone, androstenedione, oestradiol, pregnenolone, testosterone and progesterone which were prepared in a water solution (representative of cell media) at a concentration of 1µM. The control (100%) sample was a steroid sample prepared in methanol and analysed directly by mass spectrometry (no sample loss due to experimental procedures).

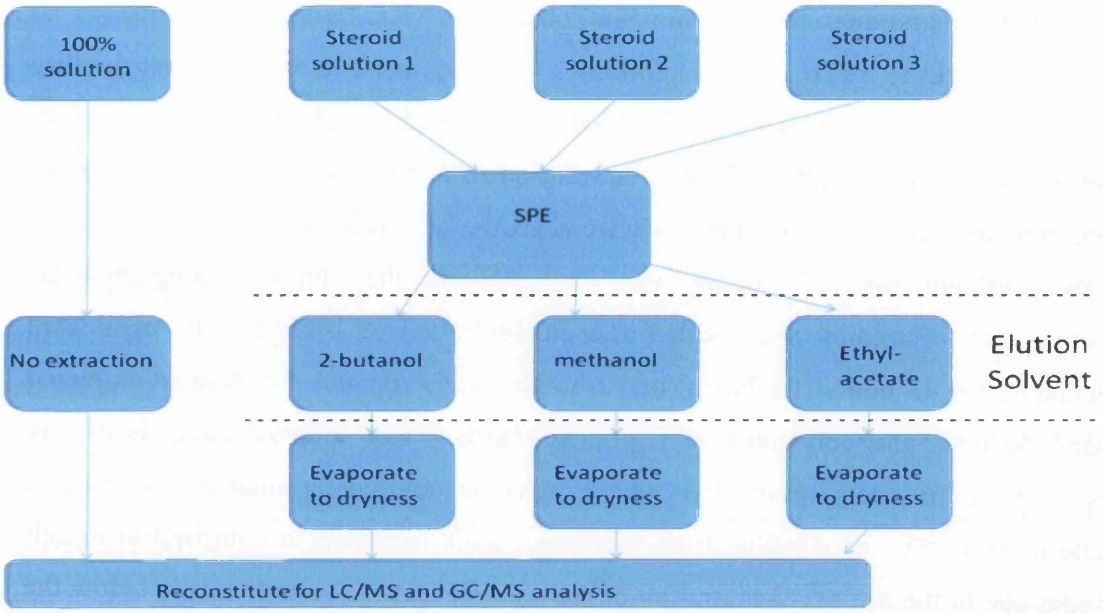

Fig 3.5: Flow chart illustrating the method for determination of the optimum solvent for steroid extractions from SPE cartridges. Steroid solutions 1, 2 and 3 and the 100% steroid solution all contain 1μM solutions of DHEA, androsterone, DHT, oestrone, androstenedione, oestradiol, pregnenolone, testosterone and progesterone. Elution solvents were 2-butanol, methanol and ethyl-acetate.

Following determination of optimum extraction solvent two 10mL samples of cell media (one containing foetal calf serum) were spiked with steroids (androsterone, testosterone, DHEA, DHT, oestrone, oestradiol, androstenedione, methyl-testosterone, pregnenolone and progesterone) each at a concentration of 50nM (in 10mL of cell media). These steroids were then extracted to investigate the effect the cell media and media constituents have on the efficiency of the SPE extraction procedure.

3.14 Method for steroid treatments of cell lines and biopsies

Following optimisation of mass spectrometry and steroid extractions methods steroid treatments of cell lines and biopsies can be completed. Initially each cell line was grown until 80% confluent in a 25mL flask, after this the media was changed and the cells incubated for 48 hours, the media was then removed and any steroids extracted, which permitted determination of the basal steroid profile. Following this treatments with a steroid from each of the steroid groups under investigation were completed, a progestin-pregnenolone, an androgen-testosterone, and an oestrogen-oestradiol.

Initially pregnenolone, testosterone and oestradiol were added (individually) to 20mL of media to make 100nM solutions as a dried solid, however after solubility experiments outlined in chapter 3.12 (and optimised in chapters 4.11 and 5.8) steroids were subsequently added as a solution in a minimal volume of methanol. The cell lines Ishikawa and HEC-1B were grown as outlined in chapter 3.2, once 80% confluent the cell media was changed and the steroids (pregnenolone, testosterone, oestradiol) were added at a concentration of 100nM. The cells were incubated for 48 hours (Ishikawa) or 72 hours (HEC-1B) and the steroids extracted from the cells and cell media by optimised SPE. This allowed analysis of any metabolism products from the added steroids and determination of further experiments. Steroid profiles from cells were uninformative in comparison to cell media due to the lower concentration of steroids present in the cells (some below the instrument limit of detection). This was advantageous as cells and cell media from the same time point can be analysed in parallel to produce a picture of both enzyme expression information and steroid profiles.

As a result of these initial experiments testosterone treatments were extended, the Ishikawa and COV434 cell lines were split into eight 75cm^2 flasks and grown until 80% confluent. The media was removed and 20mL of fresh media was added with the addition of testosterone to make 100nM solutions. After which every 8 hours for 48 hours (and at 72 hours) the cell media was removed and any steroids were extracted (optimised C_{18}). 72 hours was chosen as the treatment time for a number of reasons;

1. after 72 hours the majority of testosterone was metabolised to other steroids by each cell line,
2. at 72 hours the majority of nutrients provided by the cell media were used,
3. due to reduced nutrients the cells may become stressed which could alter steroid metabolism after 72 hours and,
4. at 72 hours the cells were 100% confluent, after this time the cells become overpopulated, possibly causing mutations and growth of multiple layers.

At each 8 hour time point the cell pellets were also removed, RNA extracted and converted to cDNA, following this real time analysis was performed to calculate steroid converting enzyme expression providing information on any temporal changes in enzyme expression over 72 hours after testosterone treatments relative to

basal conditions. (chapter 6). The other three cell lines HEC-1A, HEC-1B and RL95-2 were analysed through a similar method with steroid and RNA extractions at every 12 hours over a 72 hour period.

After mass spectrometry analysis it was possible to combine the steroid profiles from each time point and produce a picture of testosterone metabolism in each cell line, or endometrial biopsy. This allows comparisons of testosterone metabolism bio-pathways in all cell types under investigation.

3.14.1 Testosterone treatment of biopsies

Biopsy samples were separated into epithelial and stromal components. Due to the time taken to reach confluency only 4 time points were analysed for each biopsy sample these were 0, 24, 48 and 72 hours. These times were chosen as they were comparable to time points produced with the established cell lines. The biopsy samples were split into four $75cm^2$ flasks (stromal cells) or four 10cm diameter petri dishes (epithelial cells) and treated with a 100nM solution of testosterone, the steroids were extracted from the cell media via the previously optimised SPE procedure and RNA was extracted at each time point.

Together the mass spectrometry and enzyme expression profiles produced at basal level and after testosterone treatment provides important, novel information about steroid metabolism in the endometrium and its disorders. The combination of mass spectrometry and enzyme expression information will highlight any relationships between specific steroid concentrations and specific enzyme expression. This will emphasize steroids or enzymes which can be targeted for development of novel treatments for steroid responsive endometrial disorders.

3.15 References Chapter Three

[1] Way DL, Grosso DS, Davis JR, Surwit EA, Christian CD. In Vitro **19** (1983) 147-153
[2] Albitar L, Pickett G, Morgan M, Davies S, Leslie KK. Gynecologic Oncology **106** (2007) 52-64
[3] Choi M H, Chung B C. The Analyst **124** (1999) 1297-1300
[4] al-Alousi ML, Anderson R A. Steroids **67** (2002) 269-275
[5] Zhao M, Baker S D, Yan X, Zhao Y, W W Wright, B R Zirkin J P Jarow Steroids **69** (2004)721-726
[6] López de Alda M J, Barceló D. J of chrom A **892** (2000) 391-406
[7] Rose J, Holbech H, Lindholst C, Nørum U, Povlsen A, Korsgaard B, Bjerregaard P. Comparative Biochemistry and Physiology Part C **131** (2002) 531-539
[8] Chang Y-C, Li C-M, Li L-A, Jong S-B, Liao P-C, Chang L W. The Analyst **128** (2003) 363-368
[9] Buiarelli F, Coccioli F, Merolle M, Neri B, Terracciano A. Analtica Chimica Acta **526** (2004) 113-120
[10] Corbin C.J., Trant J M, Conley A J. Molecular and Cellular Endocrinology **172** (2001) 115-124
[11] Blom M J, Wassink M G, Kloosterboer H J, Ederveen A G H, Lambert J G D,. Goos H J TH. Drug metabolism and disposition **29** (2000) 76-81
[12] Sigma Aldrich Analytic Lab Info. Eluent Additives for LC/MS. Viewed online 10th November 2006.
[13] Magnisali P, Dracopoulou M, Mataragas M, Dacou-Voutetakis A, Moutsatsou P. Journal of Chromatography A. **1206** (2008) 166-177
[14] Cheng C, Tsai H-R. Anal Chim Acta **623** (2008) 168-177
[15] Miller JC, Miller JN. Statistics for analytical chemistry 2nd Edition (1992) Chapter 5 Pub Ellis Horwood.
[16] Leyssens, Royackers and Willems-Instituut GC/MS Varian Application note number 33
[17] Gomes RL, Avcioglu E, Scrimshaw M D, Lester J N. Trends in Analytical Chemistry **23** (2004) 737-744
[18] Anari M R, Bakhttiar R, Zhu B, Huskey S, Franklin R B, Evans D C. Anal chem. **74** (2002) 4136-4144.
[19] Nagaoka M, Numazawa M. Steroids **70** (2005) 831-839
[20] Diaz-Cruz MS, Lopez de Alda MJ, Lopez R, Barcelo D. J MS **38** (2003) 917-923
[21] Lin Y-H, Chen C-Y, Wang G-S. Rapid Comm in Mass Spec **21** (2008) 1973-1983
[22] Hideyuk Y, Ayako Y, Kazuta O, Sachiko I. Japanese Journal of Forensic Toxicology **17** (1999) 150-151.
[23] Xu L, Spink D C Anal Biochem. **375** (2008) 105-114.
[24] Bartzatt R. J Biochem and Biophys Methods. **47** (2001) 189-195
[25] Antignac J-P, Brosseaud A, Gaudin-Hirret I, André F, Le Bizec B. Steroids **70** (2005) 205-216
[26] Supleco Bulletin 910. Guide to solid phase extraction (1998)
[27] Zhang J, Akwa Y, El-Etr M, Baulieu E-E, Sjövall J. Biochem J. **322** (1997) 175-184
[28] Liere P, Pianos A, Eychenne B, Cambourg A, Liu S, Griffiths W J, Schumacher M, Sjövall J, Baulieu E-E. J Lipid Research **45** (2004) 2287-2302.
[29] Liu S, Griffiths W J, and Sjövall J. Anal Chem **75** (2003) 791-797.

Chapter four

Optimisation of analytical procedures for the detection and extraction of steroids

4.0 Introduction

This chapter presents the optimisation of mass spectrometry methods for the identification of steroid profiles (part one) and optimisation of steroid extraction methods from biological samples (part two).

4.0.1 Chapter 4 Part One: Optimisation and Validation of Mass Spectrometry Methods

The first part of this chapter details the optimisation of both gas and liquid chromatography linked to mass spectrometry techniques for detection of a number of steroid standards. Calibration data is included to determine which technique provides the lowest limit of detection for each steroid and to quantify steroids in biological samples.

Statistics concerning the reproducibility of the mass spectrometry techniques are presented in this chapter, providing information about confidence in the results. Also investigated and compared were a number of derivatisation procedures which act to improve the sensitivity of mass detection for certain steroids.

4.0.2 Chapter 4 Part Two: Extraction of steroids from biological samples

After steroid analysis methods were developed and optimised the extraction of steroids from biological samples was investigated.

Optimisation and validation of steroid extraction procedures (liquid-liquid and solid phase extraction SPE) was completed. This data allows determination of the most effective steroid extraction method(s) from solutions of steroid standards and biological samples.

Part One: Detection and separation of steroid standards by mass spectrometry

4.1 Optimisation of liquid chromatography mass spectrometry for detection of steroids; solvents, mobile phase additives, and quantitative calibrations

A Dionex/LC Packings HPLC system fitted with a C_{18} column was linked to the LCQ DECA XP Plus mass spectrometer. A number of different C_{18} column lengths were investigated (chapter 2 table 2.7). Various solvents, gradient systems, trap columns, mobile phase additives, injection volumes and ionisation methods were investigated to optimise the chromatographic resolution, separation and detection of each steroid defined in table 3.1.

4.1.1 Steroid analysis by LC/MS

The steroids were infused directly into the mass spectrometer in positive mode with an electrospray ionisation source and full scan mass spectra obtained over an m/z ratio range of 50-500 Da. Each steroid protonated molecular ion $[M+H]^+$ if present, was then fragmented at a collision energy >30eV to obtain fragmentation data. The major ions produced were subsequently fragmented at similar collision energies to produce further fragmentation information.

4.1.2 Androgen mass spectra and fragmentation data in LC/MS and MS/MS

All androgens (ESI source in positive mode) produced spectra with $[M+H]^+$ clearly visible and abundant. Fragmentation information was subsequently obtained in LC/MS/MS mode. For all the androgens analysed (table 4.1) an initial neutral loss of 18 mass units was observed due to a loss of water from the steroid, a subsequent second water molecule was lost from all the androgens following the first. Structurally characteristic fragments were noted to help aid steroid determination in biological samples (table 4.1). All androgen mass spectra were comparable to database steroid mass spectra.[1]

Table 4.1: LC/MS/MS fragmentation data of androgens analysed on the LCQ DECA mass spectrometer with an ESI source in positive mode.

Steroid	m/z	Assignment
Testosterone	289	$[M+H]^+$
	271	$[M+H]^+$-H_2O
	253	$[M+H]^+$-$2H_2O$
	169	Fragment
17α-methyl testosterone	303	$[M+H]^+$
	285	$[M+H]^+$-H_2O
	267	$[M+H]^+$-$2H_2O$
	211	Fragment
DHEA	289	$[M+H]^+$
	271	$[M+H]^+$-H_2O
	253	$[M+H]^+$-$2H_2O$
	223, 148	Fragments
Androsterone	291	$[M+H]^+$
	273	$[M+H]^+$-H_2O
	255	$[M+H]^+$-$2H_2O$
	199	Fragment
4-Androstene-3,17-dione	287	$[M+H]^+$
	269	$[M+H]^+$-H_2O
	251	$[M+H]^+$-$2H_2O$
Androstane 3,17-diol	293	$[M+H]^+$ not present
	275	$[M+H]^+$ -H_2O
	257	$[M+H]^+$ -$2H_2O$
DHT	291	$[M+H]^+$
	273	$[M+H]^+$-H_2O

4.1.3 Progestin mass spectra and fragmentation data in LC/MS and LC/MS/MS

Progesterone and pregnenolone both demonstrated abundant protonated molecular ion $[M+H]^+$ peaks when analysed by LC/MS using an ESI source in positive mode. The results were similar to those produced by androgens, with two neutral losses of H_2O observed in MS/MS mode. Fragmentation data was recorded in table 4.2.

Table 4.2: LC/MS/MS fragmentation data of progestins analysed on the LCQ DECA mass spectrometer with an ESI source in positive mode.

Steroid	m/z	Assignment
Progesterone	315	$[M+H]^+$
	297	$[M+H]^+$ -H_2O
	279	$[M+H]^+$ -$2H_2O$
	255, 239,215	Fragments
Pregnenolone	317	$[M+H]^+$
	299	$[M+H]^+$ -H_2O
	281	$[M+H]^+$ -$2H_2O$
	180	Fragment

4.1.4 Mass spectra and fragmentation data of oestrogens in LC/MS and LC/MS/MS

The protonated molecular species $[M+H]^+$ for oestrogens were less abundant than those produced from androgen or progestin analysis (for the same concentration of steroid). Some weak fragmentation patterns were observed table 4.3, again as with the androgen and progestin series an initial loss of water was observed in MS/MS mode. A subsequent water loss was seen with oestriol, but with oestradiol and oestrone the $-2H_2O$ signals were not present possible due to a lack of sensitivity for oestrogens in the mass spectrometer. A more sensitive technique was required for oestrogen analysis such as GC/MS analysis, or negative mode ionisation LC/MS,[2] or adoption of a derivatisation procedure.

Table 4.3: Fragmentation data LC/MS/MS of oestrogens analysed on the LCQ DECA mass spectrometer with an ESI source in positive mode.

Steroid	m/z	Assignment
Oestradiol	273	$[M+H]^+$
	255	$[M+H]^+ -H_2O$
	158	Fragment
Oestriol	289	$[M+H]^+$
	271	$[M+H]^+ -H_2O$
	253	$[M+H]^+ -2H_2O$
Oestrone	271	$[M+H]^+$
	253	$[M+H]^+ -H_2O$
	197	Fragment

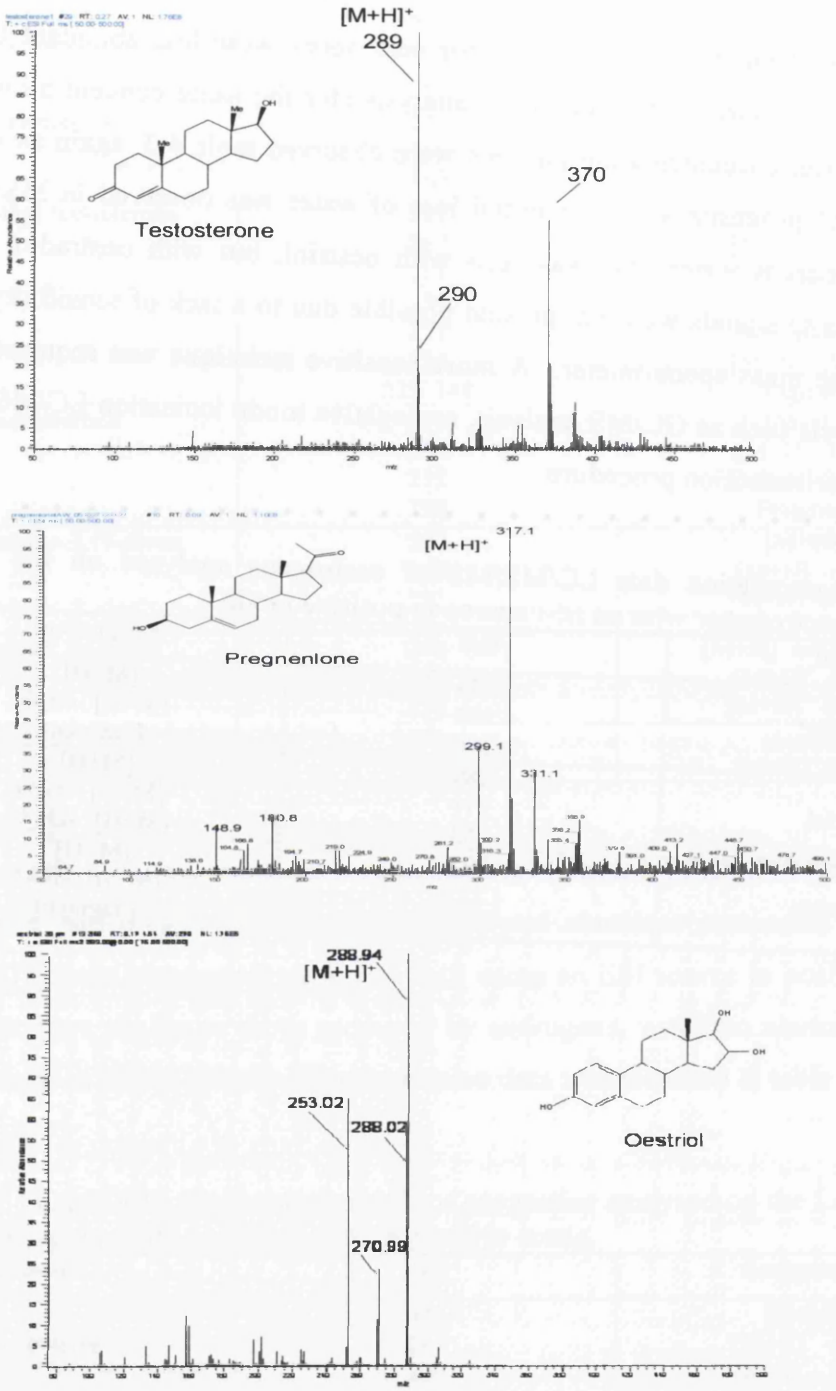

Fig 4.1: Mass spectra of a standard androgen top (testosterone), progestin middle (pregnenolone) and an oestrogen bottom (oestriol). Samples were analysed using the LCQ DECA mass spectrometer with an ESI source in positive mode by direct infusion using 3μM solutions in 50/50 methanol/water (0.1% formic acid).

4.2 Separation of steroid standards by LC/MS

For optimum separation the steroids should be fully resolved (well separated no peak overlap), and have clear mass spectra containing abundant signals for the molecular ions $[M+H]^+$ in ESI positive mode. A number of different gradient systems of methanol and water were investigated to obtain an optimised steroid separation.

A mixture of androgens, oestrogens and progestins were prepared in 50/50 methanol/water and a number of methanol/water gradient programmes were analysed to determine optimum separation and resolution. The elution order of steroids was determined by running each steroid standard separately, using the same gradient system, and comparing this to the chromatogram produced from the mixture of steroids. The optimised separation was method 4 in the table below which was a summation of a number of method development steps.

Table 4.4: Method development steps for optimisation of separation of a mixture of steroid standards by LC/MS with an ESI source in positive mode using a methanol/water gradient system with 0.1% acetic acid.

Method	Starting concentration % methanol	Time (min)	Concentration % methanol	Time (min)	Finishing concentration % methanol	Time (min)
1	70	10	80	55	100	60
2	70	10	90	55	100	60
3	50	10	75	55	100	70
4	70	10	-	-	100	70

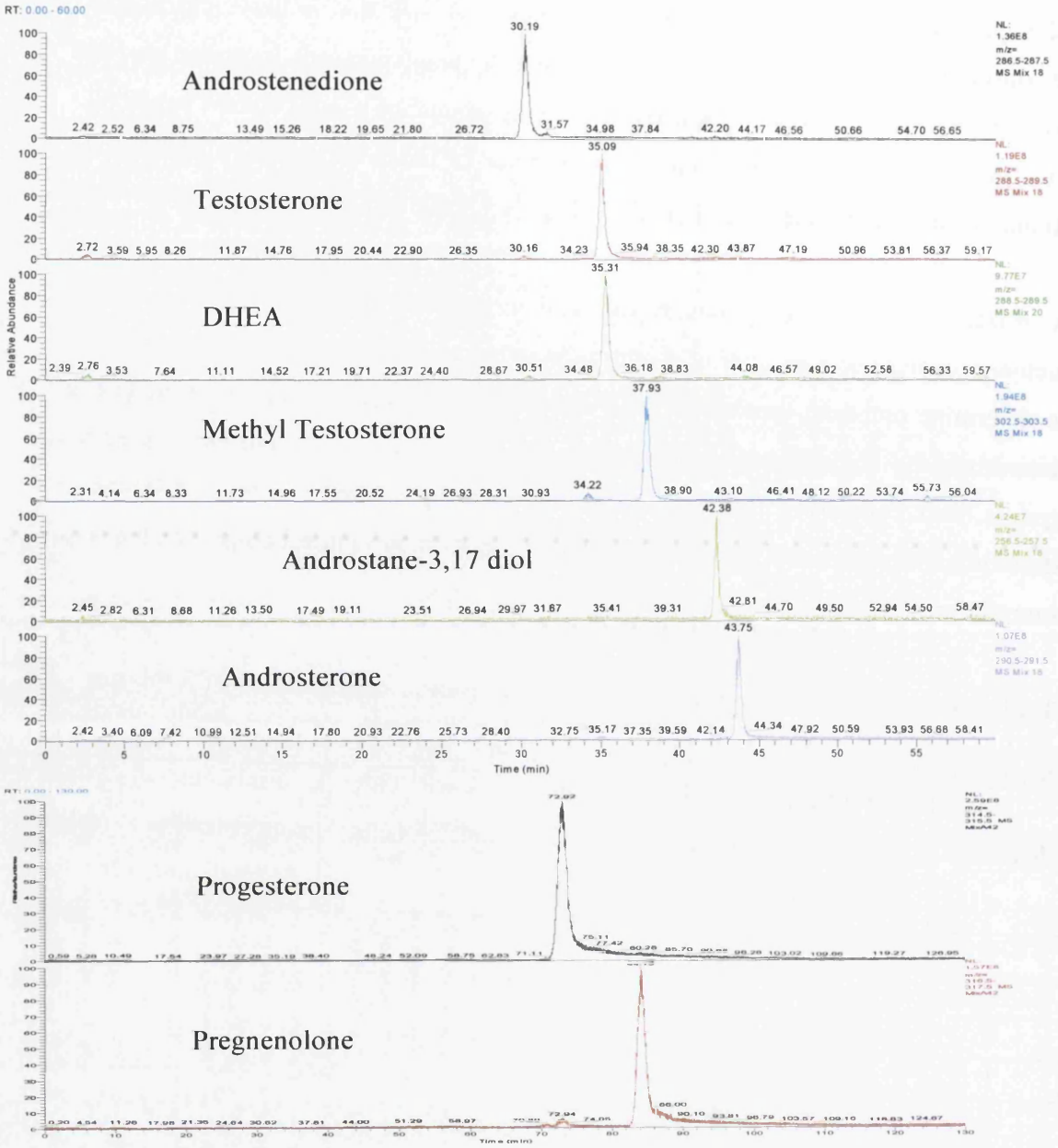

Fig 4.2: Optimised separation of eight steroids on the LCQ DECA mass spectrometer via a C_{18} column with an ESI source in positive mode using a methanol/water 0.1% acetic acid gradient system. Selected ion chromatograms of androstenedione, testosterone, DHEA, methyl-testosterone, androstane-3,17diol, androsterone, progesterone and pregnenolone selected molecular ions $[M+H]^+$ were m/z 287, 289, 289, 303, 257, 291, 315, and 317 respectively.

Figure 4.2 illustrates the optimised separation of androgens and progestins using a methanol/water elution system on a 25cm Dionex C_{18} column. This optimised separation system was transferred to biological samples, allowing positive identification of steroids through retention time and mass spectra comparisons.

Steroids which co-elute (same retention time) can be distinguished on the basis of their mass spectra and fragmentation patterns, although quantitation is not possible for co-eluting peaks and so a technique which separates these compounds is required for quantitation. Oestrogen separations were not shown here due to the lack of sensitivity in this LC/MS procedure.

4.3 Effect of mobile phase additives on resolution of steroid peaks

Additives were incorporated into the LC/MS solvents to aid ionisation, improve sensitivity and reduce peak tailing by altering the pH of the mobile phase.[3] The optimum additive for each steroid will produce high intensity well resolved peaks. The choice of additive depends on the ionisation source (ESI, APCI or CI) and the compound of interest. There are three types of mobile phase additives;

1. acids- aid detection of compounds mainly in positive mode,
2. salts- aid detection of compounds in both positive and negative mode,
3. bases- aid detection of compounds in mainly negative mode.[4]

4.3.1 Optimum additives

A number of acidic mobile phase additives (formic, acetic and trifluoroacetic acid) were investigated to improve the resolution of the androgens and progestins in LC/MS with an ESI source in positive mode. These were added to both mobile phases and all samples at a concentration of 0.1%.

Table 4.5: Acidic additives producing optimum resolution and signal intensity for a series of steroids. The percentage of each acid additive was 0.1% in all solvents and steroid solvent solutions.

Name	Optimum additive
Androstenedione	Formic acid
Testosterone	Trifluoroacetic acid
DHEA	Acetic acid
DHT	Acetic acid
Androsterone	Acetic acid
Progesterone	Formic acid
Pregnenolone	Formic acid

It was concluded that acetic acid was the overall optimum additive, as it increased resolution and signal intensity for the majority of steroids. Subsequently acetic acid

was added to mobile phase solvents and samples at a concentration of 0.1% for all positive mode LC/MS analyses. Chang and co-workers studied steroid analysis using a methanol/water elution system and concluded that the additives formic or acetic acid produce optimum responses for androgen analysis, agreeing with the work outlined above.[5]

4.4 Optimum separation by GC/MS

As stated in chapter 3 (section 3.9) and in the literature most GC/MS steroid analysis has occurred after derivatisation.[6] However, initial experiments here were undertaken without derivatisation.

4.4.1 GC/MS MD800 analysis of steroid standards

Different column temperatures were investigated (table 4.12) and an optimum procedure established to obtain high resolution peaks.

The molecular ion $[M]^{+\cdot}$ for androgens and oestrogens were abundant when analysed by GC/MS (figure 4.3). The $[M]^{+\cdot}$ molecular ions of the progestin series were less abundant, however the chromatographic peak representative of progesterone and pregnenolone were still clearly visible in the total ion chromatograms. The molecular ion indicative of cholesterol was also abundant in GC/MS analysis ($[M]^{+}$ observed at m/z 386). Following this the steroids were combined and a temperature gradient system was developed to determine the optimum separation conditions for steroids using the GC/MS MD800.

Table 4.6: Major ions present for a series of androgens using the GC/MS MD800 with an electron ionisation source (EI) in positive mode.

Steroid	m/z	Rationalisation
Testosterone	288	$[M]^{+\cdot}$
DHT	290	$[M]^{+\cdot}$
17α-methyl testosterone	302	$[M]^{+\cdot}$
DHEA	288	$[M]^{+\cdot}$
Androsterone	290	$[M]^{+\cdot}$
4-Androstene-3,17-dione	286	$[M]^{+\cdot}$

Table 4.7: Major ions present for progestins and cholesterol using the GC/MS MD800 with an electron ionisation source (EI) in positive mode.

Steroid	m/z	Rationalisation
Pregnenolone	316	$[M]^{+\cdot}$
Progesterone	314	$[M]^{+\cdot}$
Cholesterol	386	$[M]^{+\cdot}$

Table 4.8: Major ions present for a oestrogens using the GC/MS MD800 with an electron ionisation source (EI) in positive mode.

Steroid	m/z	Rationalisation
Oestrone	270	$[M]^{+\cdot}$
Oestradiol	272	$[M]^{+\cdot}$
Oestriol	288	$[M]^{+\cdot}$

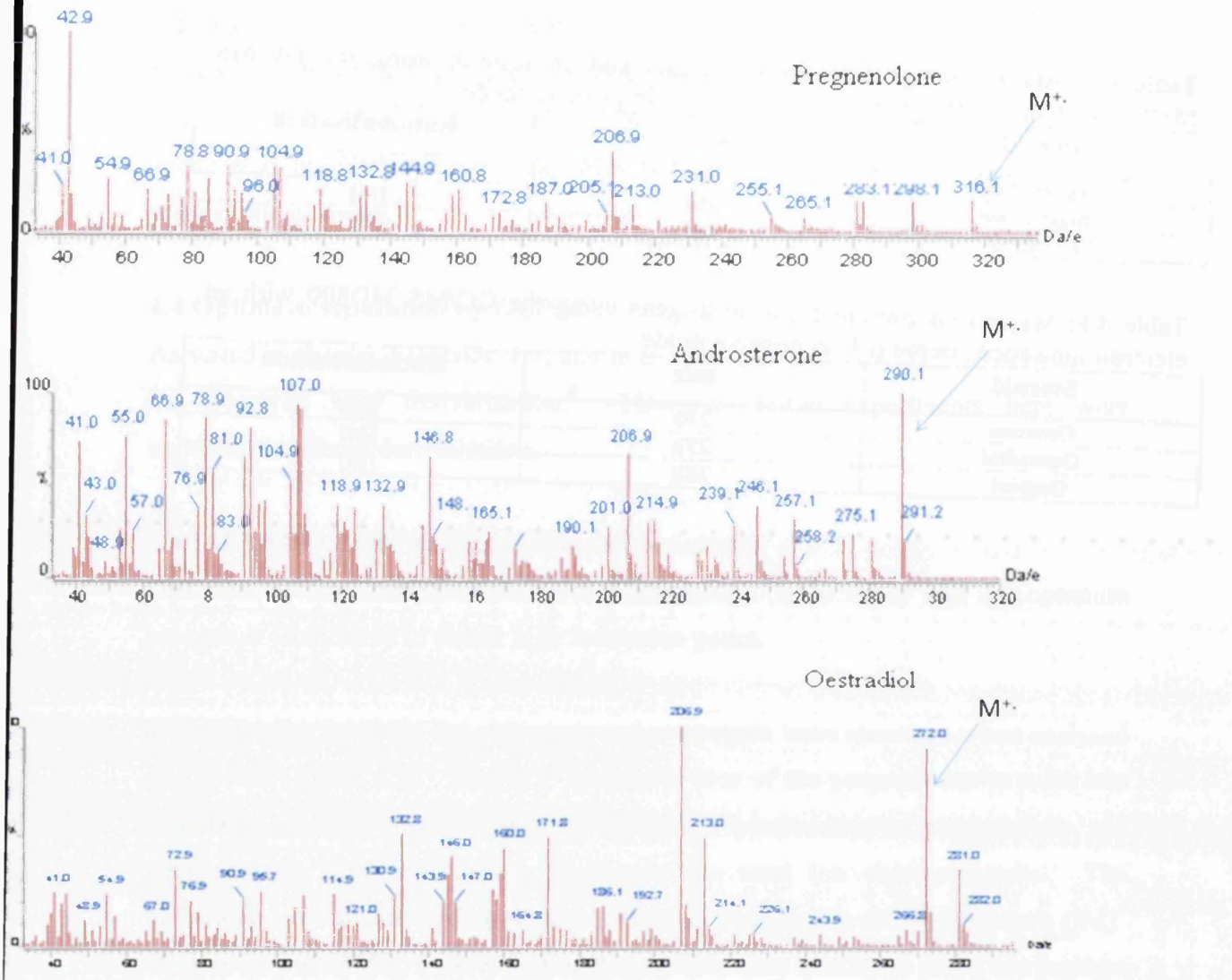

Fig 4.3: Representative mass spectra obtained on the MD800 GC/MS using an EI source in positive mode, samples were a concentration of 10µM in methanol. Top mass spectra was a progestin (pregnenolone) middle was an androgen (androsterone), and bottom was an oestrogen (oestradiol). The molecular species was clearly observed for each steroid.

Table 4.9: GC/MS MD800 Temperature programmes to optimise the chromatographic performance (separating steroid standards as a function of oven temperature).

Method	Injector temperature (°C)	Start temperature (°C)	Hold time (min)	Gradient (°C/min)	Finish temperature (°C)	Final hold time (min)
1	220	40	1	20	290	10
2	220	200	1	20	290	15
3	220	220	1	20	290	15
4	220	250	1	20	290	15

Injection numbers 1 to 4 were completed to establish a temperature gradient system using a variety of steroids. Method 4 produced an optimum separation (figure 4.4) with well resolved steroid peaks in a short time period (less than 15 minutes).

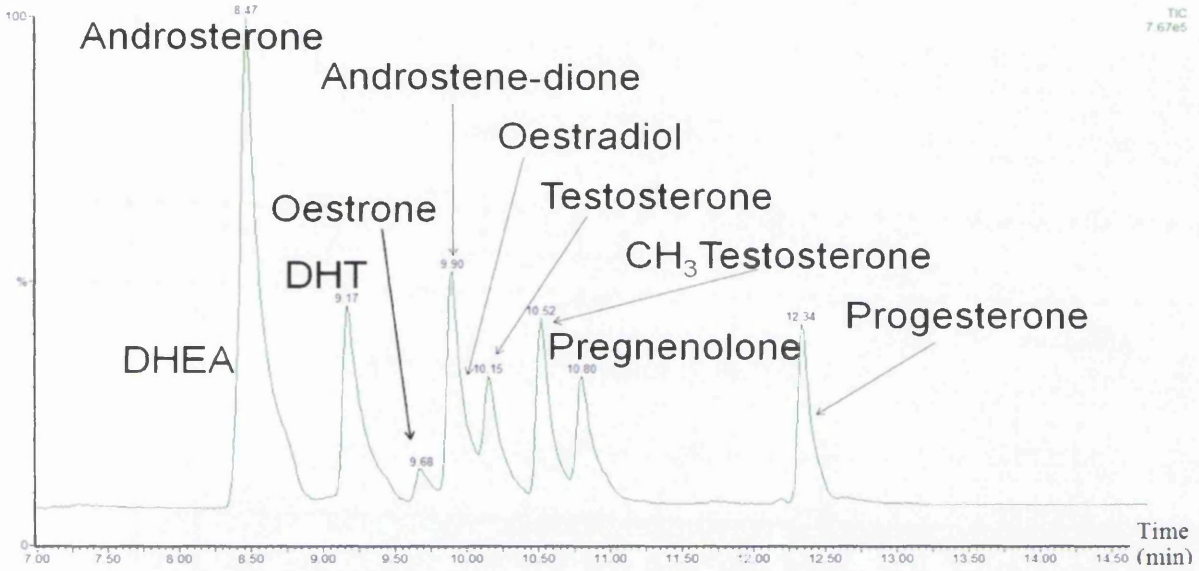

Fig 4.4: Separation of 10 steroids by GC/MS MD800 with an EI source in positive mode. Some steroids co-elute but can be distinguished from their unique peaks in the mass spectra, for example the peak on the left of the chromatogram was the co-elution of a mixture of DHEA and androsterone.

4.4.2 GC MSD analysis of steroid standards

The GC MSD was linked to the Gerstel auto-sampler, which permits pre-column sample preparation methods such as extractions and on-line derivatisation. The increased sensitivity of the GC MSD should improve standard steroid results in comparison to the GC/MS MD800 in terms of sensitivity and resolution. The steroid standards were subjected to analysis using the GC MSD to determine optimum separation parameters and the limit of detection for each steroid.

The steroid standards were infused directly into the GC MSD in positive mode using an electron ionisation source and spectra obtained for each steroid. The full scan mass spectra gave the $[M]^{+\cdot}$ for each steroid standard comparable to those produced by direct infusion to the GC/MS MD800 see tables 4.9, 4.10 and 4.11.

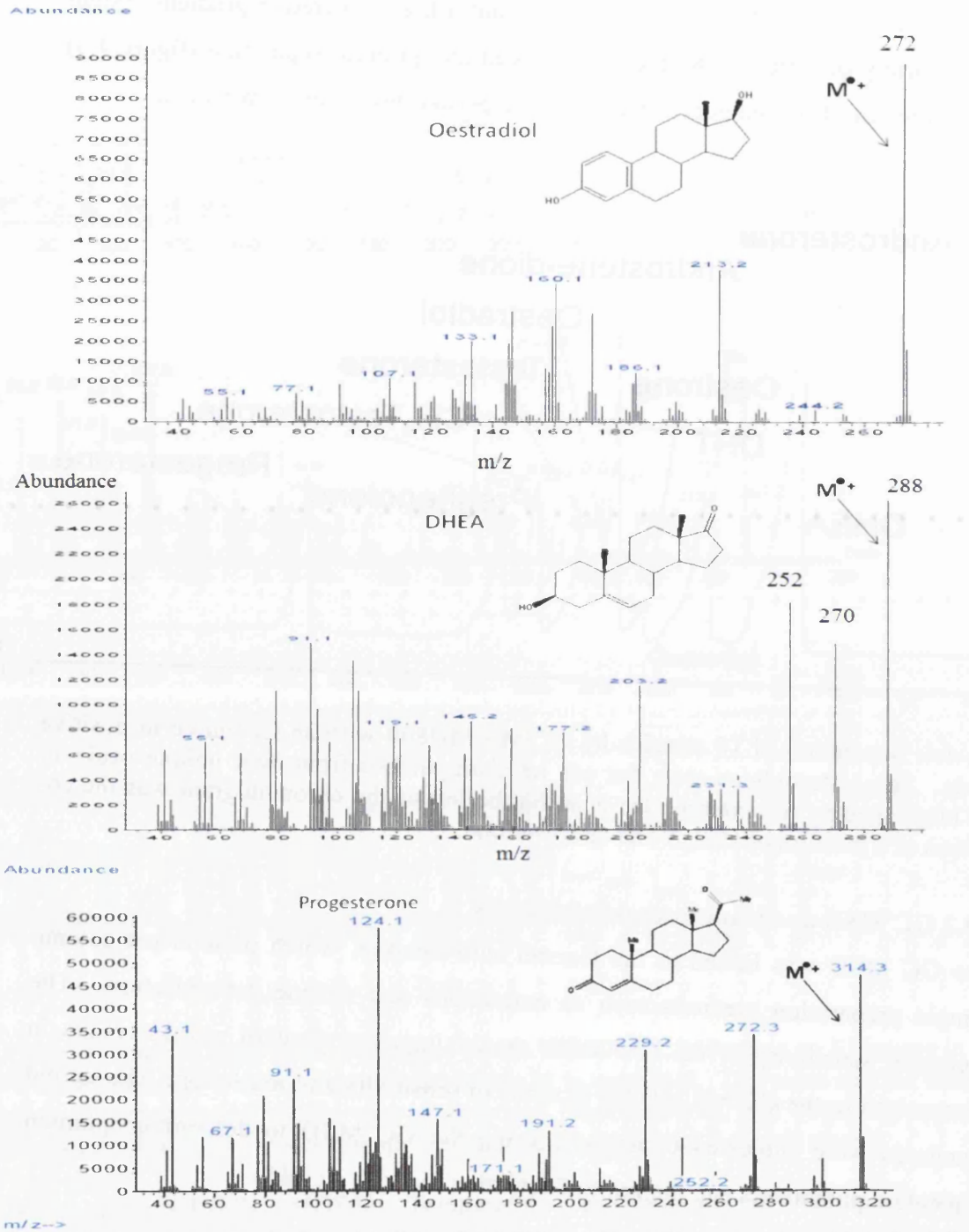

Fig 4.5: Mass spectra produced by the GC MSD with an EI source in positive mode for oestradiol (top), DHEA (middle) and progesterone (bottom). The molecular ion [$M^{\cdot+}$] were abundant for each steroid.

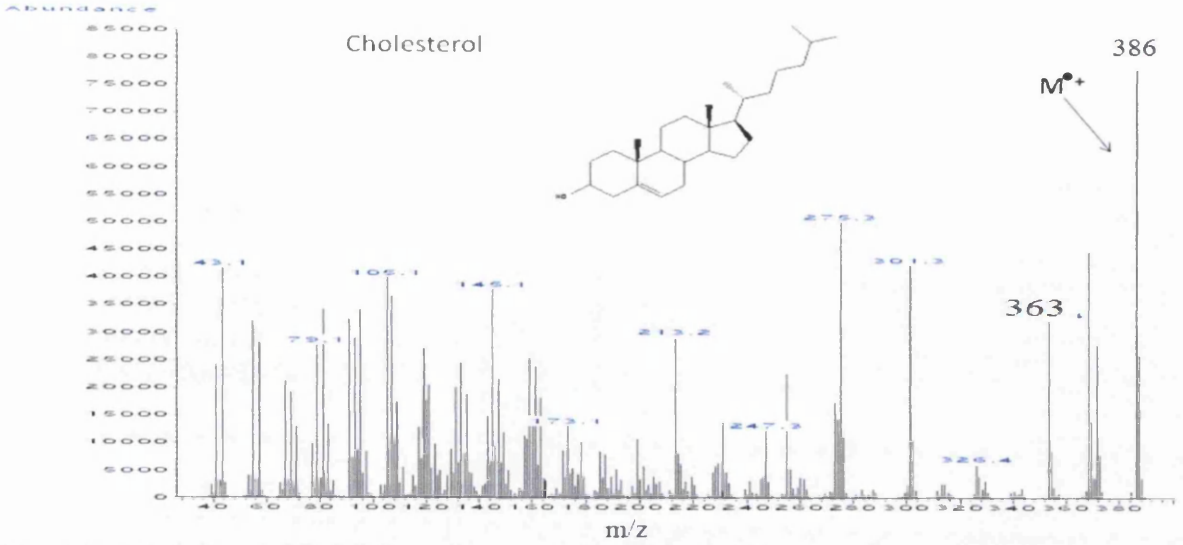

Fig 4.6: Cholesterol GC MSD mass spectrum with an EI source in positive mode. The molecular ion [$M^{\cdot+}$] was abundant for cholesterol observed at m/z 386.

Cholesterol can be easily detected using both the GC/MS MD800 and GC MSD. In figure 4.6 the $M^{\cdot+}$ molecular species was abundant. The LCQ DECA mass spectrometer was not sensitive to cholesterol, (possibly due to poor ionisation efficiency using ESI) and GC/MS offers a viable alternative for cholesterol analysis.

The ten steroids (table 3.1 and cholesterol) were subsequently combined and analysed to develop a separation technique. The optimum steroid separation was achieved using a short column HP1 and the rear programmable temperature vaporisation (PTV) injection port at 150°C, which was held for 1 minute, followed by a temperature increase of 20°C/min to 250°C, which was held for 2 minutes. There was still some co-elution of steroids using this temperature gradient system, for example testosterone and oestradiol co-elute (figure 4.7). Separation of these two compounds was possible but at the expense of good chromatography as a gradient of 0.1°C/min was required which caused significant peak broadening and tailing. Positive identification of co-eluting compounds can be determined from mass spectra generated at these times as the co-eluting steroids generate different $M^{+\cdot}$ ions, such as DHEA and androsterone which have the different $M^{+\cdot}$ ions of 288 and 290, respectively.

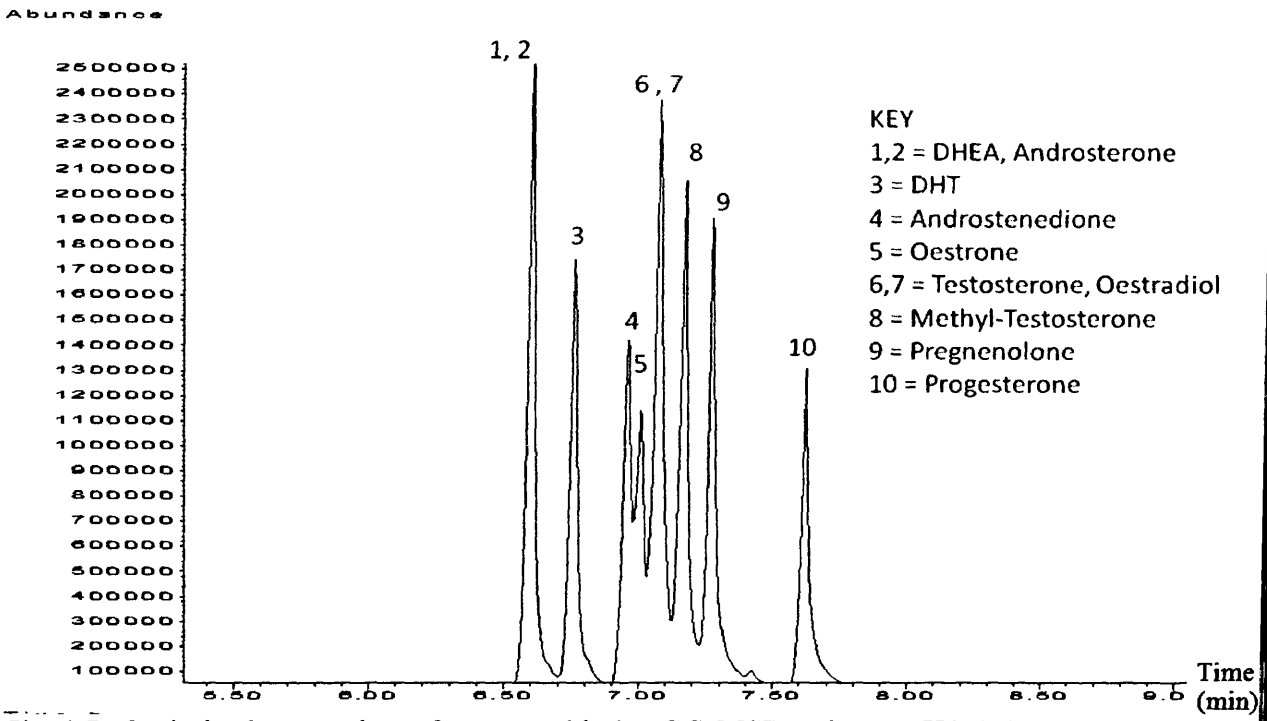

Fig 4.7: Optimised separation of ten steroids by GC MSD using an HP-1 1 metre column in positive mode with an EI source.

When comparing the GC MSD separation (figure 4.7) to that of the GC/MS MD800 (figure 4.4) it was possible to determine that the steroids can be separated in a shorter time using the GC MSD. Separation 14 minutes (GC/MS MD800) whereas separation of the same steroids using the GC MSD required just 8 minutes. The elution orders of the steroids were the same for both techniques, but the GC MSD instrument exhibited improved resolution. This was due to a combination of factors such as the improved chromatography and injection procedures on the GC MSD.

4.5 Reproducibility of steroid retention times and peak areas: variation in results with use of an internal standard

The reproducibility of each technique was measured by subjecting the same concentration and volume of a steroid solution to analysis a number of times and over many days (inter variation) and calculating the variation in the instrument response (peak area and/or retention time).

Mass spectrometers are subjected to a number of day-to-day (intra-variation) variations, such as variation in the source, instability of the mass scale, and changes

in capillary temperatures. There are also daily variations (inter-variation) associated with the LC systems, such as changes in column pressure, flow rate and column temperature. GC variations can be due to problems within the GC interface to the mass spectrometer (the transfer line from the GC oven to the ion source) or temperature variations in the GC oven which affects pressure and temperature on the column and so resolution of the compounds.

There are many techniques employed to reduce these errors through accurate measurements and optimisation of analytical techniques and apparatus. The use of a standard compound, similar to those under investigation to which the compound under investigation can be compared is applied to reduce errors associated with intra experimental variations of the instrument.[7] This standard compound can be added at two time points each of which are given a different name;

1. Surrogate internal standard- standard compound is added at the start of the experiment before extraction and undergoes all processes with the compound of interest. This includes the whole analytical procedure i.e. derivatisation and extraction. This method allows calculation of the analyte concentration present in the original sample and overcomes errors associated with experimental sample losses as well as errors associated with the analytical technique.

2. Internal standard (IS)- A standard compound is added after extraction and/or derivatisation, prior to analysis. The internal standard is added in the same concentration to each sample and a ratio of the instrument response for the analyte to the instrument response for the internal standard is calculated. The internal standard is added at a concentration of ~40% of the expected concentration range. In these experiments the IS methyl-testosterone was added after steroid extractions, prior to mass spectrometry analysis.

Instrument response reproducibility was calculated by measuring the peak area produced by a steroid over 10 infusions. The peak area recorded should be the same for each injected volume of sample and the variance of this represents the reproducibility of the technique. The variance of the ratio of peak area/internal standard peak area over a number of injections gives an error value related to

instrument reproducibility, this is expressed as the relative standard deviation (RSD) defined in equation 4.1.

Retention time reproducibility was calculated as actual retention time (Rt) and as relative retention time to the internal standard. The retention times should be the same for each steroid in every injection (same temperature/gradients). The retention time was noted for each steroid for 10 injections over 2 days, and the relative retention time to the internal standard's retention time was calculated. The variance over 10 injections and relative standard deviation (RSD) were calculated, producing an error relating to retention time reproducibility.

4.5.1 Reproducibility of instrument response (peak area) produced by analysis of androstenedione and androsterone

A mixture of androsterone and androstenedione was infused into the GC/MS MD800, GC MSD and the LCQ DECA, ten times over two days. The instrument response (peak area and retention time) was determined for each steroid in each injection. The peak area ratio, and the retention time relative to the internal standard were also calculated. The standard deviation and relative standard deviation[8] (RSD) were calculated as defined in equation 4.1.

$$RSD = \frac{\text{standard deviation} \times 100}{\text{average}} \qquad \text{(equ 4.1)}$$

RSD= relative standard deviation, average is the average peak area (or retention time) for 10 infusions into the mass spectrometer.

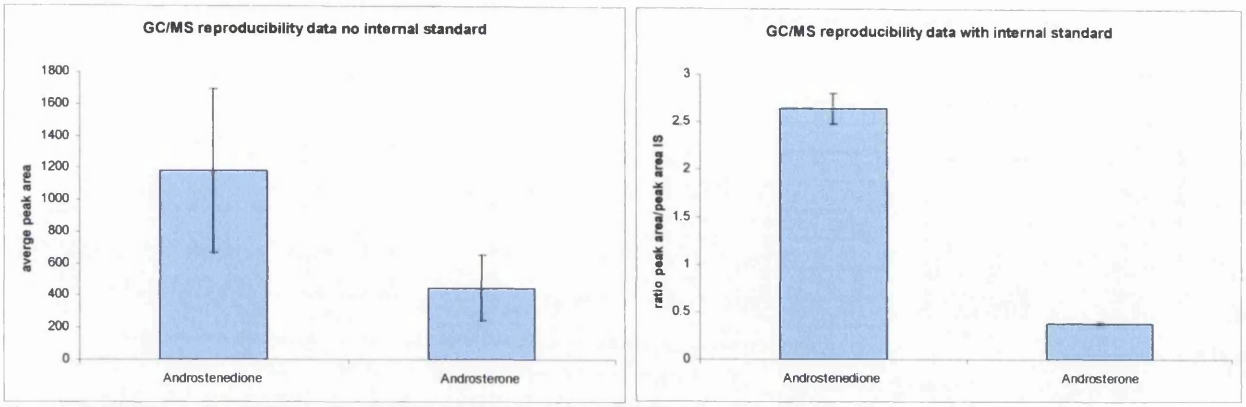

Fig 4.8: Reproducibility instrument response (peak area) for androstenedione and androsterone analysed by GC/MS MD800 in positive mode using an EI source. Graph on the left demonstrated variation without an IS and the graph on the left demonstrates variation with an IS.

Figure 4.8 illustrates the importance of an internal standard (IS). The RSD of 10 measurements of peak area was reduced from the initial error of > ±40% to only ~±6% with the use of an internal standard for both steroids. Use of an internal standard in GC/MS MD800 analysis increased the confidence in quantitation of steroids in biological samples.

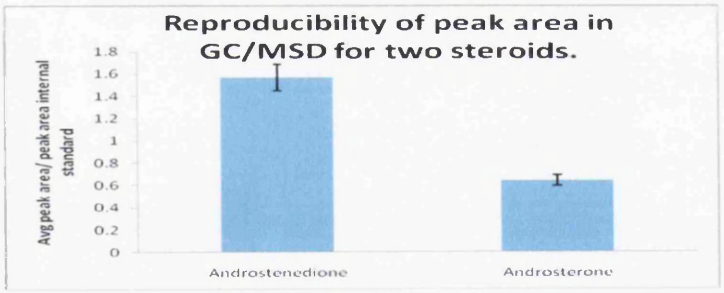

Fig 4.9: Reproducibility of peak area relating to androstenedione (m/z 286) and androsterone (m/z 290) when analysed by GC MSD in positive mode using an EI source with an internal standard (methyl-testosterone).

The RSD with use of an internal standard were ~±8% for both of the steroids analysed on the GC MSD (this was comparable to those generated by the GC/MS MD800). Without an internal standard the percentage variation for both steroids was ~±10%, therefore the GC MSD mass spectrometer was less susceptible to day-to-day instrument variations than the GC/MS MD800.

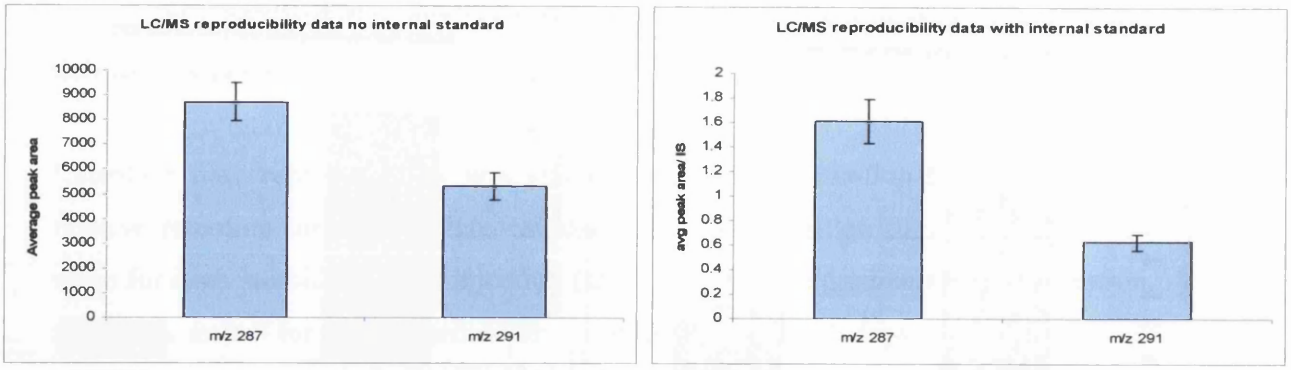

Fig 4.10: Reproducibility of instrument response (peak are) relating to androstenedione (m/z 287) and androsterone (m/z 291) when analysed by LC/MS on the LCQ DECA mass spectrometer analysed in positive mode using an ESI source. Left plot illustrates reproducibility without an internal standard right plot illustrates reproducibility with an internal standard variance was calculated as RSD.

The RSD produced with and without use of an internal standard on the LCQ DECA were similar ~±10%. From this small error it was concluded that there was little variation in the LCQ DECA mass spectrometer in terms of peak area (the technique was reproducible).

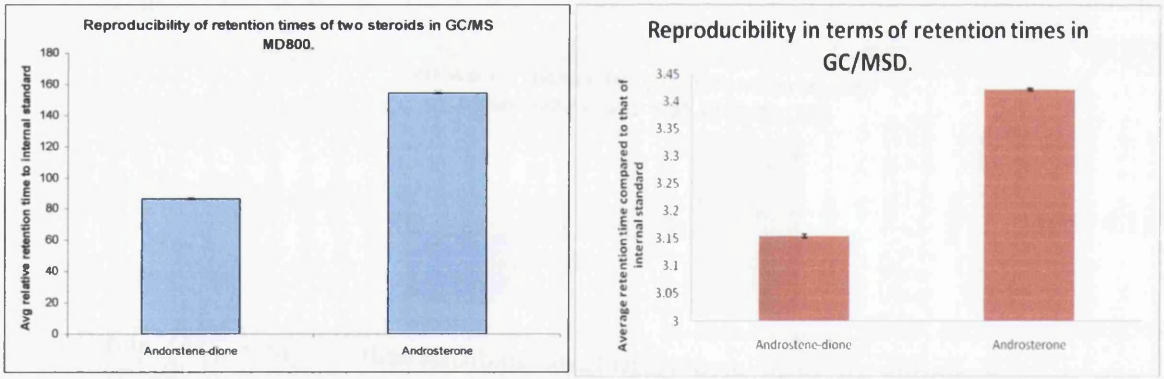

Fig 4.11: Reproducibility of retention times of androstenedione and androsterone. Left hand graph shows retention time reproducibility analysed on the GC/MS MD800, with an EI source in positive mode. The right hand graph shows relative retention times of androstenedione and androsterone analysed using the GC MSD in positive mode with an EI source. The scale on the y-axis are different due to different retention times of the steroids in the different mass spectrometers (different columns and temperature gradient systems GC/MS MD800 y-axis is seconds and GC MSD is minutes).

Figure 4.11 demonstrates the high reproducibility of the retention times of androsterone and androstenedione in gas chromatography mass spectrometry (GC/MS MD800 and GC MSD). Retention times were highly reproducible with or

without use of an internal standard. Variation in the retention time and relative standard deviation of the retention time with both gas chromatography mass spectrometers was comparable (table 4.11).

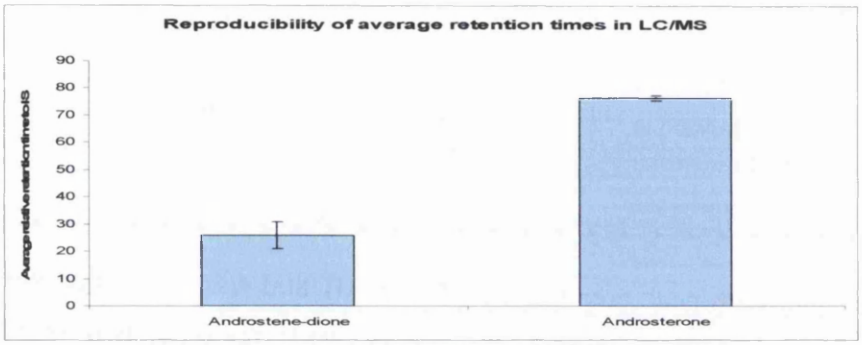

Fig 4.12: Plot showing the reproducibility of retention times of androstenedione and androsterone. These were analysed on the LCQ DECA in positive mode using an ESI source.

From the results presented above (figure 4.12) it was concluded that retention time was reproducible with a relative standard deviation of ±12.5% in LC/MS. There was some variation in retention times without an internal standard (~±20% data not shown) this could be due to incomplete initial column conditioning, pressure changes, flow rate changes or differences in chromatography causing polarity to be lower or higher than expected. Calculations of relative retention times to an internal standard reduce these errors (table 4.11 below).

4.5.2 Comparison of reproducibility for GC/MS MD800, GC MSD and LC/MS LCQ DECA

A comparison between the two GC/MS techniques and LC/MS was completed. This provides information concerning how reliable each instrument was, and which method was superior in terms of reproducibility of peak area and retention time.

Table 4.10: Reproducibility comparison of instrument response (peak areas) produced in GC/MS (GC/MS MD800 and GC MSD) and LC/MS (LCQ DECA): A comparison of RSD variations (calculated variation of 10 measurements recorded on 2 separate days).

Steroid		GC/MS (MD800)	GC MSD	LC/MS
		± RSD % variation	± RSD % variation	± RSD % variation
Without an internal standard	Androstenedione	43.38	10.4	8.86
	Androsterone	45.59	10.3	10.39
With an internal standard	Androstenedione	6.20	7.57	10.98
	Androsterone	6.21	7.59	10.68

The RSD associated with peak area for the GC/MS MD800 was very large when an internal standard was not incorporated (the average RSD for these two androgens was ±44%). This error was significantly reduced with addition of an internal standard to an average RSD error of ±6.2%. This showed a significant run-to-run variation within the GC/MS MD800 system, the reason for this large variation could be due to the manual injection procedure, instrument parameter variation, or the GC itself. The GC MSD has much reduced errors without the internal standard in comparison to the GC/MS MD800, probably due to the automated injection system and superior heating and cooling system of the oven. RSD were ~±10% without an internal standard for the GC MSD, this was comparable with results generated by Van Renterghem[9] and co-workers who investigated the reproducibility of a number of steroids using a GC MSD they calculated RDS values of between ±5.02 and 21.9% for androsterone and ±5.70 to 35.5% for androstenedione (placing the values in table 4.10 at the lower end of their results). The LC/MS system (LCQ DECA) shows small variations in the RSD for peak areas due to day-to-day instrument variation. The LCQ DECA and GC MSD were comparable in terms of RSD of peak area. This research highlights the importance of use of an internal standard for quantitative analysis. It should still be noted that even though the LCQ and GC MSD demonstrated comparable reproducibility values that the GC MSD was less sensitive than the LCQ and so cannot be used for low concentration analysis.

Table 4.11: Comparison of retention time reproducibility in GC/MS and LC/MS. A comparison of RSD variations (calculated variation of 10 measurements recorded on 2 separate days).

Steroid		GC/MS MD800	GC MSD	LC/MS
		± RSD % variation	± RSD % variation	± % RSD variation
Without an internal standard	Androstenedione	0.17	0.02	19.9
	Androsterone	0.17	0.27	5.15
With an internal standard	Androstenedione	1.14	0.05	9.98
	Androsterone	0.65	0.11	3.53

Percentage RSD variation of retention time in GC/MS was low, both techniques were highly reproducible. Table 4.11 demonstrates that retention times in the GC/MS systems were more reproducible than the LC/MS system. The RSD retention times in LC/MS were as much as ±20%, which was reduced by approximately half with addition of an internal standard. Shifts in retention times can vary throughout a chromatographic run, the percentage variation is generally reduced at longer retention times.

LC/MS and GC MSD were more reproducible in terms of peak areas than the GC/MS MD800 (no internal standard). The GC/MS techniques were significantly more reproducible in terms of retention time than the LC/MS system, however the LCQ was more sensitive for androgens and progestins in positive mode (chapter 4.5) and has the capability of MS/MS. A dual procedure for complete positive identification and quantitation of a mixture of steroids from a biological sample may be required. It was reasonable to assume that the errors associated with peak area and retention times for the other androgens, progestins and oestrogens will be comparable to those generated above.

4.6 Statistical analyses from calibration graphs using standard reference materials

The method required to obtain calibration graphs were described in chapter three (3.8). The results presented in this chapter represent the limit of detection calculated for a number of steroids obtained through calibration series via LC/MS. From calibration graphs the concentration of a specific steroid in a biological sample was determined.

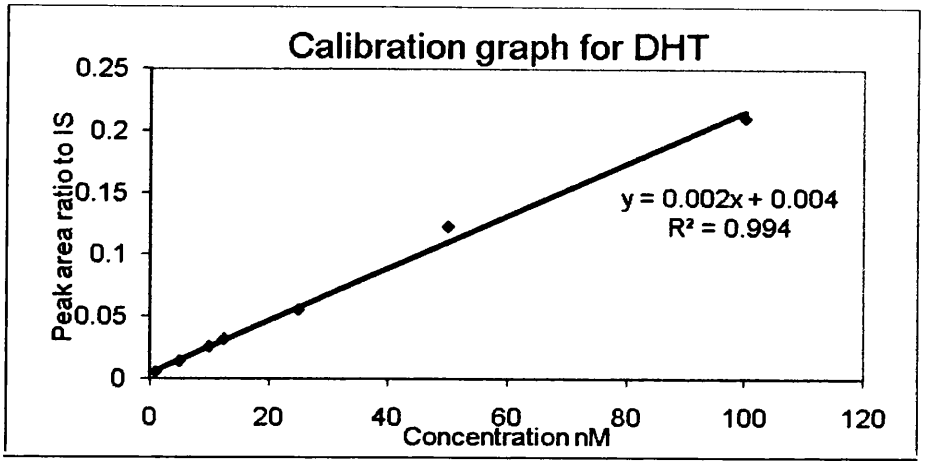

Fig 4.13: Representative calibration graph for a series of concentrations of DHT. Instrument response (peak area ratio to IS) was plotted against concentration. Analysed on the LCQ DECA mass spectrometer in positive mode using an ESI source.

Table 4.12: Limit of detection and R^2 values for 8 steroids analysed on the LCQ DECA using a C_{18} reversed-phase column ESI source in positive mode. Methyl-testosterone was the internal standard.

Steroid	Limit of detection nM	R^2
Testosterone	184	0.976
DHT	87.0	0.994
Androstenedione	36.1	0.987
DHEA	92.4	0.975
Androsterone	95.5	0.993
Androstanediol	80.5	0.969
Pregnenolone	211.7	0.998
Progesterone	83.5	0.991

The calibration graphs generated for each of the eight steroids, with the use of an internal standard were statistically significant as the R^2 values were all >0.98. Oestradiol and oestrone cannot be detected below a concentration of ~500nM, as when a steroid mixture was infused into the LC/MS system the protonated molecular ions $[M+H]^+$ were indistinguishable from background. This may be because other steroids were ionised preferentially, therefore a more sensitive method was required for oestrogen analysis.

These limits of detection were higher than the required performance limits for androgens as outlined in the WADA (World Anti-Doping Agency) 2004 for doping laboratories, which are ~10ng/mL[10,11] the limits of detection recorded here could be

reduced by at least an order of magnitude by the use of selected ion monitoring (SIM) which would produce comparable results to the WADA values. Physiological levels of steroids present in biological samples may be higher than the calculated limits above, for example DHEA-S (a steroid precursor) has been recorded at a concentration of 1μM in postmenopausal women.[12] In these experiments it was steroid metabolism under investigation, specific steroids were added at concentrations higher than the limit of detection, so they and their major metabolites can be detected. Also after experiments steroids were concentrated by extractions from large volumes of cell media and so were present at high concentration(s) in comparison to the limit of detection of each steroid. For these reasons SIM was not required in these experiments.

4.7 Statistics for GC/MS calibration graphs using the GC/MS MD800 and GC MSD

Through calibration methods and a number of calculations it was possible to calculate the R^2 value and the limit of detection for each steroid using the GC/MS MD800 and GC MSD.

Table 4.13: Limit of detection and R^2 values for nine steroids analysed by GC/MS MD800 (without an internal standard).

Steroid	Limit of detection μM	R^2
Testosterone	3.09	0.982
DHT	4.47	0.964
Androstenedione	3.04	0.983
DHEA	7.33	0.908
Androsterone	7.66	0.901
Pregnenolone	4.74	0.960
Progesterone	2.99	0.984
Oestradiol	2.25	0.989
Oestrone	9.96	0.843

These R^2 values vary significantly, this was due to errors associated with the manual injection procedure (use of an internal standard would increase the R^2 value and lower the limit of detection). To our knowledge there were no current examples of analysis of these steroids by GC/MS without prior derivatisation methods to improve the sensitivity of the technique.

Table 4.14: Limit of detection and R^2 values for nine steroids analysed by GC MSD (with an internal standard).

Steroid	Limit of detection µM	R^2
Testosterone	1.40	0.995
DHT	1.65	0.996
Androstenedione	1.10	0.998
DHEA	2.03	0.990
Androsterone	1.50	0.996
Pregnenolone	2.56	0.983
Progesterone	2.56	0.990
Oestradiol	3.32	0.983
Oestrone	1.31	0.997

Addition of an internal standard increases the R^2 value for each of the steroids analysed. All the calibrations were statistically significant now as they all have an R^2 value of over ≥ 0.98. The limit of detection was also reduced with the addition of an internal standard by an average of 1.77µM for the GC MSD.

After analysis of these steroids by the GC/MS MD800 and GC MSD it was concluded that the R^2 values were more statistically significant when using the GC MSD. The limit of detection for each steroid was reduced when using the GC MSD in comparison to the GC/MS MD800 (whether an internal standard was used or not). These conclusions along with the auto-sampler availability and improved resolution confirm that the GC MSD was a superior instrument to the GC/MS MD800. The limit of detection for each steroid can conceivably be reduced following derivatisation and/or SIM experiments.

4.8 Comparison of GC/MS and LC/MS for determination of ideal technique for analysis of standard steroids

A comparison of LC/MS and GC/MS provides information concerning the optimum analysis technique for each steroid in terms of the limit of detection. This was important because, neither LC/MS nor GC/MS is universal for low level steroid analysis. It was concluded that a dual method which includes both LC/MS and GC/MS was required to generate full steroid profiles (from cholesterol to oestradiol) in biological samples.

Table 4.15: Comparison of the limit of detection (LOD) for GC MSD and LC/MS with internal standard.

Steroid	GC MSD		LC/MS	
	LOD µM	R^2	LOD nM	R^2
Testosterone	1.40	0.995	184	0.976
DHT	1.65	0.996	87.0	0.994
Androstenedione	1.10	0.998	36.1	0.987
DHEA	2.03	0.990	92.4	0.975
Androsterone	1.50	0.996	95.5	0.993
Pregnenolone	2.56	0.983	21.2	0.998
Progesterone	2.56	0.990	83.5	0.991
Oestradiol	3.32	0.983	n/a	n/a
Oestrone	1.31	0.997	n/a	n/a

These results (table 4.15) demonstrated that the limit of detection for each steroid generated by GC/MS (GC MSD) were higher than those generated by LC/MS (with an internal standard). LC/MS was an average of ~20 times more sensitive than GC/MS. The R^2 values for both were ≥ 0.98 showing that both sets of data were statistically significant.

When a mixture of steroids were analysed by LC/MS oestradiol was almost undetectable due to ionisation suppression. The signal produced when oestradiol was infused into the GC MSD as a mixture was much improved in comparison to LC/MS. Therefore for real sample analysis both LC/MS and GC MSD were required, or a derivatisation method may be employed for single instrument full steroid analysis.

4.9 Derivatisation for improved signal in GC/MS and LC/MS

Derivatisation changes the molecule by adding a functional group which increases the ionisation efficiency of the molecule. The two derivatisation procedures investigated have been previously described (chapter 3). The first was TMS derivatisation which aids GC/MS steroid identification by derivatising the hydroxyl groups present in some, but not all steroids.[13] The second derivatisation procedure was aimed solely at increasing the mass spectrometers sensitivity to oestrogens, this was dansyl-chloride derivatisation.[14] Dansyl-chloride derivatises the phenolic hydroxyl group present in oestrogens, this procedure permits identification of oestrogens in positive mode LC/MS and GC/MS.

4.9.1 TMS derivatisation

TMS derivatisation was investigated using testosterone, oestradiol, pregnenolone and oestrone solutions all of 10μM in methanol. Each steroid was derivatised as outlined in chapter 3.10. The steroids were then analysed by direct infusion into the GC/MS MD800 in positive mode using an EI source.

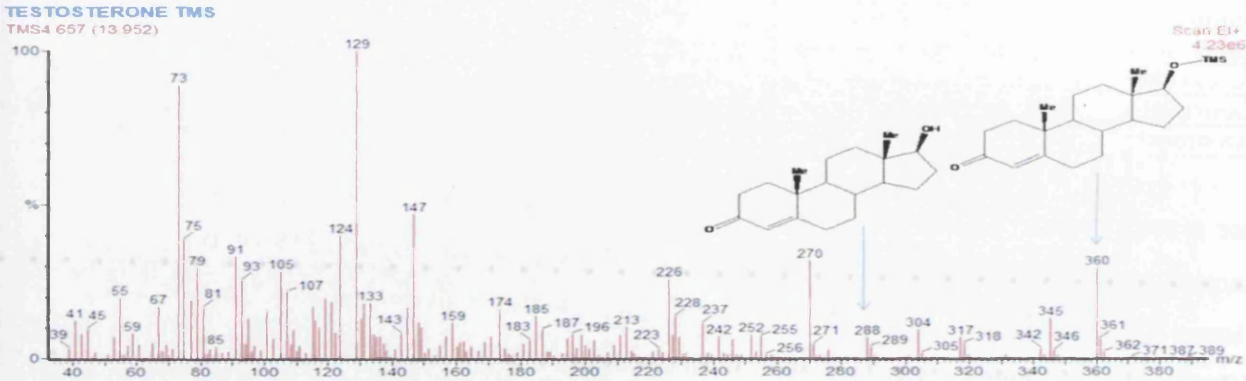

Fig 4.14: Testosterone TMS derivatisation analysed on the GC/MS MD800 in positive mode with an EI source. Testosterone-TMS derivative and some remaining testosterone were observed at 16 minutes, the derivatisation was not 100% efficient.

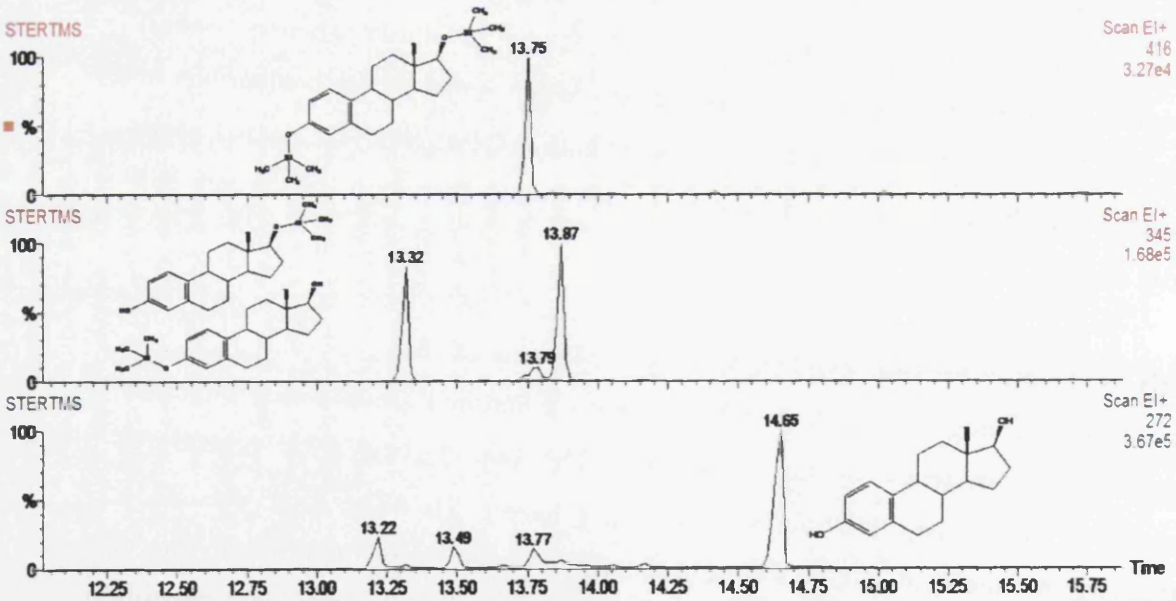

Fig 4.15: Chromatograms showing the four peaks produced after oestradiol TMS derivatisation. These chromatograms were produced on the GC/MS MD800 in positive ionisation mode using an EI source. The top peak is representative of di-derivatised oestradiol m/z 416, the middle peaks of selected mass m/z 345 were due to the two mono-dervatised compounds which can be produced with oestradiol-TMS derivatisation (OH groups at position 3 and position 17). The final peak of selected mass m/z 272 is un-derivatised oestradiol indicating that the derivatisation was not 100% efficient.

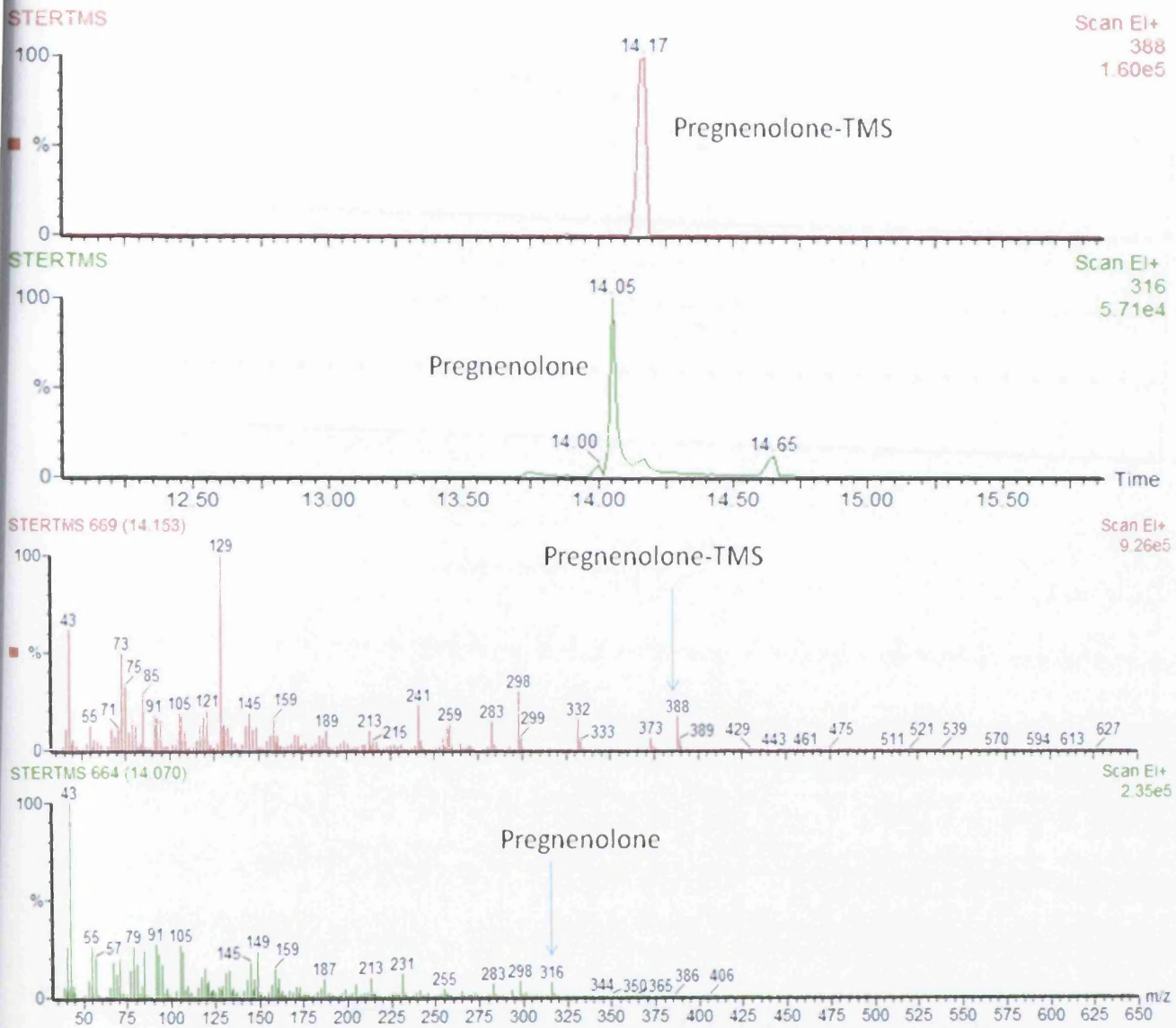

Fig 4.16: Chromatograms and mass spectra showing incomplete derivatisation of pregnenolone. Two peaks were seen in the total ion chromatogram representative of pregnenolone-TMS and un-derivatised pregnenolone. These samples were analysed in positive mode using the GC/MS MD800 with an EI source.

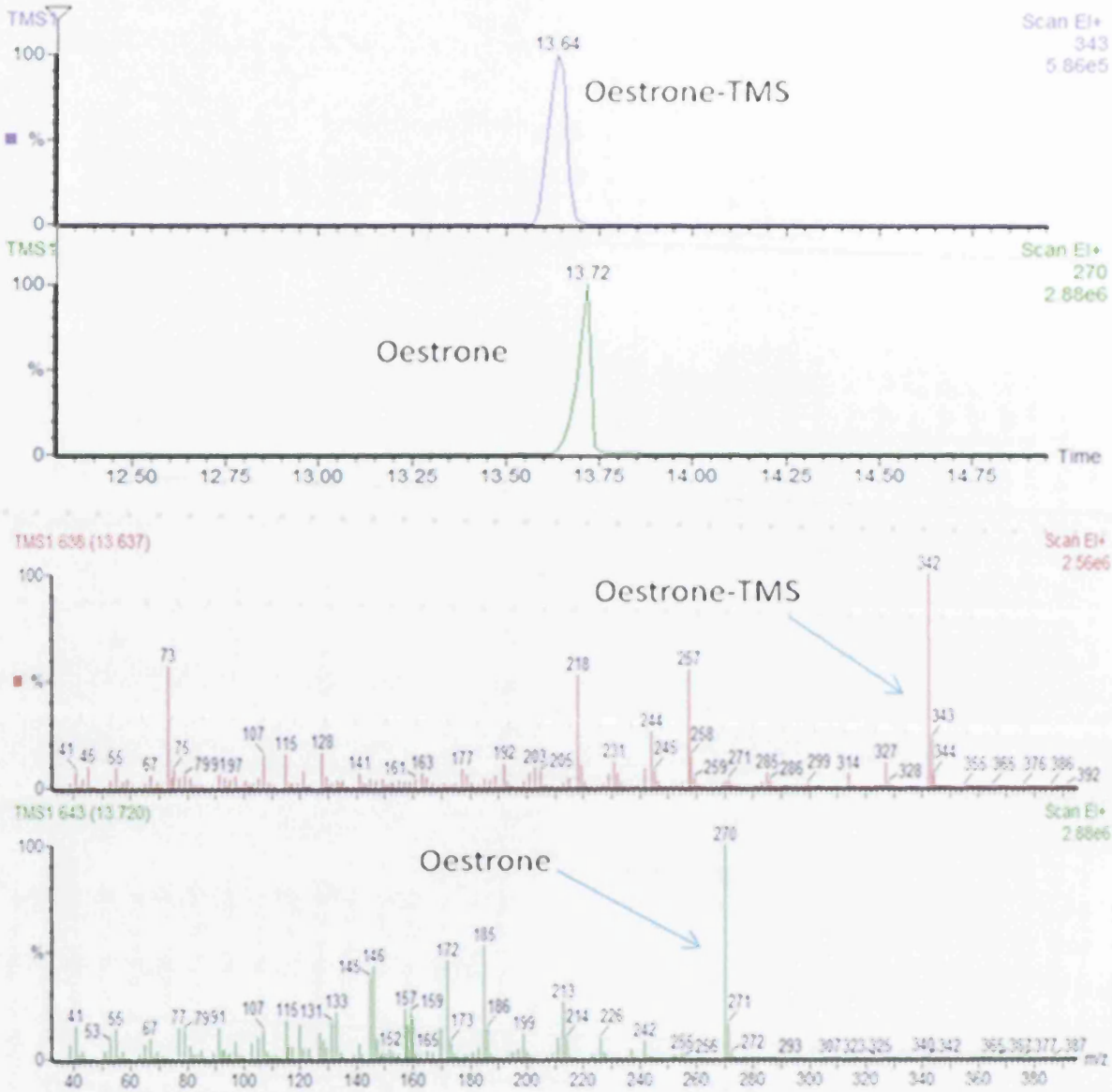

Fig 4.17: The chromatogram at the top shows two peaks after TMS derivatisation of oestrone. The top chromatogram and top mass spectrum is the derivatised oestrone m/z 342 the second chromatogram and the lower mass spectrum prove that incomplete derivatisation of oestrone has occurred as the derivatised molecular ion m/z 270 is observed. Analysed on the GC/MS MD800 using an EI source.

Figures 4.14 to 4.17 demonstrated that TMS derivatisation of the hydroxyl groups occurred with testosterone, oestradiol, pregnenolone and oestrone as the derivatised molecular ion peaks were observed with all four compounds. Testosterone conversion was the most efficient of these with little remaining underivatised testosterone present. Oestradiol-TMS chromatograms and spectra were complex because of the two mono, and one di-derivatised reaction end products (figure 4.15). The mono-derivatised compounds produced a molecular ion peak at m/z 345, and the di-derivatised compound produced a molecular ion peak of m/z 416. This leads to multiple peaks in the chromatograms representative of one compound. This new level of complexity will occur in any steroid with multiple OH groups such as androstene-diol, oestriol and 5α-androstane-3,17 diol. The complexity of multiple derivatisation sites combined with incomplete derivatisation lead to an alternative derivatisation procedure being adopted.

4.9.2 Dansyl-chloride derivatisation

This procedure was initially investigated using oestradiol, oestrone, testosterone, and pregnenolone. It has been previously shown that derivatisation of oestrogens can lead to a large decrease in their limit of detection by LC/MS.[15] Dansyl-chloride derivatisation acts only at phenolic hydroxyl groups however testosterone and pregnenolone were also studied to ascertain if any derivatisation occurs at their hydroxyl sites. ~0.1mg of each steroid were derivatised as outlined in chapter 3.10, the end products of these reactions were extracted and reconstituted in 1mL of methanol. From these stock solutions 2μL was taken and diluted in 100μL of 50/50 methanol/water 0.1% acetic acid which was directly infused into the LC/MS.

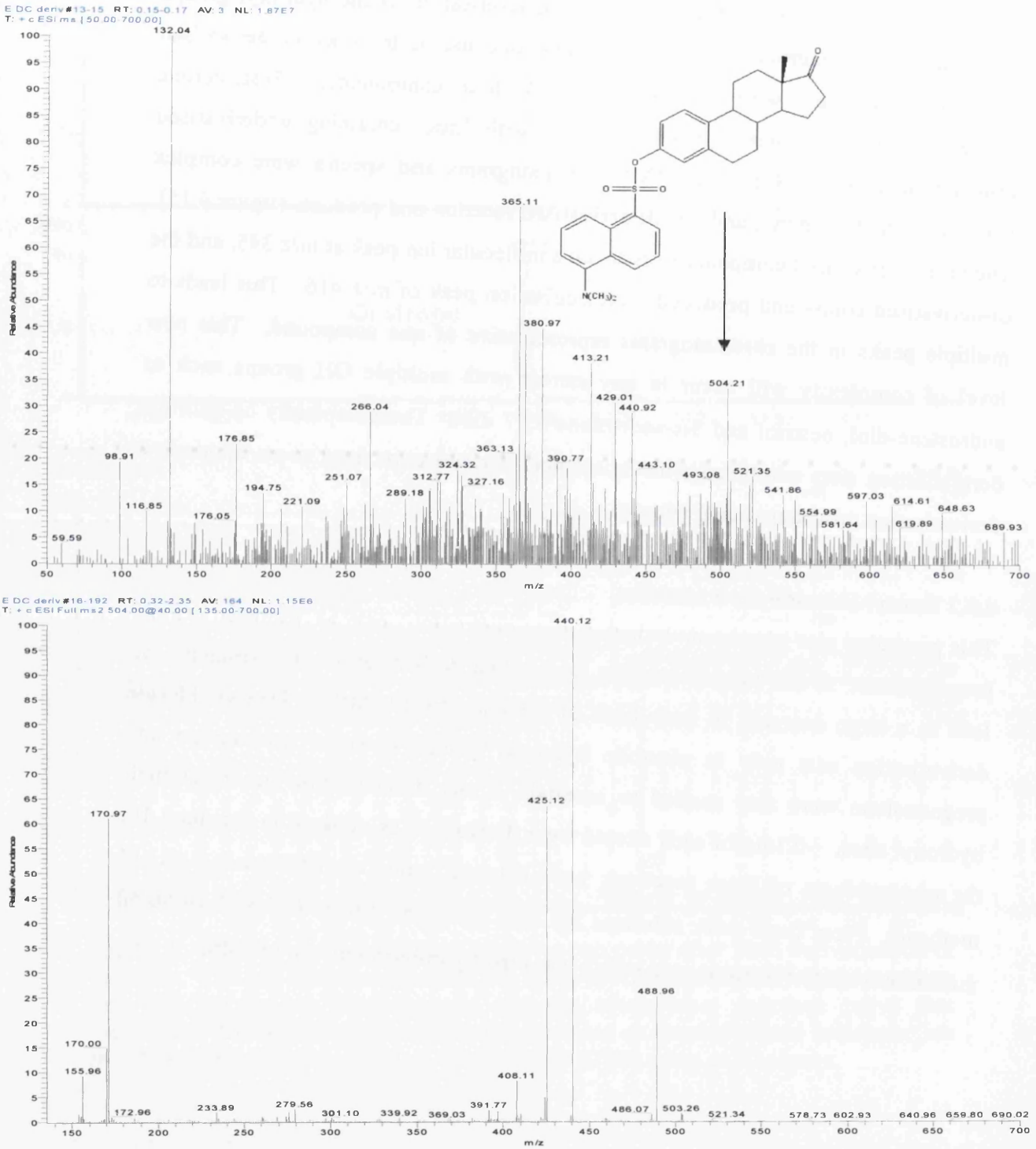

Fig 4.18: Full scan mass spectra of dansyl-chloride-oestrone (top spectra), the protonated molecular species can clearly be seen at $[M+ \text{derivative } +H]^+$ = m/z 504. This was produced from direct infusion into the LCQ DECA with an ESI source in positive mode. The LC/MS/MS generated fragmentation pattern of the protonated molecular ion (m/z 504 spectra) showing fragments which further aid identification using selected reaction monitoring (SRM).

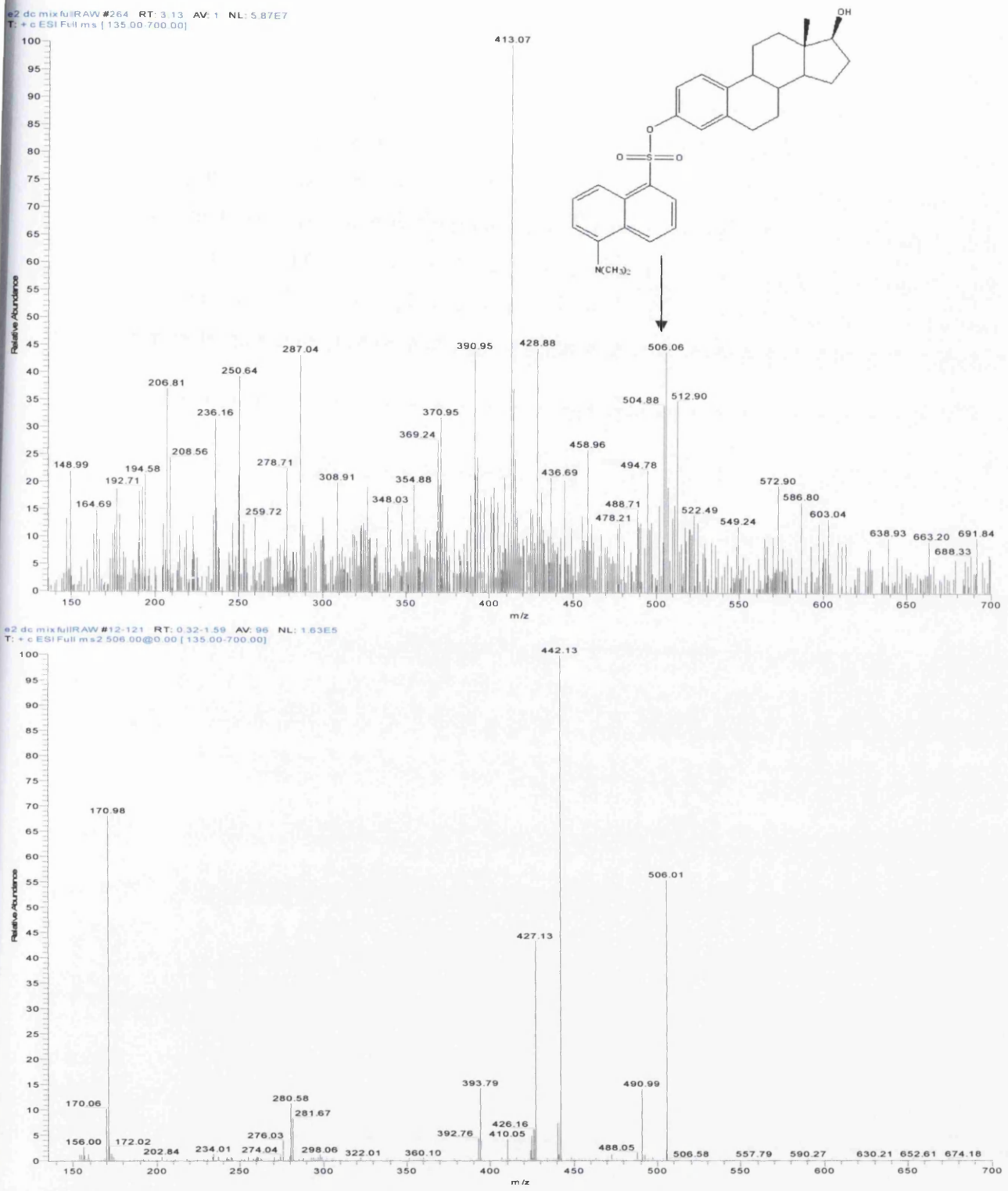

Fig 4.19: Full scan mass spectra of dansyl-chloride-oestradiol (top spectra), the protonated molecular ion can clearly be seen at [M+ derivative +H]$^+$ = m/z 506. This was produced from direct infusion into the LCQ DECA with an ESI source in positive mode. The LC/MS/MS generated fragmentation pattern of the protonated molecular ion (m/z 506-bottom spectra) showing fragments which further aid identification when using SRM.

The mass spectra (figure 4.18 and 4.19) illustrated dansyl-chloride derivatisation of oestrone and oestradiol. Both full scan mass spectra display peaks which were indicative of the derivatised oestrogens. There were no abundant peaks in either spectrum which showed underivatised oestrogens, this shows the technique was efficient, although the lack of sensitivity towards the un-derivatised oestrogens should also be noted. Development of a new separation technique was also required for unequivocal identification of the oestrogen derivatives. Dansyl chloride-oestradiol and dansyl chloride-oestrone were distinguishable due to a mass difference of 2Da, due to the 2 extra hydrogens which are present in oestradiol in comparison to oestrone.

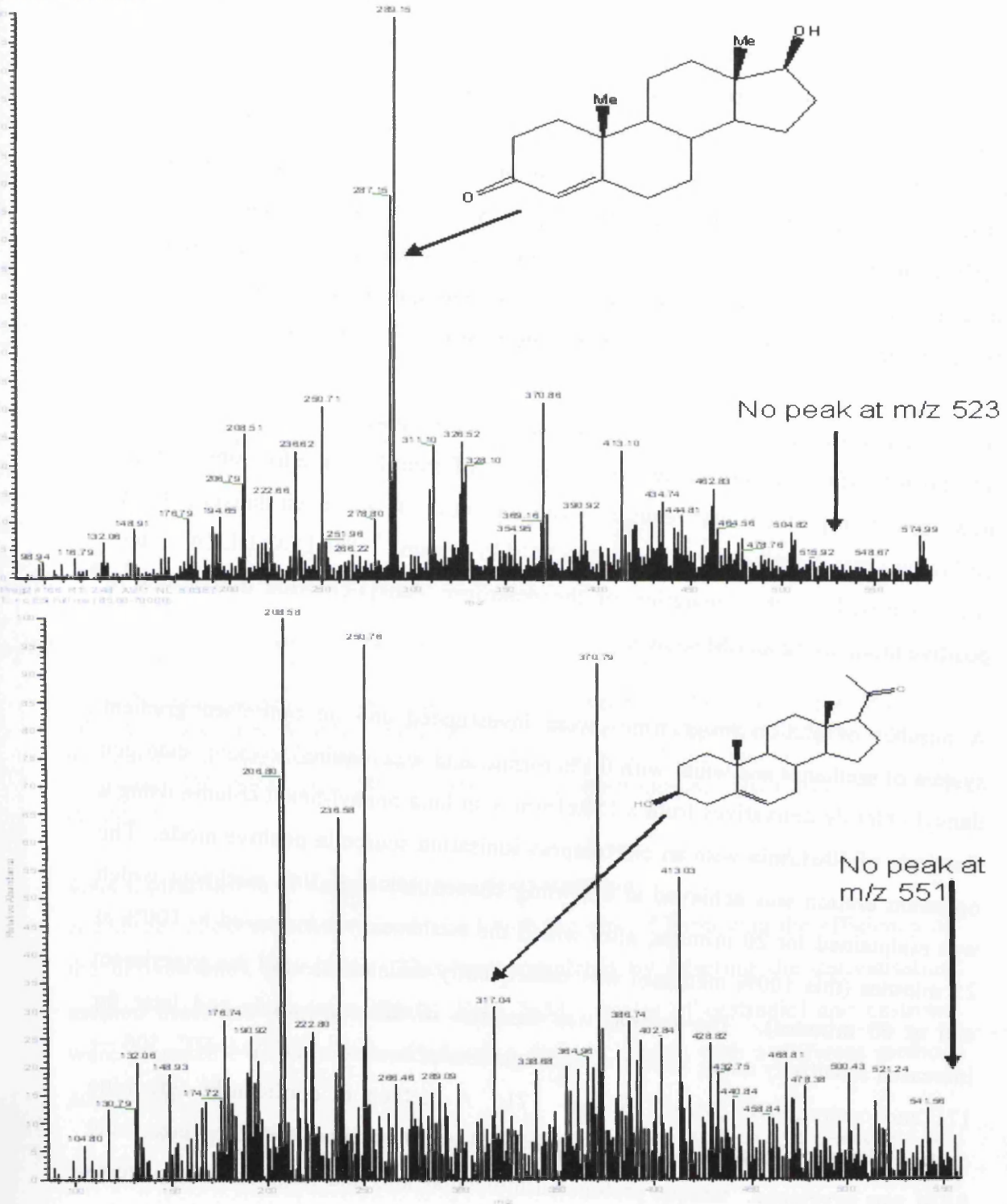

Fig 4.20: Full scan mass spectra of dansyl-chloride derivatised testosterone and dansyl chloride derivatised pregnenolone. Analysed on the LCQ DECA mass spectrometer with an ESI source in positive mode. No derivatisation has occurred as the calculated dansyl-chloride representative peaks at m/z 523 for testosterone and m/z 551 for pregnenolone were not present.

Figure 4.20 illustrates no hydroxyl group dansyl chloride derivatisation of testosterone or pregnenolone, as there were no peaks at the predicted derivatisation m/z values. In both spectra the protonated molecular ion of the underivatised steroid was abundant. The pregnenolone protonated molecular ion (figure 4.20) was less abundant than in the other spectra, this could be due to the reduced extraction efficiency of pregnenolone from the aqueous to the organic phase in the derivatisation procedure, this theory was further supported by the steroid extraction data described later in this chapter (4.14). Androgen and progestin analysis should therefore be completed prior to oestrogen derivatisation.

4.9.3 Separation of Oestrogen dansyl-chloride derivatives

The polarity of the derivatised oestrogens is now different from the free steroid and a new separation protocol was required. The separation of oestrogen dansyl chloride derivatives was described by Tai using an LC/MS system.[16] The LCQ DECA system was optimised for the separation of the oestrogen dansyl-chloride derivatives in positive mode using an ESI source.

A number of elution programmes were investigated and an optimised gradient system of methanol and water with 0.1% formic acid was required to elute oestrogen dansyl-chloride derivatives from a 150x1mm 3μm luna phenyl-hexyl column using a flow rate of 40μL/min with an electrospray ionisation source in positive mode. The optimum elution was achieved at a starting concentration of 70% methanol which was maintained for 20 minutes, after which the methanol was increased to 100% at 25 minutes (this 100% methanol was subsequently maintained until the experiment end at 60 minutes). The sample was first run in full scan mode and later for increased sensitivity using SRM for the fragments of oestradiol-DC $[M+H]^+$ 506 → 171 and oestrone-DC $[M+H]^+$ 504 → 171. A method to confidently determine oestradiol and oestrone, due to their unique molecular ions and retention times using SRM was developed. Unique protonated molecular ions and fragmentation patterns were observed for each DC-oestrogen, which in combination with unique retention times (figure 4.21) allowed positive, more sensitive identification of oestrogens by LC/MS in positive mode using an ESI source.

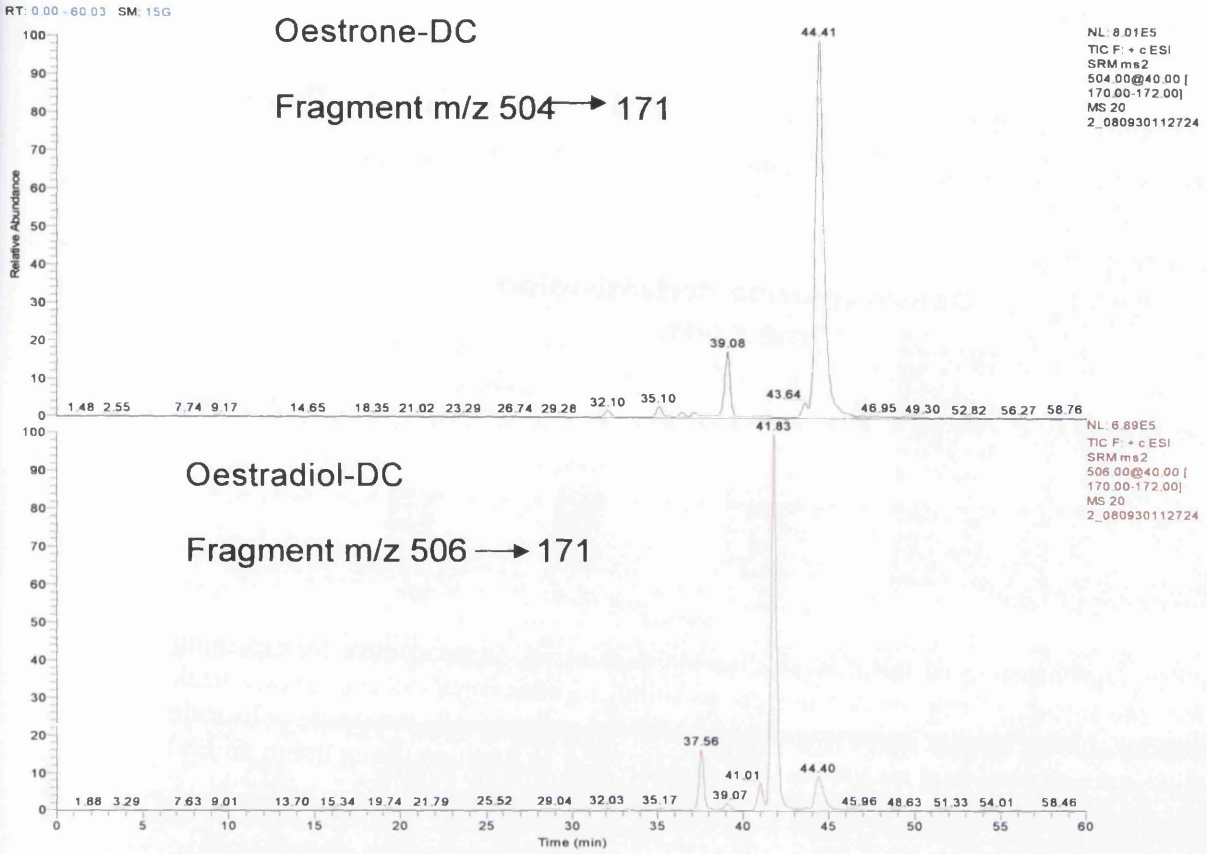

Fig 4.21: Separation of DC-oestradiol and DC-oestrone (2µM solutions) on the LCQ DECA mass spectrometer with an ESI source in positive mode using a methanol/water 0.1% formic acid using a150x1mm 3µ Luna phenyl hexyl column. Oestradiol-DC SRM m/z 506→171(top), and oestrone-DC SRM m/z 504→171 (bottom).

4.9.4 Optimisation of dansyl-chloride derivatisation

A number of experiments were devised with the aim of improving the efficiency of the derivatisation procedure. This was completed by adapting the derivatisation method described in chapter 3.10. Four 2µM samples of oestradiol and oestrone were prepared each was derivatised using dansyl-chloride with a different method adaptation;

1. (all) the whole derivatisation mixture was dried and analysed-without an extraction step
2. (2-butanol) 2-butanol was used as the extraction solvent (2-butanol was chosen as it was calculated as the optimum extraction solvent for solid phase extractions chapter 4.14),
3. (centrifuged) the derivatised mixture was centrifuged before analysis and,

4. (no buffer) derivatisation was undertaken without the sodium carbonate buffer.

These samples were then dried and reconstituted for LC/MS analysis. They were analysed using the optimised LC/MS separation procedure outlined previously.

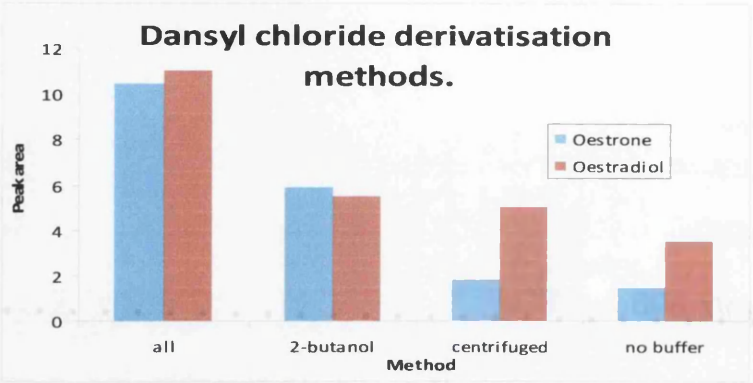

Fig 4.22: Optimisation of the dansyl-chloride derivatisation procedure by changing reaction conditions. Peak areas were proportional to concentration the largest peak area equates to the largest percentage conversion of oestrogen to the dansyl-chloride oestrogen species analysed on the LC/MS LCQ DECA in positive mode using an ESI source. Oestrone is represented in blue and oestradiol in red.

Figure 4.22 illustrated that the first derivatiastion procedure (all) was the most effective- this was analysis of the whole derivatisation mixture by LC/MS, however use of a guard column was needed to protect the analytical column from blocking. This method was adopted for all future derivatisations.

4.9.5 Limit of detection for dansyl-chloride oestrogens

The instrument's limit of detection for derivatised oestrogens was calculated by preparing a calibration series of oestradiol and oestrone, derivatised as described previously (4.9.4). Six samples ranging in concentration from 20μM to 500nM were analysed.

Table 4.16: Limit of detection and R^2 values for dansyl-chloride derivatised oestrogens. Analysed on the LCQ DECA mass spectrometer with an ESI source in positive mode.

Steroid	LOD nM	R^2
Oestradiol	316	0.9899
Oestrone	516	0.9806

These results significantly improve the oestrogen limits of detection using an LC/MS system. Previously Lin and colleagues determined that the use of dansyl chloride derivatisation increased LC/MS sensitivity to oestrogens by 1 or 2 orders of magnitude compared to the un-derivatised steroids.[17] A single instrument (LC/MS) can now be applied for full steroid analysis though C_{18} analysis of the androgens and Luna phenyl hexyl analysis of dansyl-chloride derivatised oestrogens.

4.10 Optimal steroid analysis methods

Table 4.17 outlines the optimum analysis methods for nine steroids and cholesterol. The optimum methods were determined through combination of a number of parameters, such as sensitivity of the mass spectrometer (limit of detection), complete separation and resolution of steroid standards. GC/MS analysis was required for cholesterol analysis all other steroids can be identified and quantified using the LC/MS system.

Table 4.17: Optimal analysis method for ten steroids. This table represents the ideal method for analysis in terms of sensitivity and resolution.

Steroid	Method	Requirements
Testosterone	LC/MS	ESI positive mode
DHT	LC/MS	ESI positive mode
Androstenedione	LC/MS	ESI positive mode
DHEA	LC/MS	ESI positive mode
Androsterone	LC/MS	ESI positive mode
Pregnenolone	LC/MS	ESI positive mode
Progesterone	LC/MS	ESI positive mode
Oestradiol	LC/MS	Dansyl chloride derivatisation ESI positive mode
Oestrone	LC/MS	Dansyl chloride derivatisation ESI positive mode
Cholesterol	GC/MS	EI positive mode

The results generated above were linked to recent literature via a number of sources, for example Leinonen and co-workers concluded that ESI was the ideal method for anabolic steroid analysis using a methanol/water elution system with acetic acid mobile phase additive, in comparison to other LC/MS ionisation methods,[18] agreeing with the results accumulated for androgen analysis.

A study by Díaz-Cruz and colleagues confirms the results regarding progesterone analysis, LC/MS (ESI) was superior in terms of limit of detection to GC/MS,[2] (it was conceivable that the same can be assumed for the chemically similar pregnenolone).

Anari and co-workers concluded that dansyl chloride derivatisation significantly improves LC/MS sensitivity to oestrogens, this was confirmed in these experiments.[14]

Part Two

Optimisation of extraction of steroids from biological samples

4.11 Optimisation of extraction procedures of steroids from biological samples

A number of extraction methods were investigated to determine which method extracts the widest variety of steroids most effectively as described in chapter 3.12. Initially an investigation into the solubility of the steroids in different solvents was completed.

4.12 Solubility of testosterone and pregnenolone in water and methanol

The solubility of testosterone and pregnenolone in methanol and water was determined as described in chapter 3.12.

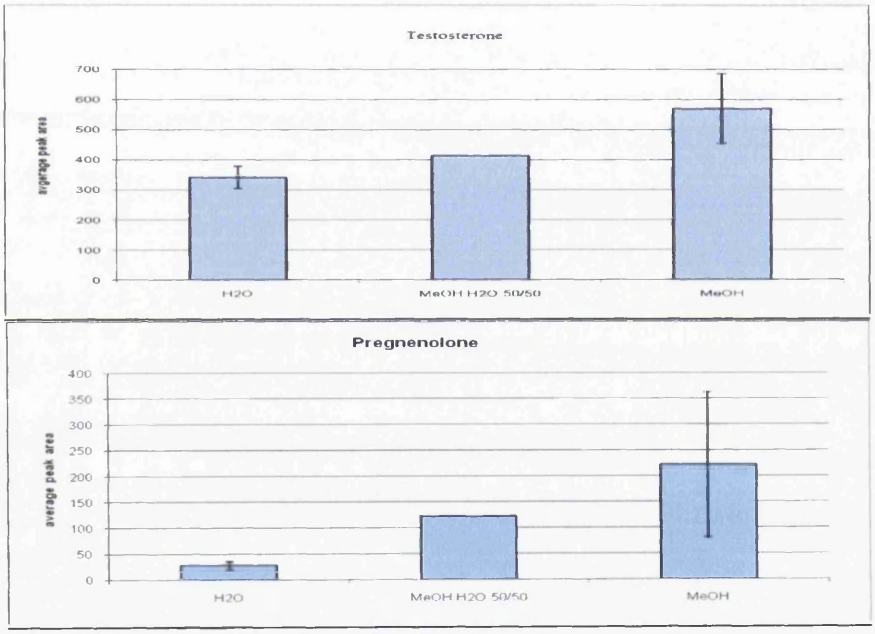

Fig 4.23: Top graph illustrates the solubility of testosterone in water, methanol/water (50/50) and methanol. Lower graph illustrates the solubility of pregnenolone in water, methanol/water 50/50 and methanol. Testosterone was more soluble in methanol than in water, with 50/50 solution having a mid-range value. Pregnenolone was more soluble in methanol than water with the half and half solution producing a mid-point value. All errors were calculated from the standard deviation of two experiments.

The percentage of organic solvent (compared to water) that steroids were dissolved in affects the concentration of the dissolved steroid. The higher the percentage of methanol in the mixture the higher the concentration of dissolved steroid. Twice as

much testosterone dissolved in methanol when compared to water, and approximately ten times the amount of pregnenolone was dissolved in methanol in comparison to water alone (figure 4.23). In the 50/50 methanol/water samples both steroids produced a mid-point concentration between the high dissolved concentrations recorded in methanol and the lower dissolved concentrations in water.

From figure 4.23 it was concluded that addition of steroids to cells (via cell media) should not be completed with the steroid as a solid or in a water solution. The ideal method was to dissolve the steroid in methanol (or other organic solvent) and add a minimal volume to the cell media. A concentration of less than 0.1% methanol in the cell media should have no negative effect on the cells, (a high methanol concentration would kill the cells).

After experiments were completed and steroids extracted solutions should be prepared in 50/50 methanol/water for LC/MS analysis. This was to reduce evaporation effects from the auto-sampler tray, and to ensure chromatographic performance was not affected which may occur with a 100% methanol solution.

4.13 Cell media extractions- simple steroid extraction methods

The optimum solvent for a wide range of steroids will remove all steroids, (androgens, oestrogens and progestins) from an aqueous solution with the highest possible percentage recovery of each. This extraction procedure can then be applied to extract steroids from cell media.

To calculate the optimum extraction solvent for simple liquid-liquid steroid extractions two steroids which widely differed in the elution sequence were chosen (testosterone and pregnenolone). The method for determination of optimum steroid extraction solvent was outlined in chapter 3.12.

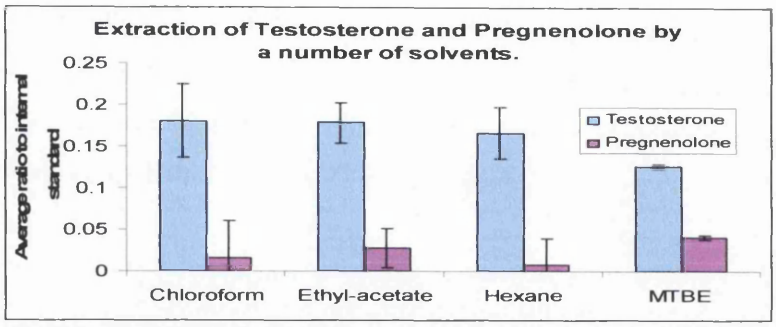

Fig 4.24: Relative extraction efficiencies of different solvents for testosterone and pregnenolone extraction from a water solution. Average peak area to an internal standard was plotted against the solvent used for extraction (chloroform, ethyl-acetate, hexane and MTBE), analysed by LC/MS in positive mode using an ESI source. Testosterone is represented in blue and pregnenolone in purple.

Ethyl-acetate was the most effective extraction solvent for testosterone, pregnenolone was extracted most effectively by MTBE. MTBE was the least effective solvent for testosterone extractions although it has been widely used previously.[19] The errors associated with pregnenolone were very high because of the lack of solubility and poor extraction of pregnenolone from the aqueous to the organic phase. As a compromise ethyl-acetate extracts both pregnenolone and testosterone in relatively high amounts and is therefore the solvent of choice for steroid extractions from water based samples.

This investigation was developed to analyse the cell media as cell media was mainly water, however many other substances were added to the media, including antibiotics, glutamine, nutrients, foetal calf serum, and other minor components. A number of steroids were added to the Ishikawa cell media (5mL of DMEM, without any added constituents), and 5mL of DMEM with full additions (antibiotic, glutamine, sodium bicarbonate, sodium pyruvate and 10% foetal calf serum as described in table 2.5). The samples were then extracted at least twice with ethyl-acetate evaporated to dryness and reconstituted in methanol/water 50/50 0.1% acetic acid for analysis by LC/MS.

Extraction of steroids from the DMEM sample (without additives) proved effective, but extraction was not possible from the media with additives. This was probably due to foetal calf serum in the media causing a suspension to form in the ethyl-

acetate, causing incomplete separation of the organic and aqueous layers, centrifuging the sample reduced this but the extraction was still ineffective. Steroids cannot be extracted effectively from media containing these additives by liquid-liquid extractions, a solid phase extraction method was developed to overcome this problem.

4.14 Development of solid phase extraction for the extraction of steroids from liquids

Solid phase extraction (SPE) was adopted as the method to extract steroids from cell media which contained interfering substances such as foetal calf serum. SPE has been widely used in steroid chemistry for a number of applications from the drug abuse detection industry in cattle and athletes to oxy-steroid concentrations in neural human biology.[20] The solid phase acts as a barrier to the interfering substances and so they were no longer problematic to the extraction procedure. The SPE procedure itself was initially investigated followed by its application to cells and cell media.

4.14.1 Solid phase extraction method validation

The SPE procedure was investigated using a 1mL solution of a 1μM mixture of pregnenolone and testosterone in water/methanol (50/50). This was completed using the SPE procedure outlined in chapter 3.13. The extracts were evaporated to dryness and re-constituted in 50/50 methanol/water 0.1% acetic acid for LC/MS analysis in positive mode using an electrospray ionisation source.

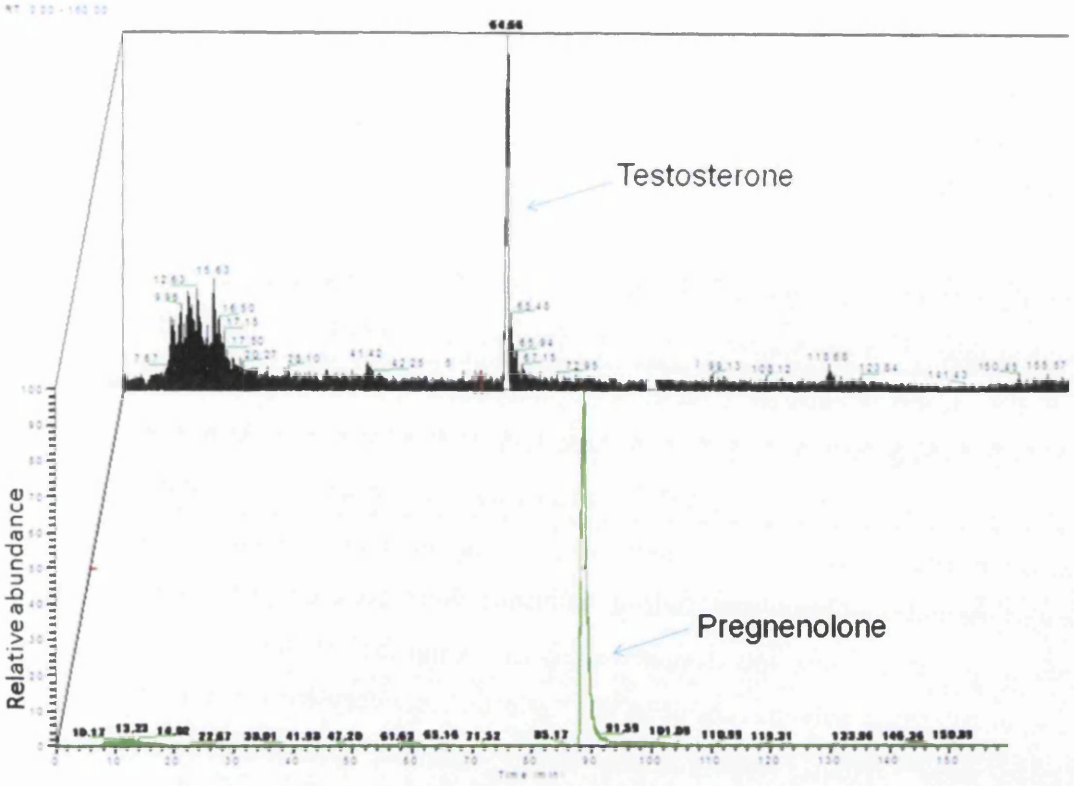

Fig 4.25: Separation of testosterone and pregnenolone after solid phase extractions from 1μM solutions, using the LCQ DECA with an ESI source in positive mode.

1μM to 50nM solutions of testosterone and pregnenolone in water were effectively extracted from water based solutions by SPE and detected by LC/MS. Further optimisation of the technique was conducted to determine the percentage recovery of these steroids and the optimum elution solvent.

4.14.2 Solid phase extractions of steroids from cells

Steroid extractions from cells did not yield high steroid concentrations after pregnenolone, testosterone and oestradiol additions (100nM concentrations). It was concluded that steroids were not present in the cells themselves in high concentrations, probably due to their lipophillic nature therefore this procedure was not optimised.

4.14.3 Optimisation of solid phase extractions of steroids from cell media

Solid phase extractions of steroids from cell media samples were optimised from the original procedure outlined in chapter 3.13 using different polarity wash solvents for

the final SPE steroid elution step. The elution wash was investigated to improve extraction efficiency of steroids from cell media, previously Cho and co-workers improved the recovery of urinary steroids by changing the elution solvent when using an Oasis HLB column.[21]

To optimise steroid extraction using C_{18} SPE cartridges, the 85% methanol wash step was investigated as described in chapter 3.13. The use of a number of solvents with a range of polarities were investigated, these were methanol, 2-butanol and ethyl-acetate with polarity indices of 5.1, 4 and 5.8, respectively. The SPE procedure was completed as previously defined with the 40% methanol wash extended to remove all traces of phenol-red after which 2mL of methanol, 2-butanol or ethyl-acetate was used to elute the steroids. The eluted steroid solutions were then evaporated to dryness and reconstituted for mass spectrometry analysis. A number of steroids were investigated to define which solvent produced the optimum recovery for a range of steroids. These were DHEA, androsterone, DHT, oestrone, androstenedione, oestradiol, pregnenolone, testosterone and progesterone. The control sample was a steroid sample prepared in methanol and analysed directly (no sample loss due to experimental procedures).

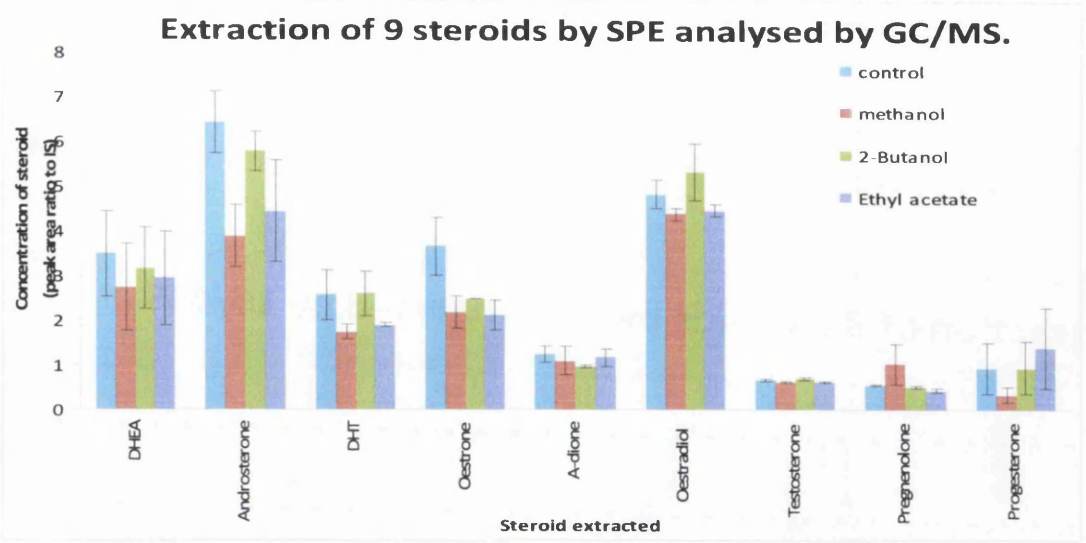

Fig 4.26: Extraction efficiency of nine steroids by SPE using three different solvents methanol, 2-butanol and ethyl-acetate. The control was a non-SPE 100% steroid solution. The peak area (proportional to concentration) was expressed as a ratio to the internal standard methyl testosterone. These results were from the GC/MS MD800 in positive mode using an EI source. Errors were produced from the standard deviation of the peak area ratio to an internal standard of two experiments.

Table 4.18: Percentage recovery of steroids when extracted by SPE using three different elution solvents analysed on the GC/MS MD800 with an EI source. Percentage recovery was calculated by assuming the control sample steroids produce a peak area representative of 100% recovery. The percentage recovery for the other steroids was relative to the contol sample.

Solvent	Recovery of steroids from SPE. (%)								
	DHEA	Andro sterone	DHT	E1	Androstene dione	E2	Testosterone	Pregnenolone	Progester one
Methanol	78.7	60.3	67.4	59.4	89.4	90.7	91.6	189	36.6
2-butanol	90.7	89.8	101	68.4	77.7	110	103	91.9	101
Ethyl-acetate	84.3	69.0	73.3	58.0	94.6	92.5	92.3	78.0	149

From the figure 4.26 and table 4.18 it was possible to determine the extraction efficiency (% recovery) for all the steroids investigated when analysed by GC/MS MD800. It can be concluded that 2-butanol was the optimum elution solvent as a range of percentage recoveries were obtained which were all over 68% with an average recovery value of 92.7% compared to 84.9% for methanol and 87.8% for ethyl-acetate.

The same samples were also subjected to LC/MS analysis. The LC/MS results (figure 4.27 and table 4.19) agree with the GC/MS results, confirming that 2-butanol was the optimum solvent for maximum steroid elution from the SPE cartridges (as this was non-derivatised LC/MS technique oestradiol was not included).

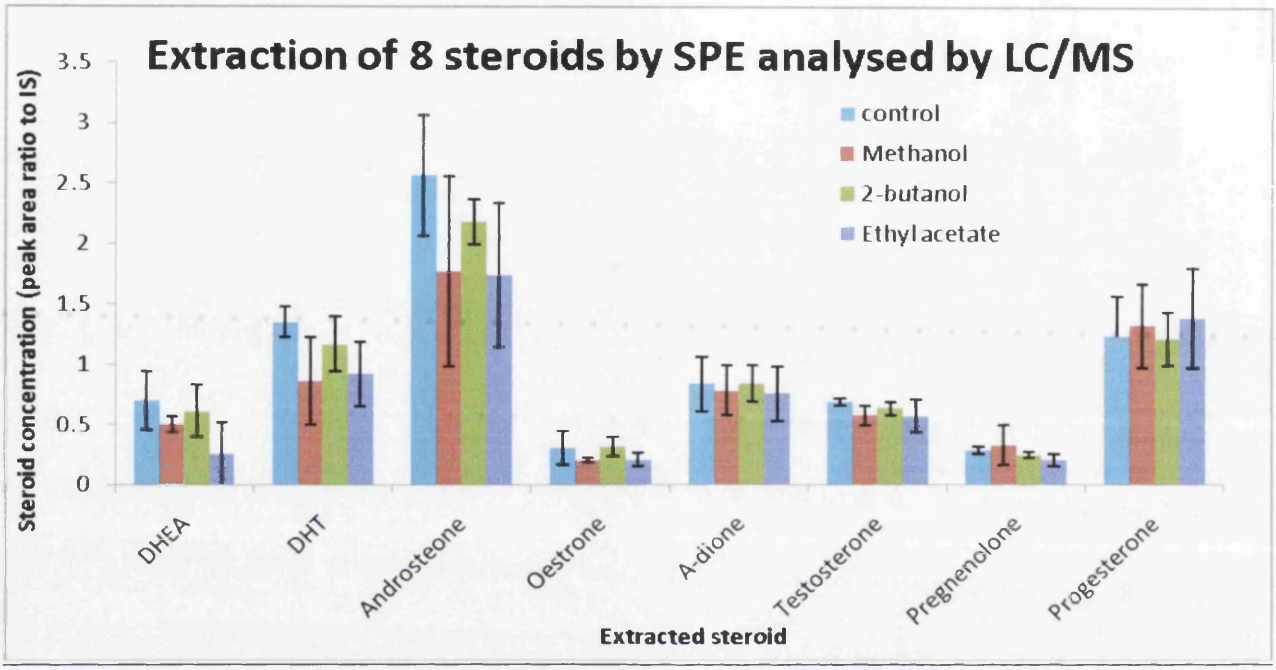

Fig 4.27: Extraction efficiency of eight steroids by SPE using three different solvents methanol, 2-butanol and ethyl-acetate. Control is a non-SPE 100% steroid solution. The peak area (proportional to concentration) was expressed as a ratio to the internal standard methyl testosterone. These steroids were detected on the LCQ DECA with an ESI source in positive mode. Errors were produced form the standard deviation of the peak area ratio to an internal standard of two experiments.

Table 4.19: Percentage recovery of steroids from SPE cartridges using methanol, 2-butanol and ethyl-acetate analysed on the LCQ DECA mass spectrometer using an ESI source in positive mode. Percentage recovery was calculated by assuming the control sample steroids produce a peak area representative of 100% recovery. The percentage recovery for the other steroids was relative to the control sample.

Solvent	Recovery of steroids from SPE. (%)							
	DHEA	DHT	Andro sterone	E1	Androstene dione	Testosterone	Pregnenolone	Progester one
Methanol	72.2	63.7	69.0	65.6	93.4	83.3	115.0	107
2-butanol	87.9	86.4	85.0	103	100.1	92.5	87.1	97.9
Ethyl-acetate	36.6	68.0	67.8	68.1	90.1	82.8	71.4	112

The percentage recoveries vary compared to those calculated for GC/MS, this was because of the differing sensitivities of each technique to different steroids. Oestradiol (E2), for example, was not detectable in LC/MS, and LC/MS analysis was more sensitive to progesterone. The overall average recoveries were similar for both techniques, the methanol average percentage recovery was 83.7%, 2-butanol was 92.5% and ethyl-acetate was 74.6% in LC/MS compared to 84.9, 92.7 and 87.8% for methanol, 2-butanol and ethyl-acetate respectively via GC/MS MD800. Both data sets conclude that 2-butanol was most effective solvent for multiple steroid extractions, as a result of this 2-butanol was employed as the steroid elution solvent for all SPE processes in these experiments.

4.15 Conclusions

The detection, extraction and derivatisation of steroids has been fully optimised and validated. These optimised methods were subsequently applied to biological samples to determine the steroid profiles and concentrations of each steroid in that profile.

The optimisation of steroid standard mass spectrometry techniques and determination of limit of detection of each steroid in each mass spectrometer permits the confident, positive, identification of steroids in water, cells and cell media. Quantitative determination of androgens and progestins in biological samples can now be assigned through calibration methods. Derivatisation of oestrone and oestradiol was completed and optimised allowing for identification and quantitation of oestrogens in biological samples.

The extraction methods of steroids from cell media has been adapted and optimised. The percentage recovery of steroids from media with foetal calf serum was now increased from virtually zero (liquid-liquid method) to an average recovery of more than 92% for a mixture of androgens, oestrogens and progestins (SPE method), producing an effective extraction procedure. The SPE method produced high recovery, clean extracts and should be routinely used in steroid extractions from complex matrices such as cell media.[22]

4.16 References Chapter Four

[1] Makin HLJ, Mass Spectra of Androgens, Estrogens and Other Steroids (2005) Wiley-Blackwell Databases.

[2] Díaz-Cruz MS, López de Alda MJ, López R, Barceló D. J MS **38** (2003) 917-923

[3] Gao S, Zhang Z-P, Karnes HT. J Chrom B **825** (2005) 98-110

[4] Agilent Technologies HPLC Application Guide and Glossary of Terms (2008). Viewed 25th November 2008 http://www.chem.agilent.com/Library/articlereprints/Public/FInal%20Advanstar%20HPLC%20Application%20Notebook.pdf

[5] Chang H, Wu S, Hu J, Asami M, Kunikane S. J Chrom A **1195** (2008) 44-51

[6] Nagaoka M, Numazawa M. Steroids **70** (2005) 831-839

[7] Scott RPW. Quantitative Chromatographic Analysis. Chrom-Ed series. Pub Library4Science, UK (2007) accessed on-line 26th November 2008 http://www.chromatography-online.org/quant/Reference-Standards/GC-and-LC/Internal-Standard-Method.html

[8] Lieberman HA, Rieger MM, Banker GS. Pharmaceutical Dosage Forms. Validation of disperse systems. Second Edition (1998) 509-510

[9] Van Renterghem P, Van Eenoo P, Van Thuyne W, Geyer H, Schänzer W, Delbeke FT. J Chrom B **876** (2008) 225-235

[10] Yuan X, Forman BM, Nuclear Receptor Signalling **3** (2005) e002

[11] WADA Technical Document- TD2004EAAS (2004)

[12] Le Bail JC, Lotfi H, Charles L, Pépin D, Habrioux G. Steroids **67** (2002) 1057-1064

[13] Gomes RL, Avcioglu E, Scrimshaw MD, Lester JN. Trends in Analytical Chemistry **23** (2004) 737-744

[14] Anari MR, Bakhttiar R, Zhu B, Huskey S, Franklin RB, Evans DC. Anal chem. **74** (2002) 4136-4144

[15] Xu X, Keefer LK, Ziegler RG, Veenstra TD. Nature Protocols **2** (2007) 1350-1355

[16] Tai S S-C, Welch MJ, Anal Chem **77** (2005) 6359-6363

[17] Lin Y-H, Chen C-Y, Wang G-S. Rapid Comm in Mass Spec **21** (2008) 1973-1983

[18] Leinonen A, Kuuranne T, Kostiainen R J MS **37** (2002) 693-698

[19] Xu CL, Chu XG, Peng CF, Jin ZY, Wang LY. J Pharma Biomedical Anal **41** (2006) 616-621

[20] Griffiths WJ, Liu S, Yang Y, Purdy RH, Sjövall J. Rapid Comm Mass Spect **13** (1999) 1595-1610

[21] Cho Y-D, Choi MH. Bull Korean Chem Soc **27** (2006) 1315-1322

[22] Grob RL, Barry EF. Modern Practice of Gas Chromatography. Fourth Edition (2004) 559-563 accessed on-line 25th November 2008 http://books.google.co.uk/books?id=DU_sglfMX6oC&pg=PA559&lpg=PA559&dq=SPE+vs+liquid-liquid+extractions&source=web&ots=QtzWZQCdMA&sig=TTaL0NCNboQovA05OFcuqT7Gsjg&hl=en&sa=X&oi=book_result&resnum=2&ct=result#PPA563,M1

Chapter Five

Steroid metabolism by endometrial cancer established cell lines, and endometrial biopsies

5.0 Introduction

This chapter describes the metabolism of testosterone by the endometrial cancer cell lines Ishikawa, HEC-1A, HEC-1B, and RL95-2 as well as the ovarian granulosa cell line COV434. These cell lines were used to determine the optimum methods for analysis of steroid profiles through mass spectrometry. Steroid concentrations were determined from the optimised calibration experiments outlined in chapter 4.2, using the internal standard methyl-testosterone.

These experimental methods were subsequently applied to endometrial biopsy samples to determine steroid profiles (and enzyme expression-chapter 6) from women with endometriosis, PCOS and ovarian cysts, unexplained infertility, endometrial polyps, and moderate atypical hyperplasia, a fertile group was also analysed.

This chapter will present cell line and biopsy experiments principally focussing on the utilisation of testosterone. The data is presented as follows;

Cell lines;

- Preliminary experiments to investigate the metabolism of pregnenolone, testosterone and oestradiol.
- Experiments regarding the utilisation of testosterone in established cell lines.
- Androgen and oestrogen production in established cell lines following testosterone treatment.
- Kinetics relating to production/metabolism of specific steroids.
- Conclusions (cell lines).

Biopsies;

- Experiments regarding the utilisation of testosterone in biopsies from fertile, endometriosis, PCOS, ovarian cyst and unexplained infertility.
- Androgen and oestrogen production in fertile biopsies (and a tubual disorder biopsy) following testosterone treatment.
- Androgen production in endometriosis, PCOS, ovarian cyst and unexplained infertility biopsies following testosterone treatment.
- Oestrogen production in endometriosis, PCOS, ovarian cyst and unexplained infertility biopsies following testosterone treatment.

- Testosterone utilisation in an endometrial hyperplasia biopsy.

- Androgen and oestrogen production in an endometrial hyperplasia biopsy following testosterone treatment.

- Testosterone utilisation in an endometrial polyp biopsy.

- Androgen and oestrogen production in an endometrial polyp biopsy following testosterone treatment.

- Conclusions biopsies.

5.1 Steroid Metabolism

Evidence suggests that the precursors to oestrogen synthesis in the endometrium are the androgens testosterone and androstenedione, which are present in normal and proliferative endometrium.[1] The majority of testosterone and androstenedione are synthesised outside the endometrium, for example in the ovary, adrenal glands or adipose tissue which enter the endometrium via the circulatory system. The conversion of these steroids to other androgens and oestrogens is described in figure 5.1.

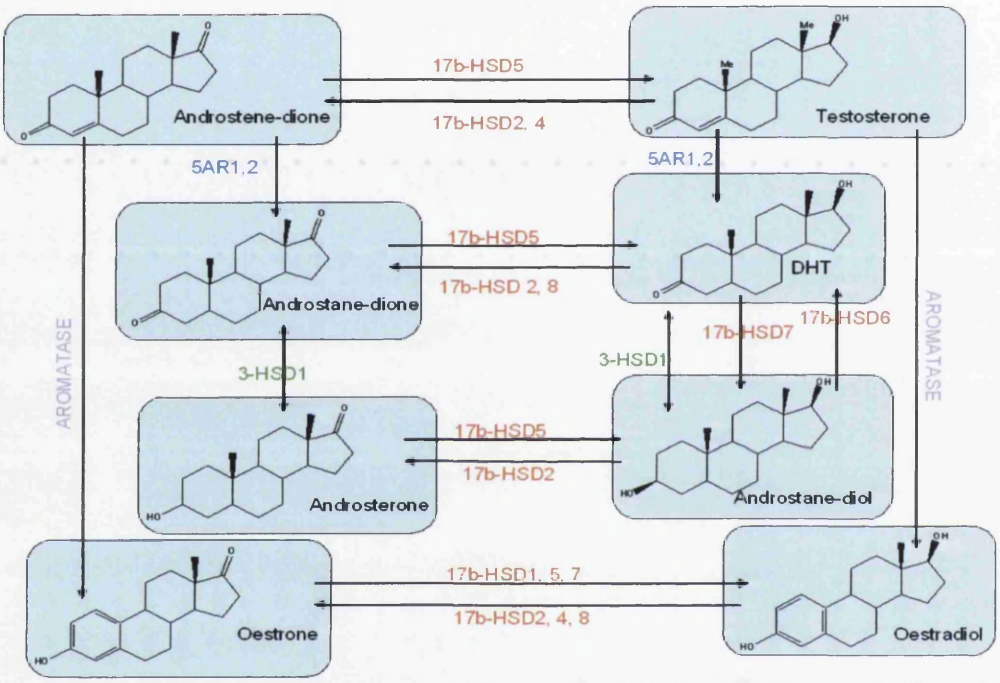

Fig 5.1: Suggested pathway of testosterone and androstenedione metabolism through steroid converting enzymes into androgens and oestrogens (the major reactions were determined from a literature search references 2, and 13-31 chapter 1). 17b-HSD = hydroxy steroid dehydrogenase which acts on position 17 of the steroid ring 3-HSD acts at position 3 (the number after the name donates the isoform). 5AR = five alpha reductase two isoforms 1 and 2. Aromatase is the rate limiting enzyme in the conversion of androgens to oestrogens.

All the HSD's mentioned in this chapter and throughout this thesis are isoforms of 17β-HSD, however to simplify the information they are expressed as HSD1, HSD2 etc.

5.2 Established cell lines: an introduction

Endometrial established cell lines have been widely used as models for studying steroid metabolism and gene expression in human endometrium.[2] All endometrial

cell lines investigated in these experiments were representative of type one cancers which typically develop from endometrial hyperplasia associated with oestrogen exposure.[3] The ovarian cell line COV434 was incorporated as it has been previously demonstrated to highly express aromatase and was employed as a positive control.[4]

5.2.1 Ishikawa cells

Ishikawa cells are a model of type one endometrial cancer derived from an endometrial adenocarcinoma in a 39 year old woman. Ishikawa cells have been widely used by numerous groups over the last twenty years.[5]

5.2.2 RL95-2 cells

RL95-2 are uterine epithelial adenosquamous cells, isolated from a 65 year old woman with grade 2 (moderately differentiated) cancer in the early 1980's.[6] These endometrioid cells grow quickly upwards in island-like formations.

5.2.3 HEC-1A and HEC-1B cells

HEC-1A and HEC-1B are similar endometrial epithelial adenocarcinoma cell lines isolated in 1968 from a grade two, endometrial carcinoma in a 71 year old woman. HEC-1B is a sub-strain of HEC-1A, the cells in the HEC-1B strain are flatter and more 'pavement' like than HEC-1A which tend to grow upwards in islands.[7] The metabolism of steroids in these cell lines may not be identical due to differences in steroid converting enzyme expression.

5.2.4 COV434 cells

The COV434 established cell line was established in 1984 from a 27 year old woman with primary ovarian granulosa cell tumour. These cells grow quickly upwards in islands. Ovarian granulosa cells are involved in the formation of the ovarian follicle, as well as conversion of androgens to oestrogens and progesterone production.[4]

5.3 Endometrial biopsies

Biopsy samples were analysed using optimised experimental procedures developed using the cell lines to produce quantitative steroid (and enzyme expression) profiles. As many patient biopsies as possible from each of the groups described in chapter one were collected (fertile and tubual disorders, PCOS, endometriosis, unexplained

infertility). Where this was not possible case studies were investigated (endometrial hyperplasia, endometrial polyp, ovarian cyst). All endometrial biopsies investigated were stromal cells (except one epithelial endometrial hyperplasia biopsy).

5.4 Steroid profiles of established cell lines

Each cell line was initially analysed to determine the steroid profile under basal conditions as described in chapter 3.14. This was completed through optimised extractions (SPE-chapter 4.14) of the culture medium following exposure to cells for 48 hours which was subsequently analysed by optimised liquid chromatography and gas chromatography mass spectrometry (chapter 4).

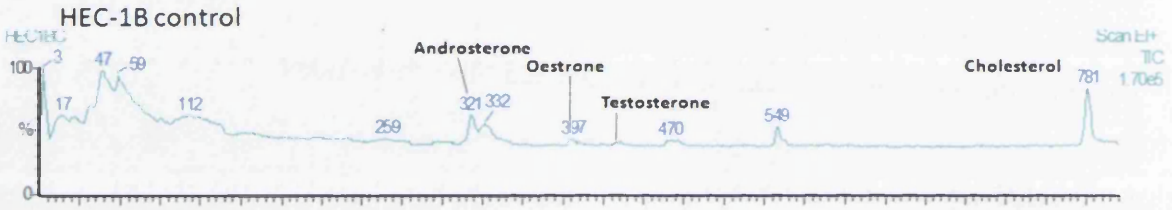

Fig 5.2: Illustrative chromatogram showing the detection of steroids in HEC-1B cell media. Androsterone, oestrone, testosterone and cholesterol were observed in HEC-1B cell media without addition of steroid precursor. Analysed using optimised procedures on the GC/MS MD800 mass spectrometer in positive mode using an EI source, (the numbers of the chromatogram refer to the retention time (seconds) of each peak).

Table 5.1: Steroid present in cell media of the established cell lines under basal conditions.

Cell line	Steroids detected
Ishikawa	Testosterone, DHT, Androsterone, Androstenedione Oestradiol, Oestrone
HEC-1A	Testosterone, DHT, Androstenedione, Androsterone Oestradiol,Oestrone
HEC-1B	Testosterone, Androsterone Oestrone Cholesterol
RL95-2	Androsterone, Testosterone Oestradiol, Oestrone
COV434	Testosterone, Androstenedione, DHT Oestradiol, Oestrone

The steroid profiles calculated in table 5.1 (no added steroids) represent steroids present under basal conditions, the presence of some of these steroids is due to foetal

calf serum (FCS) which was added to cell media as it is essential for optimum cell growth. These steroids can be removed by charcoal stripping the serum, however this process does not remove 100% of all steroids and it also removes growth factors which aid cell growth (which were important for growth of endometrial biopsies). Addition of steroids to the cell media were completed to determined the routes of steroid metabolism, three steroids were chosen for initial analysis these were pregnenolone, testosterone and oestradiol.

The metabolism of pregnenolone, testosterone and oestradiol by endometrial cell lines was investigated because,

1. pregnenolone is the precursor to androgen and oestrogen synthesis and production,[8]
2. testosterone is a major circulatory androgen,[9]
   - increased testosterone concentration has been recorded in the ovarian veins of women with endometrial cancer,[10]
   - testosterone is present at higher concentrations in endometrial tumours than in the circulatory system,[11]
   - increased circulatory testosterone concentration is associated with increased risk of developing endometrial cancer in postmenopausal women,[12]
   - testosterone is present at increased concentrations in the circulatory system of women with PCOS,[13]
   - testosterone is a precursor to oestrogens in the normal and proliferative endometrium and,[1]
3. oestradiol is the most potent oestrogen responsible for proliferation and progression of endometrial cancer,[14] and is implicated in benign endometrial conditions such as endometriosis.[15]

5.5 Treatment of Ishikawa and HEC-1B cells with pregnenolone, testosterone and oestradiol

The HEC-1B and Ishikawa cell lines were treated with 100nM solutions of pregnenolone, testosterone and oestradiol and the metabolites recorded as described in chapter 3.14. 100nM of each steroid (above biological concentration) was added to allow for low concentration products to be detected using the mass spectrometer.

Table 5.2: Steroids produced after treatments of HEC-1B and Ishikawa cells with 20mL 100nM media solutions of oestradiol, testosterone and pregnenolone.

Cell line	Steroid added (100nM concentration)	Steroids Detected
Ishikawa	Pregnenolone	Pregnenolone
HEC-1B	Pregnenolone	Pregnenolone
Ishikawa	Testosterone	Testosterone, Androstenedione, DHT, Androsterone
HEC-1B	Testosterone	Testosterone, Androstenedione, DHT, Androsterone
Ishikawa	Oestradiol	Oestrone, Oestradiol
HEC-1B	Oestradiol	Oestrone, Oestradiol

Pregnenolone was not metabolised into any other steroids when added to Ishikawa or HEC-1B cells. This suggests that the enzymes responsible for pregnenolone metabolism, P450c17 is absent in Ishikawa and HEC-1B cells. There is some literature which describes expression of P450c17 in the placental cell line JEG-3, but to our knowledge there is no evidence of expression in Ishikawa or HEC-1B cells or in the endometria,[16] therefore any steroid production in the endometrium would require a precursor distal to pregnenolone in the metabolic pathway, circulatory testosterone and androstenedione have been suggested as such precursors.[11]

Addition of oestradiol to Ishikawa and HEC-1B cells resulted in an increase in oestrone concentration. Previous studies by Chetrite and colleagues with the Ishikawa cell line determined that the majority of added oestradiol was metabolised into the sulphated (excretion) product via the enzyme oestrogen sulphotransferase.[5] However, at high oestrogen concentration the sulphotransferases become saturated and instead oestradiol was converted to oestrone by the oxidative HSDs (17β-HSD2, 4, 8) observed in figure 5.3. This was not pursued as the major objective was to explore utilisation of testosterone by endometrial cells, however this would be an ideal experiment for future work.

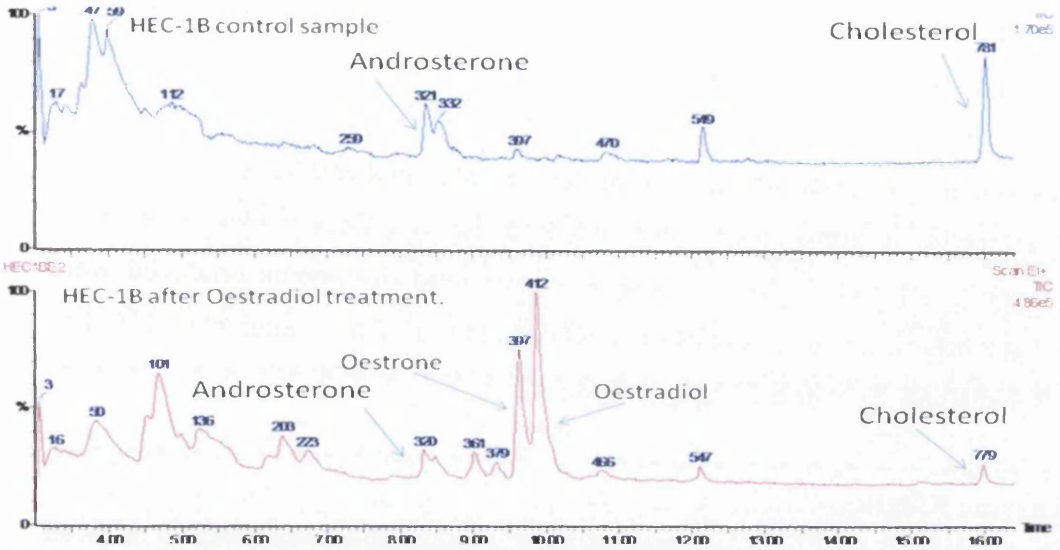

Fig 5.3: Chromatograms of HEC-1B cell lines before (top) and 72 hours after treatment with oestradiol (below) using the GC/MS MD800 mass spectrometer with an EI source in positive mode. The top chromatogram shows androsterone and cholesterol present in cell media prior to steroid treatment, the lower chromatogram has two major peaks these were due to oestradiol and oestrone (chromatograms are scaled to the most abundant peak= 100).

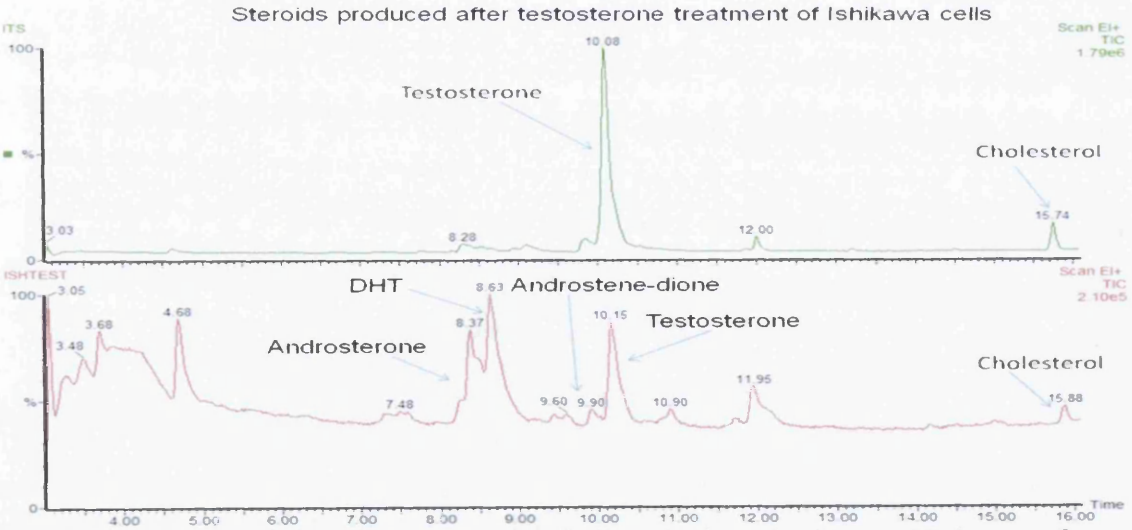

Fig 5.4: Chromatograms for Ishikawa cell lines before (top) and 48 hours after treatment with testosterone (below) using the GC/MS MD800 mass spectrometer with an EI source in positive mode. The top chromatogram shows testosterone before addition to the cells and the lower chromatogram shows production of androsterone, DHT and androstenedione.

These initial experiments revealed that testosterone produced the most informative steroid profile (the metabolites androstenedione, androsterone, and DHT were recorded figure 5.4). This experiment was extended to include more data points over

the 72 hour period permitting calculation of time dependent steroid production. The experiments were also adapted to include testosterone treatments of the established cell lines HEC-1A, RL95-2 and COV434.

5.6 Metabolism of testosterone in endometrial established cell lines

100nM solutions of testosterone were added to the cell lines Ishikawa, RL95-2, HEC-1A, HEC-1B and COV434. The androgens and oestrogens produced were recorded at 8 hour intervals (Ishikawa and COV434) and 12 hour intervals (HEC-1A, HEC-1B and RL95-2) over a 72 hour period.

5.6.1 Enzyme Kinetics

The rate of production of each steroid and its subsequent conversion rate (if observed) was calculated by analysing the change in steroid concentration over time.

If a reaction is first order the rate of reaction is dependent on the concentration and all time points and concentrations will fit the equation,

$$Ln\left(\frac{C_0}{C_t}\right) = kt \qquad \text{(equ 5.1)}$$

where C_0 is the concentration at time zero and C_t is the concentration at time t. t is time and k is the rate constant. A plot of $Ln(C_0/C_t)$ against time will produce a linear line if the reaction was first order as demonstrated in figure 5.5.

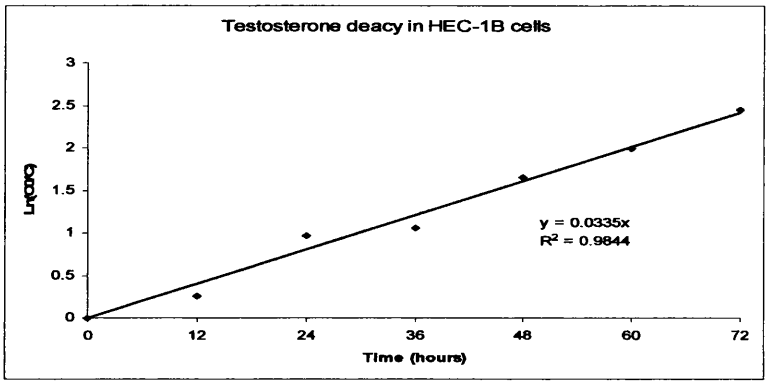

Fig 5.5: Illustration of a model first order decay of testosterone by the HEC-1B cell line.

Graphs similar to figure 5.5 were produced for each cell line, where possible, permitting calculation of kinetic data for testosterone utilisation. C_0 is not always set

at 0 hours, this is due to some steroids not being present at the start of the reaction and so C_0 has to be adjusted, in order to fit the equation.

5.7 Testosterone utilisation in established cell lines

Testosterone utilisation in each cell line was compared to provide information about differential utilisation of testosterone during the 72 hour treatment period.

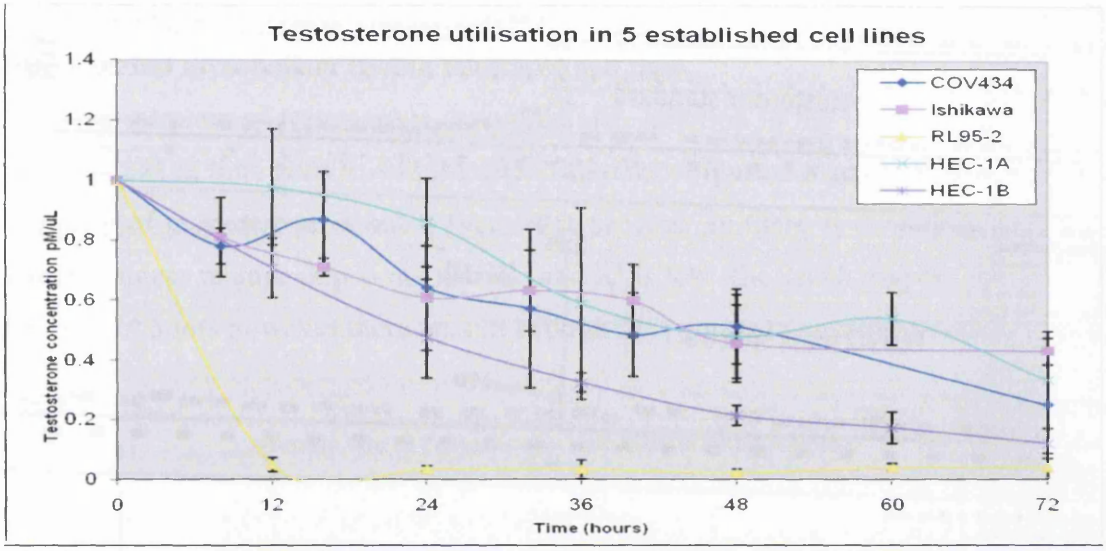

Fig 5.6: The reduction in testosterone concentration in Ishikawa (pink), COV434 (dark blue), RL95-2 (yellow), HEC-1A (light blue) and HEC-1B (purple) cell lines over 72 hours after addition of a 100nM testosterone media solution. Steroids were extracted from 10mL of cell media at each time point. Concentrations of testosterone were obtained by LC/MS using the ESI source on the LCQ DECA mass spectrometer in positive mode using methyl-testosterone as an internal standard.

Testosterone concentrations decreased over time in all cell lines, suggesting it was metabolised to other products (these products are defined in the next section). The percentage converted after 72 hours was similar in Ishikawa 57% and HEC-1A 67% cells. 75% of the testosterone has been converted after 72 hours in the COV434 cell line. The HEC-1B cell line converts 88% of the testosterone to other products in the 72 hour time period. The cell line RL95-2 metabolises the largest amount of testosterone 96% conversion to other products within the first 12 hours. To determine the nature of these products LC/MS and LC/MS/MS experiments were completed (described in chapter 4.2).

The diagram below (figure 5.7) illustrates positive identification of testosterone in RL95-2 cells due to comparative retention times to testosterone and identical mass spectra.

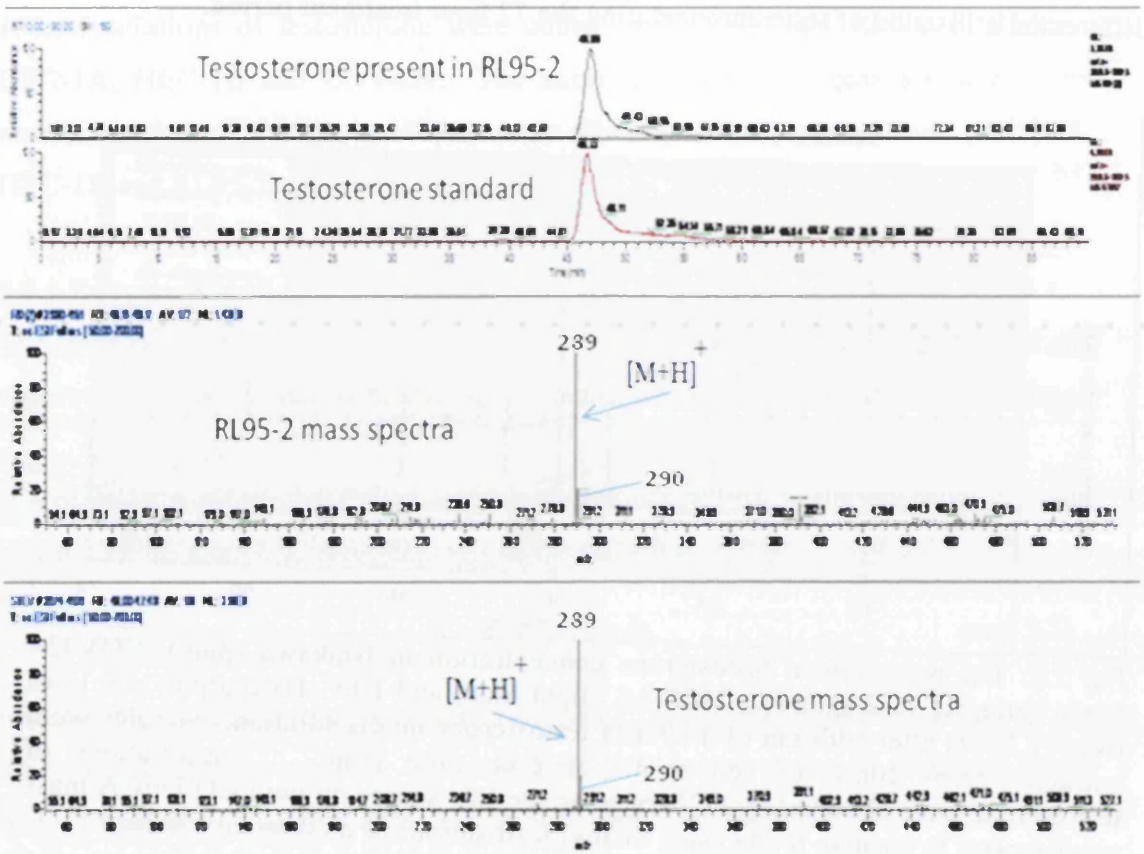

Fig 5.7: Top chromatogram and spectra shows positive determination of testosterone in RL95-2 cells via matching chromatogram and mass spectra. Obtained on the LCQ DECA mass spectrometer using an ESI source in positive mode with a C_{18} column and methanol/water 0.1% acetic acid elution system.

5.8 Steroid metabolism by established cell lines

To aid comparison between cell lines androgen concentrations have been expressed as an average ratio to the internal standard at each time point analysed via LC/MS, and oestrogen concentrations as the peak areas produced from the LC/MS/MS transitions (SRM) of 506→ 171 (oestradiol) and 504 → 171 (oestrone).

Table 5.3: Steroid nomenclature and colours on graphics (observed throughout this chapter).

Steroid	Colour on graphic
Testosterone	Red
Androstenedione	Blue
DHT	Pink
Androsterone	Yellow
Androstanediol	Green
Oestradiol	Orange
Oestrone	Black

5.8.1 Steroid metabolism by the Ishikawa cell line

The concentration of testosterone decreased after addition to the Ishikawa cell media from 100nM at time zero to ~43nM after 72 hours. Figure 5.8 suggests that the rate of decay of testosterone is not a first order process, as there is deviation from the linear (a linear relationship is not shown) and R^2 is low (the graph may be linear over the first 24 hours however there are not enough data points to confirm this).

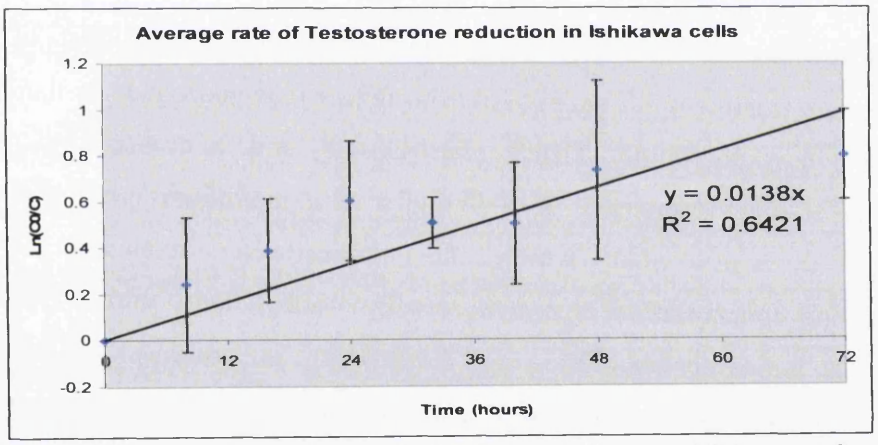

Fig 5.8: Rate of decay of testosterone in Ishikawa cells over 72 hours after addition of a 100nM testosterone media solution. Ln(C0/C) is plotted versus time to determine the rate of reaction and reaction order in Ishikawa cells.

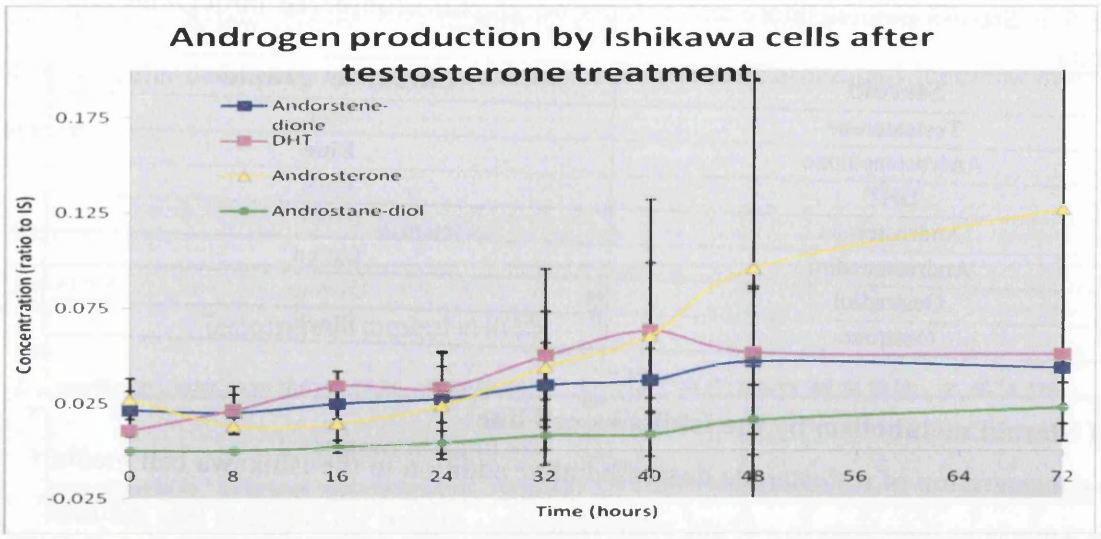

Fig 5.9: Steroid profiles of four androgens over 72 hours in Ishikawa cells after addition of a 100nM testosterone solution in 20ml of culture medium. Concentration was calculated as a ratio to the internal standard methyl-testosterone, analysed using an ESI source in positive mode on the LCQ DECA mass spectrometer with a C_{18} reversed phase column and an optimised methanol/water 0.1% acetic acid elution system. The errors bars are produced from the standard deviation of 3 experiments.

Figure 5.9 illustrates the production of androgens in Ishikawa cells over 72 hours after testosterone treatment. It was possible to detect four androgens in the steroid bio-pathway, androstenedione, DHT, androsterone and androstanediol. The concentration of DHT increased from 0 hours to a maximum concentration of 27.6nM at 40 hours after which the concentration remained constant. Androstenedione concentration increased steadily from 8 hours until it reached a plateau at 48 hours (concentration of 8.6nM). The presence of DHT and androstenedione suggests that both sides of the androgen bio-synthetic pathway were active in Ishikawa cells. The concentration of androsterone increased to a maximum at 72 hours (10.5nM), suggesting that this was a reaction end product.

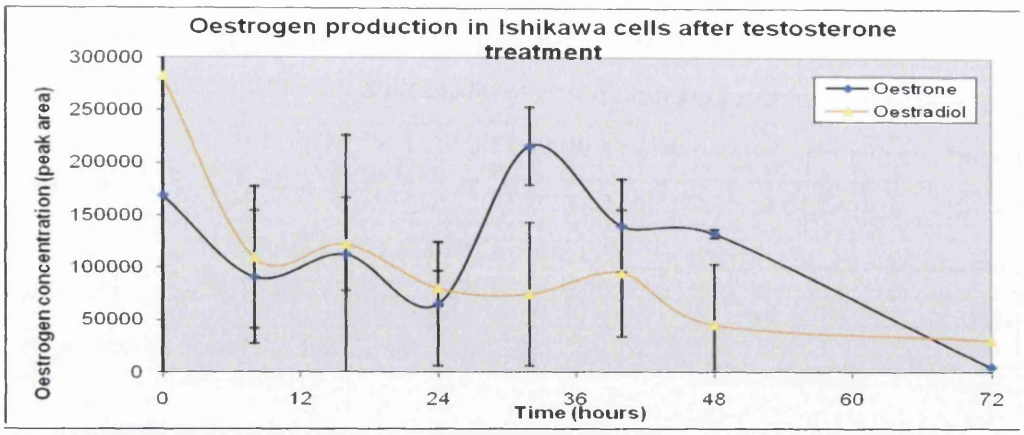

Fig 5.10: Oestrogen production in Ishikawa cells after addition of a 100nM media solution of testosterone over 72 hours. Dansyl-chloride derivatives analysed using an ESI source in positive mode on the LCQ DECA mass spectrometer using a phenyl hexyl column and an optimised methanol/water 0.1% formic acid elution system. Concentration is expressed as peak area.

In the Ishikawa cell line there were high initial concentrations of both oestrogens (due to FCS), the concentration of oestradiol was high at time zero but over time concentration decreases (figure 5.10). Oestrone concentration decreases after time zero until 24 hours, oestrone concentration then increased at 32 hours, (as the precursor androstenedione was readily available at this time). It is possible that in Ishikawa cells androstenedione was converted to oestrone at 32 hours.

The initial concentrations of oestrone and oestradiol (time zero) determined for all cell lines and biopsies were representative of oestrogens present in the cell media without any interactions with the cells. Any oestrone or oestradiol detected at this time were due to FCS and not due to conversion of added testosterone to oestrogens. Removal of oestrogens via charcoal stripping of the FCS reduce the oestrogens present, however due to the variability in removal of androgens, and progesterones coupled with removal of growth factors which aid cell growth this was not performed.

Therefore production of oestrogens from added testosterone in cell lines and biopsies was only confirmed if,

1. testosterone (or androstenedione) concentrations decreased in correlation with increased oestradiol (or oestrone) concentration after time zero and,

2. the change in oestradiol (or oestrone) concentration was significantly different from the previous data point(s) (more than the error bars).

No oestradiol (or oestrone) was being produced if,

1. despite testosterone (or androstenedione) being readily available the concentrations of oestradiol and oestrone remain constant or,
2. despite testosterone (or androstenedione) being readily available the concentrations of oestradiol and oestrone decreased. These rules were applied throughout this chapter.

5.8.2 Steroid production by RL95-2 cells after testosterone treatment

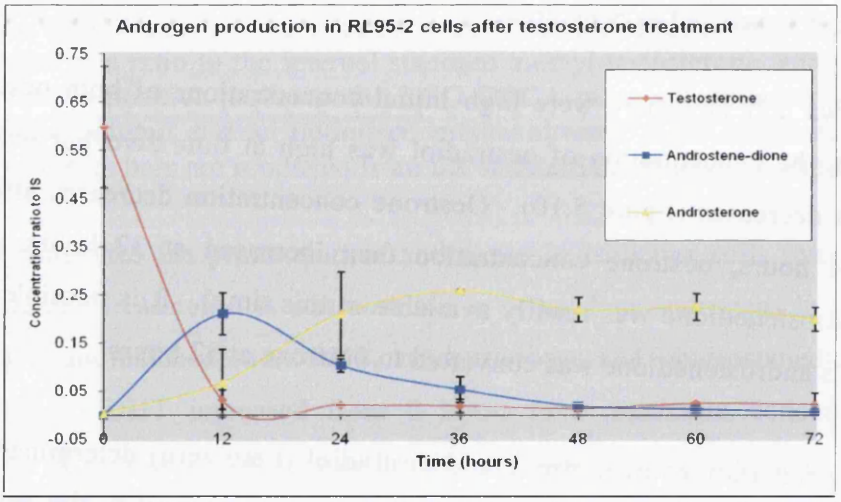

Fig 5.11: Androgens detected over 72 hours by RL95-2 cells after addition of a testosterone solution of 100nM. Concentration was calculated as a ratio to the internal standard methyl-testosterone, analysed using an ESI source in positive mode on the LCQ DECA mass spectrometer using a C_{18} reversed phase column and an optimised methanol/water 0.1% acetic acid elution system.

The majority of testosterone was metabolised by RL95-2 cells within the first 12 hours. All testosterone appeared to be converted to the major end product androsterone via the intermediate androstenedione, this was completed in the first 48 hours of the experiment. There was no DHT or androstanediol produced after testosterone treatment suggesting that only one side of the bio-pathway was active (figure 5.12). The maximum concentration of androstenedione was 46.7nM at 12 hours, and the maximum concentration of androsterone was 74.8nM at 36 hours.

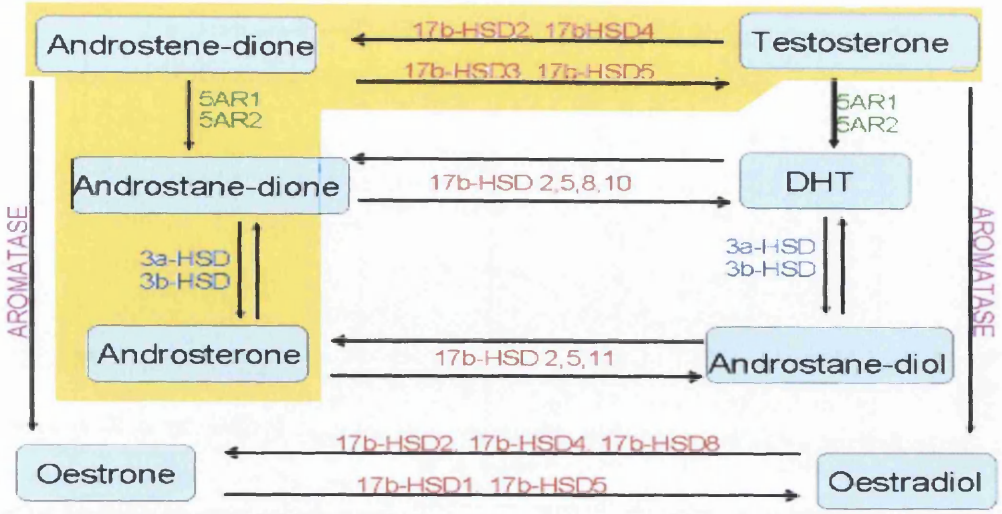

Fig 5.12: Diagram illustrating the active pathway (highlighted yellow) of androgen synthesis in RL95-2 cells.

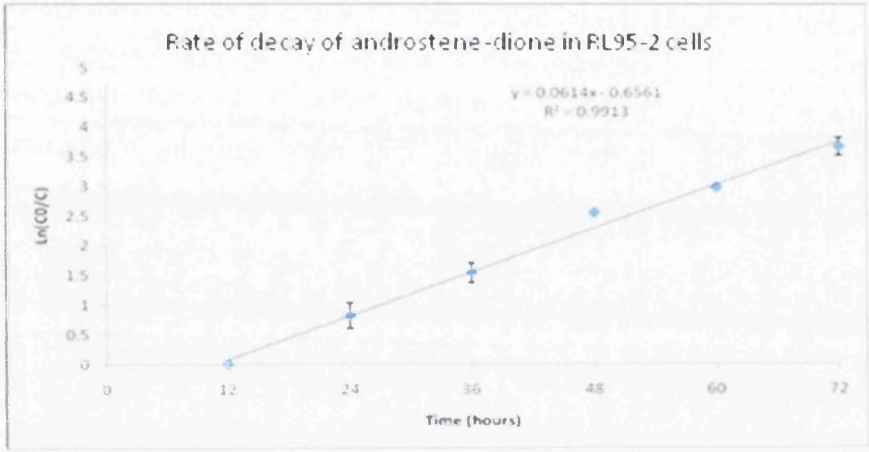

Fig 5.13: Androstenedione is produced from testosterone in RL95-2 cells over 72 hours after addition of a 100nM testosterone media solution. Androstenedione decay appears to be a first order process as a linear relationship was observed when $Ln(C_0/C)$ is plotted against time. C_0 has been adjusted to 12 hours.

The rate of the reaction was calculated with the concentration of androstenedione at 12 hours being defined as C_0 as before 12 hours there was no precursor present for this reaction (testosterone was converted to androstenedione in the first 12 hours). The metabolism of androstenedione to its end products was a first order reaction as a linear relationship is observed when concentrations is plotted against Ln(C0/C) and R^2 is 0.9913 (figure 5.13).

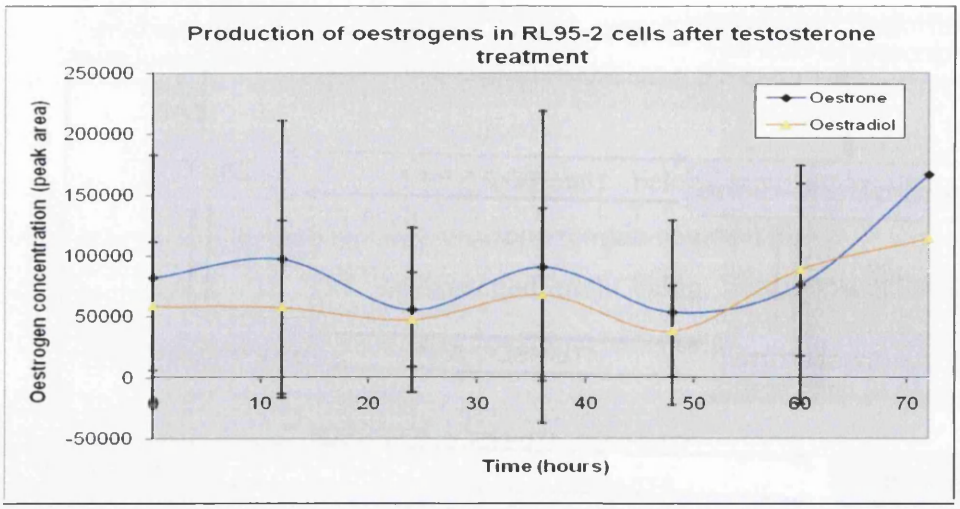

Fig 5.14: Oestrogen production in RL95-2 cells over 72 hours after addition of a 100nM testosterone media solution. Dansyl-chloride derivatives analysed using an ESI source in positive mode on the LCQ DECA mass spectrometer using a phenyl hexyl column and an optimised methanol/water 0.1% formic acid elution system.

The concentrations of oestradiol and oestrone remained constant throughout the experiment, in RL95-2 cells this suggests that there was no aromatisation of testosterone (or androstenedione) to oestrogens after testosterone treatment.

5.8.3 Steroid metabolism by HEC-1A cells after testosterone treatment

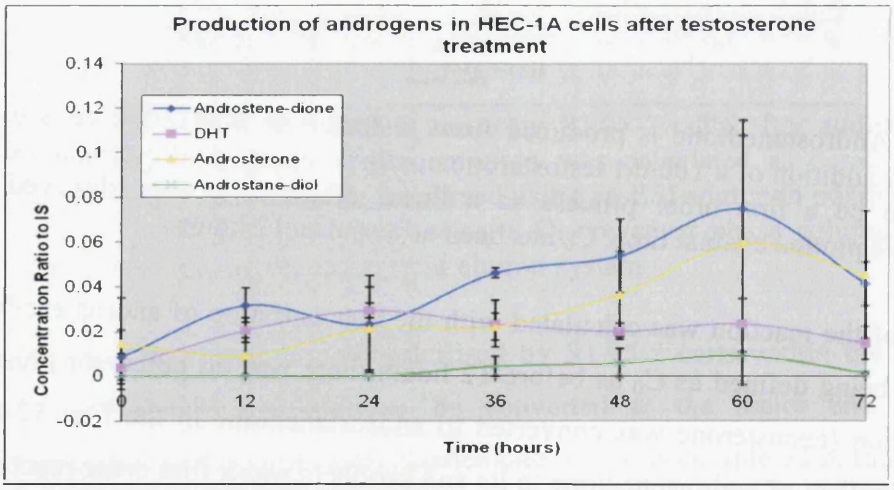

Fig 5.15: Androgen production in HEC-1A cells over 72 hours after addition of a 100nM testosterone media solution. Concentration was calculated as a ratio to the internal standard methyl-testosterone, analysed using an ESI source in positive mode on the LCQ DECA mass spectrometer using a C_{18} reversed phase column and an optimised methanol/water 0.1% acetic acid elution system.

Four androgens were detected as metabolites of testosterone in HEC-1A cells, these were androstenedione, DHT, androsterone and androstanediol. The concentrations

of androstenedione and androsterone increased to a maximum of 15.0 and 17.0nM respectively at 60 hours. The concentration of DHT reaches a maximum concentration of 11.6nM at 24 hours. The reaction end product androstanediol was produced after 24 hours and reaches a maximum at 60 hours.

Both sides of the steroid biosynthetic pathway were active in this cell line, confirmed by the presence of DHT and androstenedione.

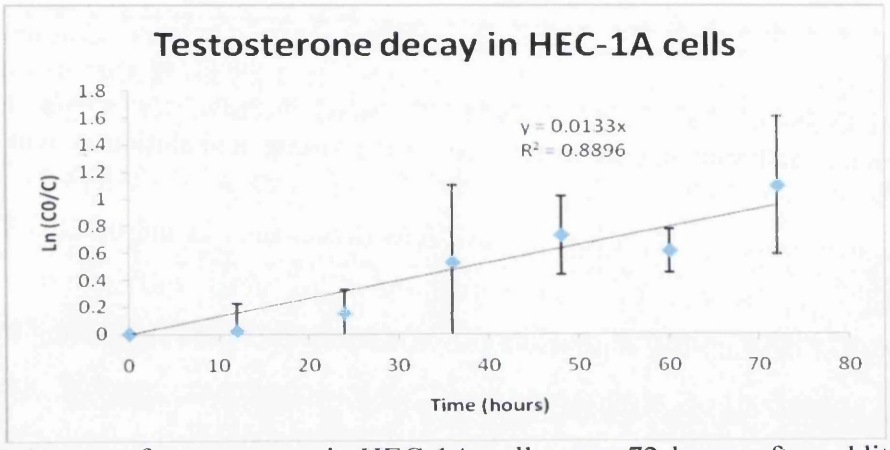

Fig 5.16: Decay of testosterone is HEC-1A cells over 72 hours after addition of a 100nM testosterone media solution. Testosterone decay appears to be a first order process as a linear relationship was observed when $Ln(C_0/C)$ is plotted against time.

The metabolism of testosterone in HEC-1A cells was probably a first order reaction, however there was some divergence probably due to the production of two testosterone metabolites (androstenedione and DHT) or production of testosterone itself. The result of this is the R^2 value is lower than expected for a first order reaction.

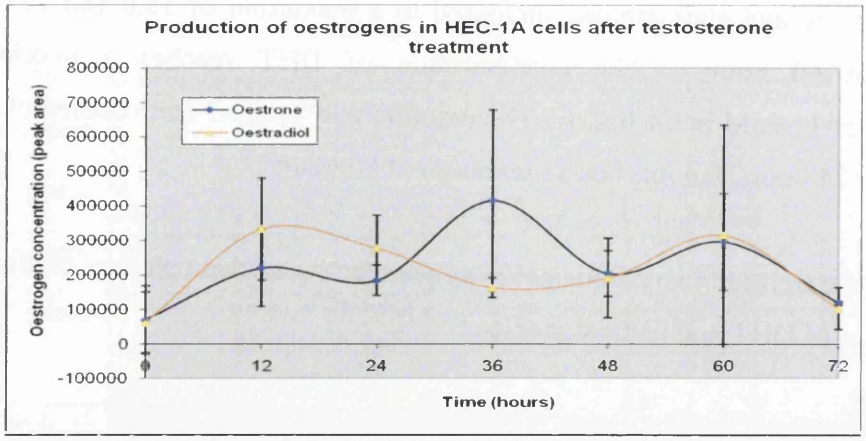

Fig 5.17: Oestrogen production in HEC-1A cells over 72 hours after addition of a 100nM/μL testosterone media solution. Dansyl-chloride derivatives analysed using an ESI source in positive mode on the LCQ DECA mass spectrometer using a phenyl hexyl column and an optimised methanol/water 0.1% formic acid elution system.

Again there were oestrogens present at time zero (lower than in the other cell line media) thought to be due to oestrogens present in foetal calf serum. The concentrations of oestradiol and oestrone increased after this time suggesting that in these cells utilisation of testosterone (and androstenedione) possibly via the aromatase enzyme was occurring. There were fluctuations in the oestrogen concentrations this could be due to inter-conversion between oestradiol and oestrone possibly through the 17β-HSDs.

5.8.4 Steroid metabolism by HEC-1B cells after testosterone treatment

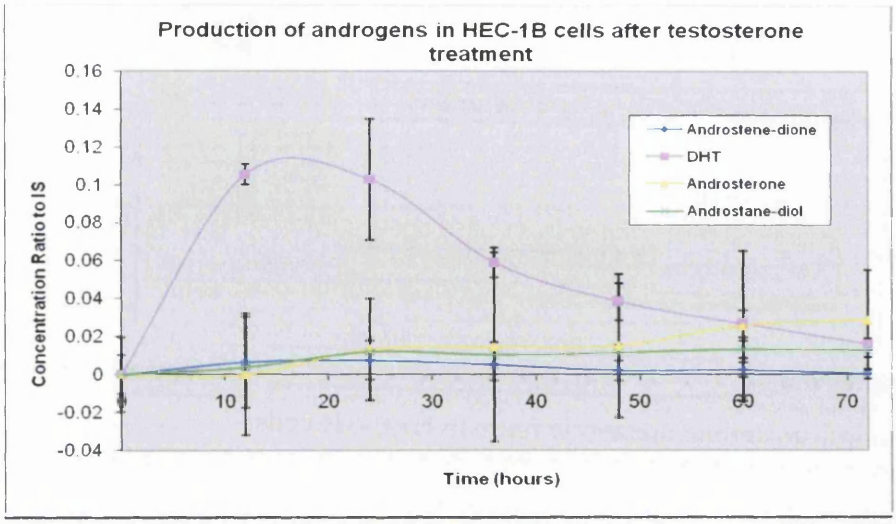

Fig 5.18: Production of androgens in HEC-1B cells over 72 hours after addition of a 100nM testosterone media solution. Concentration was calculated as a ratio to the internal standard methyl-testosterone, analysed using an ESI source in positive mode on the LCQ DECA mass spectrometer using a C_{18} reversed phase column and an optimised methanol/water 0.1% acetic acid elution system.

After addition of testosterone to the cell media of HEC-1B cells, again four androgens were detected, DHT, androstenedione, androsterone and androstanediol observed in figure 5.18. A maximum concentration of DHT of 47.6nM was detected at 12 hours, the concentration of DHT then declined throughout the remainder of the experiment with the appearance of androsterone. The concentration of androstanediol increased from 12 hours onwards to a maximum concentration of 7.87nM at 36 hours. In HEC-1B cells the major testosterone metabolism route appeared to be via production of DHT in preference to androstenedione (figure 5.19).

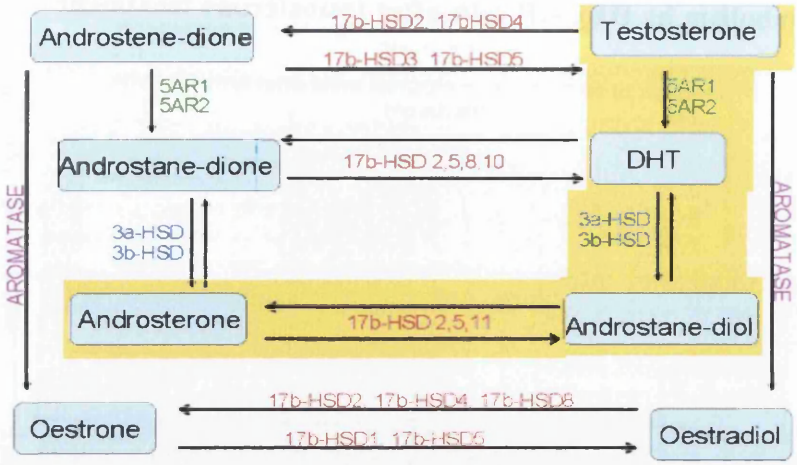

Fig 5.19: Major testosterone metabolic route in HEC-1B cells.

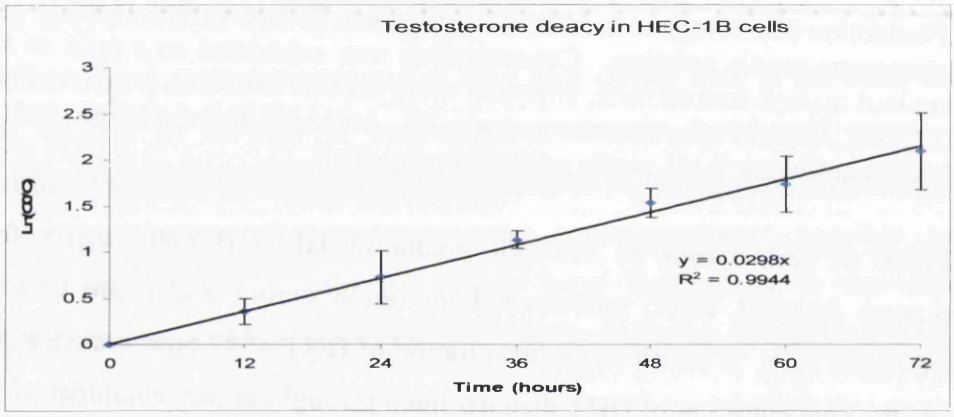

Fig 5.20: Decay of testosterone in HEC-1B cells over 72 hours after addition of a 100nM testosterone media solution. Testosterone decays appears to be first order processes as a linear relationship was observed when Ln (C_0/C_t) was plotted against time.

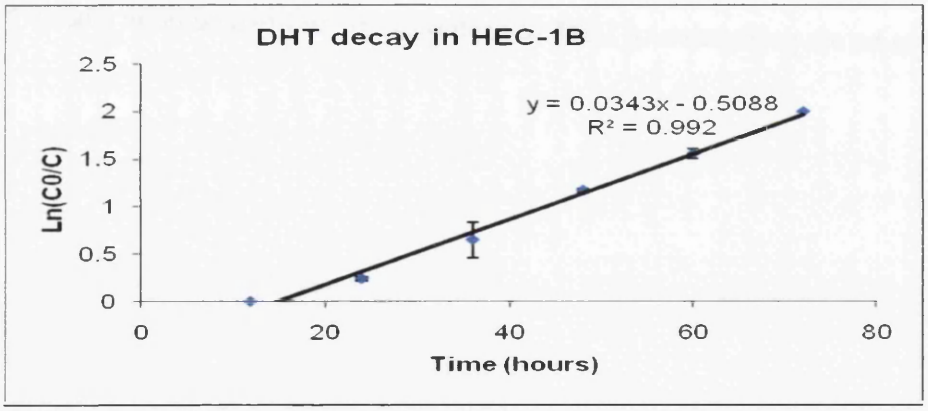

Fig 5.21: Decay of DHT in HEC-1B cells over 72 hours after addition of a 100nM testosterone media solution. DHT decays appears to be first order processes a a linear relationship was observed when Ln (C_0/C) was plotted against time. C_0 has to be altered to 12 hours as before this time no DHT is present.

Figure 5.20 illustrates that testosterone utilisation in HEC-1B cells was a first order decay. There was one major intermediate product of this reaction DHT, the highest concentration of which was produced at 12 hours and was metabolised via the 5AR enzymes. After this time DHT was converted into its metabolites again as a first order reaction (figure 5.21). Testosterone was also metabolised to the minor products androstenedione, oestrone and oestradiol.

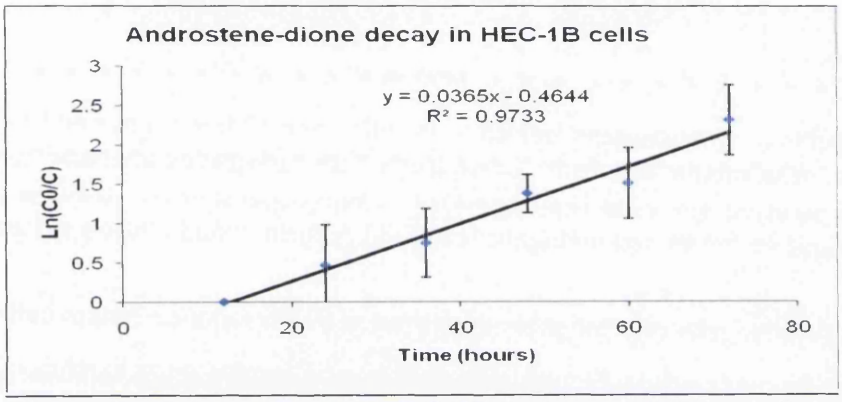

Fig 5.22: Decay of androstenedione in HEC-1B cells over 72 hours after addition of a 100nM testosterone media solution. Androstenedione metabolism appears to be a first order process as a linear relationship was observed when Ln (C_0/C) was plotted against time.

The decay of androstenedione in HEC-1B cells was also a first order process, possibly through the production of oestrone or other androgens. This was the minor product of testosterone biosynthesis, the concentrations of which were close to the limit of detection (36.1nM).

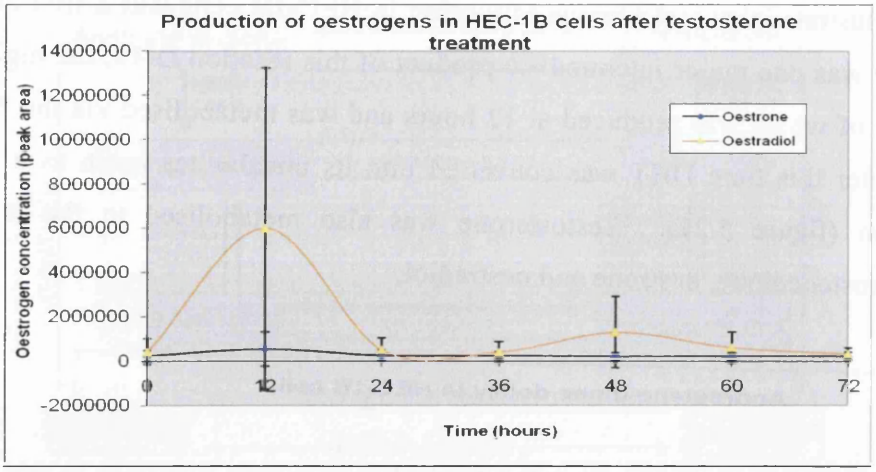

Fig 5.23: Production of oestrogens in HEC-1B cells over 72 hours after addition of a 100nM testosterone media solution. Dansyl-chloride derivatives analysed using an ESI source in positive mode on the LCQ DECA mass spectrometer using a phenyl hexyl column and an optimised methanol/water 0.1% formic acid elution system.

The amount of oestrogens present at time zero were much reduced in this cell line in comparison to the other cell lines highlighting the variation between batches of foetal calf serum composition. There was a large increase in the concentrations of oestradiol and oestrone at 12 hours suggesting that testosterone and androstenedione were being converted to oestradiol and oestrone in HEC-1B cells possibly via the aromatase enzyme. The concentration of oestrone then decreased to an almost constant value after 24 hours until the end of the experiment. The concentration of oestradiol however increased again at 48 hours, this suggests that testosterone has been metabolised to oestrogens in this cell line either through direct aromatisation or via the intermediate androstenedione (via HSDs) followed by aromatisation.

5.8.5 Steroid metabolism by COV434 cells after testosterone treatment

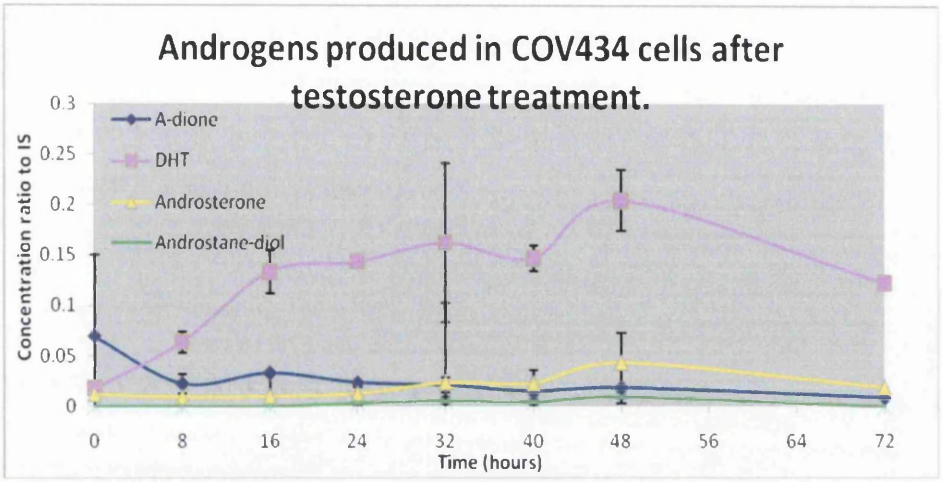

Fig 5.24: Androgen production in COV434 cells over 72 hours after addition of a 100nM testosterone media solution. Concentration is calculated as a ratio to the internal standard methyl-testosterone, analysed an ESI source in positive mode on the LCQ DECA mass spectrometer using a C_{18} reversed phase column and an optimised methanol/water 0.1% acetic acid elution system.

Four androgens were detected after addition of testosterone to the COV434 cell media (androstenedione, DHT, androsterone and androstanediol). These results suggest the major testosterone metabolism route in this cell line occurs through DHT to the end product androsterone (the route outlined in figure 5.19). The concentration of DHT increased after addition of testosterone to a maximum of 94.7nM at 48 hours. The androgenic end product was androsterone with a maximum concentration of 12.3nM recorded at 48 hours. A maximum concentration of androstanediol was detected as a reaction end product at 48 hours (12.6nM).

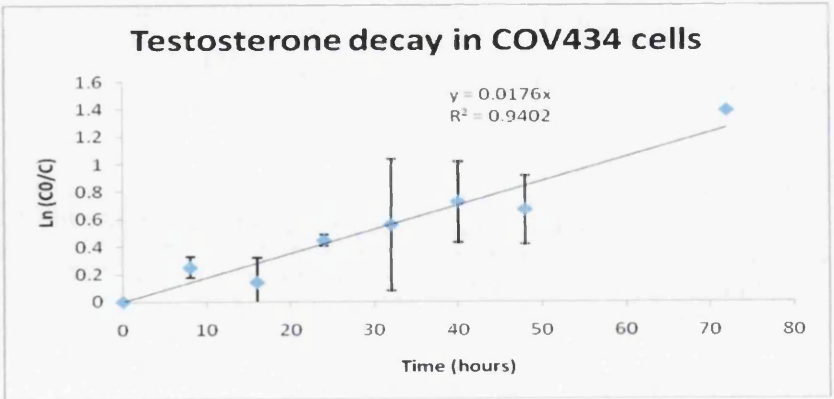

Fig 5.25: Testosterone decay in COV434 cells over 72 hours after addition of a 100nM testosterone media solution. A plot of $Ln(C_0/C)$ against time demonstrates that testosterone metabolism in COV434 was a first order process.

The metabolism of testosterone was a first order process in COV434 cells. There was an error produced at 32 hours, which was correlated with the variation in DHT concentrations at this time (figure 5.24). The explanation for this large error could be because the production rate of DHT at 32 hours was different in one experiment (possibly due to different expression of specific enzymes), or due to testosterone production.

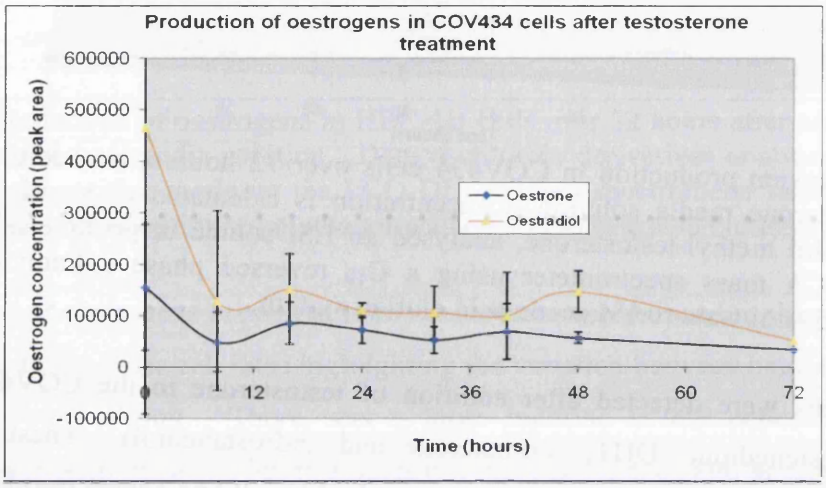

Fig 5.26: Oestrogen production in COV434 cells over 72 hours after addition of a 100nM testosterone media solution. Dansyl-chloride derivatives analysed using an ESI source in positive mode on the LCQ DECA mass spectrometer using a phenyl hexyl column and an optimised methanol/water 0.1% formic acid elution system.

Concentrations of oestradiol and oestrone were high in the cell media (observed at time zero) probably due to their presence in the FCS, after the first 8 hours the concentrations of oestradiol and oestrone decreased. The concentrations of oestradiol and oestrone then essentially remain constant suggesting that testosterone was not being metabolised to oestradiol or oestrone in COV434 cells.

5.8.6 Conclusions- cell lines

Androgens and oestrogens were detected after testosterone treatments of the cell lines, and the metabolism of testosterone was different in each cell line.

The detection of testosterone metabolites has been studied for many years, primarily in androgen responsive tissues. In 1973 Dorrington and co-workers recorded the presence of androgens (androstenedione, androsterone, DHT and androstanediol) after testosterone treatment of the seminiferous tubules isolated from male rats. They

observed localised steroid metabolism routes in this androgen responsive tissue comparable to that observed in the oestrogen responsive cell lines above,[17] suggesting that while the roles of a specific steroid in each tissue may be different the metabolism routes are similar. There is also metabolism data available for the breast cancer cell line ZR75-1, which is comparable to the data outlined above, after androgen treatment of this cell line androgen metabolism readily occurs with no detectable aromatisation to oestrogens.[18] Information about androgen metabolism in endometrial cancer cell lines is less widely available, a recent paper however described the metabolism of androstenedione in the established cell lines Ishikawa, HEC-1A, HEC-1B, and RL95-2. In the article Fournier and colleagues described metabolism of DHT, testosterone, androsterone, and androstanediol after androstenedione treatment with no reported conversions to oestrogens[19] (GC/CI-MS technique) which was directly correlated to the data recorded in these experiments.

Table 5.4 Times and maximum concentrations of androstenedione and DHT in established cell lines. Detected on the LCQ DECA mass spectrometer using a C_{18} column, with an ESI source in positive mode using an optimised methanol/water elution system with 0.1% acetic acid. Concentrations were calculated via comparison to a calibration series for each steroid as described in chapter 4.

Cell Line	Maximum concentration nM	Time hours after testosterone treatment
Androstenedione		
Ishikawa	8.6	48
RL95-2	46.7	12
HEC-1A	15.1	60
HEC-1B	Below LOD (36.1)	24
COV434	5.3	16
DHT		
Ishikawa	27.6	32
RL95-2	n/a	n/a
HEC-1A	11.6	24
HEC-1B	47.6	24
COV434	94.7	48

The highest concentration of androstenedione was recorded in the RL95-2 cell line at 48 hours, DHT was not detected in this cell line. The COV434 and HEC-1B cell lines produced the highest concentrations of DHT and the lowest concentrations of androstenedione. From these results it was possible to ascertain the principal route of testosterone metabolism in each cell line. In the RL95-2 cell line testosterone

metabolism was through androstenedione in the COV434 and HEC-1B cell lines testosterone metabolism occurred mainly through DHT. In the Ishikawa and HEC-1A cell lines testosterone metabolism occurred through both DHT and androstenedione, suggesting that both sides of the bio-pathway were active. Information concerning the expression of 5AR1, 5AR2 and a number of 17β-HSDs may explain differences in the metabolic pathways favoured in each cell line (chapters 6 and 7).

Table 5.5 Table of maximum concentrations of androsterone and androstanediol in all established cell lines. Detected on the LCQ DECA mass spectrometer using a C_{18} column, with an ESI source in positive mode using an optimised methanol/water elution system with 0.1% acetic acid. Concentrations were calculated via comparison to a calibration series for each steroid as described in chapter 4.

Cell Line	Maximum concentration nM	Time hour
Androsterone		
Ishikawa	10.5	72
RL95-2	74.9	36
HEC-1A	17.0	60
HEC-1B	8.1	72
COV434	12.3	48
Androstanediol		
Ishikawa	40.9	72
RL95-2	n/a	n/a
HEC-1A	13.0	60
HEC-1B	7.9	36
COV434	12.6	48

The highest concentration of androsterone was recorded in RL95-2 cells, again due to the simplicity of testosterone metabolism in these cells. The lowest concentration of androsterone was detected in the HEC-1B cell line. The highest concentration of androstanediol was detected in the Ishikawa cell line at 72 hours. There were similar maximum amounts of androstanediol detected in HEC-1A (60 hours) and COV434 (48 hours).

Androsterone and androstanediol were the major androgenic end products. It is conceivable that whichever way testosterone was metabolised (via DHT or androstenedione) that androsterone and androstanediol was produced due to inter-conversions through HSD enzymes.

Table 5.6 Table of maximum concentrations of oestradiol and oestrone in all established cell lines (concentrations at time zero were not included). Detected on the LCQ DECA mass spectrometer using a luna phenyl hexyl column, with an ESI source in positive mode using an optimised methanol/water elution system with 0.1% formic acid. Concentrations were calculated via comparison to a calibration series for each steroid as described in chapter 4.

Cell Line	Maximum concentration (nM)	Time hour
Oestradiol		
Ishikawa	1.55	16
RL95-2	1.45	72
HEC-1A	1.77	60
HEC-1B	7.59	12
COV434	1.87	48
Oestrone		
Ishikawa	2.53	32
RL95-2	1.95	72
HEC-1A	4.88	36
HEC-1B	2.91	12
COV434	1.01	16

The highest concentration of oestradiol was produced in the HEC-1B cell line at 12 hours and the lowest in RL95-2 cells at 72 hours. The highest concentration of oestrone was detected in the HEC-1A cell line (36 hours), and the lowest concentration was detected in COV434 cells (16 hours). These results demonstrate some oestrogen production was occurring after testosterone treatment however in comparison to androgen synthesis this was a reduced pathway. It should also be noted that there were oestrogens in the FCS under basal conditions and insensitivity to oestrogens compared to androgens in the mass spectrometer may lead to reduced sensitivity to oestrogens.

These experiments provide quantitative information concerning the metabolism of testosterone in endometrial established cell lines. The results generated determine the route of testosterone metabolism in the endometrial epithelial cancer cell lines. At high testosterone concentration androgen synthesis occurred readily, and the production of oestrogens was minor in all cell lines investigated. Oestrogen production was not a major metabolism pathway in these oestrogen responsive cell lines irrespective of aromatase expression. This unexpected result could be due to a number of factors such as saturation of the aromatase enzyme in high androgen environments, or due to the correct co-factors for the aromatisation not being present.

The mRNA expression and aromatase activity may not be directly linked which could further explain the disparities between high aromatase expression and no oestrogen production. This is further discussed in chapter 7.

5.8.7 Conclusions testosterone utilisation (reaction kinetics)

The utilisation of testosterone was investigated in the established cell lines (figures 5.8, 5.16, 5.20, and 5.25).

Table 5.7: Reaction kinetics for testosterone metabolism in established cell lines.

Cell line	Rate equation	R^2	Rate constant k	Reaction Order	Final testosterone conc nM	Half life hours
HEC-1B	0.0298x	0.9944	0.0301	1	12	23.26
COV434	0.0176x	0.9402	0.0168	1	15	39.38
RL95-2	-	-	-	-	4	-
Ishikawa	0.0138x	0.6421	0.0192	?	43	50.23
HEC-1A	0.0133x	0.8896	0.0129	~1	33	52.12

First order reactions were observed for testosterone decay in HEC-1B and COV434 cells (figures 5.20 and 5.25). The rate of conversion is directly proportional to the concentration of testosterone, this was observed because there was only one major product for both reactions, testosterone → DHT.

The kinetics of testosterone metabolism in RL95-2 cells was not possible to determine as more than 96% of the testosterone was utilised in the first 12 hours.

The decay of testosterone in Ishikawa cells is not a first order process no linear relationship was observed (figure 5.8). The other two cell lines, Ishikawa and HEC-1A produced two products when testosterone was added (DHT and androstenedione), which makes the kinetics more complex, simple relationships between reaction rate and concentration were not observed (relationships were not linear and $R^2 < 0.90$).

An increase in testosterone concentration would cause the rate of reaction to appear to decrease, causing divergences from the linear as observed in HEC-1A cells at 24 and 60 hours (figure 5.16), (a calculated decrease in the rate of reaction and R^2 values). If these data points were removed the data set becomes more linear (R^2

increases to 0.975) demonstrating the decay of testosterone was probably a first order and that a secondary process also could have been occurring in this cell line which produced testosterone. This could be attributed to expression of specific enzymes such as 17β-HSD5 (androstenedione → testosterone).

Table 5.8: Reactions kinetics for the decay of DHT and androstenedione in HEC-1B and RL95-2 cells.

Cell Line	Steroid Decay	Rate equation	R^2	Rate constant k	Reaction Order	Half Life hours
HEC-1B	DHT	0.0343x – 0.5088	0.992	0.02886	1	20.21
HEC-1B	Androstenedione	0.0365x – 0.4644	0.9733	0.03568	1	18.99
RL95-2	Androstenedione	0.0614x – 0.6561	0.9913	0.04605	1	15.05

First order decays of the testosterone products DHT and androstenedione were observed in the HEC-1B and RL95-2 cell lines (figures 5.21, 5.22 and 5.13). These relationships were observed due to the simplicity of the reactions;

DHT → → androsterone (HEC-1B)

androstenedione → → androsterone (HEC-1B and RL95-2).

In the HEC-1B cell line the conversion rates of DHT and androstenedione to their reaction products were similar to the utilisation of testosterone, half lives of 20.21 hours (DHT) and 18.99 hours (androstenedione) in comparison to 23.26 hours (testosterone). This allows us to determine that none of these decays were rate limiting in the production of androgens in the HEC-1B cell line. These decays were concentration dependent this suggests all conditions and co-factors required for the conversion were present.

These fully optimised and analytically validated methods were subsequently applied to biopsies from women with benign endometrial conditions and fertile women to evaluate the utilisation of testosterone in this setting.

5.9 Analysis of endometrial biopsies from women with benign endometrial disorders

The endometrial biopsies used in this study are summarised in table 5.9. These disorders were chosen as there is evidence of altered localised endometrial steroid metabolism in these conditions which may influence the course of the disorder;

1. Kitawaki and co-workers presented evidence of bio-accumulation of oestradiol in endometrial biopsies from women with endometriosis.[20] The role of androgens in progression of endometriosis is unknown.
2. Kaku and colleagues demonstrated high levels of oestradiol within endometrial lesions sites of women with endometrial hyperplasia[21] and this may contribute to progression to endometrial cancer. Current knowledge of steroid metabolism in endometrial hyperplasia is limited and the potential roles of androgens unknown.
3. Leon and co-workers demonstrated increased expression of 17β-HSD1 and sulphatase and decreased expression of sulphotransferase in the endometria of women with PCOS in comparison to normal endometria, which could result in altered steroid metabolism.[22] The analysis of a full steroid profile and the inclusion of analysis of more steroid converting enzymes would further elucidate altered steroid metabolism in the endometria of women with PCOS.
4. Pienkowski and colleagues discussed hormone production by ovarian cysts in prepubescent girls causing the early onset of puberty.[23] It is possible that steroid metabolism in the endometria of women with ovarian cysts is altered due to increased production of steroids by the cyst. Investigations into whether there is altered steroid metabolism in the endometria of women with ovarian cysts to our knowledge have not been completed.
5. Endometrial polyps can progress to hyperplasia and eventually endometrial cancer, suggesting an alteration from normal steroid metabolism may occur. Endometrial polyps are found in 12-34% of endometria of women with endometrial cancer suggesting progression may be hormone dependent.[24] Investigations into steroid metabolism in endometrial polyps are limited.
6. The unexplained infertility biopsies came from women who were unable to conceive, the reason could not be elucidated, but could be due to altered endometrial steroid metabolism.

The purpose of these experiments was to determine alterations in steroid metabolism routes in fertile and benign endometrial biopsies. Endometriosis biopsies were first considered (4 biopsies) followed by analysis of a smaller number of endometrial biopsies from other benign endometrial conditions. These biopsies were investigated focusing on the utilisation of testosterone and the production of the testosterone metabolites DHT, androstenedione, androsterone, androstanediol, oestradiol, and oestrone.

Testosterone treatments over 72 hours were conducted for the stromal cells from each biopsy and androgen, oestrogen and enzyme expression recorded at each time point, the epithelial and stromal cells from a epithelial endometrial hyperplasia biopsy were also treated with testosterone. A comparison of changes in enzyme expression to changes in steroid profile was then completed to ascertain any relationships between enzyme expression and steroid concentrations (chapters 6, 7).

Table 5.9: Biopsy histology showing the number of biopsies in each category and the average age and age range within each group. These biopsies were analysed by mass spectrometry or RT-PCR or used for method development.

Histology	Number of patients	Average age (years)	Age range (years)
Fertile	3	35.8	23-43
Endometriosis	4 (plus 2 RT-PCR only)	33.9	26-37
PCOS	2	32.5	25-38
Unexplained infertility	2	36	33-37
Tubual disorder	1	41	-
Endometrial polyp	1	43	-
Ovarian cyst	1	34	-
Atypical hyperplasia	1	55	-

Table 5.9 shows that the four major groups under investigation (fertile, endometriosis, unexplained infertility and PCOS) had similar average ages and age ranges. The groups with only one biopsy were investigated as case studies from which interesting preliminary data was compiled and an initial comparison of benign conditions was completed.

5.9.1 Testosterone utilisation by endometrial biopsies

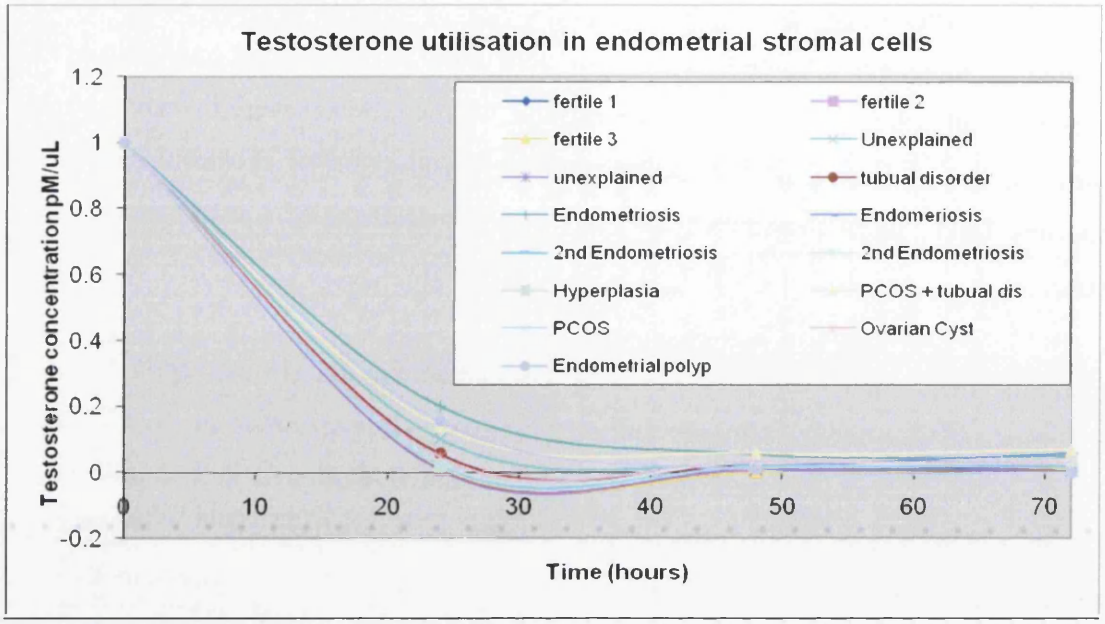

Fig 5.27: Testosterone utilisation in stromal cells from endometrial pathologies monitored over 72 hours after addition of a 100nM testosterone media solution. Concentration is calculated as a ratio to the internal standard methyl-testosterone, analysed using an ESI source in positive mode on the LCQ DECA mass spectrometer with a C_{18} reversed phase column and an optimised methanol/water 0.1% acetic acid elution system.

All stromal biopsies investigated metabolised >90% of the testosterone within the first 24 hours (figure 5.27). The concentration of testosterone was reduced in all biopsies to less than 3% of the original concentration after 48 hours. Testosterone consumption in these cells does not seem to be related to the nature of the benign disorder under clinical investigation.

5.9.2 Production of steroids following testosterone treatment by fertile biopsies.

There was no a detectable DHT at any time in any of the fertile samples (3 biopsies) or the tubual disorder sample (1 biopsy). As described later (5.9.3) the production of DHT was recorded in all endometrial disorders (except unexplained infertility), this was the major difference in testosterone metabolism in fertile biopsies relative to biopsies from all other endometrial pathologies investigated (including cell lines).

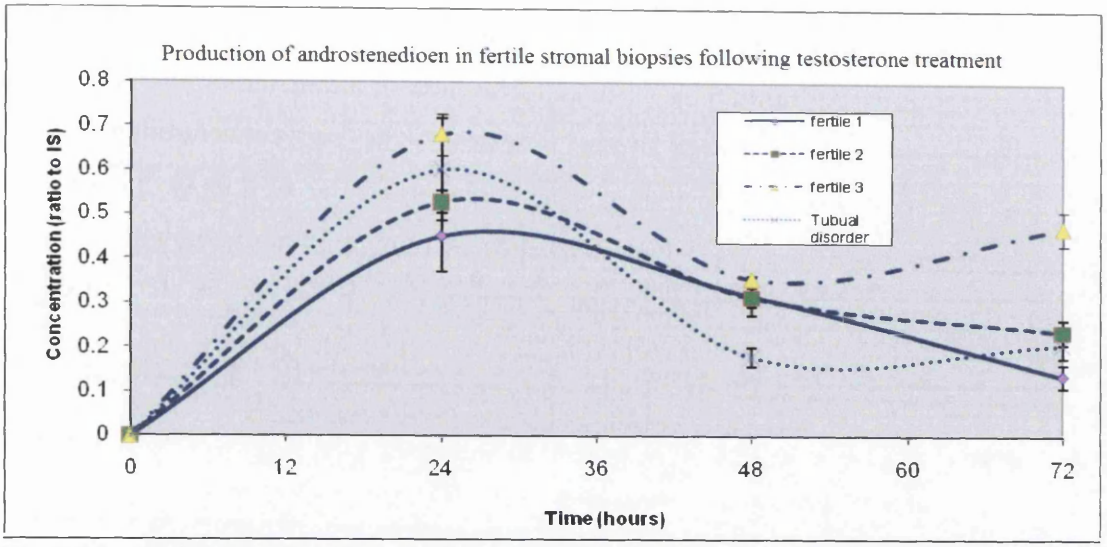

Fig 5.28: Androstenedione production in fertile biopsies over 72 hours after addition of a 100nM testosterone media solution. Concentration is calculated as a ratio to the internal standard methyl-testosterone, analysed using an ESI source in positive mode on the LCQ DECA mass spectrometer with a C_{18} reversed phase column and an optimised methanol/water 0.1% acetic acid elution system.

Endometrial biopsies from women with normal cycling endometria (fertile women) and from a woman with tubual disorder produced androstenedione 24 hours after testosterone treatment which was metabolised to other products over the next 48 hours. The maximum androstenedione concentrations produced by each fertile biopsy at 24 hours were comparable 0.103, 0.122 and 0.157μM.

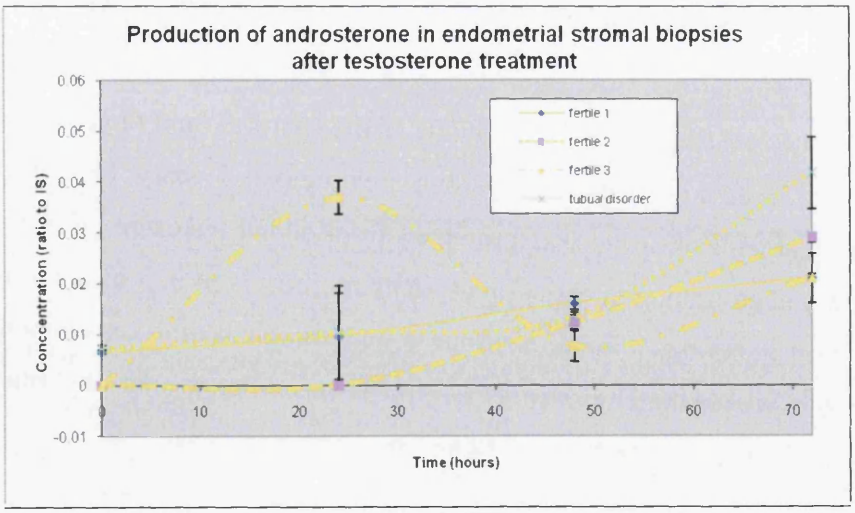

Fig 5.29: Production of androsterone in fertile biopsy samples over 72 hours after addition of a 100nM testosterone media solution. Concentration is calculated as a ratio to the internal standard methyl-testosterone, analysed using an ESI source in positive mode on the LCQ DECA mass spectrometer using a C_{18} reversed phase column and an optimised methanol/water 0.1% acetic acid elution system.

Two of the fertile biopsies and the tubual biopsy showed similar androsterone production as illustrated in figure 5.29. The concentration of androsterone increased throughout the experiment for three of the biopsies. The end concentration of androsterone was similar in all biopsies analysed an average value of 7.9nM. In one fertile sample there was different production of androsterone at 24 hours, however at the end of the experiment androsterone concentrations were similar in all fertile samples.

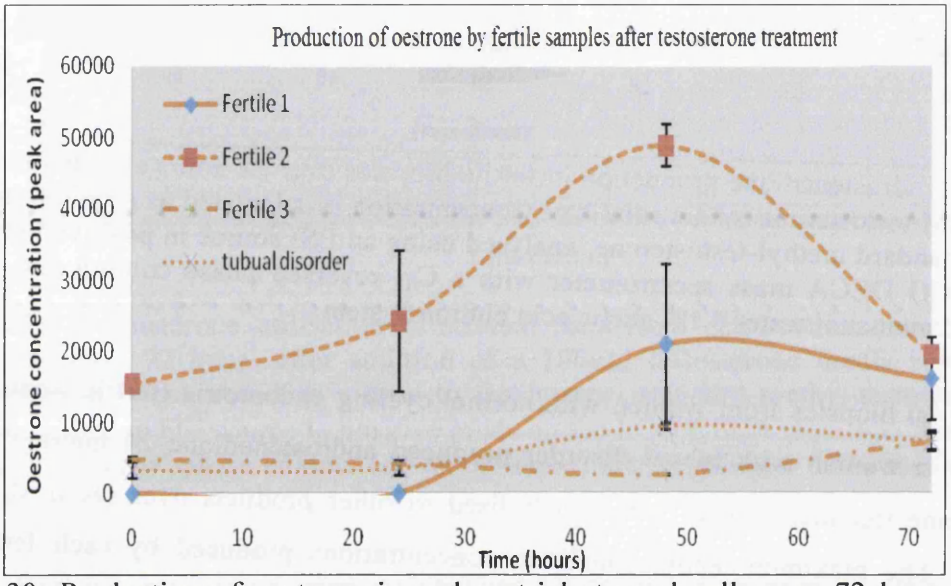

Fig 5.30: Production of oestrone in endometrial stromal cells over 72 hours after addition of a 100nM testosterone media solution. Dansyl-chloride derivative analysed using an ESI source in positive mode on the LCQ DECA mass spectrometer using a phenyl hexyl column and an optimised methanol/water 0.1% formic acid elution system.

The production of oestrone was similar in all fertile samples (and the tubual disorder biopsy, figure 5.30) following testosterone treatment. Twenty four hours after testosterone treatment oestrone was produced from added testosterone in the fertile samples with a maximum concentration at 48 hours (observed in 3 of the 4 biopsies). One fertile biopsy exhibits a larger oestrone concentration at time zero in comparison to the others, however the contour of this profile is similar to that of 2 other fertile biopsies (maximum concentrations at 48 hours).

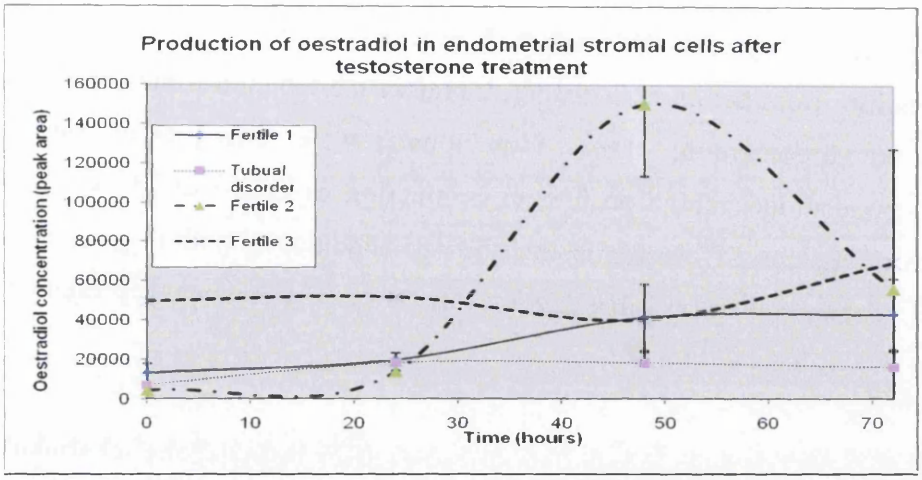

Fig 5.31: Production of oestradiol in endometrial stromal cells over 72 hours after addition of a 100nM testosterone media solution. Dansyl-chloride derivative analysed using an ESI source in positive mode on the LCQ DECA mass spectrometer using a phenyl hexyl column and an optimised methanol/water 0.1% formic acid elution system.

There was a large increase in oestradiol concentration in one fertile biopsy, at 24 and 48 hours. Oestradiol concentrations also increased in the first 24 hours to produce maxima at 48 hours for two other fertile biopsies following testosterone treatment (figure 5.31). The tubual disorder biopsy showed an increase in oestradiol concentration over time, but this was not as large as the other fertile biopsies. The low amounts of oestradiol present at time zero in conjunction with the oestrone information (figure 5.30) suggests that oestrogen production was occurring in fertile samples following testosterone treatment. Oestrogen concentrations have been measured for completion, however because the FCS is not charcoal stripped there is some variability in these results. As with the cell lines it should be noted with all biopsy samples that any oestrogens detected at the zero time point are representative of oestrogens present due to FCS in the media and not from testosterone metabolism. The conversion of testosterone to oestradiol (or oestrone) was only confirmed if the conditions outlined in chapter 5.8.1 were fulfilled.

Figure 5.28 to 5.31 illustrated similar utilisation of testosterone and production of androstenedione, androsterone, oestradiol and oestrone in fertile biopsies to the patient with tubual disorder, also there was no production of DHT by any of these biopsies. Tubual disorder is the primary reason for infertility in this woman with her clinical notes indicating two previous full term pregnancies, production of steroids

similar to the fertile biopsies suggests that there was no endometrial dysfunction as might be expected from her clinical history, therefore the tubual disorder biopsy was included in the fertile group. These four biopsies were subsequently combined together to produce an average profile for production of each steroid, which was compared to production of steroids in each benign endometrial pathology following testosterone treatment. (The average fertile value for each steroid was represented on figures 5.34 to 5.52 by a bold line.)

5.9.3 Production of DHT by endometrial biopsies after testosterone treatment

There was no detectable DHT at any time in the unexplained infertility biopsies following testosterone treatment, this was identical to the fertile biopsies, however DHT was produced in endometrial biopsies from patients with endometriosis, ovarian disorders, endometrial hyperplasia and an endometrial polyp.

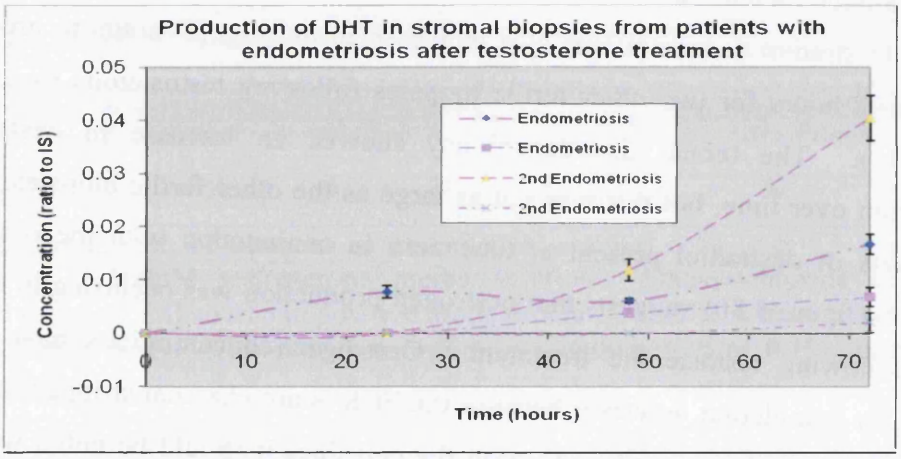

Fig 5.32: Production of DHT in endometrial stromal cells from patients with endometriosis over 72 hours after addition of a 100nM testosterone media solution. Concentration is calculated as a ratio to the internal standard methyl-testosterone, analysed using an ESI source in positive mode on the LCQ DECA mass spectrometer with a C_{18} reversed phase column and an optimised methanol/water 0.1% acetic acid elution system.

Figure 5.32 shows that DHT was produced by endometrial stromal cells of patients with endometriosis following testosterone treatment suggesting altered testosterone metabolism compared with the fertile endometrium where there was no detectable DHT. The highest concentration for each biopsy was observed after 72 hours but there was variability between samples. Therefore metabolism of testosterone to

DHT is a feature of endometriosis, the variation of which can be attributed to the disease having a complex phenotype.

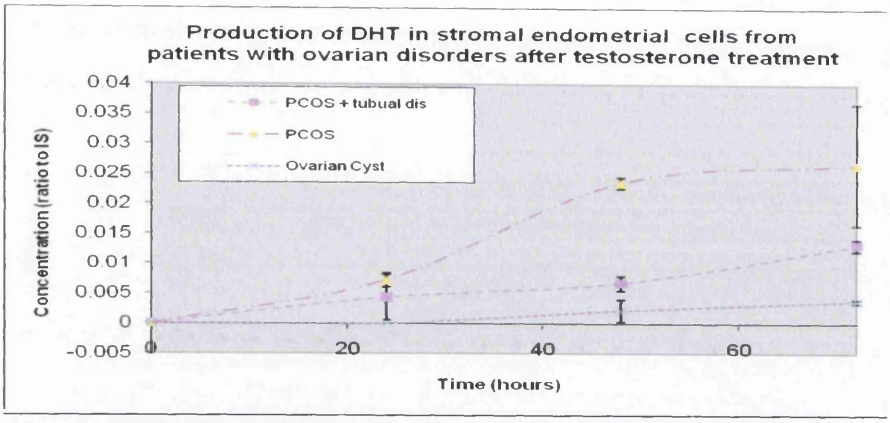

Fig 5.33: Production of DHT in endometrial stromal cells from women with ovarian disorders over 72 hours after addition of a 100nM testosterone media solution. Concentration is calculated as a ratio to the internal standard methyl-testosterone, analysed using an ESI source in positive mode on the LCQ DECA mass spectrometer with a C_{18} reversed phase column and an optimised methanol/water 0.1% acetic acid elution system.

DHT was detected in all endometrial biopsies from patients with ovarian disorders, suggesting altered testosterone metabolism compared with fertile endometria where there was no detectable DHT. The concentration of DHT increased throughout the experiment with a maximum concentration of DHT recorded in all ovarian disorders biopsies 72 hours after testosterone treatment.

5.9.3 Production of androstenedione by endometrial biopsies after testosterone treatment

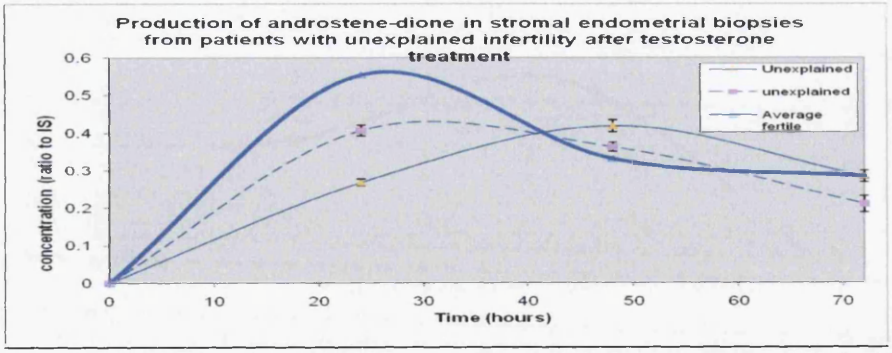

Fig 5.34: Production of androstenedione in patients with unexplained infertility after addition of a 100nM testosterone media solution. Concentration is calculated as a ratio to the internal standard methyl-testosterone, analysed using an ESI source in positive mode on the LCQ DECA mass spectrometer with a C_{18} reversed phase column and an optimised methanol/water 0.1% acetic acid elution system.

The two samples from patients with unexplained infertility had lower amounts of androstenedione present at 24 hours in comparison to the average fertile biopsies. This suggests metabolism of testosterone to androstenedione was less rapid than in fertile biopsies, however the end point concentrations were similar in all samples.

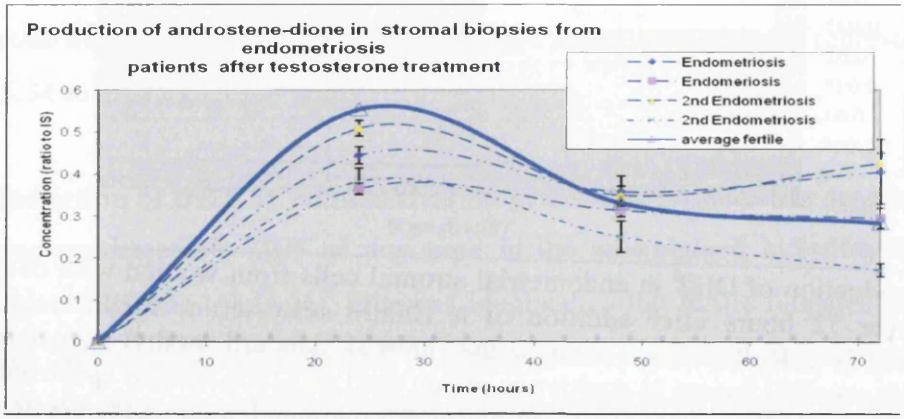

Fig 5.35: Comparison of endometriosis androstenedione production and fertile androstenedione production in endometrial stromal cells over 72 hours after addition of a 100nM testosterone media solution. Concentration is calculated as a ratio to the internal standard methyl-testosterone, analysed using an ESI source in positive mode on the LCQ DECA mass spectrometer with a C_{18} reversed phase column and an optimised methanol/water 0.1% acetic acid elution system.

Figure 5.35 illustrates that the metabolism of androstenedione in women with endometriosis was similar to that of women from the fertile group.

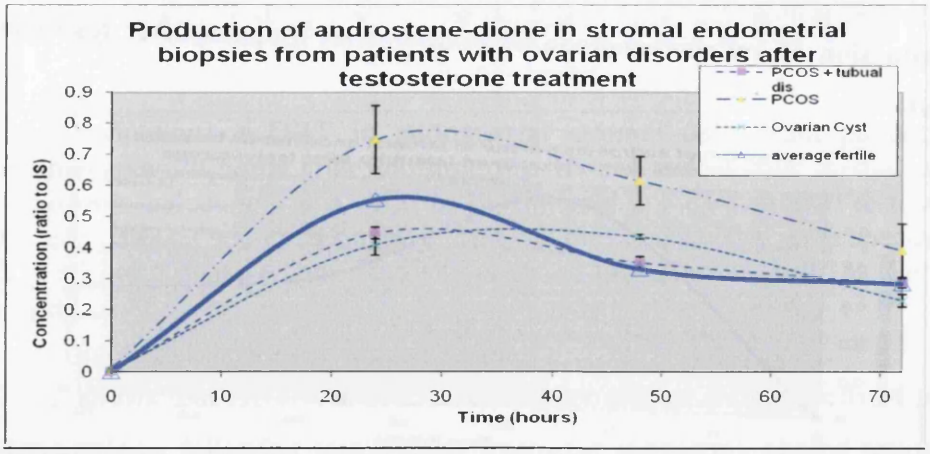

Fig 5.36: Production of androstenedione comparison between patients with ovarian abnormalities and fertile endometrial biopsies over 72 hours after addition of a 100nM testosterone media solution. Concentration is calculated as a ratio to the internal standard methyl-testosterone, analysed using an ESI source in positive mode on the LCQ DECA mass spectrometer with a C_{18} reversed phase column and an optimised methanol/water 0.1% acetic acid elution system.

The metabolism of androstenedione was similar in biopsies from patients with ovarian disorders to the average fertile biopsies. After 72 hours the amount of remaining androstenedione in the PCOS and ovarian cyst biopsies were similar to that of the average fertile sample.

5.9.4 Production of androsterone by endometrial biopsies after testosterone treatment

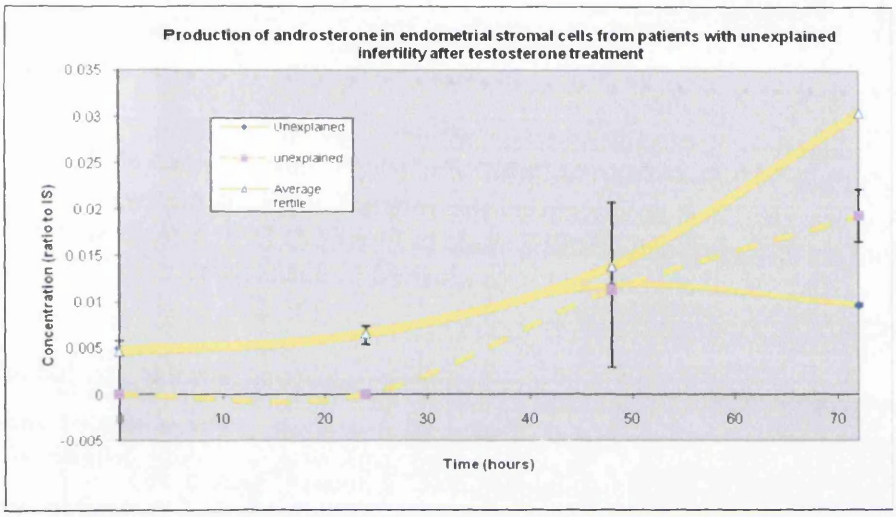

Fig 5.37: Comparison of androsterone production in endometrial stromal cells from biopsy samples from fertile and unexplained infertility patients over 72 hours after addition of a 100nM testosterone media solution. Concentration is calculated as a ratio to the internal standard methyl-testosterone, analysed using an ESI source in positive mode on the LCQ DECA mass spectrometer with a C_{18} reversed phase column and an optimised methanol/water 0.1% acetic acid elution system.

The production of androsterone in biopsy samples with unexplained infertility was simliar in both samples with an average end concentration of ~4.0nM following testosterone treatment. The amount of androsteone increased throughout the experiment over the 72 hours. The final concentration of androsterone in biopsies from patients with unexplained infertility was lower than in fertile samples.

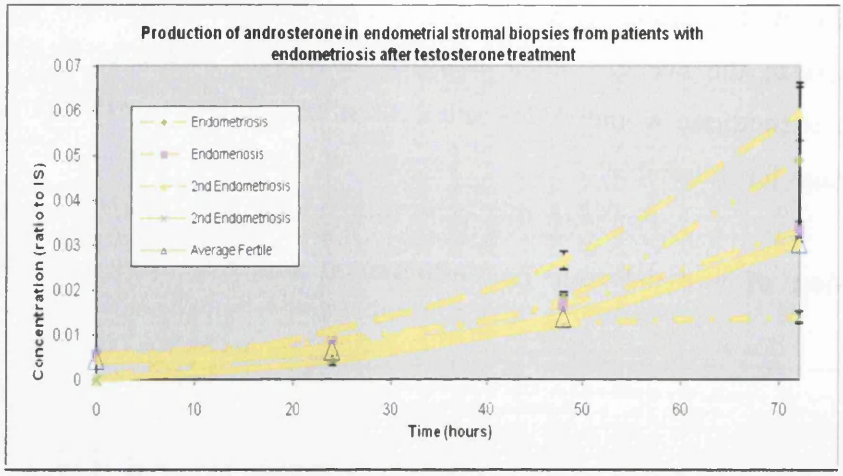

Fig 5.38: Production of androsterone in stromal cells from patients with endometriosis over 72 hours after addition of a 100nM testosterone media solution. Concentration is calculated as a ratio to the internal standard methyl-testosterone, analysed using an ESI source in positive mode on the LCQ DECA mass spectrometer with a C_{18} reversed phase column and an optimised methanol/water 0.1% acetic acid elution system.

Production of androsterone in endometriosis samples was similar to that of the averaged fertile sample following testosterone treatment. Three out of the four biopsies demonstrated a higher concentration at 72 hours (figure 5.38).

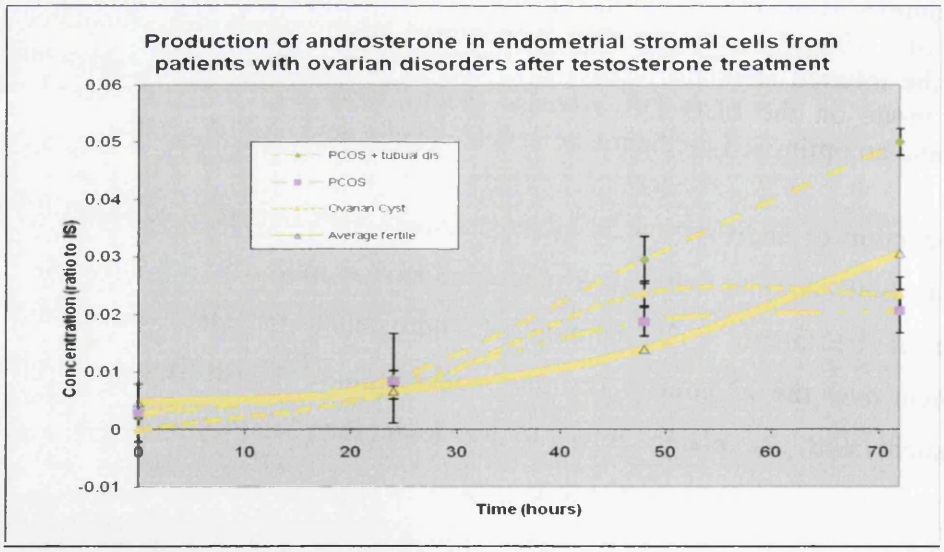

Fig 5.39: Production of androsterone in patients with ovarian disorders over 72 hours after addition of a 100nM testosterone media solution. Concentration is calculated as a ratio to the internal standard methyl-testosterone, analysed using an ESI source in positive mode on the LCQ DECA mass spectrometer with a C_{18} reversed phase column and an optimised methanol/water 0.1% acetic acid elution system.

The production of androsterone in patients with ovarian disorders was similar to the average fertile sample following testosterone treatment. All the ovarian disorder biopsy samples produced a maximum concentration of androsterone at 72 hours.

5.9.5 Production of androstanediol by endometrial biopsies after testosterone treatment

Production of androstanediol was not recorded in any of the biopsy samples following testosterone treatment. This could be related to the concentrations produced being below the limit of detection of the mass spectrometer (80.5nM). Detection of androstanediol may be possible with the inclusion of more time points as it is an intermediate steroid formed as the equilibrium between DHT (or androsterone) was achieved.

5.9.6 Production of oestrogens by endometrial biopsies after testosterone treatment

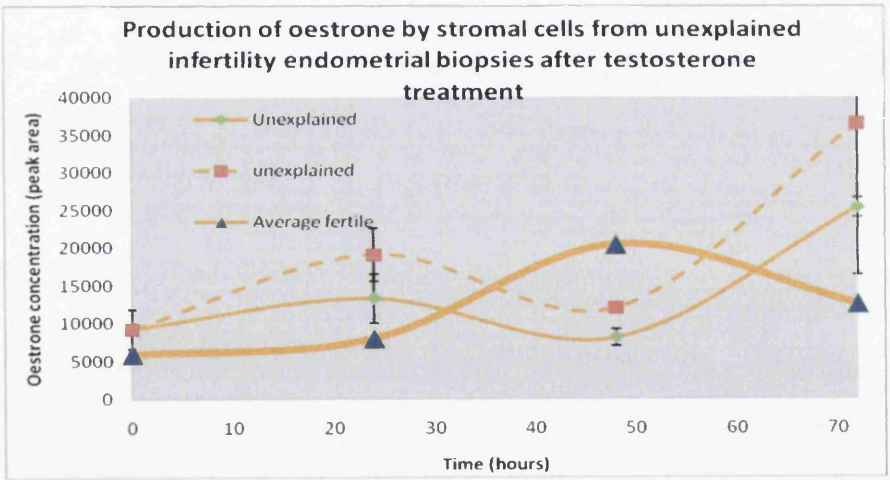

Fig 5.40: Oestrone production in unexplained infertility over 72 hours after addition of a 100nM testosterone media solution. Dansyl-chloride derivative analysed using an ESI source in positive mode on the LCQ DECA mass spectrometer using a phenyl hexyl column and an optimised methanol/water 0.1% formic acid elution system.

The two unexplained infertility biopsies produced oestrone from testosterone within the first 24 hours of the experiment. Oestrone production in unexplained infertility biopsies was similar, with decreased concentration of oestrone at 48 hours and increased oestrone concentration at 72 hours in comparison to the average fertile biopsies. This may be due to different expression of 17β-HSDs in unexplained infertility biopsies which inter-convert oestrone and oestradiol.

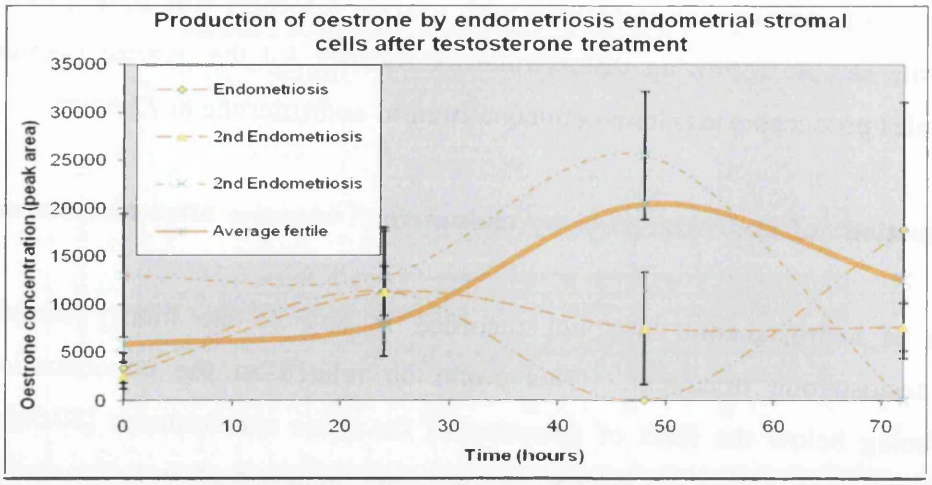

Fig 5.41: Oestrone production in endometriosis samples over 72 hours after addition of a 100nM testosterone media solution. Dansyl-chloride derivative analysed using an ESI source in positive mode on the LCQ DECA mass spectrometer using a phenyl hexyl column and an optimised methanol/water 0.1% formic acid elution system.

All endometriosis biopsies produced oestrone after addition of testosterone, suggesting the aromatase enzyme was active in these cells. After the first 24 hours the concentrations of oestrone fluctuates in the samples, possibly due to the production of oestrone in endometriosis biopsies via a number of pathways, (testosterone → oestradiol → oestrone, or testosterone → androstenedione → oestrone). A decrease in oestrone concentration in 2 of 3 endometriosis samples occurs at 48 hours.

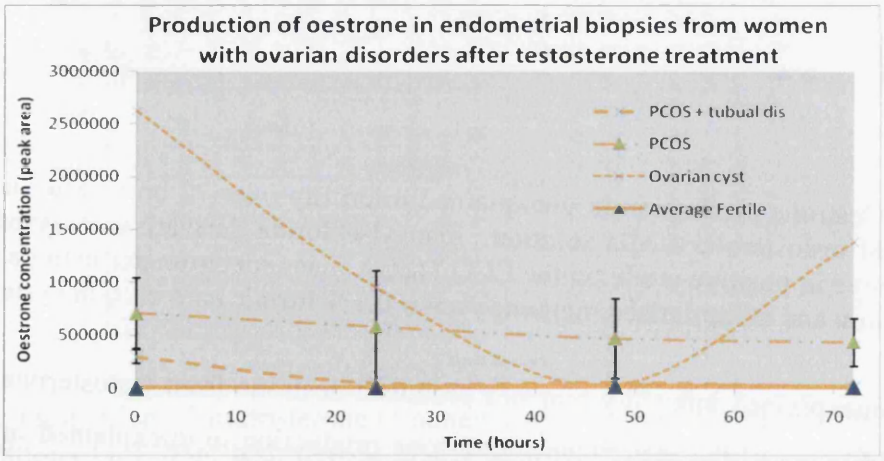

Fig 5.42: Oestrone production in ovarian disorders over 72 hours after addition of a 100nM testosterone media solution. Dansyl-chloride derivative analysed using an ESI source in positive mode on the LCQ DECA mass spectrometer using a phenyl hexyl column and an optimised methanol/water 0.1% formic acid elution system. Top graph shows all ovarian disorders, bottom graph shows ovarian disorders without the ovarian cyst sample.

A high amount of oestrone was detected at the start of the experiment (due to FCS concentrations) in the ovarian cyst sample (figure 5.42). In both PCOS biopsies the amount of oestrone decreased after time zero to a minimum at 72 hours. Oestrone concentrations were much higher in these samples than in the average fertile biopsies, however due to the very high initial concentrations any oestrone detected cannot be linked to testosterone metabolism.

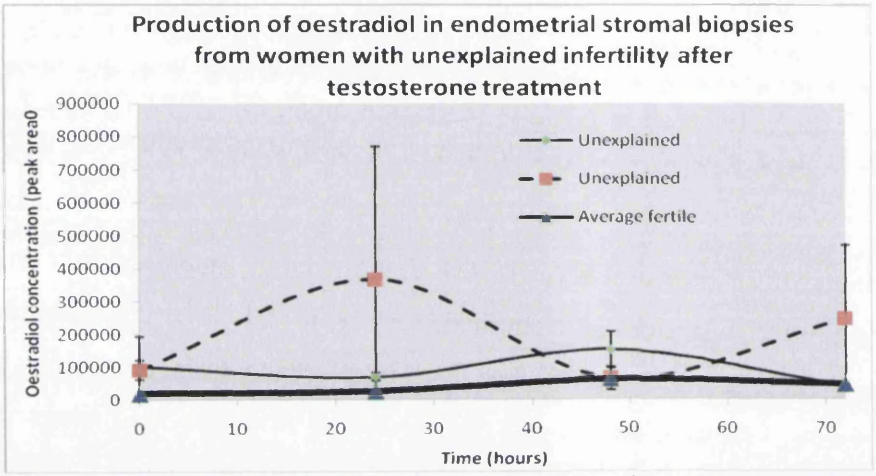

Fig 5.43: Oestradiol production in unexplained infertility biopsies over 72 hours after addition of a 100nM testosterone media solution. Dansyl-chloride derivative analysed using an ESI source in positive mode on the LCQ DECA mass spectrometer using a phenyl hexyl column and an optimised methanol/water 0.1% formic acid elution system.

The production of oestradiol was significantly higher in one of the unexplained infertility samples (dotted line) in comparison to the average fertile sample following testosterone treatment (figure 5.43). The other unexplained infertitlity biopsy (smooth line) had a similar oestradiol profile to the fertile throughout (assuming initial oestradiol concentration is discounted).

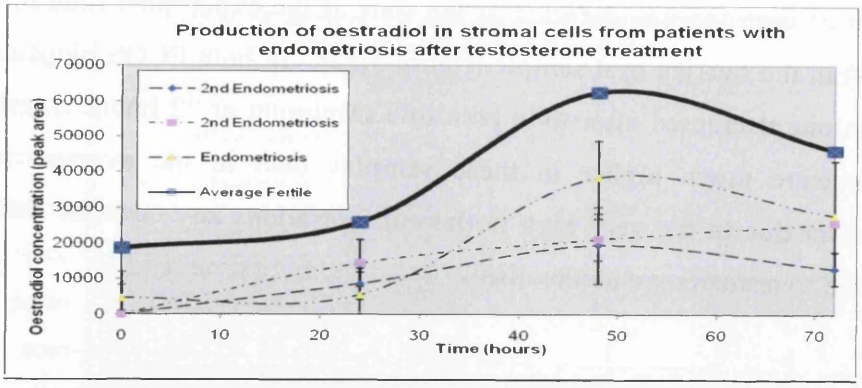

Fig 5.44: Oestradiol production in endometriosis samples over 72 hours after addition of a 100nM testosterone media solution. Dansyl-chloride derivative analysed using an ESI source in positive ionisation mode on the LCQ DECA mass spectrometer using a phenyl hexyl column and an optimised methanol/water 0.1% formic acid elution system.

All the endometriosis biopsies investigated demonstrated increases in oestradiol concentrations after testosterone treatment. The initial low concentration of oestradiol in these experiments indicates little interference from oestrogens in the foetal calf serum. Oestradiol detected after 48 and 72 hours was either due to testosterone metabolism through the aromatase enzyme or via the intermediates androstenedione and oestrone. The concentration of oestradiol in endometriosis samples was lower than the average fertiles at all time points, this was in part due to the higher initial oestradiol concentration in the fertile biopsies at time zero, however the metabolism contour is similar with a maximum oestradiol concentration in 2 of 3 endometriosis samples at 48 hours.

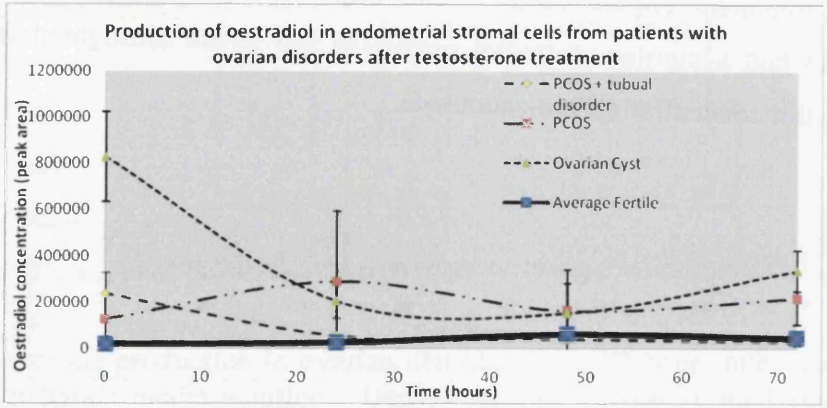

Fig 5.45: Production of oestradiol in patients with ovarian disorders over 72 hours after addition of a 100nM testosterone media solution. Dansyl-chloride derivative analysed using an ESI source in positive mode on the LCQ DECA mass spectrometer using a phenyl hexyl column and an optimised methanol/water 0.1% formic acid elution system.

Oestradiol was detected in an endometrial biopsy from a woman with an ovarian cyst and in endometrial biopsies from two women with PCOS (figure 5.45). The concentrations of oestradiol in these samples was higher than the average fertile throughout the experiments for the ovarian cyst and one PCOS biopsy, oestradiol metabolism in these samples was different from the fertile. After 24 hours the PCOS plus tubual disorder biopsy produced oestradiol in a similar manner to the fertile biopsies.

Case Studies

5.10 Testosterone metabolism by a stromal and epithelial endometrial atypical hyperplasia biopsy

Atypical endometrial hyperplasia is an oestrogen responsive condition, which can progress to endometrial cancer.[25] Atypical endometrial hyperplasia is defined by the elongation of the epithelial cells and glands, while stromal cell appearance essentially remains normal.[26] Throughout this thesis this biopsy is referred to as epithelial hyperplasia and stromal hyperplasia, however it is only in the epithelial cells that hyperplasia occurs.

In the endometrium stromal cells have been shown to directly affect steroid production in the epithelial cells,[27] however if cultured together stromal cells grow faster and steroid metabolism information regarding only the stromal cells is observed. In the endometrial hyperplasia biopsy all stromal cells were removed from the epithelial cells prior to steroid treatments to prevent this. This permitted analysis of variations in testosterone utilisation by the stromal and epithelial cells from an endometrial hyperplasia biopsy.

A biopsy was collected from a 55 year old patient with moderate atypical endometrial hyperplasia who suffered from post menopausal bleeding. This biopsy was split into 4 flasks of epithelial and 4 flasks of stromal cells and steroid profiles were determined after treatment with 100nM of testosterone.

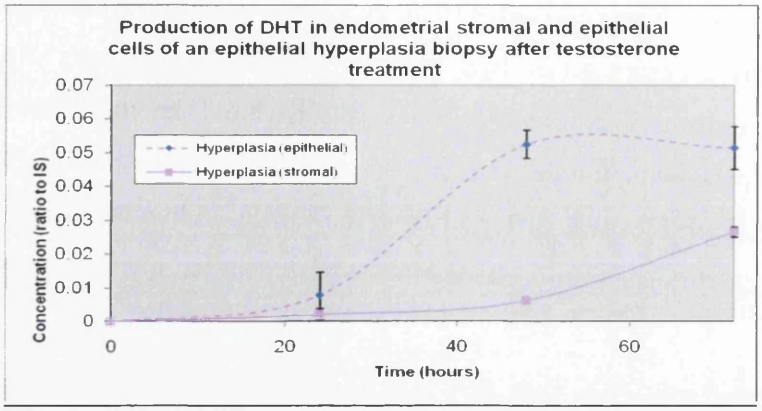

Fig 5.46: Comparison of DHT production in stromal and epithelial cells from a hyperplasia biopsy over 72 hours after addition of a 100nM testosterone media solution. Concentration is calculated as a ratio to the internal standard methyl-testosterone, analysed using an ESI source in positive mode on the LCQ DECA mass spectrometer using a C_{18} reversed phase column and an optimised methanol/water 0.1% acetic acid elution system.

There was a difference in the production of DHT in the stromal and epithelial cells of the above hyperplasia biopsy following testosterone treatment (figure 5.46). The final concentrations were 10.3 and 22.6nM in the stromal and epithelial cells, respectively. Production of DHT occurred in this hyperplasia biopsy, no DHT was detected in any fertile samples following testosterone treatment, demonstrating an altered androgenic profile after testosterone treatment of this hyperplasia biopsy in comparison to the fertile biopsies.

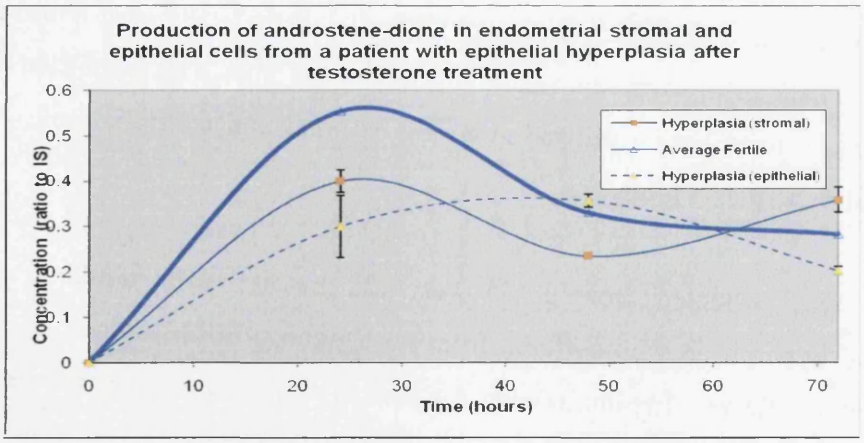

Fig 5.47: Production of androstenedione comparisons between stroma and epithelia from an endometrial hyperplasia biopsy and fertile stromal cells over 72 hours after addition of a 100nM testosterone media solution. Concentration is calculated as a ratio to the internal standard methyl-testosterone, analysed using an ESI source in positive mode on the LCQ DECA mass spectrometer using a C_{18} reversed phase column and an optimised methanol/water 0.1% acetic acid elution system.

The stromal hyperplasia biopsy investigated produced androstenedione in a similar pattern to the fertile biopsies but at lower concentrations (until 72 hours) following testosterone treatment. The epithelial production of androstenedione after testosterone treatment has a maximum at 48 hours where a minimum is observed in the stromal cells (figure 5.47).

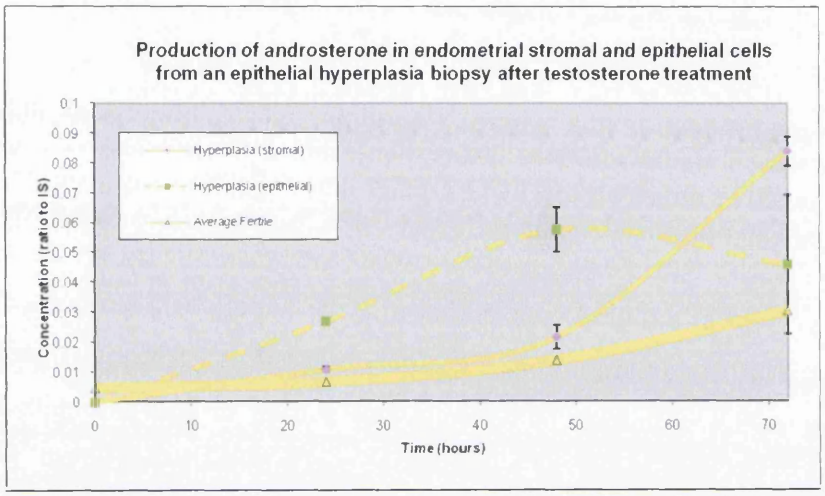

Fig 5.48: Production of androstreone in stromal and epithelial cells from a hyperplasia biopsy over 72 hours after addition of a 100nM testosterone media solution. Concentration is calculated as a ratio to the internal standard methyl-testosterone, analysed using an ESI source in positive mode on the LCQ DECA mass spectrometer using a C_{18} reversed phase column and an optimised methanol/water 0.1% acetic acid elution system.

The stromal hyperplasia sample demonstrated altered production of androsterone compared to the fertiles, with higher concentrations produced at 72 hours (figure 5.48). The epithelial hyperplasia cells produced higher concentrations of androsterone than the stromal cells at 48 hours 16.5nM, but at 72 hours the concentration of androsterone was higher in the stromal cells 24.1nM.

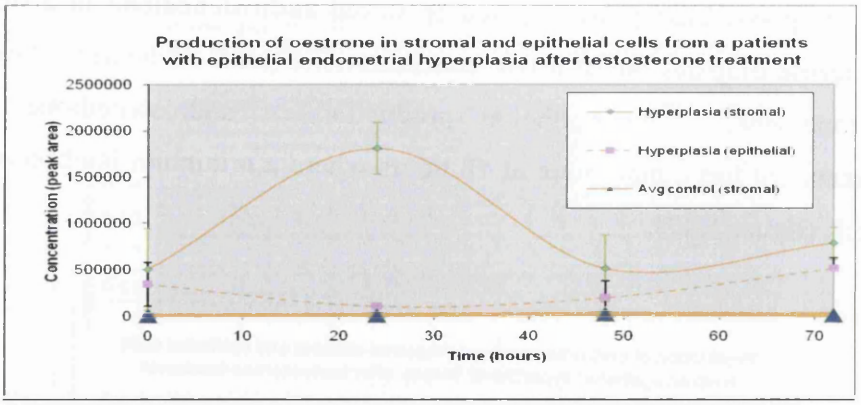

Fig 5.49: Oestrone production in a hyperplasia sample over 72 hours after addition of a 100nM testosterone media solution. Dansyl-chloride derivative analysed using an ESI source in positive mode on the LCQ DECA mass spectrometer using a phenyl hexyl column and an optimised methanol/water 0.1% formic acid elution system.

Oestrone was present at a higher concentration in the hyperplasia stromal cells than fertile biopsies with a maximum concentration observed at 24 hours (figure 5.49). After 72 hours the concentration of oestrone was similar in both the epithelial and stromal cells. The production of oestrone was significantly different from the averaged fertile biopsies for stromal cells throughout the experiment, with a higher concentration observed in the hyperplasia stromal cells after 24 hours. Oestrone was produced by the epithelial cells after testosterone treatment with a maximum at 72 hours. Oestrone production from testosterone by both the epithelial and stromal cells from the hyperplasia biopsy may occur via oestradiol (aromatisation) followed by conversion to oestrone by the HSDs, or from testosterone to androstenedione (via HSDs) and to oestrone by aromatase, (RT-PCR is required to confirm expression of these enzymes in these biopsies).

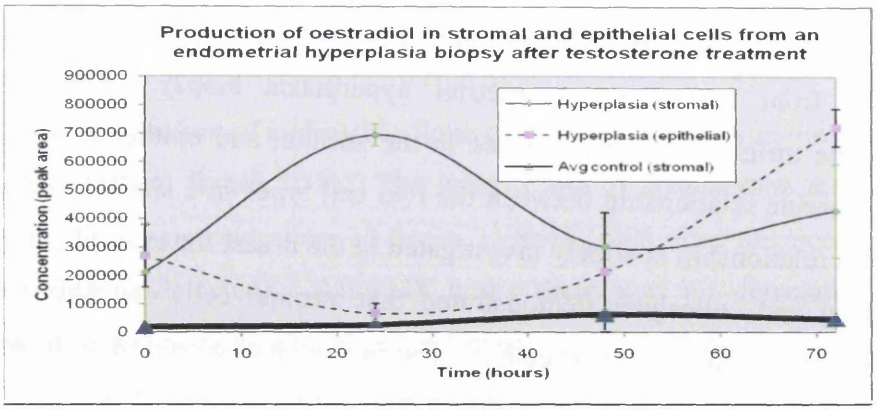

Fig 5.50: Production of oestradiol in stromal and epithelial cells from an endometrial hyperplasia biopsy over 72 hours after addition of a 100nM testosterone media solution. Dansyl-chloride derivative analysed using an ESI source in positive mode on the LCQ DECA mass spectrometer using a phenyl hexyl column and an optimised methanol/water 0.1% formic acid elution system.

There were differences in the production of oestradiol in the stromal and epithelial cells from the hyperplasia sample following testosterone treatment (figure 5.50). In the first 24 hours the highest concentration of oestradiol was observed in the stromal cells, at 72 hours the highest oestradiol concentration was observed in the epithelial cells. The concentration of oestradiol in the stromal cells from the endometrial hyperplasia biopsy was higher throughout the experiment than the averaged stromal fertile biopsies. Oestradiol may be produced from added testosterone (or androstenedione) in both hyperplasia cell types via the aromatase enzyme, this can occur via two pathways;

testosterone → androstenedione → oestrone → oestradiol,

testosterone → oestradiol.

The stromal hyperplasia cells produced different steroid production of androsterone, DHT, oestrone and oestradiol compared to the fertile stromal biopsies. Despite these observations being for only one example of this pathology, changes in all of the testosterone metabolites investigated except androstenedione (compared to the fertile) is consistent with altered testosterone utilisation. It was expected that hyperplasia samples will produce more oestrogens through highly expressed aromatase[28] in comparison to fertile samples, this was confirmed here by high oestrogen concentrations. Production of DHT was also significantly different compared to the fertile, suggesting a possible role for DHT in endometrial hyperplasia progression.

It was concluded that there were different rates of steroid metabolism in stromal and epithelial cells from the same endometrial hyperplasia biopsy. *In-vitro* the differences in the utilisation of testosterone in the stromal and epithelial cells may result in an paracrine relationship between the two cell types in a similar manner to the breast. This relationship is widely investigated in the breast for example previous work by Wilson and colleagues demonstrated that stromal cells can alter steroid metabolism in surrounding epithelial cells.[29] The inclusion of a co-culture technique would confirm this relationship in the endometrium.

5.11 Testosterone metabolism by an endometrial polyp biopsy

A biopsy was collected from a 43 year old patient with an endometrial polyp. Steroid profiles were calculated after treatment of the stromal cells with 100nM media solutions of testosterone.

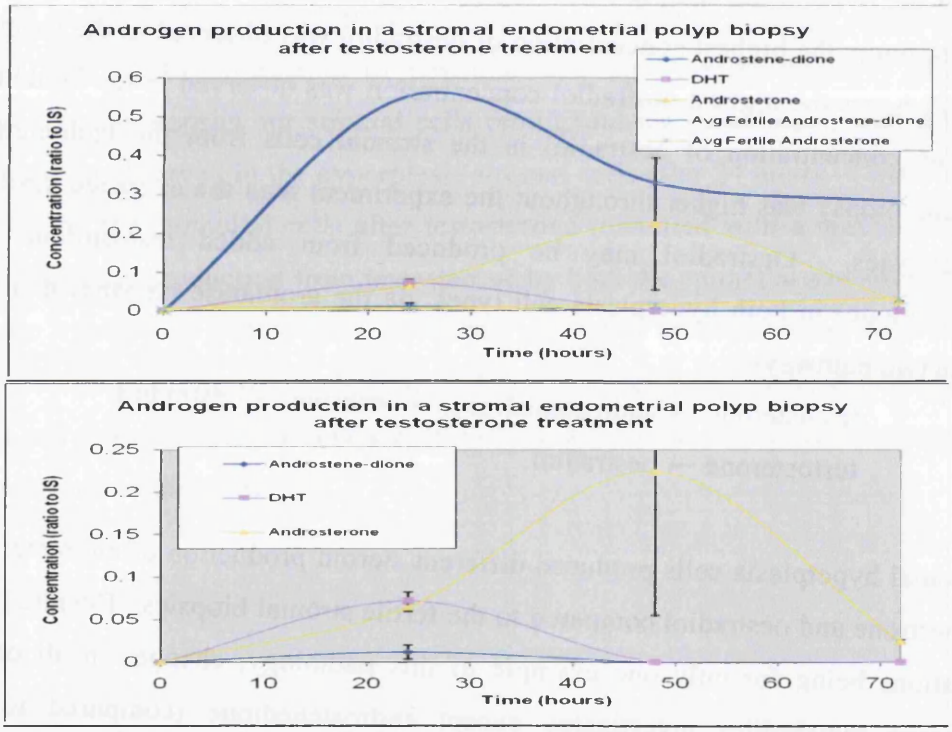

Fig 5.51: Production of steroids in an endometrial polyp stromal biopsy over 72 hours after addition of a 100nM testosterone media solution. Top graph compares the testosterone metabolites produced by the average fertile biopsies to the endometrial polyp, bottom graph has a reduced scale and illustrates production of androstenedione, DHT and androsterone in an endometrial polyp without the inclusion of the fertile biopsies. Concentration is calculated as a ratio to the internal standard methyl-testosterone, analysed using an ESI source in positive mode on the LCQ DECA mass spectrometer with a C_{18} reversed phase column and an optimised methanol/water 0.1% acetic acid elution system.

The endometrial polyp biopsy demonstrated a significantly different testosterone metbolism profile in comparison to the fertile biopsies (figures 5.51 and 5.52). There was a small concentration of androstenedione detected at 24 hours in the endometrial polyp biopsy (bottom figure 5.51). The initial route of testosterone metabolism is through DHT (max concentration 24 hours 31.8nM), this does not occur in fertile biopsies (no DHT detected). After 48 hours there was no detectable DHT or androstenedione by the endometrial polyp biopsy. Androsterone was then produced as an androgenic end product (maximum concentration of 65.0nM at 48 hours) at higher concentrations than observed in the fertile biopsies.

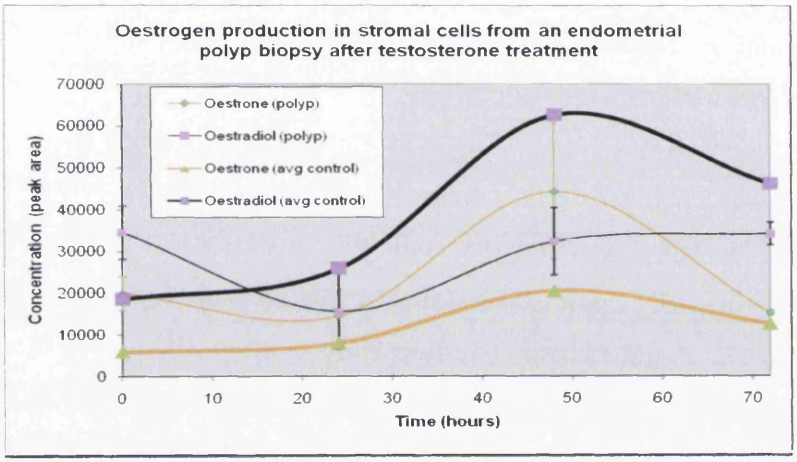

Fig 5.52: Oestrogen production in a stromal biopsy from an endometrial polyp over 72 hours after addition of a 100nM testosterone media solution. Average fertile concentrations are presented as the wider lines. Oestradiol in black and oestrone in orange. Dansyl-chloride derivatives analysed using an ESI source in positive mode on the LCQ DECA mass spectrometer using a phenyl hexyl column and an optimised methanol/water 0.1% formic acid elution system.

Oestrogen production was occurring in this endometrial polyp sample following testosterone treatment, with an increase in concentration of both oestrone and oestradiol observed at 48 hours. The concentration of oestrone was higher at all time points than in the fertile biopsies, and the concentration of oestradiol was reduced at all time points relative to the fertile biopsies. Oestradiol can be produced in the endometrial polyp biopsy via two pathways;

testosterone → oestradiol,

testosterone → androstenedione → oestrone → oestradiol.

Despite these observations being for only one example of this pathology, changes in all of the testosterone metabolites investigated was consistent with an altered testosterone utilisation in this endometrial polyp biopsy (compared to the fertile).

5.12 Conclusions biopsy steroid metabolism

Testosterone was metabolised rapidly in all endometrial biopsies irrespective of the pathology. The role of testosterone only as a precursor to oestrogen synthesis is restricted. Testosterone is involved in regulation of a number of transcription factors, genes and proteins in the endometrium such as the metalloproteinase MMP-1 which is involved in implantation and menstruation.[30] Testosterone has been defined as being important in normal endometrial function and may also be involved in progression of some endometrial disorders.

The major difference in testosterone metabolism between biopsy samples was the synthesis of DHT. DHT was not detected in any of the fertile (4 biopsies) or unexplained infertility (2 biopsies) samples, but was present in endometrial biopsies from patients with endometriosis (4 biopsies), ovarian disorders (3 biopsies), endometrial hyperplasia (1 biopsy), and an endometrial polyp (1 biopsy). Although the numbers of biopsies in the hyperplasia, endometrial polyp and unexplained infertility groups were small, it was concluded that DHT production was associated with benign endometrial pathologies following testosterone treatment. The role DHT plays in progression of these disorders has not been confirmed, although it has been described by Ito and colleagues to be involved in regulation of androgen action and cellular proliferation in normal and cancerous endometria.[31] The role of DHT in androgen dependent tumours is important, it is described at the most potent androgen, important in proliferation in steroid responsive prostate cancer.[32] It is possible that DHT also plays a vital role in the progression of proliferative endometrial disorders and alteration of the differentiation function in this tissue.

A previous investigation by Lovely and co-workers defined the presence of DHT in the endometria of women with PCOS due to high circulatory androgen levels which induced endometrial AR expression.[33] However it was concluded that any DHT recorded in the experiments reported here was due to localised (cellular) steroid metabolism as the biopsies investigated have been through at least 3 passages to

obtain enough cells for experimentation, any residual DHT from the circulatory system will have been removed in this process. In agreement with this Leon and colleagues determined that localised steroid biosynthesis occurs in the endometria of women with PCOS independently of circulatory steroid concentration.[34] It is probable that increased DHT concentrations recorded in endometria of women with PCOS were due to increases in both circulatory and localised DHT production.

The metabolism of androstenedione in all endometrial disorders was not significantly altered from the fertiles to differentiate between pathologies. The end concentrations of androstenedione were similar in all samples (except endometrial polyp).

The metabolism of testosterone to androsterone in all endometrial disorders was not significantly altered from the fertiles to differentiate between pathologies. A similar increase in concentration was observed in all samples with a maximum at 72 hours, this is because androsterone is an androgenic end product produced irrespective of which side of the bio-pathway was active.

5.12.1 Conclusions oestrogens

Both oestrone and oestradiol were produced in the fertile biopsies probably via the aromatase enzyme. The biopsies here were taken at the early proliferative stage and it is possible that the production of oestradiol and oestrone could be due to aromatase expression at this stage of the menstrual cycle, RT-PCR experiments will permit the determination of aromatase expression in these fertile biopsies and correlations with oestrogen production if observed.

Oestrone concentration decreased in both PCOS samples from the high initial concentration observed at time zero. Oestradiol profiles for both PCOS biopsies differ significantly, again a high concentration of oestradiol due to FCS makes trends difficult to determine.

In the ovarian cyst biopsy a similar contour was observed for oestradiol and oestrone concentrations after testosterone treatment. There was a very high initial concentration of both present at time zero, this high concentration was metabolised to other products over the next 48 hours possibly through conversion via either 17β-

HSDs or oestrogen sulphotransferases. At 72 hours the concentration of both oestradiol and oestrone increased again, probably due to the aromatisation of testosterone and/or androstenedione.

5.12.2 Conclusions endometriosis

The production of androstenedione and androsterone in stromal cells derived from the endometria of women with endometriosis was similar to the fertile biopsies following testosterone treatment. The metabolism of DHT, oestrone and oestradiol in all endometriosis biopsies was different from the fertile biopsies, inclusion of enzyme expression information may be able to explain these differences.

There was no uniformity in the profiles for the significantly altered steroids (DHT, oestrone, oestradiol) in the endometriosis biopsies probably due to differences in stage or severity of the endometriosis in each individual (as described in chapter 1.6.2). It was also expected that large variations in enzyme expression between biopsies may therefore occur.

Production of DHT may be important in endometriosis patients as duel treatments may be required for these women to conceive, the first to combat the ovarian dysfunction and the second to alter steroid metabolism in their endometrium. This altered androgen metabolism in the endometria of women with ovarian disorders may cause problems with uterine receptivity.

5.12.3 Conclusions Unexplained Infertility

Steroid metabolism by the two biopsies from patients with unexplained infertility demonstrated similar steroid profiles to the fertile biopsies for testosterone, androstenedione, oestrone and produced no DHT.

There was a significantly lower concentration of androsterone recorded at 72 hours in the first unexplained infertility biopsy (2.55 compared to 7.88nM average fertile) and the concentration of oestradiol was similar to the fertile. The second unexplained infertility biopsy had a similar profile for androsterone and an increased concentration of oestradiol relative to the fertile. The altered steroid profile whether androgen or oestrogen related could be significant enough to cause infertility in these

women, however the similarities in production of all other steroids after testosterone treatment (especially no production of DHT) provides no positive conclusion. It is possible that another reason for infertility in these women such as quality of the ovum or foetal bone fragments could be the main reason for their infertility.[35]

5.13 Conclusions Chapter Five

Initial investigations into steroid metabolism in cell lines permitted optimisation of experimental procedures which were applied to endometrial biopsy samples from women with endometriosis, as there was previous evidence of altered steroid metabolism. This was extended to include a smaller number of benign endometrial pathologies. Pregnenolone, testosterone and oestradiol treatments of the cell lines indicated that pregnenolone was not metabolised to any other steroids suggesting the enzymes responsible for pregnenolone metabolism were not active in these endometrial cell lines, and that a steroid below pregnenolone in the bio-pathway is responsible for oestrogen production in the endometria. Oestradiol was metabolised to oestrone probably through conversion via specific 17β-HSDs, addition of oestradiol did not provide any new information about steroid metabolism in the endometria.

Steroid treatments with the bio-available androgen, testosterone provided novel information about steroid synthesis in established cell lines and benign endometrial conditions. Steroid metabolism varied in the cell lines and biopsies under investigation. Testosterone metabolism in all conditions occurs via the initial metabolites;

1. DHT,
2. androstenedione,
3. oestradiol or,
4. DHT and androstenedione depending on the cell line or pathology.

Production of these steroids may occur via a number of enzymes (5AR1, 5AR2, 17β-HSD2, 4, 8, and aromatase), the significance the expression of each of these enzymes has on the steroid profile was determined in chapters 6 and 7.

Testosterone metabolism in fertile biopsies was representative of testosterone metabolism by the RL95-2 cell line: testosterone to androstenedione to androsterone

(no DHT). When analysing androgen metabolism in healthy samples this cell line could be recommended as a model. Ishikawa and HEC-1A metabolise testosterone into both androstenedione and DHT which was comparable to biopsies from patients with endometriosis and ovarian disorders. The endometrial polyp biopsy metabolises testosterone primarily to DHT this was representative of androgen metabolism in the HEC-1B and COV434 cell lines. This highlights the importance of selecting the correct cell line for investigations into steroid metabolism in endometrial disorders. Production of oestrogens by the cell lines was minimal, however a number of biopsies produced oestradiol or oestrone after testosterone treatment (PCOS, hyperplasia), it is therefore expected that these biopsies express the aromatase enzyme and actively convert androgens to oestrogens.

The production of androgens in preference to oestrogens was unexpected especially in the cell line COV434 which highly expressed the aromatase enzyme. It is possible that the aromatase enzyme has become saturated in the high androgen environment. This phenomenon has been described previously by Havelock and Thompson who both saw saturation of the aromatase enzyme in ovarian granulosa cells in high androgen environments with the result of DHT being produced in preference to oestrogens.[36,37] This is similar to the results obtained for the COV434 cell line in these experiments.

The inclusion of steroid converting enzyme expression data should provide additional information on the routes to the altered steroid metabolism in these conditions in comparison to fertile biopsies. This was conducted and the results were recorded in chapter 6, following this a comparison of steroid profiles and steroid converting enzyme expression was completed to determine any correlations between the two as described in chapter seven.

5.14 References Chapter Five

[1] Bukulmez O, Hardy DB, Carr BR, Auchus RJ, Toloubeydokhti T, Word RA, Mendelson CR. J Clin Endocrinol Metab **93** (2008) 3471-3477

[2] Glasser S, Aplin J, Giudice LC, Tabobzadeh S. The Endometrium Pub: Informa Health Care (2002) 443-445

[3] Albitar L, Pickett G, Morgan M, Davies S, Leslie K K Gynecologic Oncology **106** (2007) 52-64

[4] Zhang H, Vollmer M, De Geyer M, Litzistorf Y, Ladewig A, Dürrenberger M, Guggenheim R, Miny P, Holzgreve W, De Geyter C. Molecular Human Reproduction **6** (2000) 146-153

[5] Chetrite G, Pasqualini J R J Steroid Biochem. Biol. **61** (1997) 27-34

[6] Way DL, Grosso DS, Davis JR, Surwit EA, CD Christian. InVitro **19** (1983) 147-158 (now renamed In Vitro Cellular and developmental biology)

[7] American Type Culture Collection,UK www.lgcpromochem-atcc.com accessed 12th November 2008

[8] Thiboutot D, Jabara S, McAllister JM, Sivarajah A, Gilliland K, Cong Z, Clawson G. J Invest Dermatol **120** (2003) 905-914

[9] Rivera-Woll LM, Papalia M, Davis SR, Burger HG. Human Repro Update **10** (2004) 421-432

[10] Segawa T, SHozu M, Murakami K, Kasai T, Shinohara K, Nomura K, Ohno S, Inoue M. **11** (2005) 2188-2194

[11] Ito K, Utsunomiya H, Suzuki T, Saitou S, Akahira J-I, Okamura K, Yaegashi N, Sasano H. Mol and Cell Endocrin **248** (2006) 136-140

[12] Allen NE, Key TJ, Dossus L, Rinaldi S, Cust A, Lukanova A, Peeters PH, Onland-Moret NC, Lahmann PH, Berrino F, Panico S, Larrañaga N, Pera G, Tormo MJ, Sánchez MJ, Quirós JR, Ardanaz E, Tjønneland A, Olsen A, Chang-Claude J, Linseisen J, Schulz M, Boeing H, Lundin E, Palli D, Overvad K, Clavel-Chapelon F, Boutron-Ruault M-C, Bingham S, Khaw K-T, Bueno-de-Mesquita HB, Trichopoulou A, Trichopoulos D, Naska A, Tumino R, Riboli E, Kaaks R. Endocrine-Related Cancer **15** (2008) 485-497

[13] Giudice LC, Best Practise and Clinical Endocrin and Met **20** (2006) 235-244

[14] Utsunomiya H, Ito K, Suzuki T, Kitamura T, Kanedko C, Nakata T, Niikura H, Okanura K, Yaegashi N, Sasano H. Clinical cancer research **10** (2004) 5850-5856

[15] Lukanova A, Kaaks R. Cancer Epidemiology, biomarkers and prevention Review **14** (2005) 98-102

[16] Zhang P, Hammer F, Bair S, Wang J, Reeves WH, Mellon SH. DNA and Cell Biol **18** (1999) 197-208

[17] Dorrington JH, Fritz I B. Biochem and Biophys Research Comm **54** (1973) 1425-1431

[18] Thèriault C, Labrie F. J Steroid Biochem and Mol Biol **38** (1991) 155-164

[19] Fournier M-A, Poirier D. Mol and Cell Endo **301** (2009) 142-145

[20] Kitawaki J, Kado N, Ishihara H, Koshiba H, Kitaoka Y, Honjo H. J Steroid Biochem and Mol Biol **83** (2003) 149-155

[21] Kaku T, Hirakawa T, Sakai K, Amada S, Kobayashi H, Nakano H. Gynecologic Oncology 72 (1999) 51-55

[22] Leon L, Bacallao K, gabler F, Romero C, Valladares L, Vega M. Steroids **73** (2008) 88-95

[23] Pienkowski C, Baunin C, Gayrard M, Lemasson F, Vaysse P, Tauber M. Paediatric and adolescent gynecology. Evidence-Based Clinical Practise **7** (2004) 66-76

[24] Hileeto D, Fadare O, Martel M, Zheng W. World Journal of Surgical Oncology **3**:8 (2005) doi:10.1186/1477-7819-3-8

[25] Zaino RJ, Kauderer J, Liu Trimble C, Silverberg SG, Curtin JP, Lim PC, Gallup DG. Cancer **106** (2006) 804-811

[26] Horn L-C, Meinel A, Handzel R, Einenkel J. Pathology **11** (2007) 297-311

[27] Arnold JA, Kaufman DG, Seppälä M, Lessey BA. Human Reproduction **16** (2001) 836-845

[28] Li H, Chen X, Qiao J, Inter J of Gyne and Obste **100** (2008) 10-12

[29] Wilson CL, Sims AH, Howell A, Miller CJ, Clarke RB. Endo related Cancer **13** (2006) 617-628

[30] Ishikawa T, Harada T, Kubota T, Aso T. Reproduction **133** (2007) 1233-1239

[31] Ito K, Suzuki T, Akahira J-I, Moriya T, Kaneko C, Utsunomiya H, Yaegashi N, Okamura K, Sasano H. Int J. Cancer **99** (2002) 652-657

[32] Carruba G, Granata OM, Farruggio R, Cannella S, Bue AL, Leake RE, Pavone-Macaluso M, Castagnetta LAM. Steroids **61** (1996) 41-46
[33] Lovely LP, Appa Rao KB, Gui Y, Lessey BA. Steroid Biochem and Mol Bio **74** (2000) 235-241
[34] Leon , Bacallao K, Gabler F, Romero C, Valladares L, Vega M. Steroids **73** (2008) 88-95
[35] Elsford K, Claman P. Fertility and Sterility **79** (2003) 1028-1030
[36] Havelock JC, Rainey WE, Carr BR. Mol and Cell Endocrinology **228** (2004) 67-78
[37] Thompson MA, Adelson MD, Kaufman LM, Marshall LD, Coble DA. Cancer Research **48** (1988) 6491-6497

Chapter six

Real time polymerase reaction (RT-PCR) for analysis of steroid converting enzyme expression in established endometrial cell lines and biopsies

6.0 Introduction

This chapter describes basal expression data for the enzymes aromatase, 17β-HSD1, 17β-HSD2, 17β-HSD4, 17β-HSD5, 17β-HSD7, 17β-HSD8, 5AR1 and 5AR2 (described in chapter 1.3 and table 6.0) in the endometrial epithelial cell lines Ishikawa, HEC-1A, HEC-1B, RL95-2 and the ovarian granulosa cell line COV434 (aromatase positive). In order to access expression of these enzymes analysis of their RNA was determined by quantitative real-time, reverse transcriptase PCR (QRT-PCR). RNA expression of steroid converting enzymes in the established cell lines under basal conditions (starting quantity no steroid treatment) provided information from which an estimated steroid profile was determined. The mass spectrometry data obtained after steroid treatments of these cell lines permitted a comparison of metabolic profiles to enzyme expression which could validate the original hypothesis (chapter 7).

Following optimisation of techniques and methodologies using established cell lines the same experimental methods to determine enzyme expression were applied to endometrial biopsy samples obtained from fertile, endometriosis, PCOS patients and patients diagnosed with unexplained infertility, an endometrial polyp or ovarian cyst.

Basal enzyme expression profiles were compared to highlight similarities and differences in RNA expression in a number of endometrial pathologies. The differences in enzyme expression between fertile biopsies and endometrial cancer cell lines (or endometrial disorders) could be essential to understanding altered steroid metabolism in these pathologies. This could highlight specific previously unrecognised enzyme targets, antagonism of which could lead to novel treatments for specific endometrial disorders.

Temporal changes in RNA expression after testosterone treatments were recorded in all samples. Testosterone treatments of biopsies and cell lines were conducted over 72 hours and enzyme expression was measured throughout this time. This permitted analysis of changing RNA expression after testosterone treatment in each cell line or biopsy. Again the different pathologies were compared to highlight differences and similarities in enzyme expression profiles over 72 hours after testosterone treatment.

A flow chart outlining the experiments undertaken to analyse RNA enzyme expression if the steroid converting enzymes is described in figure 6.0.

Table 6.0: Steroid converting enzymes nomenclature and suggested reactions under investigation in these experiments, (the major reactions were determined from a literature search references 2, and 13-31 chapter 1). All the HSD's here are isoforms of 17β-HSD, however to simplify the information they are expressed as HSD1, HSD2 etc.

Steroid converting enzyme	Major reactions in androgen/oestrogen synthesis	Other reactions
Aromatase	Testosterone → Oestradiol Androstenedione → Oestrone	-
HSD1	Oestrone → Oestradiol	DHEA →Androstene-diol
HSD2	Oestradiol → Oestrone Testosterone → Androstenedione DHT → Androstane-dione Androstanediol → Androsterone	20α-progesterone →Progesterone
HSD4	Testosterone → Androstenedione Oestradiol → Oestrone	Peroxisomal fatty acid metabolism
HSD5	Androstenedione → Testosterone Androstane-dione → DHT Androsterone → Androstanediol Oestrone → Oestradiol	Progesterone→ 20α-hydroxyl progesterone
HSD7	Oestrone → Oestradiol DHT → Androstanediol	Cholesterol biosynthesis
HSD8	DHT → Androstane-dione Testosterone → Androstenedione Oestradiol → Oestrone	Fatty acid metabolism
5AR1	Testosterone → DHT Androstenedione → Androstane-dione	-
5AR2	Testosterone → DHT Androstenedione → Androstane-dione	-

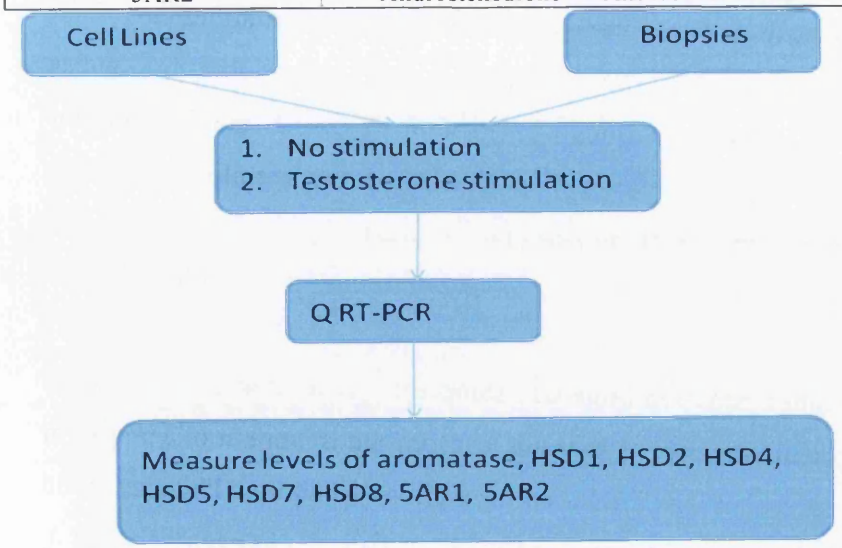

Fig 6.0: Schematic describing the approach taken to analyse expression of RNA relating to specific steroid converting enzymes in cell lines and biopsies. 1. Corresponds to basal RNA expression and 2 corresponds to changes in expression after testosterone treatment, this was determined for a number of time points over 72 hours for each experiment.

Information concerning the expression levels of some of these enzymes was available in the literature, allowing comparisons of the results obtained here to previously described observations. There was not however one study which encompasses the range of steroid converting enzymes or the number of endometrial pathologies investigated here, and there are no examples of a comparative study which incorporates multiple enzyme expression data with testosterone metabolism mass spectrometry information (chapter 7).

This chapter will present cell line and biopsy experiments principally focussing on the expression of specific steroid converting enzymes. The data is presented as follows;

-Primer design.

Cell lines;

- Relative basal expression of aromatase, 17β-HSD1, 2, 4, 5, 7, 8 and 5AR1 and 2.
- Changing enzyme expression following testosterone treatment (72 hours) in each cell line.
- Conclusions (cell lines).

Biopsies;

- Comparison of basal expression of aromatase, 17β-HSD1, 2, 4, 5, 7, 8, 5AR1 and 2 in stromal cells from fertile endometrial biopsies (four samples) to;
  a) endometriosis biopsies (six samples),
  b) endometrial biopsies from women with PCOS (2 samples) and an endometrial biopsy from a woman with an ovarian cyst (1 sample),
  c) unexplained infertility biopsies (2 samples),
  d) an endometrial hyperplasia biopsy (stromal and epithelial cells from 1 sample) and,
  e) an endometrial polyp biopsy (1 sample)
- Changing enzyme expression following testosterone treatment (72 hours) in all endometrial biopsies.
- Conclusions (cell lines).

6.1 Primer design and housekeeping genes for quantitative real-time reverse transcription polymerase chain reaction (RT-PCR)

QRT-PCR was employed in these experiments to determine RNA expression of the steroid converting enzymes as described in chapter 3.4. The quality of the primer pair was important; all specific primer pairs were designed using Beacon Design 2.0 software (Premier Biosoft, USA) to ensure the reaction was as efficient as possible.

All primers were between 15 and 30 base pairs in length, and were tested for primer dimer formation or for annealing non-specifically. A blast search on all primers was run in the Beacon Design software to make sure the primers would not anneal to other targets. In addition analysis of the melting curves was completed in all experiments and the presence of a single homogeneous melt curve peak for all reactions was confirmed (this was indicative of a single PCR product being amplified in each reaction). In order to generate meaningful data that can be compared from sample to sample it was important to quantify as well as normalise the data with the inclusion of a normalising gene. The normalising gene is typically a 'housekeeping gene' whose expression should be constant under the experimental conditions under investigation. The housekeeping gene in these experiments was GADPH (glyceraldehyde-3-phosphate-dehydrogenase) which has been well characterised and widely used.[1] As expression of the housekeeping gene was constant any variation in the threshold cycle (Ct) of the housekeeping gene can be attributed to other sources of variation such as efficiency of the reverse transcription reaction, yield of RNA purification and variation in the number of cells from which RNA was purified. The standard curves and the samples were run in triplicate to provide statistical improvement.

6.2 Relative enzyme expression in cell lines

To compare basal RNA expression levels for each steroid converting enzyme between cell lines a number of RT-PCR experiments were devised. 100ng/μL of RNA from each of the five cell lines was converted to cDNA combined together and diluted to make a standard curve. Onto this curve the expression of each steroid converting enzyme for each cell line under basal conditions was applied. This provides comparative starting quantity expression information for each enzyme in each of the cell lines, for example we observed which cell line has the highest (and

lowest) aromatase expression. Enzyme expression in biopsy samples was also applied to this calibration series to determine enzyme expression profiles in a number of endometrial pathologies. Expression of each enzyme under basal conditions was compared between cell lines to determine significantly similar expression. Statistical analysis was performed using the Minitab 1.5 software package. For every set of data an unpaired t-test was performed for the normally distributed RT-PCR data obtained for the basal expression of steroid converting enzymes in endometrial cell lines. Statistical analysis of the changes in fold expression relative to basal expression after testosterone treatment were also calculated by this method (6.3 onwards). A calculated significance P value <0.05 was considered statistically significant.

6.2.1 Aromatase expression

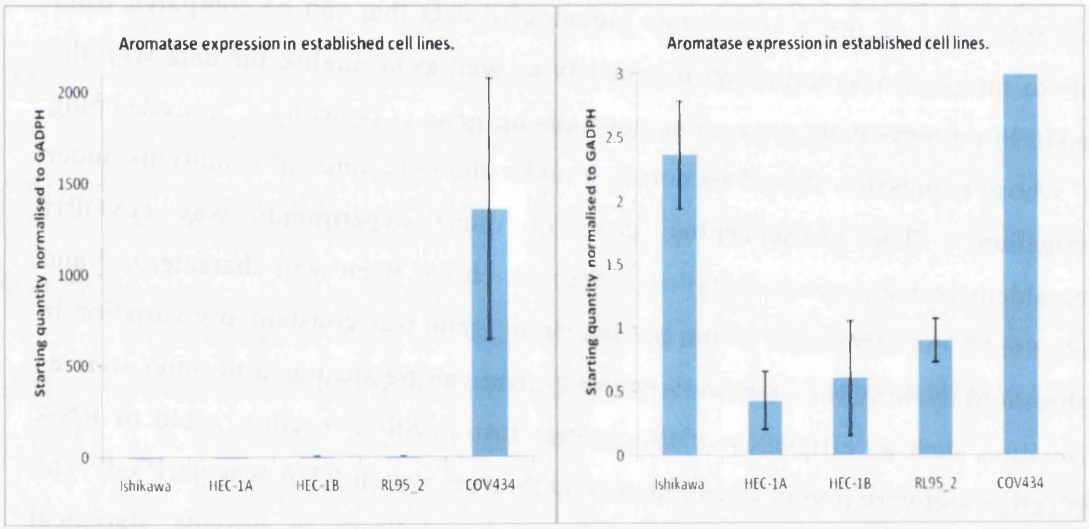

Fig 6.1: Relative basal expression of aromatase in the Ishikawa, HEC-1A, HEC-1B, RL95-2 and COV434 established cell lines. Each cell line was grown in specific medium (chapter 2.4) harvested and RNA extracted. Experiments were completed in triplicate and representative images are shown. Specific primers outlined in table 2.6 were used to establish aromatase expression levels through RT-PCR. Graph on the right is a reproduction of the graph on the left with a reduced scale.

The aromatase enzyme catalyses the conversion of testosterone to oestradiol and androstenedione to oestrone. Expression levels of aromatase determined by QRT-PCR were high in COV434 cells in agreement with work by Havelock and colleagues.[2] Expression levels of aromatase in HEC-1A, HEC-1B and RL95-2 were similar, (the difference in expression of aromatase in these cell lines was not significantly different $P> 0.05$). Ishikawa expression of aromatase was lower than

COV434 but was statistically significantly higher than that found in HEC-1A, HEC-1B, and RL95-2 cells (All P< 0.041).

6.2.2 17β-HSD1 expression

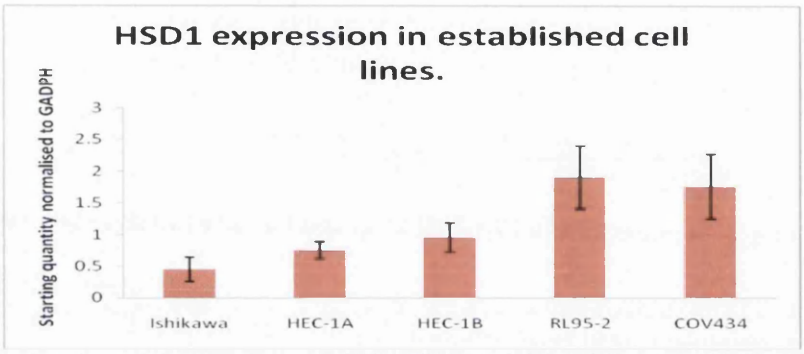

Fig 6.2: Relative basal expression of 17β-HSD1 in the Ishikawa, HEC-1A, HEC-1B, RL95-2 and COV434 established cell lines. Each cell line was grown in specific medium (chapter 2.4) harvested and RNA extracted. Experiments were completed in triplicate and representative results are shown. Specific primers outlined in table 2.6 were used to establish HSD1 expression levels through RT-PCR.

The enzyme HSD1 catalyses the conversion of oestrone to oestradiol. Expression levels of HSD1 determined by QRT-PCR were highest in RL95-2 and COV434 cells, the differences in expression of HSD1 between RL95-2 and COV434 were not statistically significant (P> 0.05). HEC-1A and HEC-1B were determined to have similar expression levels of HSD1 (which were not significantly different P> 0.05). HEC-1A and HEC-1B expression of HSD1 was lower than RL95-2 and COV434 but higher than that found in Ishikawa. Ishikawa cells had statistically significantly (lower) expression of HSD1 in comparison to COV434 cells (P= 0.014)

6.2.3 17β-HSD2 expression

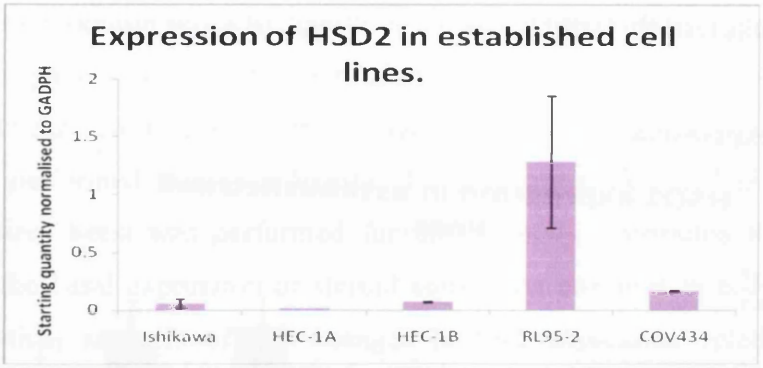

Fig 6.3: Relative basal expression of 17β-HSD2 in the Ishikawa, HEC-1A, HEC-1B, RL95-2 and COV434 established cell lines. Each cell line was grown in specific medium (chapter 2.4) harvested and RNA extracted. Experiments were completed in triplicate and representative results are shown. Specific primers outlined in table 2.6 were used to establish HSD2 expression levels through RT-PCR.

The enzyme HSD2 catalyses the conversion of testosterone to androstenedione, DHT to androstane-dione, androstanediol to androsterone and oestradiol to oestrone. Expression levels of HSD2 determined by QRT-PCR was significantly higher in RL95-2 cells in comparison to all other cell lines ($P< 0.05$ for all comparisons). COV434 and HEC-1B cells have similar low expression levels of HSD2. The differences in expression of HSD2 in HEC-1B and COV434 cells was determined not to be statistically significant $P= 0.78$. Ito and colleagues analysed a number of cell lines for HSD2 expression these were HEC-1A, HEC-1B, RL95-2, Ishikawa and KLE. Their results produced by northern blot analysis demonstrated no expression of HSD2 in Ishikawa and HEC-1B cells and low expression in HEC-1A cells. The RL95-2 cell line was shown to express HSD2 over 100 fold higher than in HEC-1A cells.[3] The starting quantities in figure 6.3 illustrated higher HSD2 expression in RL95-2 cells which was comparable to Ito's results. It was probable that in our investigations HSD2 expression was detected in Ishikawa, HEC-1B and HEC-1A cells because of the use of the more sensitive technique of RT-PCR which cannot be detected through northern blot analysis, QRT-PCR has been described as being more sensitive than northern blot; ~8ng of RNA can be detected by northern blot[4], whereas ~1fg can be detected by QRT-PCR (although around 10fg is required for reliable detection).[5]

6.2.4 17β-HSD4 expression

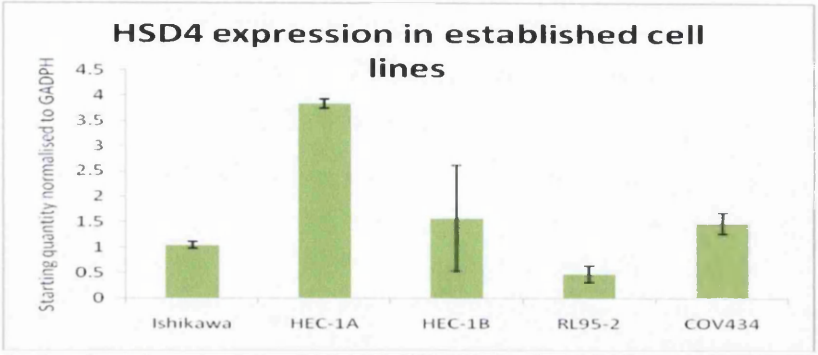

Fig 6.4: Relative basal expression of 17β-HSD4 in the Ishikawa, HEC-1A, HEC-1B, RL95-2 and COV434 established cell lines. Each cell line was grown in specific medium (chapter 2.4) harvested and RNA extracted. Experiments were completed in triplicate and representative results are shown. Specific primers outlined in table 2.6 were used to establish HSD4 expression levels through RT-PCR.

The enzyme HSD4 catalyses the conversion of testosterone to androstenedione, and oestradiol to oestrone. Expression levels of HSD4 determined by QRT-PCR were significantly higher in HEC-1A cells in comparison to all other cell lines ($P< 0.05$). HEC-1B and Ishikawa and RL95-2 exhibited similar starting quantity expression of HSD4. The differences in expression of HSD4 in HEC-1B, Ishikawa and RL95-2 were determined not to be statistically significant $P> 0.05$. In the cell lines COV434 expression of HSD4 was significantly lower than HEC-1A ($P = 0.044$) but higher than that recorded in RL95-2 cells.

6.2.5 17β-HSD5 expression

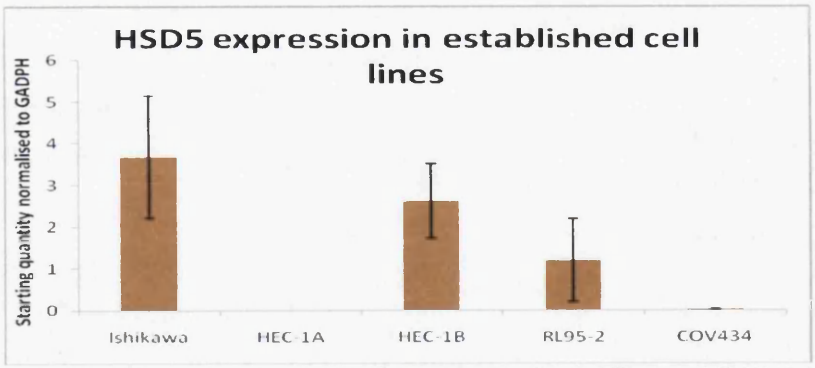

Fig 6.5: Relative basal expression of 17β-HSD5 in the Ishikawa, HEC-1A, HEC-1B, RL95-2 and COV434 established cell lines. Each cell line was grown in specific medium (chapter 2.4) harvested and RNA extracted. Experiments were completed in triplicate and representative results are shown. Specific primers outlined in table 2.6 were used to establish HSD5 expression levels through RT-PCR.

The enzyme HSD5 catalyses the conversion of androstenedione to testosterone, androstane-dione to DHT, androsterone to androstanediol and oestrone to oestradiol. Expression levels of HSD5 determined by QRT-PCR were highest in Ishikawa cells. The expression of HSD5 in COV434 and HEC-1A was negligible. HSD5 expression in HEC-1B and RL95-2 was lower than in Ishikawa and higher than in COV434 or HEC-1A cell lines.

6.2.6 17β-HSD7 expression

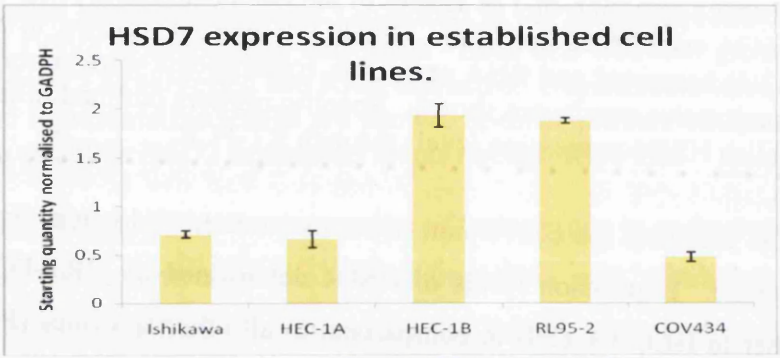

Fig 6.6: Relative basal expression of 17β-HSD7 in the Ishikawa, HEC-1A, HEC-1B, RL95-2 and COV434 established cell lines. Each cell line was grown in specific medium (chapter 2.4) harvested and RNA extracted. Experiments were completed in triplicate and representative results are shown. Specific primers outlined in table 2.6 were used to establish HSD7 expression levels through RT-PCR.

The enzyme HSD7 catalyses the conversion of oestrone to oestradiol. Expression levels of HSD7 determined by QRT-PCR were highest in RL95-2 and HEC-1B cells and lowest in COV434 cells. The expression of HSD7 was similar in the HEC-1B and RL95-2 cell lines (the difference in expression of HSD7 between HEC-1B and RL95-2 cells was determined not to be statistically significant P= 0.41). HEC-1A and Ishikawa also demonstrated similar HSD7 expression (the difference in expression of HSD7 in Ishikawa and HEC-1A cells was determined not to be statistically significant P= 0.50).

6.2.7 17β-HSD8 expression

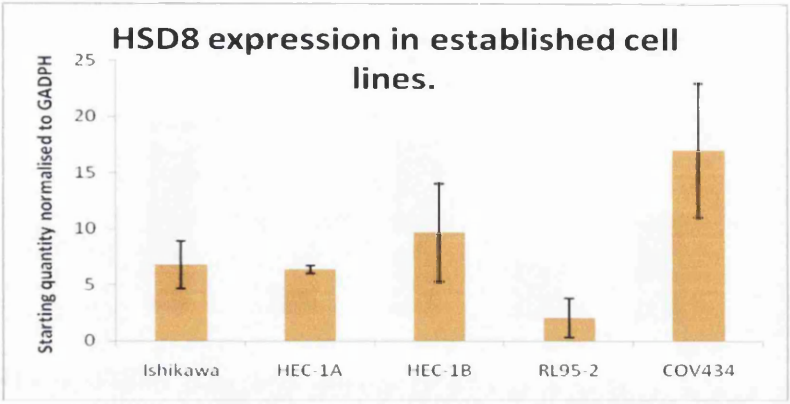

Fig 6.7: Relative basal expression of 17β-HSD8 in the Ishikawa, HEC-1A, HEC-1B, RL95-2 and COV434 established cell lines. Each cell line was grown in specific medium (chapter 2.4) harvested and RNA extracted. Experiments were completed in triplicate and representative results are shown. Specific primers outlined in table 2.6 were used to establish HSD8 expression levels through RT-PCR.

The enzyme HSD8 catalyses the conversion of oestradiol to oestrone and androstanedione to DHT. Expression levels of HSD8 determined by QRT-PCR were highest in COV434 cells. Expression of HSD8 in COV434 was significantly higher than in RL95-2 cells (P= 0.006), (RL95-2 demonstrated the lowest expression of HSD8). Expression of HSD8 was similar in Ishikawa, HEC-1A, and HEC-1B cells. The difference in expression of HSD8 in Ishikawa, HEC-1A, and HEC-1B cells was determined not to be statistically significant P>0.24 for all comparisons.

6.2.8 5AR1 expression

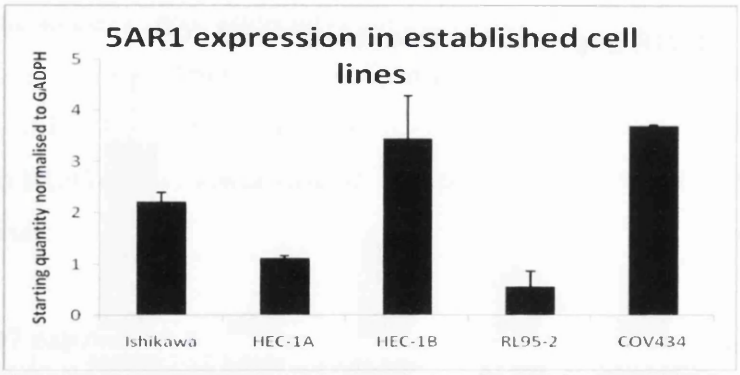

Fig 6.8: Relative basal expression of 5AR1 in the Ishikawa, HEC-1A, HEC-1B, RL95-2 and COV434 established cell lines. Each cell line was grown in specific medium (chapter 2.4) harvested and RNA extracted. Experiments were completed in triplicate and representative results are shown. Specific primers outlined in table 2.6 were used to establish 5AR1 expression levels through RT-PCR.

The enzyme 5AR1 catalyses the conversion of testosterone to DHT and androstenedione to androstane-dione. Expression levels of 5AR1 determined by QRT-PCR were highest in HEC-1B and COV434 cells. The difference in expression of 5AR1 between HEC-1B and COV434 cells were determined not to be statistically significant ($P= 0.73$). The lowest expression level of 5AR1 was detected in the RL95-2 cell line which was significantly lower than recorded in HEC-1B ($P= 0.029$) or COV434 ($P< 0.0001$) cells. Expression of 5AR1 in Ishikawa and HEC-1A was higher than in RL95-2 and lower than in HEC-1B and COV434 cells, (these differences were found to be not statistically significant).

6.2.9 5AR2 expression

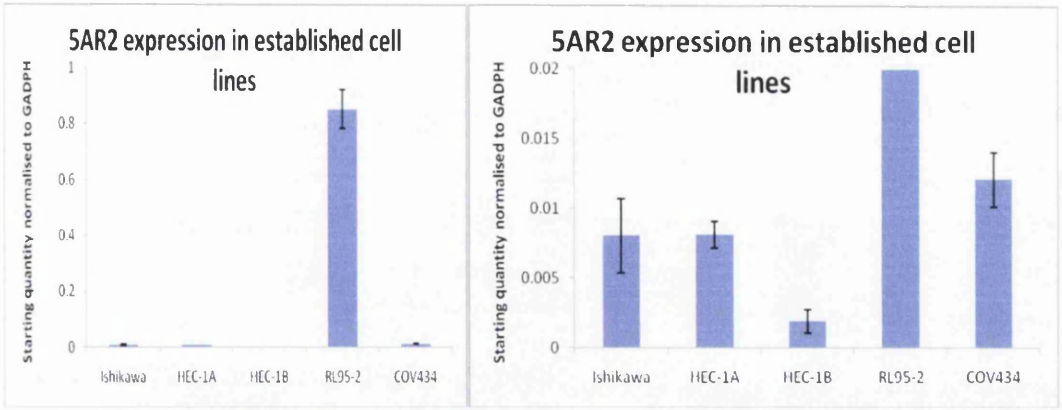

Fig 6.9: Relative basal expression of 5AR2 in the Ishikawa, HEC-1A, HEC-1B, RL95-2 and COV434 established cell lines. Each cell line was grown in specific medium (chapter 2.4) harvested and RNA extracted. Experiments were completed in triplicate and representative results are shown. Specific primers outlined in table 2.6 were used to establish 5AR2 expression levels through RT-PCR. The graphs above are identical however the graph on the right has a reduced scale to allow observations of low level expression of 5AR2.

The enzyme 5AR2 catalyses the conversion of testosterone to DHT and androstenedione to androstane-dione. Expression level of 5AR2 determined by QRT-PCR were significantly higher in RL95-2 cells in comparison to all other cell lines investigated ($P= 0.002$ for all comparisons). When the scale was reduced it was revealed that Ishikawa, HEC-1A and COV434 had similar expression of 5AR2 and HEC-1B demonstrated the lowest expression value. The differences in expression of 5AR2 in Ishikawa, HEC-1A, and COV434 cells were determined not to be statistically significant $P> 0.17$. HEC-1A, Ishikawa and COV434 expression of 5AR2 was lower than RL95-2 but higher than that found in HEC-1B cells.

6.2.10 Summary of basal enzyme expression in established cell lines

Table 6.1: Relative expression of enzymes investigated in established cell lines. Enzyme expression (high, medium or low) was relative to expression in the other cell lines calculated from a mixed calibration series. Cell lines indicated in red show the highest relative expression and those indicated in blue show the lowest expression of that specific enzyme.

Enzyme	Cell Line		
	High expression	Medium expression	Low expression
Aromatase	COV434	Ishikawa, RL95-2, HEC-1A, HEC-1B	
HSD1	RL95-2, COV434	HEC-1A, HEC-1B	Ishikawa
HSD2	RL95-2	COV434	Ishikawa, HEC-1A, HEC-1B
HSD4	HEC-1A	Ishikawa, HEC-1B, COV434	RL95-2
HSD5	Ishikawa, HEC-1B	RL95-2	COV434, HEC-1A
HSD7	RL95-2, HEC-1B	Ishikawa, HEC-1A	COV434
HSD8	COV434, HEC-1B	Ishikawa, HEC-1A	RL95-2
5AR1	HEC-1B, COV434	Ishikawa, HEC-1A	RL95-2
5AR2	RL95-2	Ishikawa, HEC-1A, COV434	HEC-1B

Each cell line expressed the specific steroid converting enzymes under investigation at different quantities under basal conditions, from these relative expression values it was possible to hypothesise a variety of metabolic pathways may be active after addition of testosterone. The differences in basal expression of specific enzymes was correlated to the initial metabolites of testosterone as described in chapter 7.

Ishikawa cells exhibited the highest relative expression of HSD5, this enzyme catalyses the conversion of androstenedione to testosterone and oestrone to oestradiol, after addition of testosterone to Ishikawa cells it was postulated that the metabolite androstenedione may be converted back into testosterone via the highly expressed HSD5 enzyme.

HEC-1A cells exhibited high expression of HSD4, after testosterone treatment of this cell line androstenedione is a probable metabolite due to conversion via the highly expressed HSD4.

HEC-1B cells exhibited high expression of 5AR1 and HSD7, after testosterone treatment it was expected that these cells will produce the metabolite DHT (through 5AR1).

RL95-2 cells exhibited high expression of HSD1, HSD2, HSD7 and 5AR2, the significantly high expression of HSD2 in comparison to the other cell lines suggested that after testosterone treatments that the major initial metabolite will be androstenedione (via HSD2) following this metabolism of androstenedione is expected to occur via the highly expressed 5AR2 enzyme (to androstanediol).

COV434 cells expressed aromatase, HSD1, HSD8 and 5AR1 in the highest amount relative to the other cell lines, it was expected from these results that after addition of testosterone, DHT will be metabolised via 5AR1, androstenedione via HSD8 and oestradiol via aromatase.

This represents a simplistic view of steroid metabolism (simple substrate-product relationships), it is probable that generated experimental data will be more complex due to the different reactions possible. For example an enzyme may bind a number of substrates to produce a number of products. Enzyme affinity for each substrate may differ (some enzymes may have a higher affinity for a specific substrate at low expression levels than others).

6.3 Changes in gene expression after Testosterone treatment in established cell lines

Following determination of basal starting quantity expression of mRNA for each enzyme testosterone treatments of the cell lines were conducted as described in chapter 3.14 and changes in expression were recorded at specific time intervals. Significant changes in enzyme expression were determined relative to basal enzyme expression using the unpaired t-test as described previously, (the times any significant changes occur and P values are summarised in table 6.3)

For ease of comparison the same enzymes are represented by the same colours throughout this chapter and chapter 7.

Table 6.2: Enzyme nomenclature and corresponding colours in chapters 6 and 7.

Enzyme	Colour
Aromatase	Blue
HSD1	Red
HSD2	Pink
HSD4	Green
HSD5	Brown
HSD7	Yellow
HSD8	Orange
5AR1	Black
5AR2	Purple

The changes in RNA expression levels for all enzymes assessed throughout the experiments were expressed as fold expression relative to the housekeeping gene GADPH (expression divided by expression amount of GADPH in each sample). The expression of each enzyme was then normalised to 1 at time zero (under control conditions) changes in fold expression relative to this time throughout the 72 hours were observed.

6.3.1 Changes in enzyme expression in the Ishikawa cell line

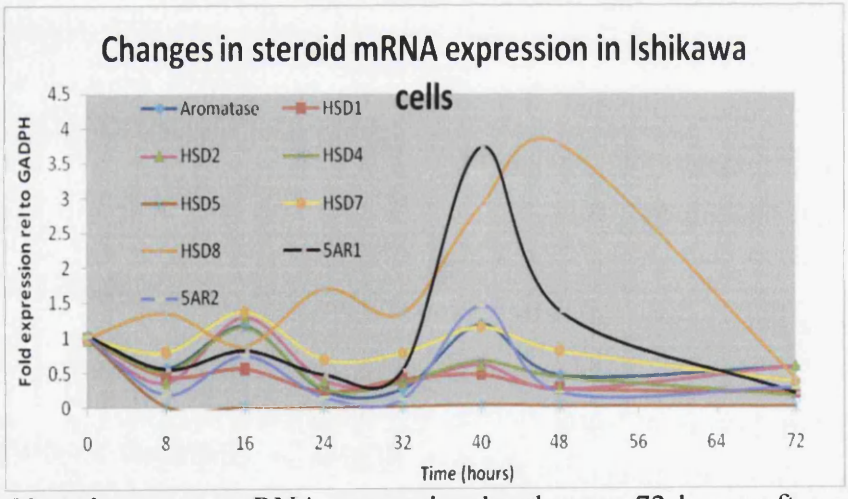

Fig 6.10: Changing enzyme RNA expression levels over 72 hours after addition of testosterone to Ishikawa cell media. Ishikawa cells were grown in specific medium (chapter 2.4) harvested and RNA extracted. Specific primers outlined in table 2.6 were used to establish expression of each enzyme through RT-PCR.

Highest fold expression changes were observed for the enzymes HSD8 (48hours) and 5AR1 (40 hours). 5AR1 converts testosterone to DHT and androstenedione to androstane-dione with this increased expression at 40 hours it was expected that an

increase in the reaction product concentration will be observed this was confirmed in chapter 7.

6.3.2 Changes in enzyme expression in the RL95-2 cell line

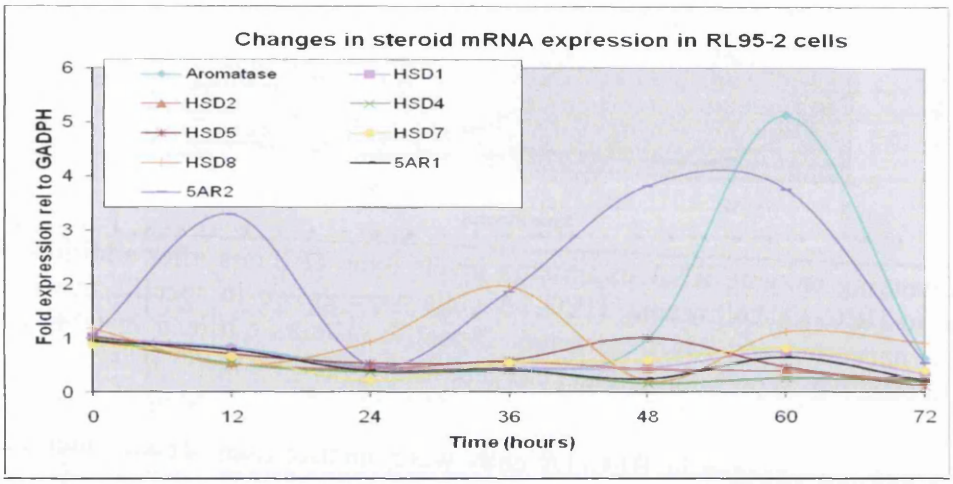

Fig 6.11: Changing enzyme RNA expression levels over 72 hours after addition of testosterone to RL95-2 cell media. RL95-2 cells were grown in specific medium (chapter 2.4) harvested and RNA extracted. Specific primers outlined in table 2.6 were used to establish expression of each enzyme through RT-PCR.

Expression of all enzymes (except 5AR2, HSD8 and aromatase) was reduced at all time points relative to time zero. Expression of 5AR2 was high at 12, 48, and 60 hours. 5AR2 catalyses the conversion of testosterone to DHT and androstenedione to the end product androsterone through androstane-dione. Corresponding mass spectral steroid profiles were combined to determine any steroid-enzyme relationships. Aromatase expression increased at 60 hours (figure 6.11), this could be linked to an increase in the reaction products oestrone and/or oestradiol if the reaction substrate (testosterone or androstenedione) were available, however in these experiments this is not recorded as all testosterone was converted to androsterone (through androstenedione) before 60 hours as described in chapter 5.8.2)

6.3.3 Changes in enzyme expression in the HEC-1A cell line

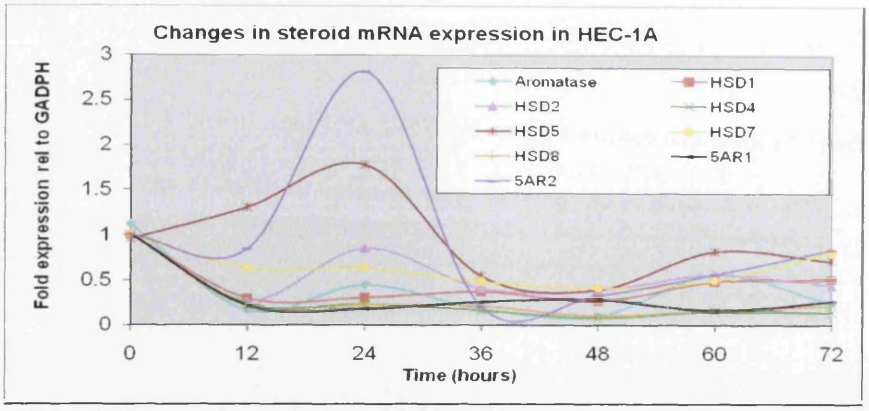

Fig 6.12: Changing enzyme RNA expression levels over 72 hours after addition of testosterone to HEC-1A cell media. HEC-1A cells were grown in specific medium (chapter 2.4) harvested and RNA extracted. Specific primers outlined in table 2.6 were used to establish expression of each enzyme through RT-PCR

The fold expression changes in HEC-1A cells were smaller than for all other cell lines. Figure 6.12 illustrates that expression of all enzymes (except HSD5 and 5AR2) decreased after testosterone treatment. Significant changes in fold expression were observed with the enzymes 5AR2 and HSD5 relative to basal expression (P= 0.025 and 0.033 respectively) both at 24 hours. Correlation between these results and changes in steroid profiles are defined in chapter 7.

6.3.4 Changes in enzyme expression in the HEC-1B cell line

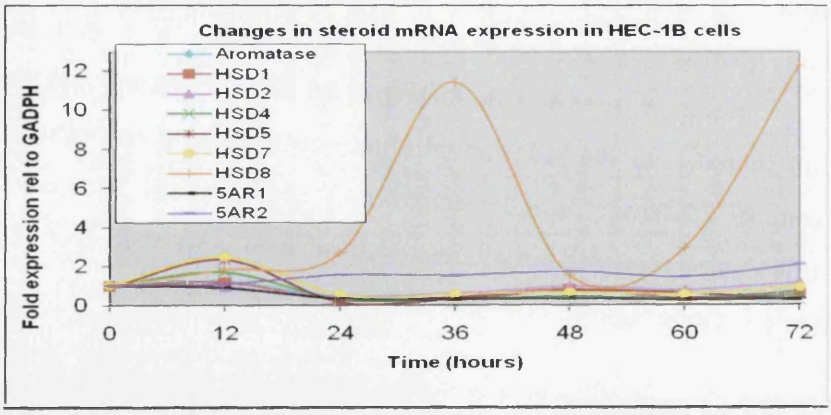

Fig 6.13: Changing enzyme RNA expression levels over 72 hours after addition of testosterone to HEC-1B cell media. HEC-1B cells were grown in specific medium (chapter 2.4) harvested and RNA extracted. Specific primers outlined in table 2.6 were used to establish expression of each enzyme through RT-PCR.

Expression of most of the enzymes increased at 12 hours after which expression levels were essentially constant throughout the experiment. Figure 6.13 illustrates

that only HSD8 demonstrated significant changes in fold expression relative to time zero in HEC-1B cells at 36 hours (P=0.005) and 72 hours (P= 0.003). HSD8 converts testosterone to androstenedione, increased expression at 36 and 72 hours should correlate with increased androstenedione concentration at these time.

6.3.5 Changes in enzyme expression in the COV434 cell line

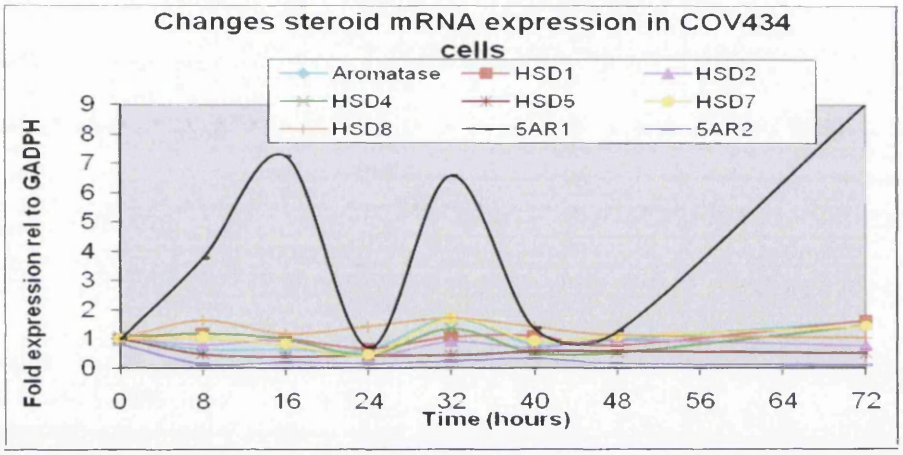

Fig 6.14: Changing enzyme RNA expression levels over 72 hours after addition of testosterone to COV434 cell media. COV434 cells were grown in specific medium (chapter 2.4) harvested and RNA extracted. Specific primers outlined in table 2.6 were used to establish expression of each enzyme through RT-PCR.

Changes in expression levels of all steroid converting enzymes (except 5AR1) were negligible compared to time zero. Fold expression of 5AR1 relative to time zero increased significantly in COV434 cells, at 12, 32 and 72 hours (P= 0.043, 0.006 and 0.047 respectively). It was expected that at these time points the concentration of the steroid produced by 5AR1 (DHT) will increase; this was confirmed in chapter 7.

6.3.6 Conclusions established cell lines

Basal enzyme starting quantities provided information concerning the likely route of steroid bio-synthesis. Changes in expression levels of each enzyme through the 72 hours after testosterone treatment highlighted enzymes which expression levels changed significantly (relative to basal expression) in each cell line. Further investigation into each of these combined with the mass spectrometry generated steroid profiles were completed in chapter 7. This allows any trends in enzyme expression and/or relationships between enzyme expression and changes in steroid concentration to be observed.

Table 6.3: Significant enzyme expression changes (relative to basal expression) over 72 hours after testosterone treatment of the cell lines Ishikawa, RL95-2, HEC-1A, HEC-1B, and COV434.

Cell Line	Enzyme changing	Time change rel to zero (hours)	P values	Steroid conversion reaction
Ishikawa	HSD8	40	0.035	Androstane-dione →DHT
		48	0.038	Oestrone→Oestradiol
	5AR1	40	0.041	Testosterone → DHT
RL95-2	5AR2	12	0.029	Androstenedione → Androstane-dione (→Androsterone)
		48	0.037	
		60	0.029	
	Aromatase	60	<0.001	Androgens →Oestrogens
HEC-1A	5AR2	24	0.025	Androstenedione → Androstane-dione (→Androsterone)
	HSD5	24	0.033	Androstenedione →Testosterone
HEC-1B	HSD8	36	0.005	Androstane-dione →DHT
		72	0.003	Oestrone→Oestradiol
COV434	5AR1	0	0.043	Testosterone → DHT
		16	0.006	
		72	0.047	

From the table 6.3 and table 6.1 it was possible to observe the enzymes which were important in all the cell lines in terms of high relative starting quantity expression or significant fold expression changes were aromatase, 5AR1, 5AR2, HSD2, HSD5 and HSD8. Specific inhibition of one of these enzymes may change the steroid profile significantly, resulting in normal steroid metabolism being re-established, and halting progression of proliferation. For example finasteride a 5AR inhibitor alters steroid metabolism, and has been used for treatment of benign prostatic hyperplasia and androgenetic alopecia.[6]

A sensitive, reproducible method was determined for the analysis of enzyme expression in endometrial established cell lines. These experimental methods were applied to biopsy samples to obtain information about basal enzyme expression and temporal changes in enzyme expression following testosterone treatment in benign endometrial conditions.

6.4 Relative expression of steroid converting enzymes in a number of endometrial pathologies (biopsies)

Studies of basal enzyme expression relative to the averaged fertile biopsies in the biopsy groups under investigation (endometriosis, PCOS and unexplained infertility) were completed. Studies into basal enzyme expression (relative to the averaged fertile biopsies) in biopsies from a patient with an endometrial polyp, a patient with an ovarian cyst and in stromal and epithelial cells from a patient with endometrial hyperplasia were also conducted. The number of biopsies in each endometrial disorder group was described in chapter 5 (table 5.9).

Biopsies from each of the groups were obtained as there is evidence of altered enzyme expression relating to steroid metabolism in these conditions. This altered expression is thought to cause bio-accumulation of steroids which aid progression and proliferation of the disorders. For example in endometriosis biopsies from both the eutopic and ectopic endometrium there is evidence of increased aromatase and sulphatase activity[7], and increased HSD1 and reduced HSD2 expression which leads to bio-accumulation of oestradiol.[8]

In biopsies from the endometria of women with PCOS it has been shown that there was increased expression of HSD1 and decreased expression of HSD2 in comparison to healthy endometrial tissue again causing bio-accumulation of oestradiol.[9]

The unexplained infertility biopsies come from women who are unable to conceive, but the reason cannot be explained by any of the tests available today, this was an interesting group to study as one of the factors contributing towards their infertility could be an altered steroid metabolism due to abnormal expression of specific steroid converting enzymes in their endometria.

Women who have endometrial hyperplasia (or non-invasive proliferation) have been recorded as having altered enzyme endometrial expression of HSD2, 5AR1 5AR2 (all decreased) and HSD5, (increased) relative to fertile biopsies (discussed further in 6.5.5).[10]

To confirm these results the expression of these enzymes was investigated in fertile biopsies and in biopsies from the specific endometrial disorders. The work was also extended to include all steroid converting enzymes described in table 6.0 to produce a wider enzyme expression profiles with the aim of elucidating important enzymes which have been previously overlooked.

6.4.1 Comparison of basal starting quantity expression of steroid converting enzymes in stromal cells isolated from fertile and endometriosis endometrial biopsies

The similarity in basal steroid converting enzyme expression in fertile biopsies (4 samples) allowed averaged data to be obtained with relatively small standard deviations. Endometriosis biopsies cannot be grouped by this method as RNA enzyme expression can vary considerably between samples, possibly due to the stage or severity of the endometriosis in each individual (described in chapter 1.6.3). It was hypothesised that as the condition progresses enzyme expression will alter. Unfortunately the severity of endometriosis in each biopsy was not recorded in these experiments and so this hypothesis cannot be validated. Six endometriosis biopsies were investigated, three of the women were described as having secondary endometriosis (2nd endometriosis), these women had previously conceived and had developed endometriosis since their pregnancies.

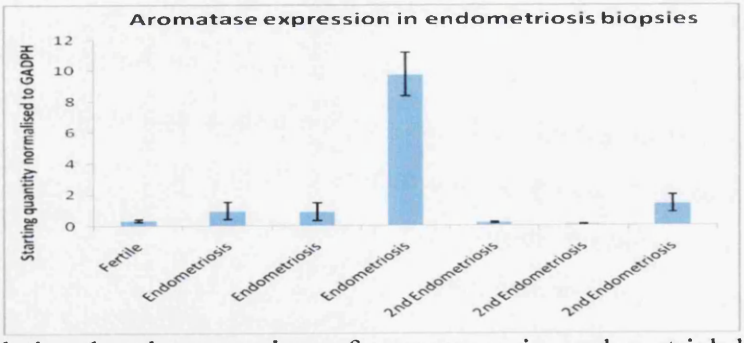

Fig 6.15: Relative basal expression of aromatase in endometrial biopsies from averaged fertile and endometriosis. All biopsy cells were grown in specific medium (chapter 2.4) harvested and RNA extracted. Specific primers outlined in table 2.6 were used to establish aromatase expression through RT-PCR.

Figure 6.15 illustrated aromatase expression in four of the six endometriosis samples was higher than the average fertile biopsies. Increased aromatase expression in endometriosis biopsies relative to fertile samples agrees with observations by Attar

and co-workers.[11] There were two samples which have lower aromatase expression than the fertile sample this could be due to the disease being at an early stage in these women.

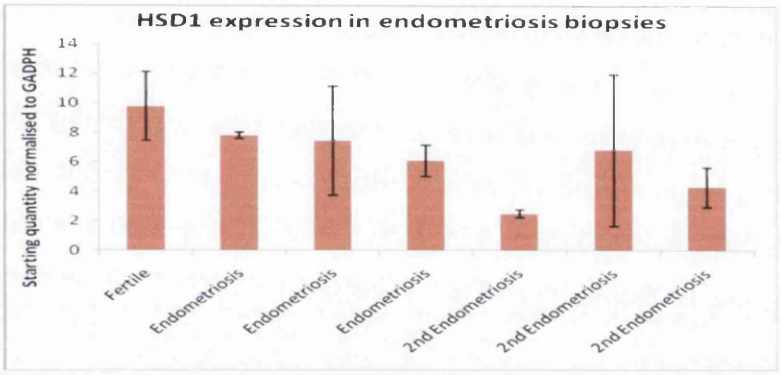

Fig 6.16: Relative basal expression of HSD1 in endometrial biopsies from averaged fertile and endometriosis samples. Endometriosis biopsy cells were grown in specific medium (chapter 2.4) harvested and RNA extracted. Specific primers outlined in table 2.6 were used to establish HSD1 expression through RT-PCR.

All endometriosis biopsies investigated demonstrated lower or comparable HSD1 expression relative to the average fertile sample (figure 6.16). HSD1 expression was found to be increased at deep-invasive endometriosis sites by Dassen[12] and colleagues, the disparity in these results compared to those in figure 6.16 may be due to the biopsies in Dassen's study being taken directly from the ectopic endometrium (lesion sites) and not the endometrium itself, (the endometriotic lesion sites are inflammation sites and it was expected that at these sites there will be an increase in multiple enzyme expression and steroid concentrations).

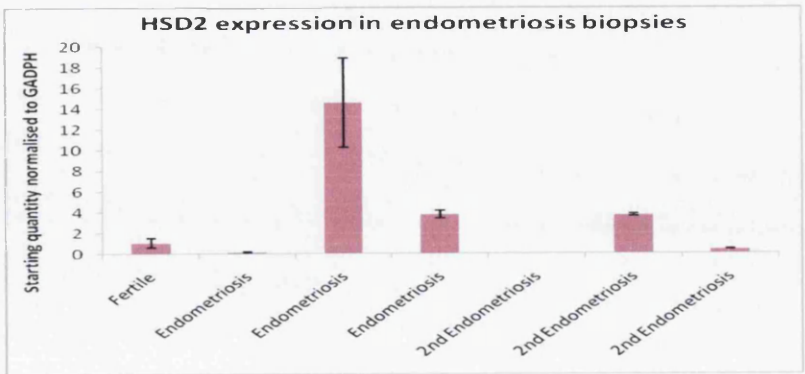

Fig 6.17: Relative basal expression of HSD2 in averaged fertile and endometriosis biopsies. Endometriosis biopsy cells were grown in specific medium (chapter 2.4) harvested and RNA extracted. Specific primers outlined in table 2.6 were used to establish HSD2 expression through RT-PCR.

Bulun and colleagues recorded a decrease in expression of HSD2 in endometriosis biopsies relative to fertile biopsies resulting in bioaccumulation of oestradiol.[13] HSD2 expression was decreased in three of the six endometriosis samples investigated in these experiments in comparison to the fertile as illustrated by figure 6.17. Three of the samples have increased HSD2 expression relative to the fertile this difference in expression levels could again be attributed to severity of the disease, however there is some variation in the literature concerning the down regulation of HSD2 from fertile to endometriosis samples, Day and colleagues reported some studies demonstrating an increase in HSD2 expression, although the majority of experiments record decreased expression of HSD2 in endometriosis biopsies.[14,15,16]

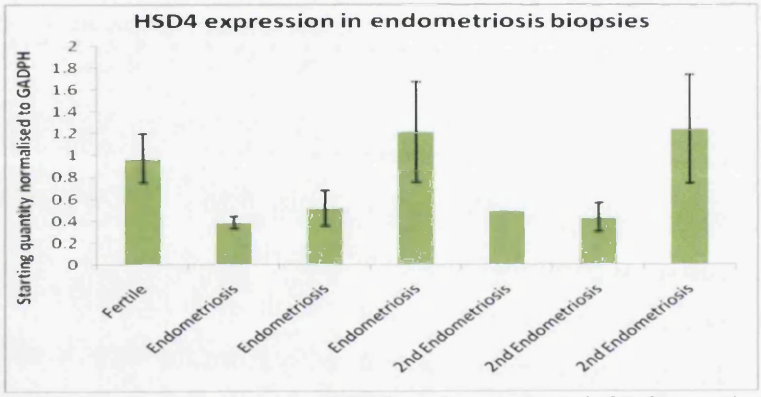

Fig 6.18: Relative basal expression of HSD4 in averaged fertile and endometriosis biopsies. Endometriosis biopsy cells were grown in specific medium (chapter 2.4) harvested and RNA extracted. Specific primers outlined in table 2.6 were used to establish HSD4 expression through RT-PCR.

Expression of HSD4 in four of six endometriosis samples was less than the fertile group (figure 6.18). Two biopsies were recorded as having comparable HSD4 expression to the fertile samples. This agrees with work by Dassen and co-workers who recorded decreased expression of HSD4 in endometriosis biopsies in comparison to fertile biopsies.[12]

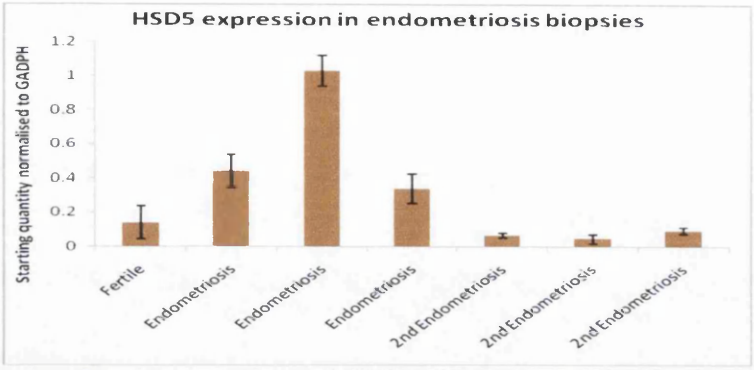

Fig 6.19: Relative basal expression of HSD5 in averaged fertile and endometriosis biopsies. Endometriosis biopsy cells were grown in specific medium (chapter 2.4) harvested and RNA extracted. Specific primers outlined in table 2.6 were used to establish HSD5 expression through RT-PCR.

Three of the six endometriosis biopsies illustrated in figure 6.19 demonstrated higher expression of HSD5 than the fertile group. Similarly high HSD5 expression has recently been recorded in endometriosis samples by Šmuc and colleagues.[17] The other three samples have HSD5 expression comparable to the fertile, again variation was attributed to severity.

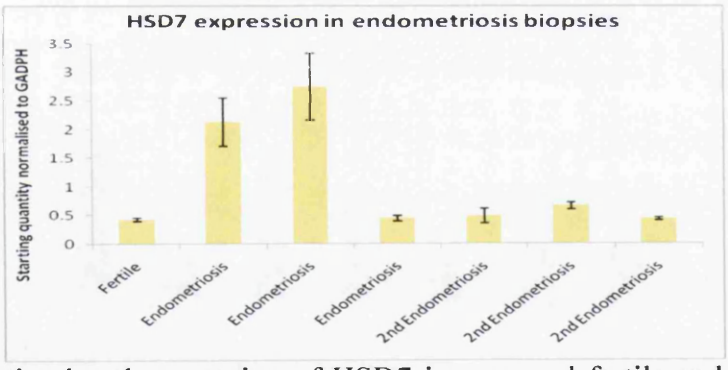

Fig 6.20: Relative basal expression of HSD7 in averaged fertile and endometriosis biopsies. Endometriosis biopsy cells were grown in specific medium (chapter 2.4) harvested and RNA extracted. Specific primers outlined in table 2.6 were used to establish HSD7 expression through RT-PCR

HSD7 expression in endometriosis biopsies was either higher or comparable to the averaged fertile sample as illustrated by figure 6.20. Šmuc and co-workers recorded increased HSD7 expression in endometriosis samples relative to fertile samples, confirming these results.[18]

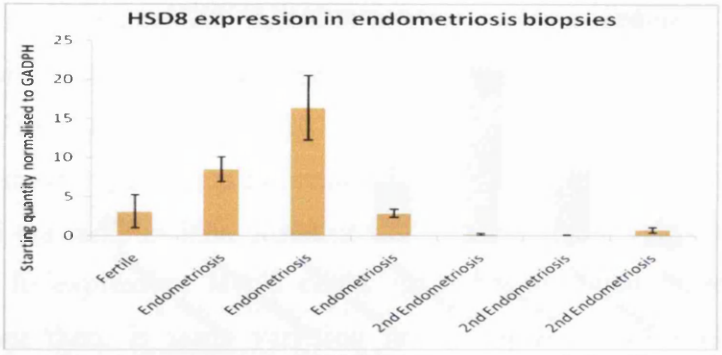

Fig 6.21: Relative basal expression of HSD8 in averaged fertile and endometriosis biopsies. Endometriosis biopsy cells were grown in specific medium (chapter 2.4) harvested and RNA extracted. Specific primers outlined in table 2.6 were used to establish HSD8 expression through RT-PCR.

HSD8 was expressed at levels similar to or less than expression levels of the fertile sample in four endometriosis biopsies (figure 6.21). This agrees with previous work from Šmuc and co-workers stating oxidative HSDs (HSD2, 4, 6 and 8) have similar or reduced expression levels relative to the fertile samples.[19] HSD8 was however highly expressed in two endometriosis samples, again this was probably due to the progression of the disease in these patients.

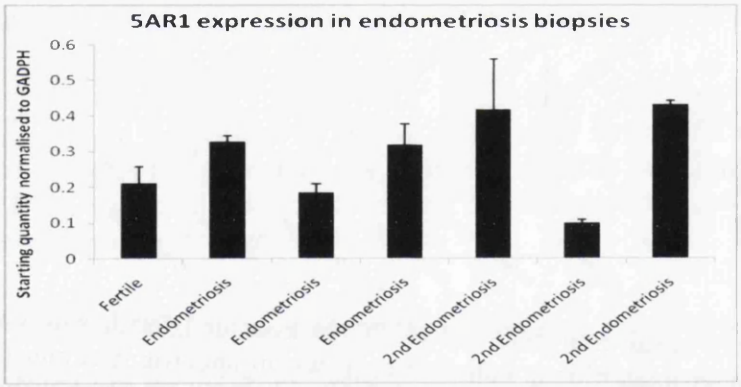

Fig 6.22: Relative basal expression of 5AR1 in endometrial biopsies in comparison to averaged fertile biopsies. Endometriosis biopsy cells were grown in specific medium (chapter 2.4) harvested and RNA extracted. Specific primers outlined in table 2.6 were used to establish 5AR1 expression through RT-PCR.

5AR1 expression was increased in four of the six endometriosis samples relative to the fertile group (figure 6.22). 5AR1 expression has been detected in endometriosis samples in previous studies, Carneiro and co-workers detected 5AR1 expression in 83% of endometria from endometriosis suffers, agreeing with the above results.[20]

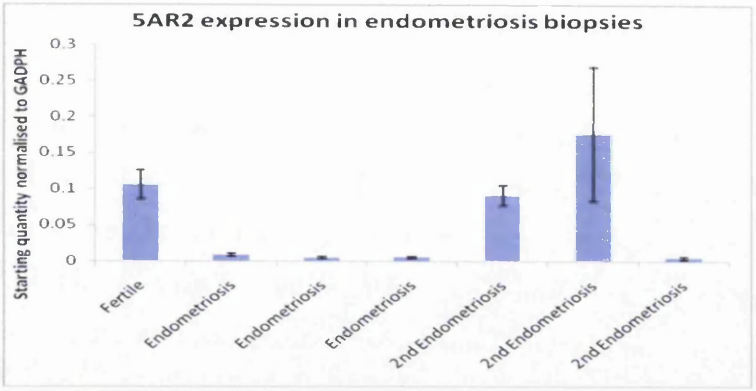

Fig 6.23: Relative basal expression of 5AR2 in averaged fertile and endometriosis biopsies. Endometriosis biopsy cells were grown in specific medium (chapter 2.4) harvested and RNA extracted. Specific primers outlined in table 2.6 were used to establish 5AR2 expression through RT-PCR.

Expression of 5AR2 was reduced relative to the fertile group in four of the six endometriosis biopsies (figure 6.23). 5AR2 expression was detected in two of six endometriosis biopsies a study by Carneiro and colleagues, this correlates with the results recorded in the experiments described in figure 6.23.[20]

6.4.2 Conclusions Endometriosis samples

Endometriosis biopsies were difficult to investigate due to the variation between samples. If the biopsies were grouped according to the stage of endometriosis (minimal, mild, moderate, severe) changes in basal enzyme expression through the different stages of endometriosis may be apparent. This made any data analysis difficult to determine for the group as a whole (expression was not determined to be significantly different from the fertiles for all endometriosis biopsies for each enzyme investigated).

The general trends recorded in these experiments were high aromatase, 5AR1, HSD7, and HSD5 starting quantity expression, and low expression of 5AR2, HSD4, and HSD1 relative to the average fertile sample. Šmuc and colleagues demonstrated expression of the reductive HSDs (1, 5 and 7) was up-regulated in endometria from endometriosis samples (relative to fertile biopsies), leading to bio-accumulation of the potent oestrogen oestradiol which is essential of progression of endometriosis, in the same study by Šmuc expression of the oxidative HSDs (2, 4 and 8) was found to be comparable to or lower than fertile samples.[19] The majority of endometriosis samples investigated in these experiments agreed with these observations (except

HSD1). Carneiro and colleagues observed increased expression of 5AR1 and decreased expression of 5AR2 in the majority of endometriosis biopsies under investigation, the results accumulated in these experiments confirm Carneiro's results.[20] The altered enzyme expression profiles produced by the endometriosis samples relative to the fertile biopsies indicated that a number of steroid metabolism pathways were active in this pathology, furthermore a different steroid pathway should be observed between the two groups after testosterone treatment. This agrees with the experimentally obtained steroid profiles described in chapter 5.9.

6.4.3 Comparison of average starting quantity expression of steroid converting enzyme RNA in ovarian disorder biopsies to fertile biopsies

The endometria of women with ovarian disorders were investigated. The two ovarian disorders under investigation were PCOS (2 biopsies) and ovarian cyst (1 biopsy). One patient with PCOS was also described as having tubual disorder, in chapter five it was recorded that testosterone metabolism in a woman with only tubual disorder was similar to the fertile biopsies. It was therefore probable that in the biopsy from the woman with PCOS and tubual disorder any recorded alterations in testosterone metabolism or enzyme expression would be influenced by the PCOS condition and not tubual disorder. In all the graphs below this biopsy was described as PCOS plus tubual disorder to permit observations between the two PCOS biopsies.

Ovarian cysts and PCOS while both ovarian conditions are different disorders determined by different clinical pathologies. PCOS patients have 2 of these 3 symptoms, circulatory hyperandrogenism, oligo-ovulation (or annovulation), and a number of cysts on the ovary (chapter 1.6). These factors may cause altered steroid metabolism in the endometrium of women with PCOS.

Presence of cysts in the ovaries can affect the menstrual cycle and cause pelvic pain. Cunat and colleagues demonstrated ovarian cysts (themselves) expressing aromatase which could lead to an increase in circulatory oestrogens, which could in turn affect steroid metabolism and proliferation in the endometrium.[21] The patient investigated in this thesis was described as having chronic pelvic pain which may suggest the cyst was proliferating and expressing aromatase and oestradiol. The expression of steroid

converting enzymes in endometrial tissue from women with ovarian cysts is not widely investigated (in comparison to PCOS), as the cyst is generally removed eliminating the problem.

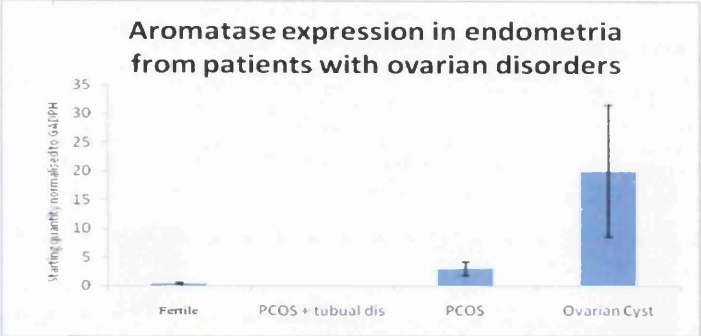

Fig 6.24: Relative basal expression of aromatase in averaged fertile and ovarian disorder biopsies. Ovarian disorder biopsies were grown in specific medium (chapter 2.4) harvested and RNA extracted. Specific primers outlined in table 2.6 were used to establish aromatase expression through RT-PCR.

Figure 6.24 illustrates basal aromatase expression in the endometria from women with ovarian disorders relative to fertile biopsies. There was little aromatase expression in the PCOS (plus tubual disease) sample or the fertile biopsies. This agrees with work by Bacallao who detected no aromatase expression in endometrial tissue from fertile women and women with PCOS.[9] The other PCOS biopsy and the ovarian cyst biopsy disagree with this both recording higher aromatase expression in comparison to the fertile sample (figure 6.24).

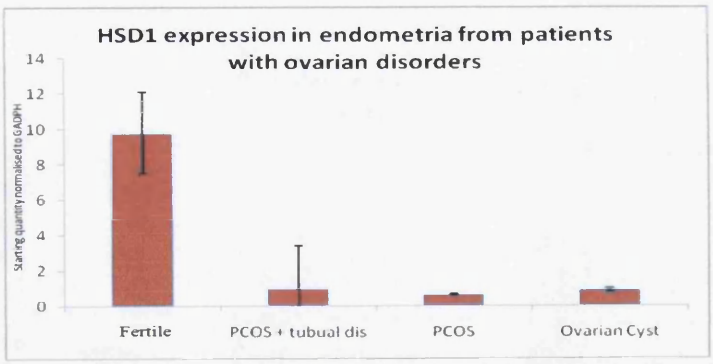

Fig 6.25: Relative basal expression of HSD1 in averaged fertile and ovarian disorder biopsies. Ovarian disorder biopsies were grown in specific medium (chapter 2.4) harvested and RNA extracted. Specific primers outlined in table 2.6 were used to establish HSD1 expression through RT-PCR.

Figure 6.25 illustrates that HSD1 expression was reduced in all ovarian disorder samples relative to the average fertile biopsies. HSD1 expression was comparable in all ovarian disorders.

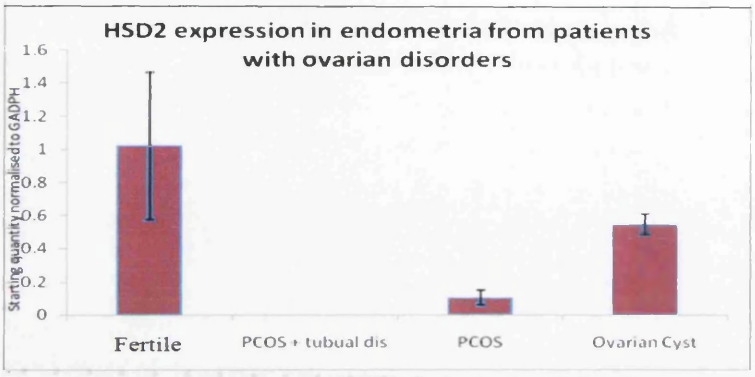

Fig 6.26: Relative basal expression of HSD2 in averaged fertile and ovarian disorder biopsies. Ovarian disorder biopsies were grown in specific medium (chapter 2.4) harvested and RNA extracted. Specific primers outlined in table 2.6 were used to establish HSD2 expression through RT-PCR.

Figure 6.26 illustrates HSD2 expression was reduced in all ovarian disorder samples relative to the averaged fertile sample. This reduced expression of HSD2 in the PCOS biopsies did not agree with mRNA enzyme expression information recorded by Leon and co-workers in 2008, who found similar HSD2 expression in fertile and endometriosis biopsies, the reason for this disparity could be because Leon obtained his biopsies from the mid secretary phase whereas in these experiments they were taken from the proliferative phase.[22]

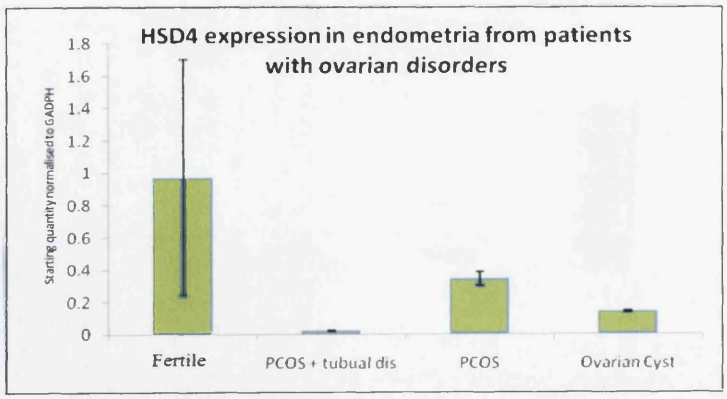

Fig 6.27: Relative basal expression of HSD4 in averaged fertile and ovarian disorder biopsies. Ovarian disorder biopsies were grown in specific medium (chapter 2.4) harvested and RNA extracted. Specific primers outlined in table 2.6 were used to establish HSD4 expression through RT-PCR.

Figure 6.27 illustrates expression of HSD4 was reduced in all ovarian disorder biopsies relative to the averaged fertile sample.

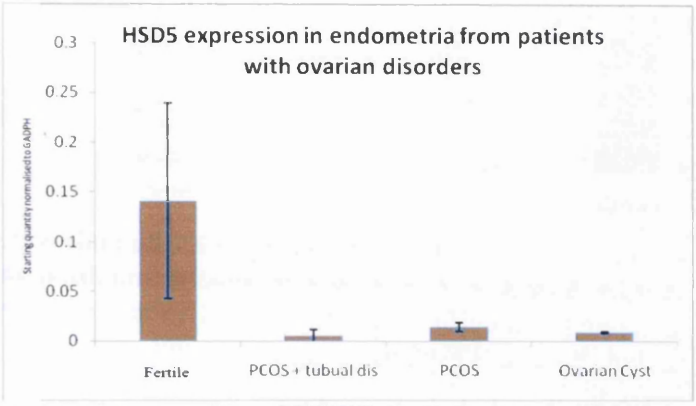

Fig 6.28: Relative basal expression of HSD5 in averaged fertile (control) and ovarian disorder biopsies. Ovarian disorder biopsies were grown in specific medium (chapter 2.4) harvested and RNA extracted. Specific primers outlined in table 2.6 were used to establish HSD5 expression through RT-PCR.

Figure 6.28 illustrates that HSD5 expression was low in all ovarian disorder biopsies relative to the fertile samples. The expression levels of HSD5 were comparable in the ovarian cyst and both PCOS biopsies.

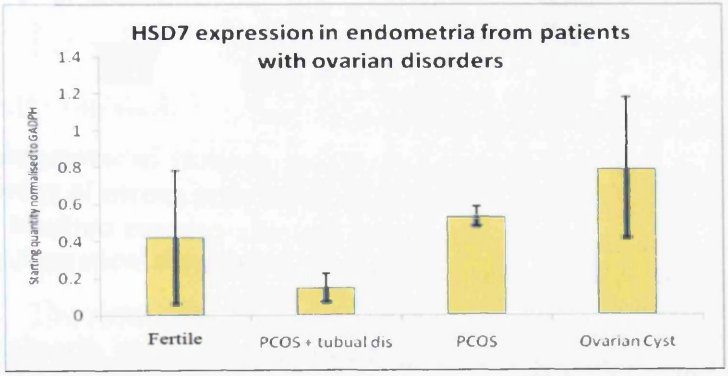

Fig 6.29: Relative basal expression of HSD7 in averaged fertile (control) and ovarian disorder biopsies. Ovarian disorder biopsies were grown in specific medium (chapter 2.4) harvested and RNA extracted. Specific primers outlined in table 2.6 were used to establish HSD7 expression through RT-PCR.

Figure 6.29 illustrates the PCOS biopsy and the ovarian cyst biopsy exhibited high comparable starting quantity expression of HSD7 relative to the fertile (and the PCOS plus tubual disorder biopsy).

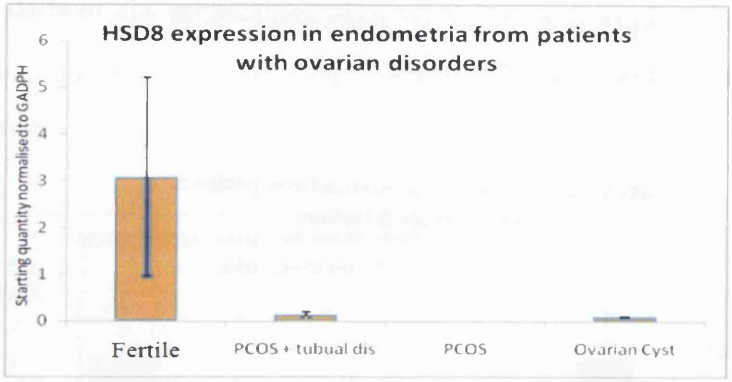

Fig 6.30: Relative basal expression of HSD8 in averaged fertile and ovarian disorder biopsies. Ovarian disorder biopsies were grown in specific medium (chapter 2.4) harvested and RNA extracted. Specific primers outlined in table 2.6 were used to establish HSD8 expression through RT-PCR.

Figure 6.30 illustrates low HSD8 expression in all ovarian disorder biopsies in comparison to the fertile biopsies.

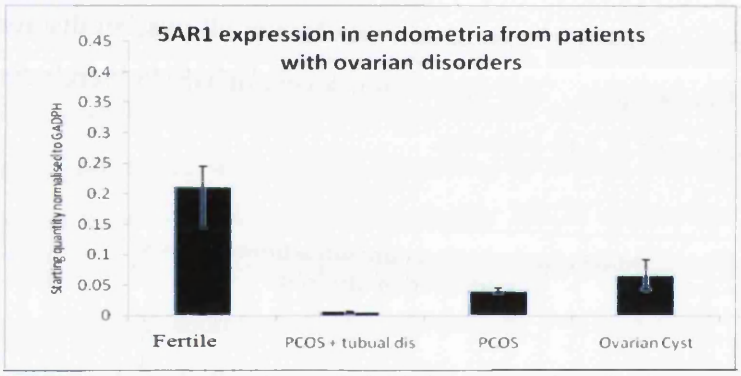

Fig 6.31: Relative basal expression of 5AR1 expression in averaged fertile and ovarian disorder biopsies. Ovarian disorder biopsies were grown in specific medium (chapter 2.4) harvested and RNA extracted. Specific primers outlined in table 2.6 were used to establish 5AR1 expression through RT-PCR.

Figure 6.31 illustrates low expression of 5AR1 in all ovarian disorder biopsies in comparison to the average fertile sample.

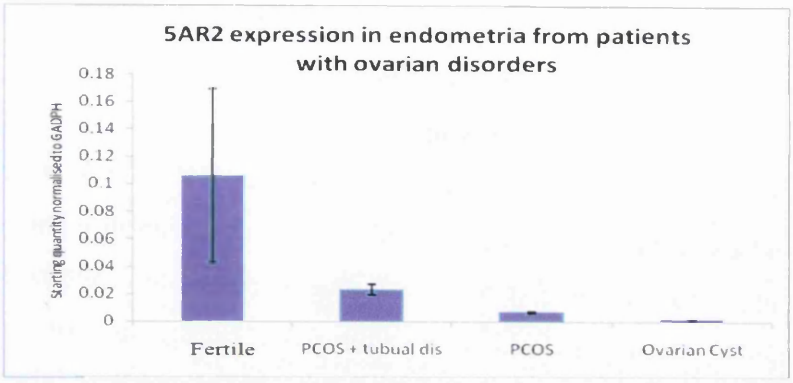

Fig 6.32: Relative basal expression of 5AR2 in averaged fertile and ovarian disorder biopsies. Ovarian disorder biopsies were grown in specific medium (chapter 2.4) harvested and RNA extracted. Specific primers outlined in table 2.6 were used to establish 5AR2 expression through RT-PCR.

Figure 6.32 illustrated that 5AR2 expression in all ovarian disorder biopsies was lower than the fertile sample.

6.4.4 Conclusions ovarian disorders

Basal enzyme expression in PCOS biopsies allows confirmation of altered enzyme expression of previously investigated enzymes. The majority of previous work has been centred specifically on oestrogen metabolism and the bio-accumulation of oestradiol[23] via increased expression of aromatase and HSD1 or decreased expression of HSD2. To our knowledge comparative investigations into the expression levels of HSD 4, 5, 7, 8, 5AR1 or 5AR2 in the endometria of women with PCOS or ovarian cysts has not been completed.

There is less information about steroid metabolism in the endometria of women with ovarian cysts. The data described in this thesis suggested that ovarian cysts can affect endometrial steroid metabolism as there was altered enzyme expression under basal conditions and altered steroid profiles following testosterone treatment relative to the fertile biopsies (chapter 5).

There were similarities between the starting quantity expression for both PCOS samples and the ovarian cyst biopsy (lower expression of HSD1, 2, 4, 5, 8, 5AR1, 2, and significantly higher expression of aromatase and comparable HSD7 expression relative to the fertile group). Altered endometrial enzyme expression in patients with ovarian disorder suggests that ovarian cysts and PCOS affect steroid metabolism in

the endometrium in a similar manner. This could contribute towards infertility described in these women since hormone changes regulate endometrial receptivity. It could also lead to progression of an endometrial disorder such as hyperplasia or endometrial cancer. It is probable there were significant roles for these enzymes and the steroids they produce in the progression of endometrial disorders in women with PCOS. Giudice stated that unopposed oestrogen and increased androgens aid the progression to endometrial hyperplasia and endometrial cancer in women with PCOS. It is possible that this progression occurs through altered endometrial enzyme expression.[24]

6.4.5 Comparison of basal starting quantities of enzymes in averaged fertile biopsies to biopsies from patients with unexplained infertility

Two biopsies from women with unexplained infertility were analysed and compared to the average fertile biopsies to determine relative expression of nine steroid converting enzymes outlined in table 6.0.

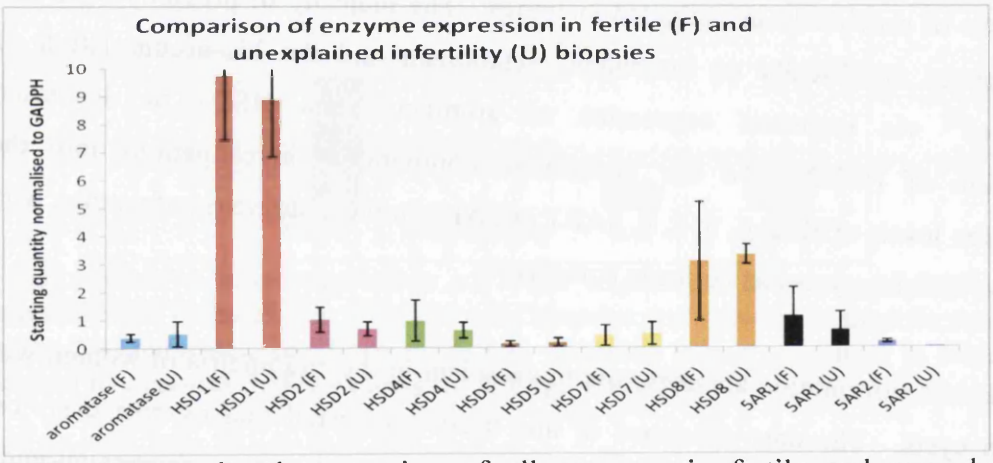

Fig 6.33: Average basal expression of all enzymes in fertile and unexplained infertility biopsies. Two unexplained infertility (U) and four fertile biopsies (F) were grown in specific medium (chapter 2.4) harvested and the RNA extracted. Specific primers described in table 2.6 were used to establish expression levels of steroid converting enzymes through RT-PCR.

All enzymes analysed in the unexplained infertility group (2 biopsies) and the fertile group (4 biopsies) demonstrated similar basal enzyme expression values for all steroid converting enzymes (figure 6.33). These results suggest that in the endometria of these two women, steroid metabolising enzyme expression was not a factor contributing towards infertility. This correlates with the steroid profiles

described in chapter 5.8 which showed similar metabolism of testosterone, and production of androstenedione, androsterone, oestradiol and oestrone in comparison to the fertile biopsies. The unexplained infertility biopsies also produced no DHT which was identical to the fertile biopsies (further discussed in chapter 7.2). More samples are required to confirm these preliminary results described in this thesis.

6.4.6 Case Reports

Statistical analysis of the data sets cannot be confidently assigned to groups with low number of samples. Case studies were described for biopsies from a woman with endometrial hyperplasia and a woman with an endometrial polyp. Initial observations were recorded, however the numbers in each group limit any conclusions regarding that condition due to variation between patients, however these were interesting to study and the observations recorded showed some interesting preliminary data. Progression of this work to include analysis of more biopsies from these groups via these optimised methods would be an ideal continuation of this project.

6.4.7 Basal starting quantities of steroid converting enzymes in stromal and epithelial cells from a patient with endometrial hyperplasia compared to fertile biopsies

A hyperplasia biopsy was obtained from a 55 year old woman with moderate atypical hyperplasia and post menopausal bleeding, this was split into epithelial and stromal cells. Starting quantity expression of the enzymes outlined in table 6.0 were recorded under basal conditions.

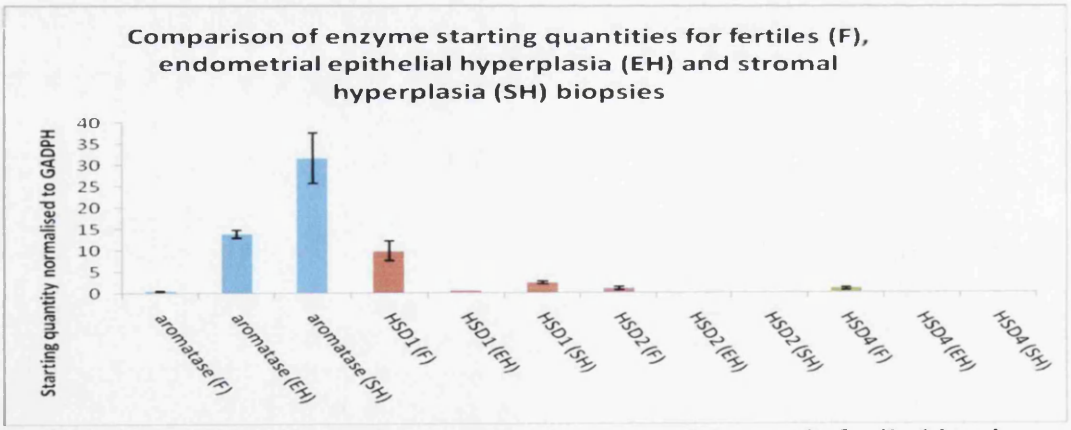

Fig 6.34: Comparison of basal expression in averaged (stromal) fertile biopsies and epithelial and stromal cells from an endometrial epithelial hyperplasia biopsy. All biopsies were grown in specific medium (chapter 2.4) harvested and the RNA extracted. Specific primers described in table 2.6 were used to establish expression levels of steroid converting enzymes through RT-PCR. EH= endometrial epithelial hyperplasia, SH= stromal cells from a patient with endometrial epithelial hyperplasia, F= averaged fertile stromal biopsies (4 samples).

Figure 6.34 illustrated that aromatase expression was significantly increased in the stromal cells from the hyperplasia biopsy in comparison to the fertile biopsies (P=0.004). Increased aromatase expression in endometrial hyperplasia has been reported by Li and colleagues, and the treatment of endometrial hyperplasia with aromatase inhibitors is often administered[25] (although some inhibitors reduce global oestrogen synthesis). There was low expression of HSD1 in both hyperplasia samples in comparison to the fertile biopsies, Utsunomiya and colleagues confirmed these results (no expression of HSD1 in hyperplasia using an immunoreactivity method).[26] Utsunomiya also recorded decreased HSD2 expression lower in 25% of hyperplasia biopsies. HSD2 expression recorded in this investigation was decreased in both the stromal and epithelial hyperplasia biopsies in comparison to the fertile (figure 6.35), agreeing with some of Utsunomiya's results. Further experiments with more samples will be required to confirm the initial observations described in this thesis.

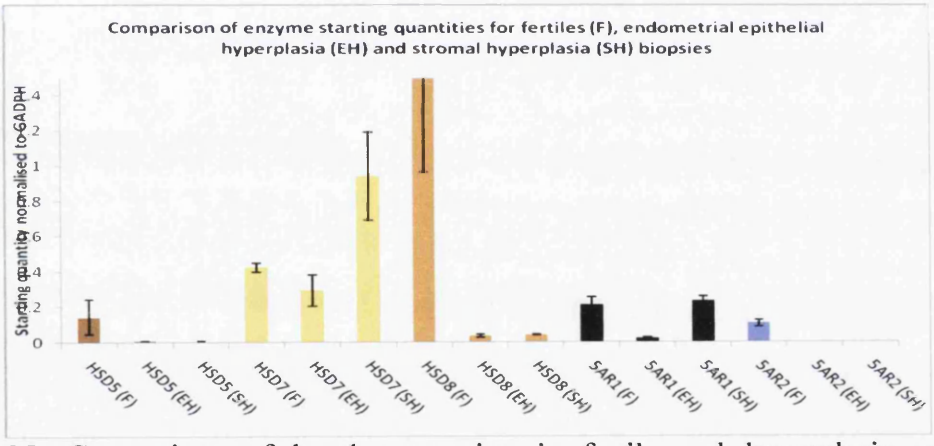

Fig 6.35: Comparison of basal expression in fertile and hyperplasia samples (epithelial and stromal). Endometrial epithelial hyperplasia, endometrial stromal cells from a patient with endometrial hyperplasia and fertile biopsies were grown in specific medium (chapter 2.4) harvested and the RNA extracted. Specific primers described in table 2.6 were used to establish expression levels of steroid converting enzymes through RT-PCR. EH= endometrial epithelial hyperplasia, SH= stromal cells from a patient with endometrial epithelial hyperplasia, F= averaged fertile stromal biopsies.

HSD5 expression was higher in the hyperplasia epithelial cells than the hyperplasia stromal cells. Ito and colleagues showed increased expression of HSD5 in endometrioid cancer biopsies relative to the hyperplasia and fertile samples. In these experiments both hyperplasia biopsies have lower HSD5 expression than the fertile

biopsy (this was contradictory to Ito's second conclusion).[10] Expression of 5AR1 and 5AR2 in the hyperplasia (epithelial and stromal) biopsy was reduced in comparison to the fertile sample. This agrees with another study by Ito and co-workers who recorded low expression of both 5AR isoforms in hyperplasia biopsies.[27] To our knowledge comparative investigations into the expression levels of HSD4, HSD7, and HSD8 in endometrial hyperplasia biopsies have not been completed.

PCOS patients are at a higher risk of developing endometrial hyperplasia (and possibly endometrial cancer) due to increased androgens and unopposed oestrogens.[28] It is possible that the endometria from women with PCOS are progressing towards hyperplasia. A comparison of the expression levels of each steroid converting enzyme in the endometria of the ovarian cyst and PCOS biopsies to the stromal hyperplasia biopsy demonstrated similar trends for all enzymes (a decrease in HSD1, 2, 4, 5, 8 and 5AR2, an increase in aromatase, and comparable expression of HSD7 and 5AR1 relative to the average fertile biopsies), suggesting progression in these biopsies to endometrial hyperplasia.

6.4.8 Comparison of basal starting quantities of steroid converting enzymes in an endometrial polyp biopsy to fertile biopsies

Starting quantity expression under basal conditions for the enzymes outlined in table 6.0 were analysed in an endometrial polyp biopsy from a 43 year old woman. An endometrial polyp is a benign growth in which steroid metabolism is thought to be similar to the normal endometrium, if this was true enzyme expression in the average fertile and the endometrial polyp sample should be identical. However in chapter 5.11 this biopsy demonstrated altered steroid metabolism (compared to fertile biopsies) and so altered enzyme expression was expected.

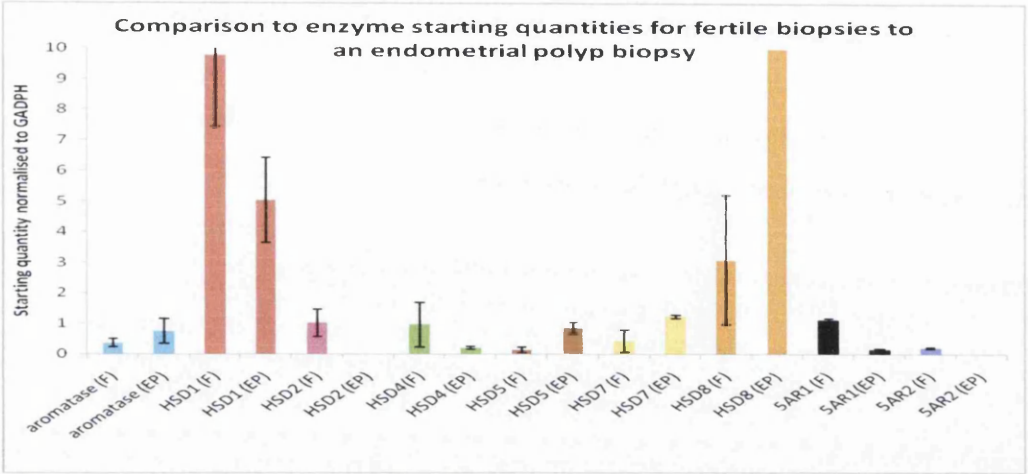

Fig 6.36: Comparison of basal expression of nine steroid converting enzymes in fertile and endometrial polyp biopsies. An endometrial polyp biopsy (EP) and the fertile biopsies (F) were grown in specific medium (chapter 2.4) harvested and the RNA extracted. Specific primers described in table 2.6 were used to establish expression levels of steroid converting enzymes through RT-PCR.

Figure 6.36 illustrated a decrease in the starting quantity expression of HSD1, HSD2, HSD4, 5AR1 and 5AR2 in the endometrial polyp biopsy compared to the average fertile biopsies. There was increased expression of aromatase, HSD5, HSD7 and HSD8 (figure 6.36). Aromatase expression in the biopsy from an endometrial polyp was higher than the basal expression levels in the average fertile sample, this did not agree with expression information from Pal and co-workers who observed aromatase expression to be similar in endometrial polyps and fertile samples.[29] Further experiments with more samples will be required to confirm the initial observations described in this thesis.

The combination of enzyme expression profile for the endometrial stromal hyperplasia and the mass spectrometry information from chapter 5 this suggests that this endometrial polyp biopsy could be progressing towards hyperplasia. This was supported by the similar trends in expression of a number of enzymes in both pathologies relative to the fertile biopsies, (increased expression of aromatase and HSD7, and decreased expression of HSD1, HSD2, HSD4 and 5AR2).

6.4.9 Summary of enzyme expression in fertile biopsies and benign endometrial disorders

A direct comparison between basal expression of each enzyme in each condition relative to the fertile biopsies was completed (table 6.4).

Table 6.4: Basal enzyme expression in benign endometrial pathologies relative to the averaged fertile biopsies. H was higher expression than the 95th percentile of the average fertiles, L was lower expression than the 95th percentile of the averaged fertiles and, – was comparable expression to the averaged fertiles. Expression of specific enzymes was determined by RT-PCR with specific primers as outlined in table 2.6 (arom= aromatase).

Pathology	arom	HSD1	HSD2	HSD4	HSD5	HSD7	HSD8	5AR1	5AR2
Unexplained Infertility	-	-	-	-	-	-	-	-	-
Endometriosis	H	L	*	L	H	*	*	H	*
PCOS	-	L	L	L	L	L	L	L	L
Ovarian Cyst	H	L	L	L	L	L	L	L	L
Hyperplasia Epithelial	H	L	L	L	L	L	L	L	L
Hyperplasia Stromal	H	L	L	L	L	H	L	-	L
Endometrial polyp	H	L	L	L	H	H	H	L	H

* basal expression varied significantly between endometriosis biopsies making comparison by 95th percentile method not possible.

The results quoted for endometriosis samples in table 6.4 demonstrate increased (or decreased) expression in the majority of endometriosis biopsies relative to the fertile biopsies, (this was not possible with HSD2 or HSD8 expression due to the large variation in basal expression of endometriosis enzymes also half exhibited increased and half decreased expression of each enzyme relative to the fertile biopsies). Unexplained infertility biopsies were observed to exhibit similar enzyme expression and steroid profiles to fertile biopsies, again confirming the hypothesis that endometrial steroid metabolism was not altered in these women suggesting steroid metabolism was not contributing towards infertility. There was variation in expression of a number of enzymes in all other benign conditions relative to the fertile biopsies. This could explain the variation in testosterone utilisation and production of the specific steroids determined in chapter 5. Relative to the fertile biopsies, one PCOS biopsy demonstrated higher aromatase expression the other exhibited lower aromatase expression, this highlights the variation between biological samples, an expansion of this investigation to include further PCOS

biopsies would determine the relationship between aromatase expression in PCOS endometria relative to the fertile group.

6.5 Changes in enzyme expression after testosterone treatment over 72 hours in endometrial biopsies

Testosterone treatment of biopsies was completed over four time points over 72 hours (0, 24, 48 and 72 hours) as described in chapter 3.14. Changes in enzyme expression throughout the experiment for each endometrial pathology were determined (expressed as fold expression relative to GADPH). The expression of each enzyme was then normalised to 1 at time zero (under basal conditions) changes in expression relative to this time throughout the 72 hours were calculated. This highlights the enzymes which demonstrated the largest changes in fold expression throughout the experiments after testosterone treatment. Following determination of changes in enzyme expression after testosterone treatment correlations between changing steroid concentrations and enzyme expression were determined (chapter 7).

6.5.1 Changes in enzyme expression in fertile biopsies

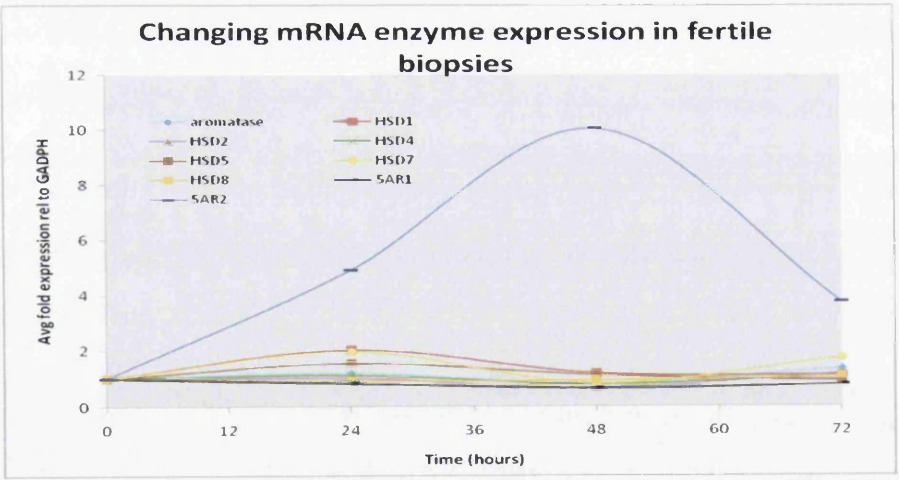

Fig 6.37: Changes in enzyme expression levels over 72 hours after testosterone treatment in average fertile stromal biopsies. Fertile biopsies were grown in specific medium (chapter 2.4) harvested and RNA extracted. Specific primers described in table 2.6 were used to establish expression levels of steroid converting enzymes through RT-PCR.

There were significant changes in expression levels of the 5AR2 enzyme produced from averaged data from four fertile biopsies (figure 6.37). The expression was significantly increased at 24 hours relative to zero (P= 0.016) a maximum fold

increase was observed at 48 hours. The expression of all other enzymes remains essentially constant throughout the experiment. It was postulated that at 24 and 48 hours there would be an increase in the reaction product androsterone and a decrease in the reaction precursor androstenedione this was confirmed in chapter 7.

6.5.2 Changes in enzyme expression in unexplained infertility biopsies

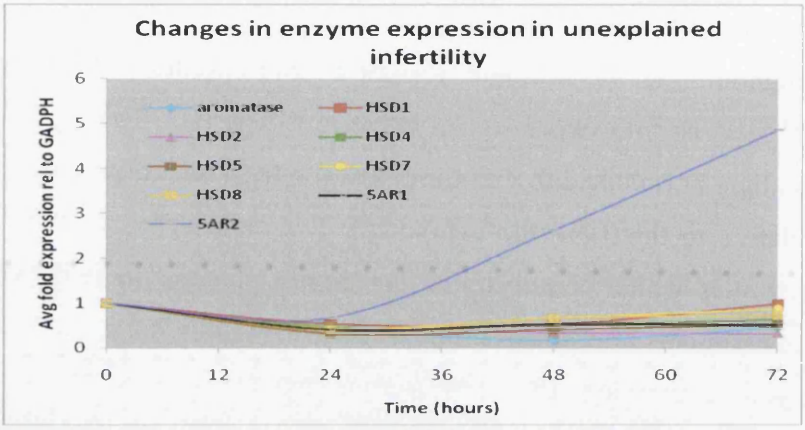

Fig 6.38: Changes in enzyme expression levels over 72 hours after testosterone treatment in average unexplained infertility biopsies. Unexplained infertility biopsies were grown in specific medium (chapter 2.4) harvested and RNA extracted. Specific primers described in table 2.6 were used to establish expression levels of steroid converting enzymes through RT-PCR.

5AR2 expression increased at 48 and 72 hours relative to time zero in the unexplained infertility biopsies, as illustrated in figure 6.38. As with the fertile biopsies expression of all other enzymes remained constant throughout the experiment. A change in 5AR2 expression was comparable to the fertile biopsies (although observed later in the unexplained infertility biopsies).

6.5.3 Changes in enzyme expression in endometriosis biopsies

The endometriosis biopsies were grouped together to determine changes in enzyme expression after testosterone treatment this was possible as at time zero all enzyme expression was normalised to one. This allows investigation into changes in enzyme expression irrespective of basal enzyme expression.

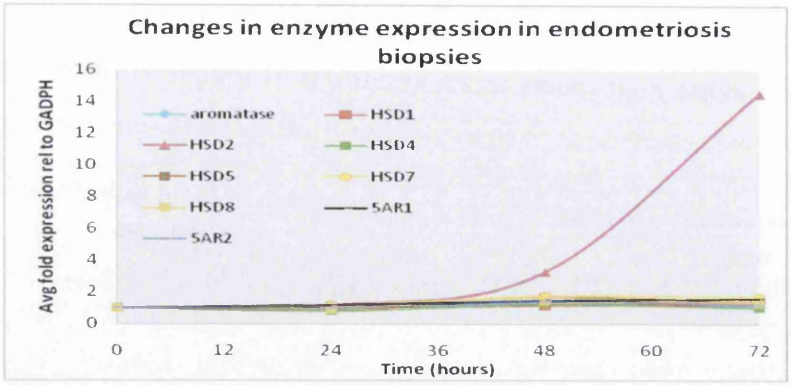

Fig 6.39: Changes in enzyme expression levels over 72 hours after testosterone treatment in average endometriosis stromal biopsies. Endometriosis biopsies were grown in specific medium (chapter 2.4) harvested and RNA extracted. Specific primers described in table 2.6 were used to establish expression levels of steroid converting enzymes through RT-PCR.

Figure 6.39 illustrates a change in expression of the enzyme HSD2 at 48 and 72 hours in the endometriosis biopsies.

6.5.4 Changes in enzyme expression in endometrial biopsies from patients with PCOS

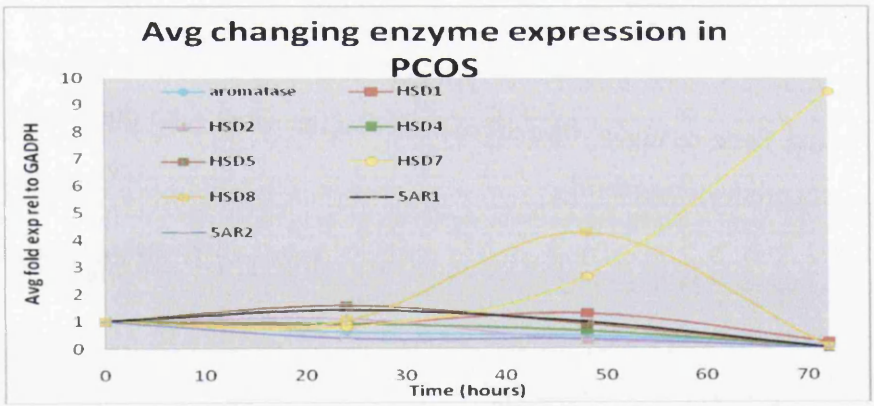

Fig 6.40: Changes in enzyme expression levels over 72 hours after testosterone treatment in average PCOS stromal biopsy. PCOS biopsies were grown in specific medium (chapter 2.4) harvested and RNA extracted. Specific primers described in table 2.6 were used to establish expression levels of steroid converting enzymes through RT-PCR.

Figure 6.40 illustrates a change in HSD7 enzyme expression at 48 and 72 hours in the PCOS biopsy. HSD8 expression was increased at 48 hours and any correlations between enzyme expression and steroid concentrations were outlined in chapter 7. Expression of all the other enzymes remains essentially constant after time zero.

Case Reports

6.5.5 Changes in enzyme expression in an endometrial biopsy from an ovarian cyst

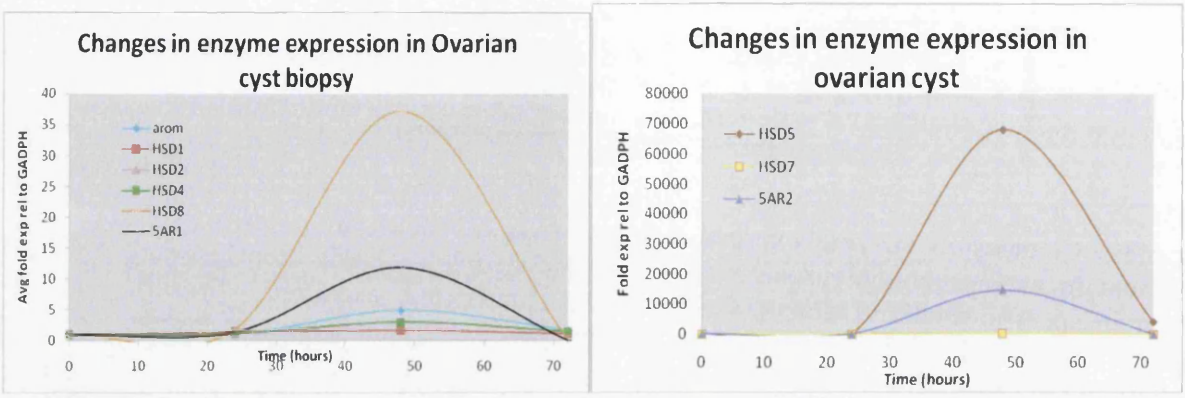

Fig 6.41: Changes in enzyme expression levels over 72 hours after testosterone treatment in average ovarian cyst stromal biopsy. An ovarian cyst biopsy was grown in specific medium (chapter 2.4) harvested and RNA extracted. Specific primers described in table 2.6 were used to establish expression levels of steroid converting enzymes through RT-PCR (two separate graphs are shown as the increase in expression was larger for HSD5, 7 and 5AR2 in comparison to the other enzymes).

There were large changes in the expression levels of a number of enzymes in the stromal biopsy from a patient with an ovarian cyst (figure 6.41). At 48 hours the expression levels of aromatase, HSD8 and 5AR2 were increased in relation to basal expression. These large changes were all recorded at the same time point which may be indicative of a misleading result.

6.5.6 Changes in enzyme expression in endometrial biopsy from an endometrial hyperplasia biopsy

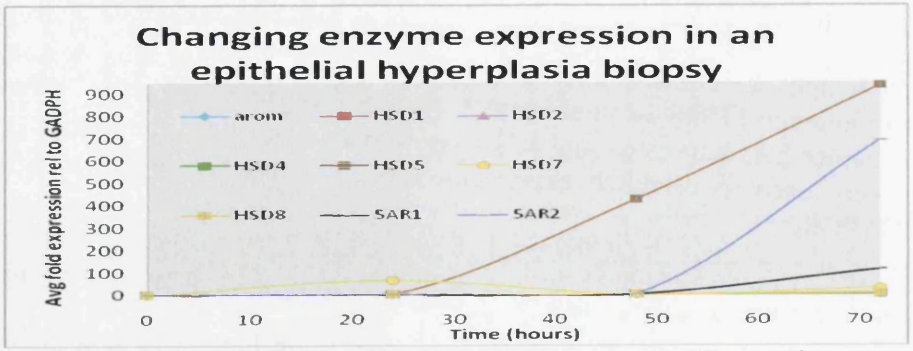

Fig 6.42: Changes in enzyme expression levels over 72 hours after testosterone treatment of an epithelial hyperplasia biopsy. An endometrial hyperplasia biopsy was grown in specific medium (chapter 2.4) harvested and RNA extracted. Specific primers described in table 2.6 were used to establish expression levels of steroid converting enzymes through RT-PCR.

Significant changes in enzyme expression relative to time zero were recorded in the enzymes HSD5, HSD7, 5AR1 and 5AR2 in the epithelial hyperplasia biopsy. HSD7 increases at 24 and 72 hours relative to time zero. HSD5 expression was increased at 48 and 72 hours, and expression of 5AR1 and 5AR2 was increased at 72 hours relative to time zero (figure 6.42). Expression of all other enzymes was constant throughout the experiment.

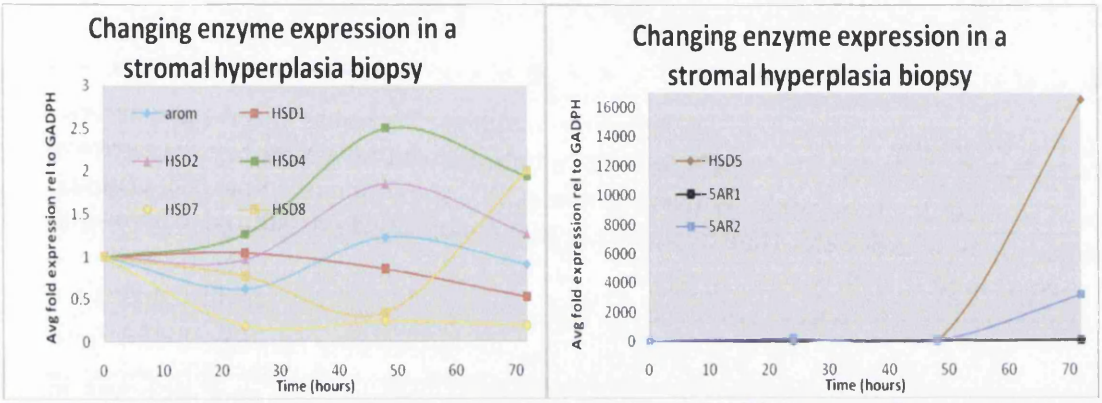

Fig 6.43: Changes in enzyme expression levels over 72 hours after testosterone treatment in stromal cells from an endometrial hyperplasia biopsy. An endometrial stromal biopsy was grown in specific medium (chapter 2.4) harvested and RNA extracted. Specific primers described in table 2.6 were used to establish expression levels of steroid converting enzymes through RT-PCR.

Figure 6.43 illustrates increased expression of three enzymes in the hyperplasia stromal biopsy. These changes were higher than recorded in the epithelial cells, but were recorded with the same enzymes HSD5, 5AR1 and 5AR2 all of which showed increased expression at 72 hours. Expression of HSD2, HSD4 and aromatase increased 48 hours after testosterone treatment, all other enzyme expression remained essentially constant throughout the experiment.

6.5.7 Changes in enzyme expression in an endometrial sample from a patient with an endometrial polyp

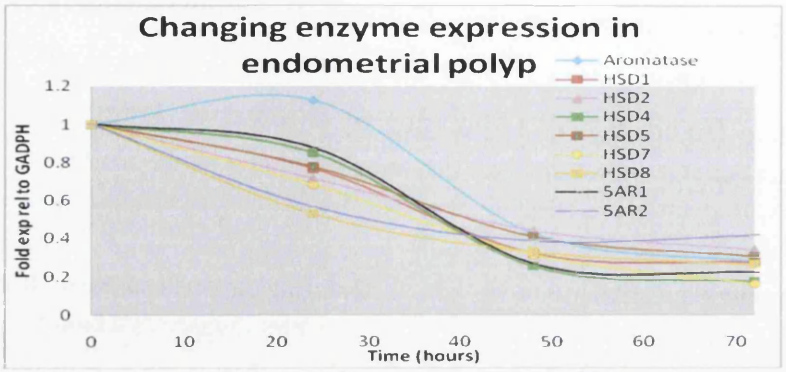

Fig 6.44: Changing expression of all enzymes over 72 hours after testosterone treatment in an endometrial polyp biopsy. An endometrial polyp biopsy was grown in specific medium (chapter 2.4) harvested and RNA extracted. Specific primers described in table 2.6 were used to establish expression levels of steroid converting enzymes through RT-PCR.

At 24 hours all enzymes (except aromatase) were reduced in comparison to time zero, another decrease in expression of all enzymes was observed after 48 hours in the endometrial polyp sample as illustrated in figure 6.44. Aromatase expression increased after 24 hours and decreased after this time.

6.5.8 Conclusions biopsies

A table of temporal changes in enzyme expression levels for each endometrial pathology was compiled. This was directly compared to steroid metabolism profiles in chapter 7.

Table 6.5: Temporal changes in enzyme expression in seven endometrial pathologies relative to basal expression after testosterone treatment (72 hours).

Endometrial pathology	Enzymes which exhibit large fold expression changes rel to time zero	Steroid conversion reaction
Fertile	5AR2 (P= 0.016)	Androstenedione → Androstane-dione Testosterone → DHT
Unexplained Infertility	5AR2	Androstenedione → Androstane-dione Testosterone → DHT
Endometriosis	HSD2	Testosterone → Androstenedione Oestradiol → Oestrone
Ovarian Cyst	Aromatase HSD5 HSD7 HSD8 5AR1/5AR2	Androgens →Oestrogens Androstenedione →Testosterone Oestrone → Oestradiol Oestradiol →Oestrone DHT→Androstane-dione Testosterone → DHT Androstenedione → Androstane-dione
PCOS	HSD7 HSD8	Oestrone → Oestradiol Oestradiol →Oestrone DHT→Androstane-dione
Hyperplasia Epithelial	HSD7 HSD5 5AR1/5AR2	Oestrone → Oestradiol Androstenedione →Testosterone Testosterone → DHT Androstenedione → Androstane-dione
Hyperplasia Stromal	HSD5 5AR1/5AR2	Androstenedione →Testosterone Testosterone → DHT Androstenedione → Androstane-dione
Endometrial Polyp	None	

The enzyme expression data, (basal expression (summarised in table 6.4) and large changes in enzyme expression relative to basal expression table 6.5) highlighted enzymes which could be targeted for inhibition that were not present in fertile samples but were highly expressed in endometrial disorders possibly leading to altered steroid metabolism. Cells lines were more homogenous than the biopsies, which leads to less variation between experiments and in enzyme expression which permitted the use of statistical tests. Unlike the cell lines there were less biopsies available from each group (the case studies only investigated one biopsy) and biological variation between patients was more apparent.

HSD2 inhibition in endometriosis samples may be a viable target or 5AR1 expression in hyperplasia, PCOS or ovarian cyst patients. HSD5 expression increased in hyperplasia and ovarian cyst patients and HSD7 expression increased in the ovarian disorders following testosterone treatment and so these could also be viable targets. The level of influence expression of each of these enzymes has on the production of a specific steroid(s) requires confirmation before inhibitor development.

6.6 Conclusions chapter six

Initial experiments with established cell lines permitted optimisation of cell culture techniques and experimental methods, as well as RNA extraction, reverse transcription and RT-PCR. After a sensitive, reproducible method was determined it was subsequently applied to biopsy samples.

The basal expression of nine steroid converting enzymes was recorded in all cell lines and biopsies. A comparison of basal enzyme expression in biopsies which exhibit similar testosterone metabolism profiles was conducted. Following this testosterone treatments were completed over 72 hours and changes in expression of each enzyme recorded.

Experiments with cell lines and biopsies highlight the same enzymes as important for steroid metabolism. There were a number of enzymes which were either highly expressed (high basal expression) or produced the highest changes in fold expression after testosterone treatment relative to basal expression. These enzymes were aromatase, 5AR1, 5AR2, HSD2, HSD5, HSD8 and (to a lesser extent) HSD7.

Changes in enzyme expression were linked to changes in steroid concentration(s) in chapter 7 to determine if expression of a specific enzyme(s) can directly affect the steroid profile.

6.7 References

[1] AB Applied Biosystems Technical Resources RT-PCR accessed online 15th December 2008 www.ambion.com/techlib/basics/rtpcr/index.htlm

[2] Havelock J C, Rainey W E, Carr B R. Mol and Cell Endocrinology **228** (2004) 67-78

[3] Ito K, Suzuki T, Moriya T, Utsunomiya H, Sugawara A, Konno R, Sato S, Sasano H. The J of Clinical Endo and Metab **86** (2001) 2721-2727

[4] Applied Biosystems. The Basics: Northern Analysis. Accessed online 23rd February 2009 http://www.ambion.com/techlib/basics/northerns/index.html

[5] Singh R, Recinos RF, Agresti MMS, Schaefer RB, Bosbous MBS, Gosain AK. Plastic and Reconstructive Surgery **177** (2006) 2227-2234

[6] Rahimi-Ardabili B, Pourandarjani R, Habibollahi P, Mualeki A. BMC Clincal Pharmacology **6** (2006) doi:10.1186/1472-6904-6-7

[7] Purohit A, Fusi L, Brosens J, Woo LWL, Potter BVL, Reed MJ. Human Reproduction **23** (2008) 290-297

[8] Kitawaki J, Kado N, Ishihara H, Koshiba H, Kitaoka Y, Honjo H. J Steroid Biochem and Mol Biol **83** (2002) 149-155

[9] Bacallao K, Leon L, Gabler F, Soto E, Romero C, Valladares L, Vega M. J steroid Biochem Mol Biol **110** (2008) 163-169

[10] Ito K, Utsunomiya H, Suzuki T, Saitou S, Akahira J-I, Okamura K, Yaegashi N, Sasano H. Mol and Cell Endocrin **248** (2006) 136-140

[11] Attar E and Bulun S E. Human Reproduction Update **12** (2006) 49-56

[12] Dassen H, Punyadeera C, Kamps R, Delvoux B, Van Langendonckt A, Donnez J, Husen B, Thole H, Dunselman G, Groothuis P. Human Repro **22** (2007) 3148-3158

[13] Bulun S E, Gurates B, fang Z, Tmaura M, Sebastian S, Zhou J, Amin S, Yang S. J of Repro Immunology **55** (2002) 21-33

[14] Day JM, Tutill HJ, Purohit A, Reed MJ. Endocrine-Related Cancer **15** (2008) 665-692

[15] Carneiro MM, Morsch DM, Camargos AF, Spritzer PM, Reis FM. Gynecol Endocrin **23** (2007) 188–192

[16] Matsuzaki S, Canis M, Pouly JL, Botchorishvili R, De´chelotte PJ, Mage G. Fertility Sterility **86** (2006) 548–553

[17] Šmuc T, Kristan K, Bajc G, Šinlovec J, Ribič-Pucelj M, Husen B, Thole H, Lanišnik-Rižner T. (Eds) Weiner H, Maser E, Lindahl R Plapp B. Enzymology and Molecular Biology of Carbonyl Metabolism chapter **13** (2007) 350-359

[18] Šmuc T, Puceli M R, Šinlovec J, Husen B, Thole H, Rižner T L. Gynecological Endocrinology **23** (2007) 105-111

[19] Šmuc T, Hevir N, Pucelj M R, Husen B, Thole H, Rižner T L. Mol and Cell Endo Article in Press (2008) accepted July 2008 doi:10.1016/j.mce.2008.07.020

[20] Carneiro M M, Morsch D M, Camargos AF, Reis FM, Spritzer PM. British Journal of Obstetrics and Gynaecology **115** (2008) 113-117

[21] Cunat S, Rabenoelina F, Daurès, Katsaros D, Sasano H, Miller WR, Maudelonde T, Pujol P. J of Steroid Biochem and Mol Biol **93** (2005) 15-24

[22] Leon , Bacallao K, Gabler F, Romero C, Valladares L, Vega M. Steroids **73** (2008) 88-95

[23] Lukanova A, Kaaks R. Cancer Epidemiology, biomarkers and prevention Review **14** (2005) 98-102

[24] Giudice LC. Best Practise in Clinical Endocrinology and Meta **20** (2006) 235-244

[25] Li H, Chen X, Qiao J, Inter J of Gyne and Obste **100** (2008) 10-12

[26] Utsunomiya H Suzuki T, Kaneko C, Takwyama J, Nakamura J, Kimura K, Yoshihama M, Harada N, Ito K, Konno R, Sato S, Okamura K, Sasano H. J Clinical Endo and Metab **86** (2001) 3436-3443

[27] Ito K, Suzuki T, Akahira J, Moriya T, Kaneko C, Utsunomiya H, Yaegashi N, Okamura K, Sasano H. Int J of Cancer **99** (2002) 652-657

[28] Pillay OC, Wong Te Fong LF, Crow JC, Benjamin E, Mould T, Atiomo W, Menon PA, Leonard AJ, Hardiman P. Human Repro **21** (2006) 924-929

[29] Pal L, Niklaus A L, Kim Mimi, Pollack S Santoro N. Human Repro **23** (2008) 80-84

Chapter seven

Testosterone utilisation by endometrial cells: Comparison of metabolic (mass spectrometry) and enzyme expression profiles

7.0 Introduction

This chapter describes the combination of mass spectrometry and enzyme expression data (RT-PCR), under basal conditions (prior to testosterone treatment) and after testosterone treatment creating a unique view of testosterone metabolism in the endometrium. From these results important metabolism routes and enzymes have been observed in endometrial cell lines and in the endometria of women with endometriosis suggesting altered testosterone metabolism pathways in comparison to fertile biopsies. Preliminary data from a limited number of endometrial biopsies from women with other benign disorders (PCOS, ovarian cyst, endometrial hyperplasia, and endometrial polyp) also demonstrated altered testosterone metabolism in comparison to the fertile group. Two biopsies from women with unexplained infertility were also investigated in this chapter.

Expression profiles for aromatase, 17β-HSD1, 17βHSD2, 17β-HSD4, 17β-HSD5, 17β-HSD7, 17β-HSD8, 5AR1 and 5AR2 which catalyse the steroid conversion reactions described in chapter 6 were investigated for each cell line and pathology. Positive identification of steroids was determined through optimised mass spectrometry (LC/MS and LC/MS/MS) analysis relative to identical steroid standards (chapters 4 and 5). The data presented in this chapter is a combination of the results obtained in chapters 5 and 6.

A combination of enzyme expression and steroid profiles after testosterone treatment permitted a comparison of;

1. fertile biopsies to cell lines,
2. fertile biopsies to endometriosis biopsies and,
3. fertile biopsies to each benign endometrial pathology.

From preliminary data a model of testosterone metabolism was suggested in fertile biopsies through hyperplasia biopsies to endometrial cancer cell lines (figure 7.1), and from fertile biopsies to all other biopsy pathologies- endometriosis (6 biopsies), unexplained infertility (2 biopsies), PCOS (2 biopsies), ovarian cyst (1 biopsy), endometrial hyperplasia (1 biopsy) and endometrial polyp (1 biopsy), as illustrated in figure 7.2.

This provides a unique method for determination of changes in the steroid profile and/or enzyme expression which may characterize each endometrial disorder. The information regarding testosterone metabolism and enzyme expression in the endometria of women with PCOS, unexplained infertility, endometrial hyperplasia and endometrial polyp was limited in comparison to the fertile and endometriosis groups and the cell lines as there were low numbers of samples in these groups, nevertheless it allowed us to demonstrate some interesting preliminary data, covering a range of endometrial conditions.

This chapter will compare cell line and biopsy experiments principally focussing on the combination of testosterone metabolism pathways (recorded in chapter 5) and the expression of steroid converting enzymes (recorded in chapter 6). The data is presented as follows;

- Androgen production and relation to enzyme expression by cell lines and endometrial biopsies following testosterone treatment
- Roles of androgens in the human endometrium
- Oestrogen production and aromatase expression by cell lines and endometrial biopsies following testosterone treatment
- Comparison of testosterone metabolism by cell lines to fertile endometrial biopsies
- Comparison of enzyme expression by cell lines with similar testosterone metabolism profiles (Ishikawa and HEC-1A, COV434 and HEC-1B)
- Correlations between enzyme expression and steroid concentration by cell lines and biopsies
- Summary
- Conclusions
- Discussion
- Further work

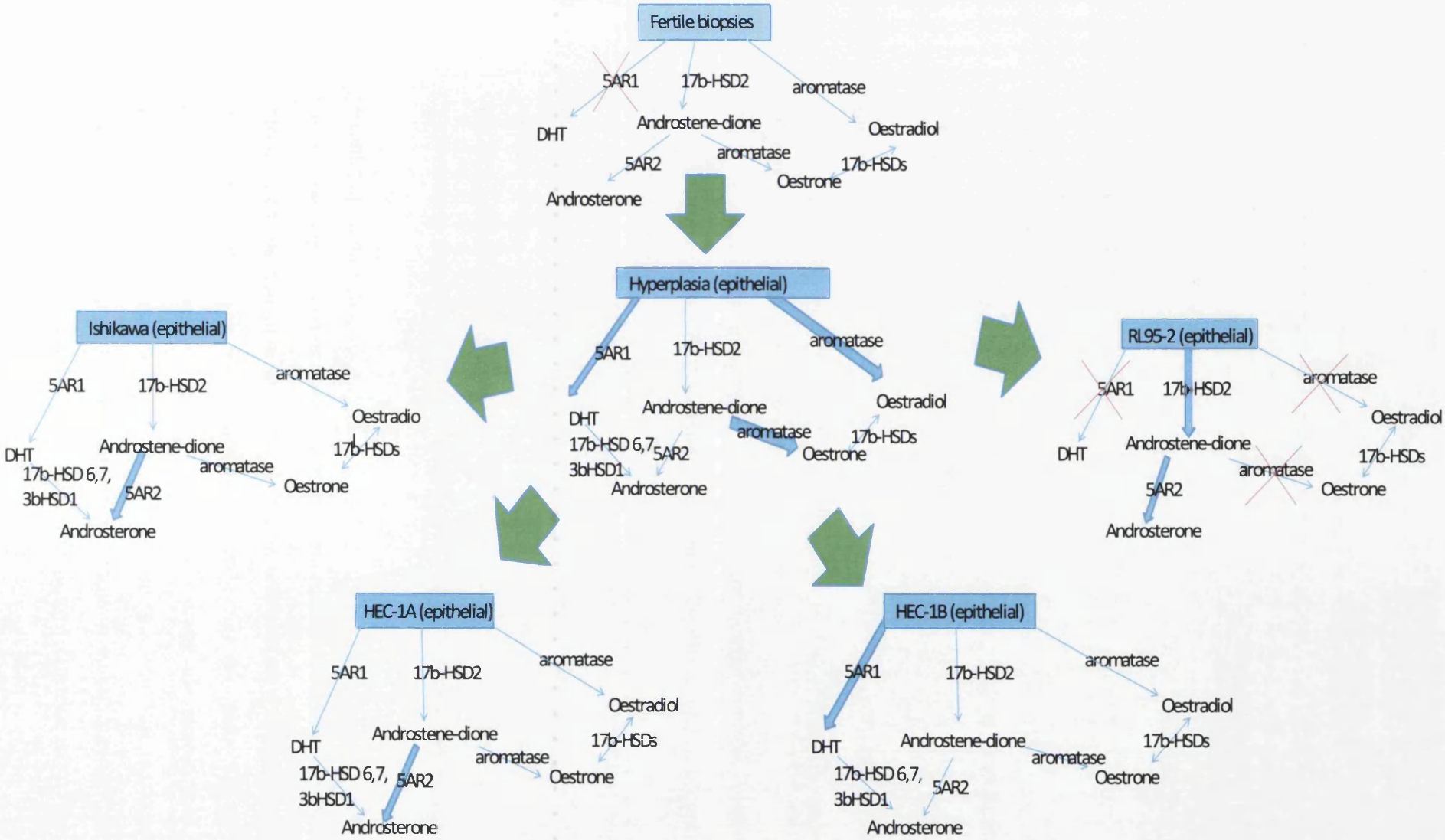

Fig 7.1: Alteration in steroid metabolism from 4 fertile biopsies to 1 epithelial hyperplasia biopsy to the established cell lines. An arrow with a red cross indicates reaction is not occuring, increased arrow size indicates this reaction route is increased (relative to the fertile biopsies). Enzymes which catalyse each conversion are recorded on each arrow.

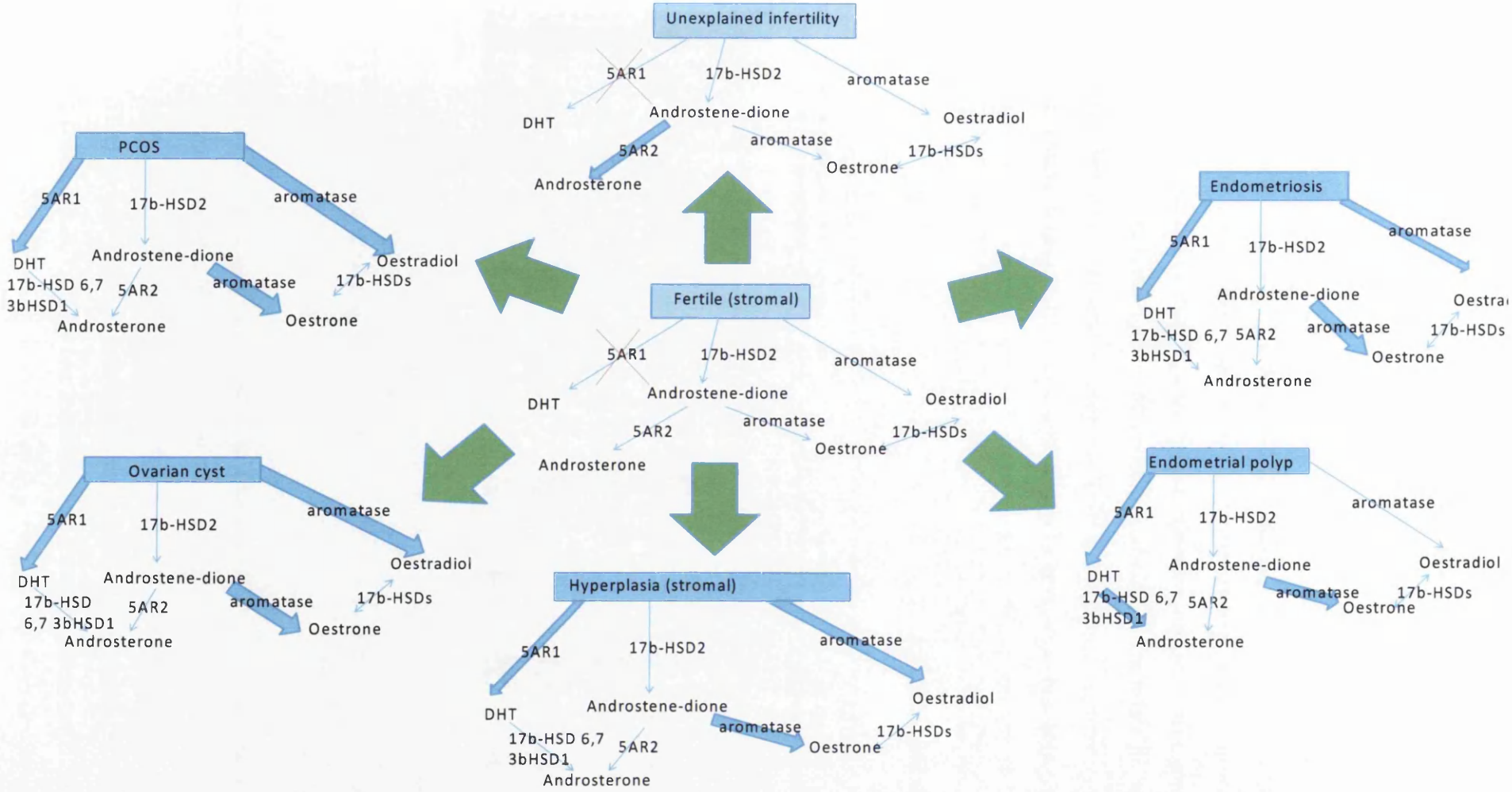

Fig 7.2: Alteration in steroid metabolism from stromal cells from 4 fertile biopsies to biopsies from each pathology (endometriosis (6 biopsies), unexplained infertility (2 biopsies), PCOS (2 biopsies) endometrial polyp (1 biopsy), endometrial hyperplasia (1 biopsy), and ovarian cyst (1 biopsy). An arrow with a red cross indicates reaction is not occuring, increased arrow size indicates this reaction route is increased (relative to the fertile biopsies). Enzymes which catalyse each conversion are recorded on each arrow.

7.1 Androgen production in established cell lines and endometrial biopsies from fertile women and women with benign endometrial disorders

The initial route of testosterone metabolism varied in the cell lines and clinical biopsies, in each case the major metabolite was correlated with high basal enzyme expression of 5AR1 or the oxidative 17β-HSDs (HSD2, 4 and 8) prior to testosterone treatment. Expression of these specific enzymes can be used to determine the chief route of testosterone utilisation, for example if DHT was produced high expression of 5AR1 was observed and if androstenedione was produced high basal expression of HSD2, 4 or 8 was observed. A mixture of DHT and androstenedione was correlated with expression of 5AR1 and expression of either HSD2, 4 or HSD8 (as illustrated in figures 7.3 and 7.4 and described in table 7.1). Therefore the major route of testosterone metabolism in endometrial cells can be estimated by analysis of the expression of these four enzymes.

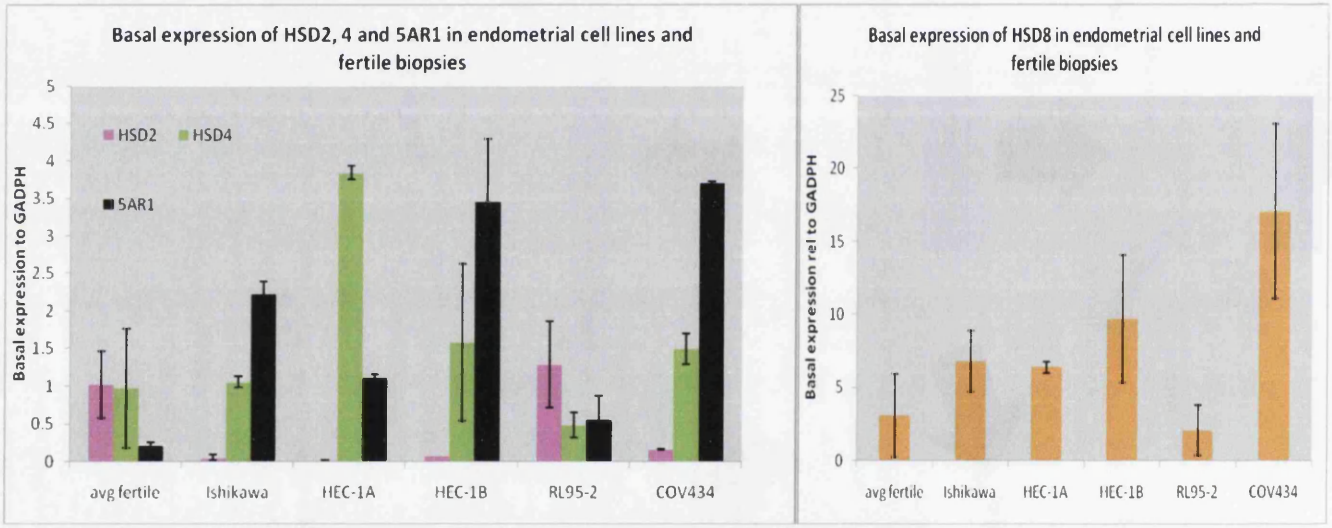

Fig 7.3: Plots illustrating the basal expression levels of HSD2, 4, 8 and 5AR1 in endometrial cell lines in comparison to fertile endometrial biopsies. Cell lines and biopsies were grown in specific media outlined in chapter 2.4. Expression of HSD2, 4, 8 and 5AR1 were calculated by RT-PCR with the use of specific primers as described in chapter 2.6.

The maximum concentration of DHT observed appears to be related to the basal expression of 5AR1, for example the COV434 line exhibited the highest 5AR1 expression under basal conditions and the highest concentration of DHT was recorded. The RL95-2 cells exhibited the lowest expression of 5AR1 and no DHT was produced. The combination of mass spectrometry and QRT-PCR suggested a

relationship between 5AR1 expression and DHT production (this relationship was further investigated in the cell lines Ishikawa, HEC-1B and COV434 figures 7.12, 7.17 and 7.18).

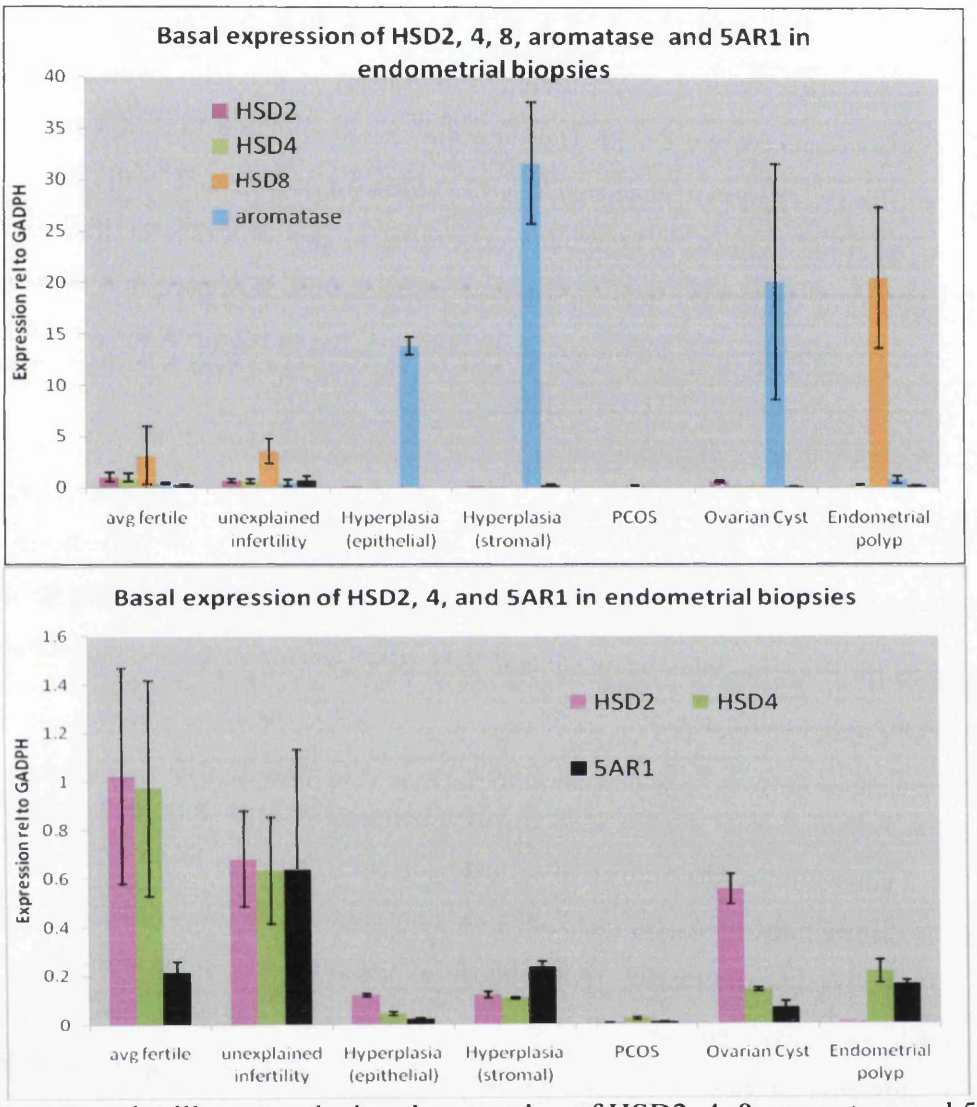

Fig 7.4: Top plot illustrates the basal expression of HSD2, 4, 8, aromatase and 5AR1 in endometrial biopsies, bottom plot illustrates the expression of HSD2, 4 and 5AR1. Cell lines were grown in specific media outlined in chapter 2.4. Expression of aromatase, HSD2, 4, 8, aromatase and 5AR1 was calculated by RT-PCR with the use of specific primers as described in table 2.6.

The 5-alpha reductases catalyse the conversion of testosterone to DHT or androstenedione to androstanedione. Specific enzymes and/or isoforms have been shown to exhibit different affinities for testosterone, for example 5AR2 was described by Baxter and colleagues as having a higher affinity for testosterone than 5AR1.[1] The opposite of this was concluded in these experiments where 5AR1 expression appeared to correlate with DHT production suggesting that this enzyme had a higher affinity for testosterone than 5AR2. This was confirmed in the RL95-2 cell line which highly expressed 5AR2 and according to Baxter's results this would result in production of DHT after addition of testosterone, however this was not observed in these experiments which suggests that conditions required for the 5AR2 conversion were not present in RL95-2 cells.

In fertile biopsies, biopsies from patients with unexplained infertility and RL95-2 cells the majority of testosterone was rapidly converted to androstenedione in correlation with high expression of HSD2, HSD4 and/or HSD8. In fertile and unexplained infertility biopsies oestrone and oestradiol were also produced probably through the aromatase enzyme.

Endometrial biopsies from fertile women, two women with unexplained infertility and RL95-2 cells produced no DHT after testosterone treatment, in correlation with this they exhibited low expression 5AR1 in comparison to the oxidative HSDs. There was a large variation in 5AR1 basal expression levels between the two unexplained infertility biopsies (figure 7.4) which was attributed to biological variation, however steroid profiles produced after testosterone treatment of both unexplained infertility biopsies were comparable to the fertile biopsies suggesting that DHT production via 5AR1 was not occurring in either of these biopsies and the major route of testosterone utilisation was through oxidation via HSD2, 4 or 8 to androstenedione.

Basal expression of 5AR1 was similar in COV434 and HEC-1B cells, and so the expression of HSD2 and HSD8 in these cell lines was compared (HSD4 expression- the other enzyme which converts testosterone to androstenedione was not significantly different between the two cell lines (P= 0.626) and so was not included

in this comparison). The basal expression of both HSD2 and HSD8 was higher in COV434 cells in comparison to HEC-1B, which was correlated with higher concentration of androstenedione produced by the COV434 cell line, suggesting HSD2 and/or HSD8 were converting testosterone to androstenedione in these cell lines.

The majority of endometriosis biopsies investigated demonstrated increased 5AR1 expression relative to the fertile group (figure 6.22), which was linked to DHT production after testosterone treatment (no production of DHT by fertile group). Production of androstenedione was recorded in all endometriosis biopsies in a similar profile to the fertile biopsies (figure 5.35) possibly due to expression of one or more of the oxidative 17β-HSDs (HSD2, 4 or 8). Following determination of these observations in endometriosis biopsies, other benign endometrial conditions were investigated (chapters 5 and 6) to ascertain how typical these observations were in relation to endometrial disorders.

In the COV434 and HEC-1B cell lines and biopsies from an endometrial polyp, and endometrial stromal hyperplasia, production of DHT was recorded in preference to androstenedione after testosterone treatment. This was correlated to high basal expression of 5AR1 relative to the oxidative HSDs in these conditions suggesting this was required for the conversion of testosterone to DHT in preference to androstenedione.

A mixture of androstenedione and DHT was produced after testosterone treatment of the Ishikawa and HEC-1A cell lines and biopsies from the endometria of women with endometriosis. In correlation with this these cell lines and biopsies all expressed at least one of the oxidative 17β-HSDs (HSD2, 4 or 8) and 5AR1. In the ovarian cyst, PCOS and epithelial hyperplasia biopsies 5AR1 expression was low in comparison to the oxidative 17β-HSDs (HSD2, 4 and 8) so it was expected that androstenedione would be the major androgenic product, however following testosterone treatment 5AR1 expression increased which corresponded with an increase in DHT production.

Table 7.1: Observed enzyme expression related to the production of DHT and/or androstenedione in cell lines and endometrial biopsies.

Androgen produced	High expression	Medium expression	Low expression	Cell Line/biopsy
DHT	5AR1	HSD4 HSD8	HSD2	HEC-1B COV434 Endometrial polyp
Androstenedione	HSD2, (HSD4 or HSD8)	n/a	5AR1	RL95-2 Fertile Unexplained infertility
Androstenedione and DHT	-	5AR1 HSD2, (HSD4 or HSD8)	-	Ishikawa HEC-1A Endometriosis Ovarian disorders Endometrial hyperplasia

7.2 The roles of androgens in the endometrium

The expression of HSD2, 4 8, and 5AR1 and production of corresponding steroids (androstenedione and DHT) in the endometrial cancer cell lines and biopsies suggests there maybe roles for these enzymes and androgens in endometrial function. The roles of the androgens; androstenedione, DHT and androsterone in endometrial function and progression to endometrial disorders may be numerous.

The major role of androstenedione is as a circulatory precursor of adrenal (or adipose) origin which enters the endometrium and is converted through aromatisation to oestrogens.[2] Other roles of androstenedione in the endometrium were described by Maliqueo and colleagues as being induction of cellular proliferation and a decrease in apoptosis of normal endometrial stromal cells.[3] Androstenedione has also been described as producing oestrogenic effects, such as causing abnormal menstrual cycling and progression to endometrial hyperplasia.[4] Androstenedione may therefore cause cellular proliferation in endometrial disorders, however androstenedione production after testosterone treatment was observed in fertile biopsies (figure 5.28) suggesting that androstenedione is produced in the normal endometrium and is not indicative of a proliferative disorder.

An increased concentration of DHT has been previously recorded in breast cancers[5,6] and it has been shown to cause proliferation and progression of prostate cancers.[7] DHT has also been shown to affect cellular proliferation in normal endometria by Ito

and colleagues,[8] and is described as being a more potent androgen than testosterone in both the normal and cancerous endometria. DHT may therefore cause cellular proliferation and/or progression of endometrial disorders which produce DHT, (this would include the cell lines Ishikawa, HEC-1A, HEC-1B, (COV434) and endometria from women with endometriosis, PCOS, ovarian cysts, endometrial polyps and endometrial hyperplasia).

The role of androsterone in the endometrium has not been defined, it is present in serum of normal females[9] and is described as being a seven times weaker androgen than testosterone.[10] It was essentially the reaction end product in these experiments, and was produced via DHT or androstenedione following testosterone treatment.

Further investigations into the roles of specific androgens possibly by specific steroid treatments or selective enzyme inhibition may elucidate their roles in endometrial disorders and cancers.

7.3 Aromatase expression and oestrogen production in endometrial cell lines and biopsies

Several studies of steroid metabolism in breast cancer have lead to the hypothesis that in endometrial cancer and other endometrial disorders where aromatase is expressed an increase in oestradiol production may contribute to cellular proliferation.[11,12] When investigating the endometrial cell lines Ishikawa, HEC-1A, HEC-1B and RL95-2 following testosterone treatment it was therefore expected that oestradiol would be produced via the aromatase enzyme. This would be confirmed by increased oestradiol and oestrone concentration recorded by mass spectrometry and QRT-PCR confirming aromatase expression. The ovarian granulosa cell line COV434 was included as a positive control which highly expressed aromatase and so was expected to produce large concentrations of oestradiol (and oestrone) after testosterone treatment.

The results obtained did not fit this hypothesis, oestradiol and oestrone were not recorded as major metabolites of testosterone after treatment of any cell line. A range of aromatase expressions were recorded in the endometrial cell lines

suggesting that irrespective of aromatase expression little or no oestrogen production occurred after testosterone treatment.

From the combination of mass spectrometry (chapter 5) with enzyme expression (chapter 6) it was possible to conclude that the major route of testosterone metabolism was via the androgens androstenedione and/or DHT in correlation with expression of the oxidative 17β-HSDs (2, 4 and 8) or 5AR1 as described previously, this resulted in the focus of this thesis being the determination of testosterone utilisation via androgen production. Oestrogen production was low in comparison, however due to the significant amount of literature dedicated to oestrogen analysis in steroid responsive tissues it was not disregarded.

The preferential production of androgens rather than oestrogens following testosterone treatment could be explained by investigating the reaction mechanisms. Aromatisation of testosterone to oestradiol, or androstenedione to oestrone is a complex multi-stage reaction which requires multiple co-factors and is widely described as the rate limiting step in oestrogen synthesis.[13] In comparison, the conversions of testosterone to DHT or testosterone to androstenedione are simple one step reactions. The affinity that each enzyme has for testosterone or the availability of co-factors in each cell line may also be key to understanding the metabolism routes, for example 5AR1 may have a higher affinity for testosterone than aromatase so in the COV434 cell line which highly expresses both enzymes production of DHT may occur in preference to oestradiol after testosterone treatment, inhibition of 5AR1/2 would confirm this hypothesis.

It was also possible that testosterone treatments resulted in saturation of the aromatase enzyme inhibiting conversion of androgens to oestrogens. Havelock and co-workers described that in environments of high androgen concentration ovarian granulosa cells (in the presence of FSH) converted testosterone to DHT through the 5-α reductases,[14] in preference to aromatisation of oestrogens. This probably occurred in the COV434 cell line which highly expressed aromatase, but oestrogen concentrations did not increase following testosterone treatment (figure 5.26). To our knowledge there is no evidence of testosterone saturation of aromatase in

endometrial cell lines however, previously Thompson and colleagues demonstrated saturation of aromatase in the ovarian cell line 2774 at approximately a 5μM concentration of testosterone,[15] and George and colleagues demonstrated testosterone saturating aromatase in the rat brain at concentrations of 100nM.[16] This could explain the observations of little or no oestrogens detected in the endometrial cell lines following testosterone treatments in these investigations.

Oestradiol and oestrone were detected in both the Ishikawa and COV434 cell lines under basal conditions before testosterone treatment this was due to oestrogens present in the FCS. The concentrations of oestradiol and oestrone decreased in the first eight hours after testosterone treatment of both cell lines, possibly due to conversion to either sulphated oestrogens or other oestrogen analogues (figures 5.10 and 5.26). RL95-2 cells did not produce any oestrogens after testosterone treatment, the concentrations of oestradiol and oestrone remained essentially constant throughout the experiment. At 60 hours there was an increase in aromatase expression in RL95-2 cells (figure 6.11), this was not correlated with increased oestradiol or oestrone concentrations as there were no reaction precursors available (all testosterone had been converted to androsterone through the intermediate androstenedione in the first 36 hours).

Both oestradiol and oestrone were produced by the fertile biopsies following testosterone treatment, suggesting the aromatase enzyme was active in these cells. It is possible that aromatase in the fertile biopsies does not become saturated at the testosterone concentrations used in these experiments and that the essential co-factors for aromatisation were present. These results agree with some recent studies which recorded low levels of oestradiol in the endometria of fertile women,[17] however the majority of past studies have recorded little or no oestrogen production in fertile endometria, detection here may be due to the improved sensitivity of the mass spectrometry system in comparison to the previously used methods of RIA and TLC.[18,19]

The roles of aromatase and oestradiol in progression of endometriosis, endometrial cancer and in endometrial hyperplasia have been widely investigated, with an

increase in both leading to progression of these disorders.[20,21,22] In these investigations it was possible to observe an increase in aromatase expression relative to the fertile group in the majority of endometriosis biopsies (4 of 6 biopsies) and in epithelial and stromal hyperplasia samples (1 biopsy) and in the ovarian cyst (1 biopsy) and endometrial polyp (1 biopsy), this was correlated with increased oestradiol and/or oestrone concentration relative to the fertile group as described in chapter 5 (however concentrations of oestradiol and oestrone due to the FCS recorded throughout these experiments makes positive correlations difficult to determine). These results suggested there may be a role for aromatase and oestradiol (or oestrone) in these disorders, although the major metabolism route was still via DHT and/or androstenedione in correlation with the expression of oxidative HSDs and/or 5AR1.

The majority of work describing endometrial steroid metabolism has been centred on aromatase and oestrogens, the information presented in this thesis suggests that androgens may also play a significant part in the development of endometrial disorders. This hypothesis could not have been reached if oestrogens were added directly to the endometrial cells, addition of an upstream, biologically abundant, steroid was essential to obtain a more complete picture of steroid metabolism in the endometrium.

7.4 Comparison of testosterone metabolism from fertile endometrial biopsies to established cell lines

Enzyme expression in the cell lines/biopsies which produced similar steroid profiles was compared to confirm important enzymes which result in flux through specific steroid pathways. This comparison was also completed to determine the enzymes whose expression does not affect the steroid profile, together these results elucidated and eliminated enzyme targets.

Endometrial cancer cell lines are often used as models to investigate endometrial function, as a result of these experiments it was shown that certain cell lines have similar characteristic steroid profiles to specific endometrial pathologies (chapter 5). For example the RL95-2 cell line and the fertile biopsies produced a similar

androgen profile after testosterone treatment, which was correlated with similar expression of a number of enzymes outlined in figure 7.5.

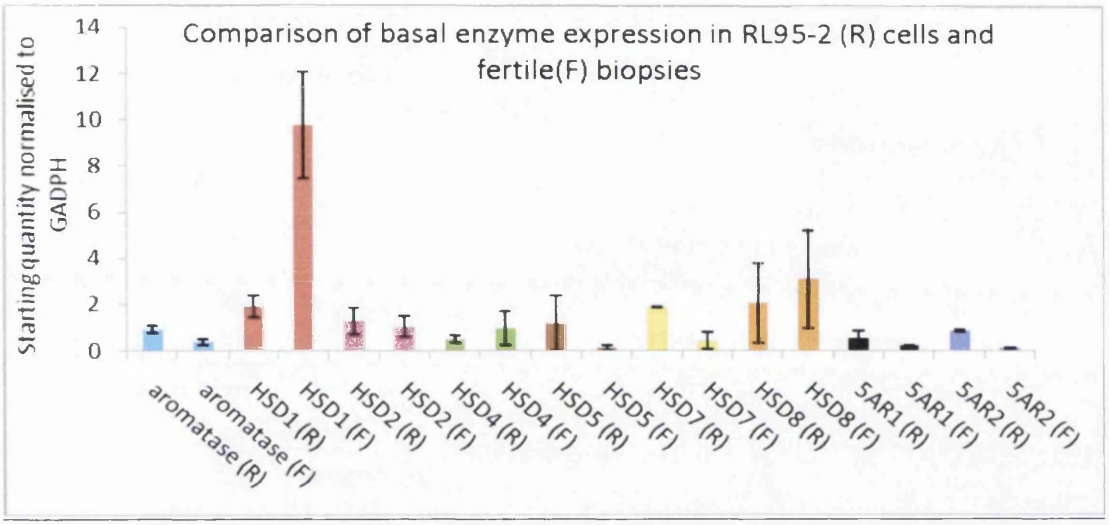

Fig 7.5: Comparison of basal expression levels of nine steroid converting enzymes in the RL95-2 cell line and 4 averaged fertile biopsies. Cells were grown in specific media outlined in chapter 2.4. Expression of all enzymes was calculated by RT-PCR with the use of specific primers as described in chapter 2.6.

Expression of a number of enzymes was comparable in RL95-2 cells and fertile biopsies, (HSD2, HSD4, HSD8, 5AR1) which resulted in the similar route of testosterone utilisation. If an investigator desired to study steroid metabolism in the fertile endometrium this cell line would be an ideal choice, however it should be noted that the oestrogen profiles differ possibly due to the reasons outlined previously (chapter 7.3).

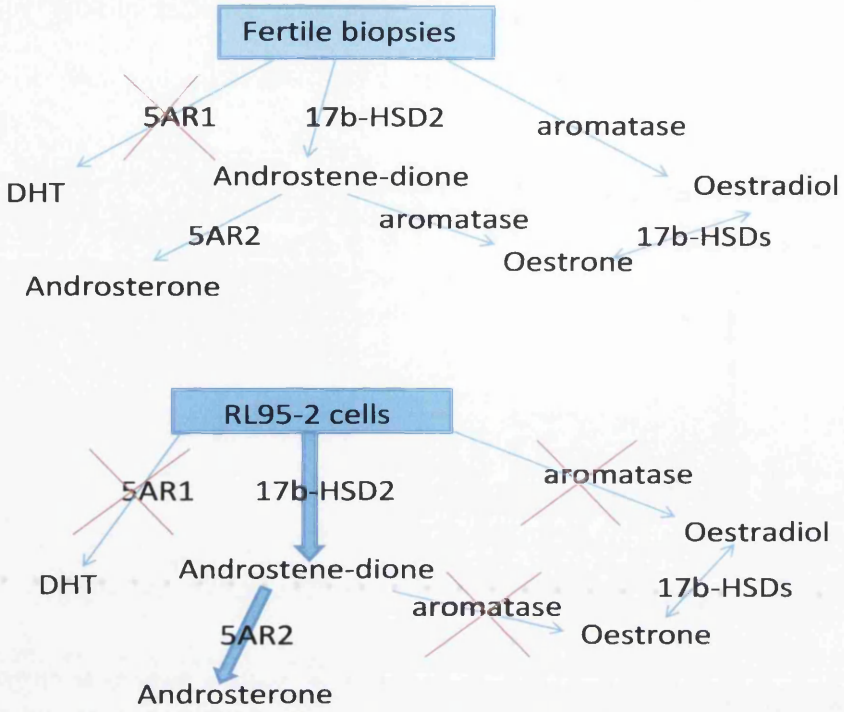

Fig 7.6: Alteration in routes of testosterone metabolism from fertile biopsies to RL95-2 cells. An arrow with a red cross indicates reaction was not occurring, increased arrow size indicates reaction route was increased relative to the fertile biopsies. Enzymes which catalyse each conversion are recorded on each arrow.

The route of androgen metabolism was similar in fertile biopsies and RL95-2 cells. Increased expression of HSD2, 4, 8 and 5AR2 in RL95-2 cells relative to the fertile biopsies was correlated to increased concentrations of androstenedione and androsterone after testosterone treatment suggesting these are important enzymes involved in these conversions. Testosterone was converted to oestradiol in the fertile biopsies but this was not recorded in RL95-2 cells.

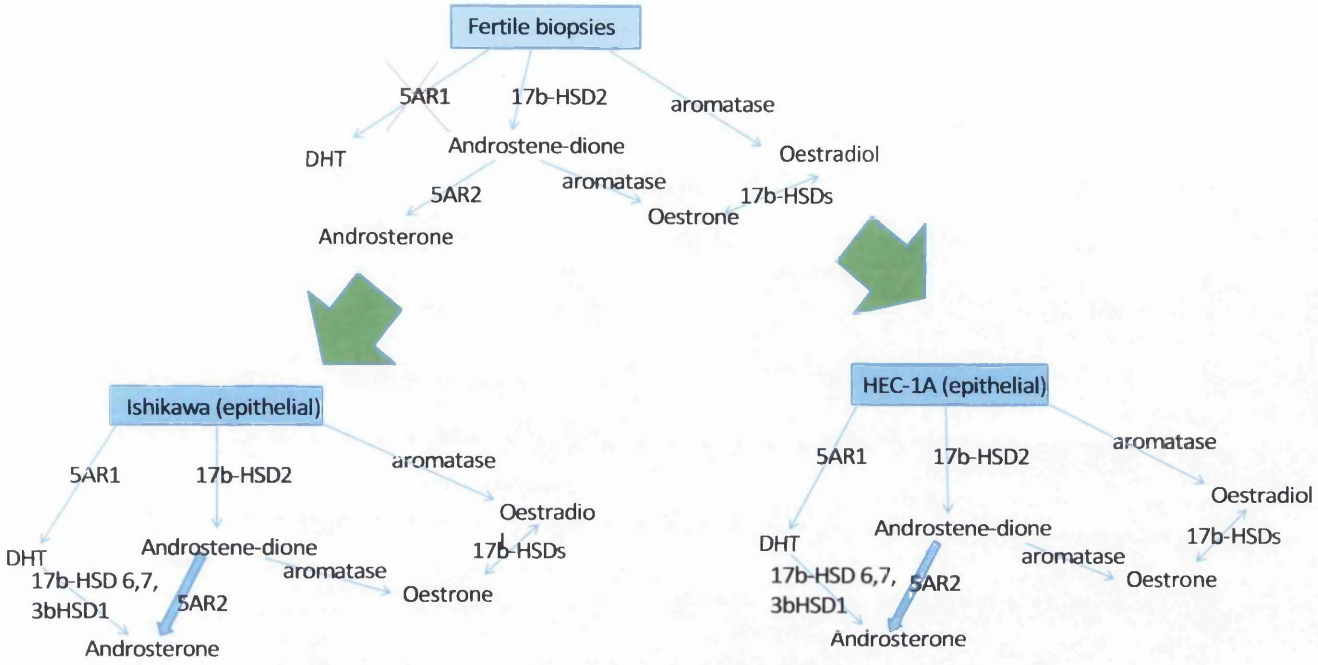

Fig 7.7: Alteration in routes of testosterone metabolism from stromal fertile biopsies to Ishikawa and HEC-1A cells. An arrow with a red cross indicates reaction was not occurring, increased arrow size indicates reaction route was increased (relative to the fertile biopsies). Enzymes which catalyse each conversion are recorded on each arrow.

There were alterations in testosterone metabolism from fertile biopsies to HEC-1A and Ishikawa cells as illustrated by figure 7.7. Production of DHT in HEC-1A and Ishikawa cells, (which was not observed in fertile biopsies) was correlated with increased expression of 5AR1 relative to the fertile biopsies figure 7.3. HSD2, HSD4 and HSD8 were expressed in both cell lines, which was correlated with the production of androstenedione suggesting these enzymes were involved in this conversion. The HEC-1A and Ishikawa cell lines demonstrated increased androsterone concentration after testosterone treatment which was linked to increased expression of 5AR2 relative to the fertile biopsies.

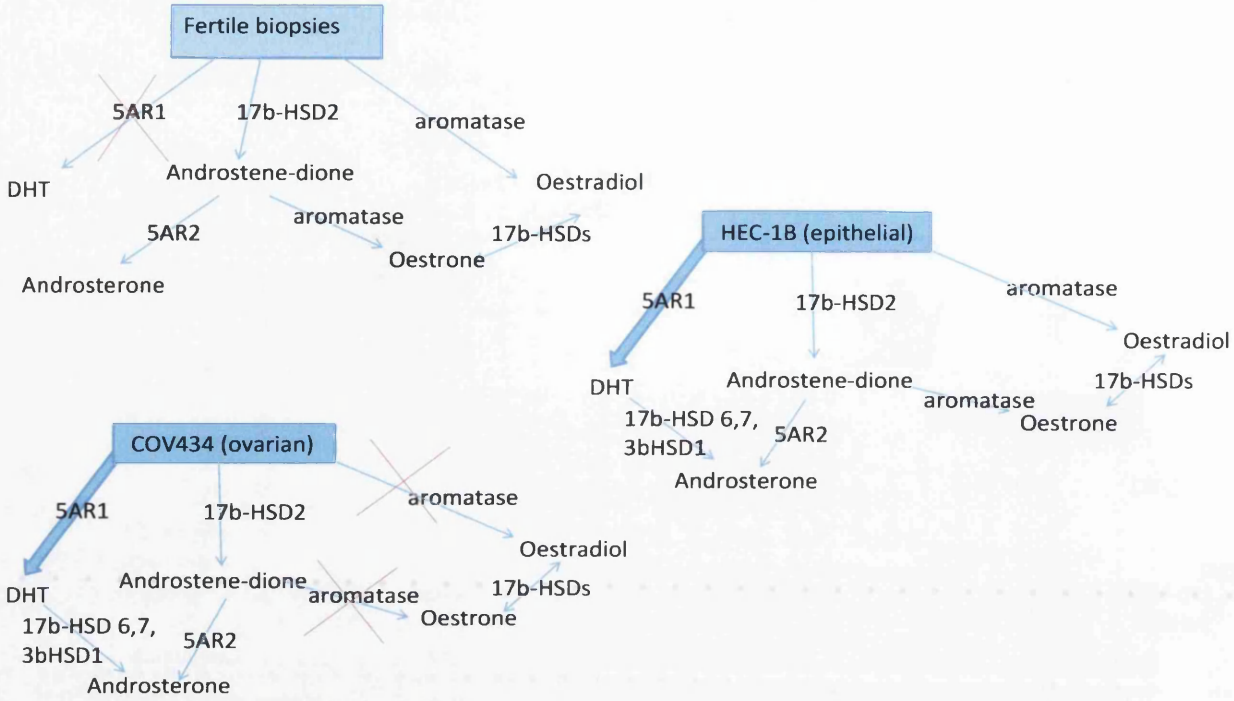

Fig 7.8: Alteration in routes of testosterone metabolism from fertile biopsies to HEC-1B and COV434 cells. An arrow with a red cross indicates reaction was not occurring, increased arrow size indicates this reaction route was increased (relative to the fertile biopsies). Enzymes which catalyse each conversion are recorded on each arrow.

There were alterations in testosterone metabolism from fertile biopsies to HEC-1B and COV434 cells as illustrated by figure 7.8. In COV434 and HEC-1B cells androstenedione was still produced following testosterone treatment but at a lower concentration than by the fertile biopsies. This was correlated to reduced expression of HSD2 relative to the fertile biopsies (figure 7.3). There was some conversion of androgens to oestrogens in HEC-1B cells although the major route of testosterone metabolism was through DHT in association with high expression of 5AR1 (figure 7.3).

7.5 Comparisons of cell lines with similar steroid profiles

Basal enzyme expression of the nine steroid converting enzymes under investigation was compared in cell lines with similar testosterone metabolism routes (HEC-1B and COV434, Ishikawa and HEC-1A), this was completed to determine enzymes which are important (and irrelevant) for a similar testosterone metabolism pathway.

The major route of testosterone metabolism in COV434 and HEC-1B cells was through DHT which was correlated with high expression of 5AR1 relative to the fertile biopsies.

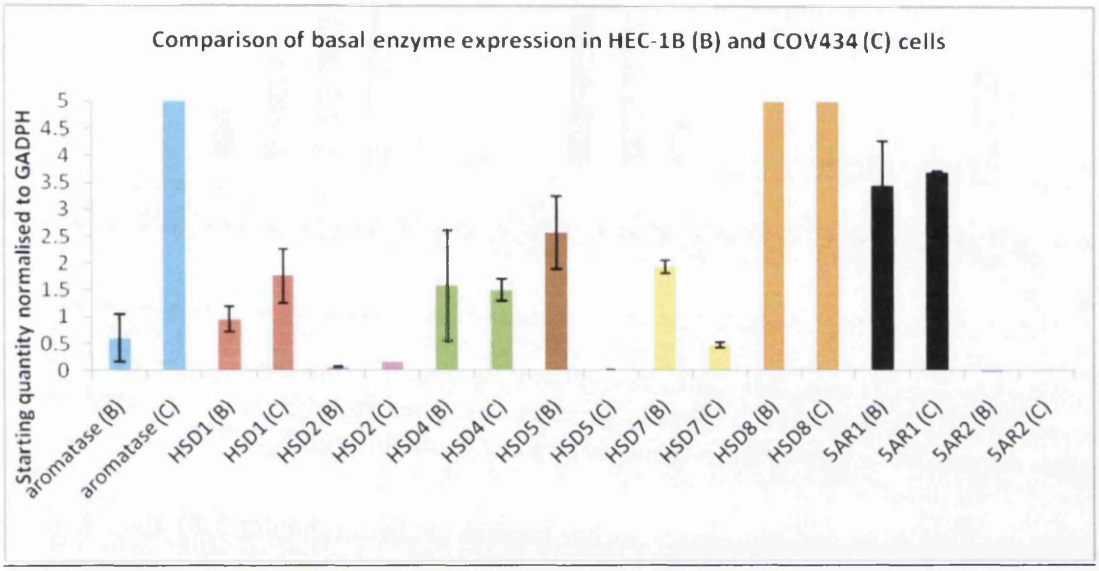

Fig 7.9: Comparison of basal expression of steroid converting enzymes in COV434 and HEC-1B cells. Each cell line was grown in specific medium (chapter 2.4) harvested and RNA extracted. Specific primers described in table 2.6 were used to establish expression levels of steroid converting enzymes through RT-PCR.

HEC-1B and COV434 cells demonstrated similar steroid metabolism profiles and exhibited low (similar) expression of 5AR2, midpoint expression of HSD4, and high expression of 5AR1 and HSD8 under basal conditions relative to the other cell lines (figure 7.9). The difference in expression of HSD2 and HSD8 (both higher in COV434) was correlated with the higher concentration of androstenedione recorded in COV434 cells suggesting these enzyme were responsible for androstenedione production. There were differences in the expression of HSD1 and HSD2, both were higher in COV434. There was significantly increased expression of HSD5 (P= 0.019) and HSD7 (P= 0.000) in HEC-1B cells in comparison to COV434. When attempting to correlate the higher expression of HSD5 and HSD7 in HEC-1B cells to steroid concentration no associations were apparent, suggesting these enzymes were not responsible for production of any of the steroids detected in these experiments.

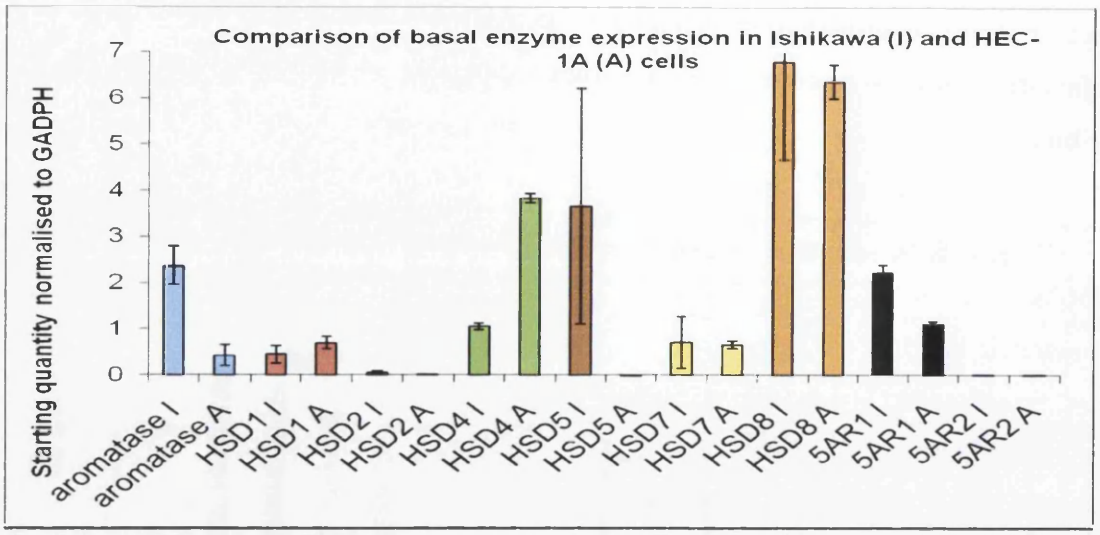

Fig 7.10: Comparison of basal expression of steroid converting enzymes in Ishikawa and HEC-1A cells. Each cell line was grown in specific medium (chapter 2.4) harvested and RNA extracted. Specific primers described in table 2.6 were used to establish expression levels of steroid converting enzymes through RT-PCR.

Ishikawa and HEC-1A demonstrated similar steroid profiles (chapter 5.8) and basal expression of a number of enzymes was similar, for example both demonstrated low expression of HSD1, HSD2, and 5AR2 (figure 7.10), they also exhibited similar midpoint expression of HSD7, and HSD8 (chapter 6.3), which suggests these were the enzymes which dictated the similar routes of testosterone metabolism recorded in these cells. Figure 7.10 illustrates significant differences in the basal expression of the enzymes aromatase (P= 0.001) and 5AR1 (P= 0.008) both higher in Ishikawa. Expression of HSD5 was also higher in Ishikawa cells. 5AR1 was expressed in Ishikawa cells at twice the amount of HEC-1A cells under basal conditions, which was correlated with approximately twice the amount of DHT produced in Ishikawa cells (maximum of 27.6nM (Ishikawa) compared to a maximum of 11.6nM in HEC-1A cells) again suggesting 5AR1 was involved in the conversion of testosterone to DHT.

While the metabolism of androgens in the Ishikawa and HEC-1A cell lines was similar their oestrogen profiles differed. Initial oestrogen information was not produced by added testosterone, but due to the high concentrations of oestrogens due to the FCS. The concentration of oestradiol and oestrone in the HEC-1A cell line increased at the start of the experiment and then remained essentially constant

throughout the experiment (figure 5.17). The oestrone concentration in the Ishikawa cell line decreased in the first 8 hours then remained constant throughout the experiment (figure 5.10). Oestradiol concentration decreased in the Ishikawa cell line from the high serum concentrations at time zero to a much reduced concentration at 72 hours (figure 5.10). Castagnetta[23] and co-workers investigated oestradiol metabolism in the Ishikawa and HEC-1A cell lines, Ishikawa cells were demonstrated to convert the majority of added oestradiol into sulphated oestrogens and other oestrogen derivatives in preference to oestrone. This agrees with the observed decrease in oestradiol concentration in the Ishikawa cell line investigated in this thesis. HEC-1A cells inter-convert the majority of added oestradiol to oestrone (or reverse) through the 17β-HSD enzymes, agreeing with the constant concentrations of the two oestrogens recorded in these experiments.

The differences in oestrogen metabolism in these cell lines was related to different expression of the HSD isoforms, HSD4 (oestradiol to oestrone) and HSD5 (oestrone to oestradiol) (figure 7.11). A significantly higher expression of HSD4 (P= 0.038) was recorded in HEC-1A cells in comparison to Ishikawa cells. These results were supportted by Castagnetta and colleagues who determined that Ishikawa cells demonstrated higher expression of the HSD5 in comparison to HEC-1A cells.[24] Higher expression of HSD4 in HEC-1A cells was also correlated with higher concentrations of androstenedione (from testosterone).

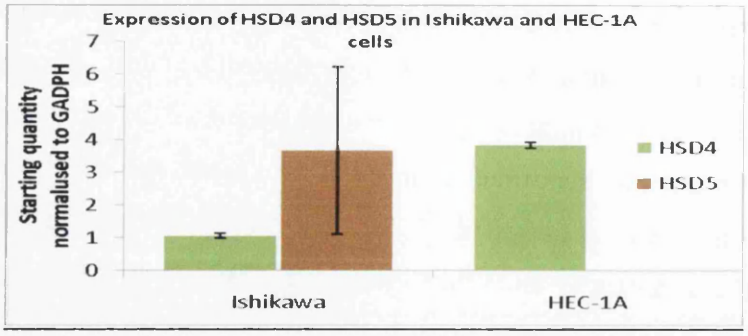

Fig 7.11: Comparison of basal expression of HSD4 (green) and HSD5 (brown) in Ishikawa and HEC-1A cell lines. Each cell line was grown in specific medium (chapter 2.4) harvested and RNA extracted. Specific primers for HSD4 and HSD5 described in table 2.6 were used to establish expression levels of steroid converting enzymes through RT-PCR.

Irrespective of the metabolism of FCS originated oestradiol and oestrone to their reaction end products, aromatase can still act to convert the precursors, testosterone or androstenedione to the oestrogens, oestradiol and oestrone. Possible correlations between expression of aromatase and oestrogen concentration was observed in both Ishikawa and HEC-1A cell lines is discussed later (figures 7.14 and 7.16).

7.6 Changes in enzyme expression combined with steroid profiles for endometrial cell lines and biopsies (and an ovarian cell line) following testosterone treatment

Following addition of testosterone to the cell lines and biopsies the steroid-enzyme relationships described previously were further investigated by looking over a longer time course. Enzyme expression at a number of time points throughout a 72 hour period (as described in chapter 6), was combined with steroid profiles produced in chapter 5 to determine if any changes in enzyme expression could be correlated with a change in the steroid profile.

This allowed observations of any relationships between changing expression and changes in steroid concentration following testosterone treatment.

The enzymes and steroids were chosen because;

1. they have been shown to be important in DHT or androstenedione metabolism (HSD2, HSD4, HSD8, 5AR1),

2. they exhibited a significant increase in fold expression ($P < 0.05$) after testosterone treatment relative to basal expression and/or,
3. they were involved in oestrogen synthesis (aromatase).

The changes in expression levels of the specific enzyme(s) and the changes in steroid concentration(s) were combined together. The histogram on each graph represents enzyme expression at each time point (relative to GADPH) after testosterone treatment. Enzyme expression was normalised to 1 at time zero allowing expression changes relative to basal expression levels to be observed. The scatter graph (with smooth lines joining each data point) and scale on the right of each graph represents the concentration of that steroid(s). Androgen concentration was represented as a ratio to the internal standard methyl-testosterone, (to simplify the graphs the axes are just labelled as concentration). Oestrogen concentration was represented by peak area which is directly proportional to concentration. The combination of these two data sets onto the same graph provided a method for observing correlations between changes in enzyme expression and steroid concentration(s).

7.6.1 Correlations between enzyme expression and steroid concentrations in the Ishikawa cell line after testosterone treatment

Ishikawa cells exhibited high basal expression of HSD5 relative to all the other cell lines. The enzymes which demonstrated significant changes relative to basal expression after testosterone treatment were 5AR1 ($P = 0.041$ at 40 hours) and HSD8 ($P < 0.04$ at 40 and 48 hours). Relationships between enzyme expression and steroid concentration were determined.

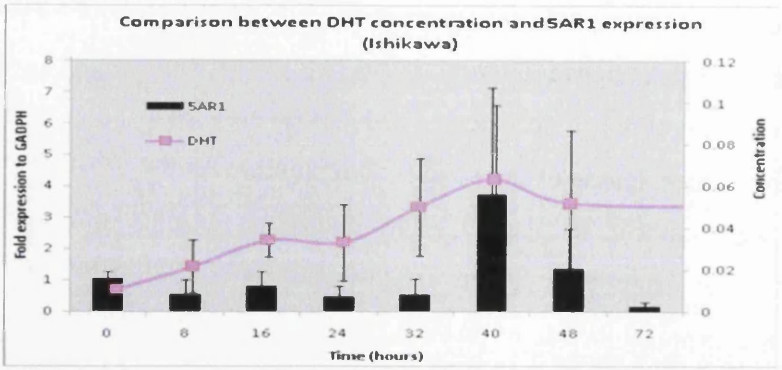

Fig 7.12: Correlation between 5AR1 expression and DHT concentration in Ishikawa cells over 72 hours after addition of a 100nM testosterone media solution. Ishikawa cells were grown in specific medium (chapter 2.4) harvested and RNA extracted. Specific primers outlined in table 2.6 were used to establish 5AR1 expression levels through RT-PCR. DHT concentrations were obtained from the average values of three experiments on the LCQ DECA mass spectrometer using an ESI source in positive mode with a C_{18} reversed phase column with an optimised methanol/water 0.1% acetic acid elution system.

5AR1 catalyses the conversion of testosterone to DHT. It was possible to observe a trend between increasing expression of 5AR1 and increasing concentration of DHT in the Ishikawa cell line (figure 7.12), this suggests 5AR1 was converting testosterone to DHT.

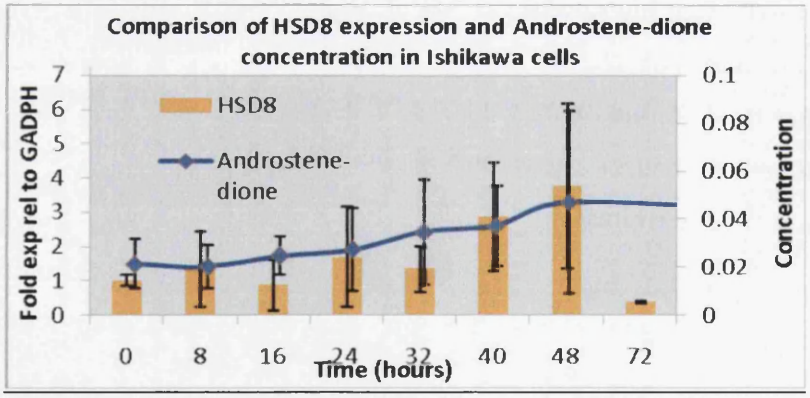

Fig 7.13: Correlations between HSD8 expression and androstenedione concentration in Ishikawa cells over 72 hours after addition of a 100nM testosterone media solution. The Ishikawa cell line was grown in specific medium (chapter 2.4) harvested and RNA extracted. Specific primers outlined in table 2.6 were used to establish HSD8 expression levels through RT-PCR. Androstenedione concentrations were obtained from the average values of three experiments on the LCQ DECA mass spectrometer using an ESI source in positive mode with a C_{18} reversed phase column and an optimised methanol/water 0.1% acetic acid elution system.
HSD8 catalyses the conversion of testosterone to androstenedione. It was possible to observe a trend between increasing concentration of androstenedione and increasing

HSD8 expression in the Ishikawa cell line (figure 7.13), this suggests HSD8 was converting testosterone to androstenedione.

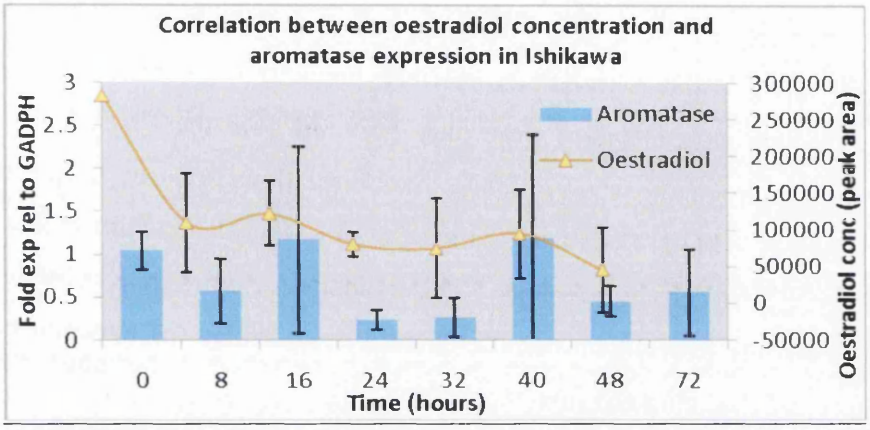

Fig 7.14: Correlations between oestradiol concentration and aromatase expression in Ishikawa cells over 72 hours after addition of a 100nM testosterone media solution. The Ishikawa cell line was grown in specific medium (chapter 2.4) harvested and RNA extracted. Specific primers outlined in table 2.6 were used to establish aromatase expression levels through RT-PCR. Oestradiol concentrations were obtained from the average values of three experiments on the LCQ DECA mass spectrometer using an ESI source in positive mode using a luna phenyl-hexyl column with optimised methanol/water 0.1% formic acid elution system.

Aromatase converts testosterone to oestradiol. Figure 7.14 shows a possible correlation between aromatase expression and oestradiol concentration, however the high concentration of oestradiol (due to FCS) prior to testosterone treatment (0 hours) and the errors associated with aromatase expression make any relationships difficult to determine. This graph is included in this chapter to provide a full picture of testosterone utilisation by the Ishikawa cell line, however oestrogen production was a secondary pathway and the primary focus of this work was to determine the route of testosterone metabolism through androgen production.

7.6.2 Correlations between enzyme expression and steroid concentrations in the RL95-2 cell line after testosterone treatment

The metabolism of testosterone was rapid in RL95-2 cells in comparison to the other cell lines, (the majority of the androgenic end product androsterone was produced after 36 hours). Any initial correlations between testosterone converting enzyme expression and steroid concentration were only be valid over the first 36 hours as after this no reaction precursor was available. No correlations between the changing expression of 5AR2, HSD2, HSD8 or aromatase and steroid concentrations were observed following testosterone treatment. The inclusion of more data points within the first 36 hours of the experiment could elucidate any correlations between steroid concentration(s) and changing enzyme expression.

7.6.3 Correlations between enzyme expression and steroid concentrations in the HEC-1A cell line after testosterone treatment

HEC-1A cells demonstrated the highest relative basal expression of HSD4 in comparison to all other cell lines (figure 6.4). The enzymes which exhibited significant changes in fold expression after testosterone treatment were 5AR2 ($P= 0.025$ at 24 hours) and HSD5 ($P= 0.033$ at 24 hours). High expression of 5AR2 was expected to correlate with decreased concentration of androstenedione, which was observed at 24 and 72 hours (figure 5.15).

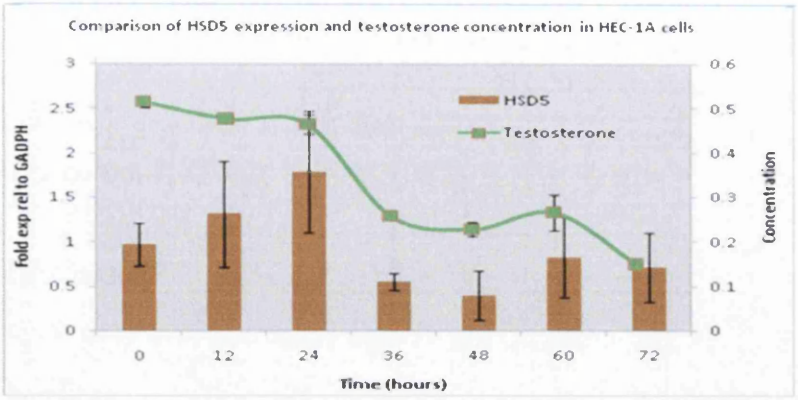

Fig 7.15: Correlation between testosterone concentration and HSD5 expression in HEC-1A cells over 72 hours after addition of a 100nM testosterone media solution. The HEC-1A cell line was grown in specific medium (chapter 2.4) harvested and RNA extracted. Specific primers outlined in table 2.6 were used to establish HSD5 expression levels through RT-PCR. Testosterone concentrations were obtained from average values on the LCQ DECA mass spectrometer using an ESI source in positive mode with a C_{18} reversed phase column and an optimised methanol/water 0.1% acetic acid elution system.

The concentration of testosterone decreased throughout these experiments as it was metabolised to other steroids, (this readily occurred due to the high initial testosterone concentration, and expression of HSD2, 4 8 and 5AR1). HSD5 catalyses the conversion of androstenedione to testosterone. Testosterone concentration increased at 24 and 60 hours in correlation with increased expression of HSD5, suggesting HSD5 was converting androstenedione to testosterone in HEC-1A cells.

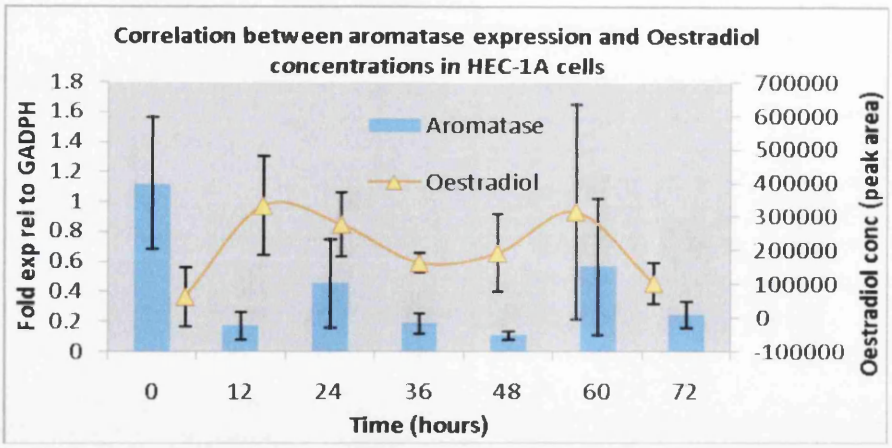

Fig 7.16: Correlation between oestradiol concentration and aromatase expression in HEC-1A cells over 72 hours after addition of a 100nM testosterone media solution. The HEC-1A cell line was grown in specific medium (chapter 2.4) harvested and RNA extracted. Specific primers outlined in table 2.6 were used to establish aromatase expression levels through RT-PCR. Oestradiol concentration was obtained from average values on the LCQ DECA mass spectrometer using an ESI source in positive mode using a luna phenyl-hexyl column with optimised methanol/water 0.1% formic acid elution system.

Aromatase converts testosterone to oestradiol and androstenedione to oestrone. Conversion of testosterone to oestrogens in HEC-1A cells was a secondary process, with the major metabolism route being androgen production, however there was some oestradiol produced as illustrated in figure 7.16. A trend between the increasing concentration of oestradiol and increasing expression of aromatase was observed suggesting aromatase was converting testosterone to oestradiol in HEC-1A cells. Again this graph is included in this chapter to provide a complete picture of testosterone utilisation by the HEC-1A cell line, however oestrogen production was a secondary pathway and the primary focus of this work was to further determine the route of testosterone metabolism which was mainly through androgen production.

7.6.4 Correlations between enzyme expression and steroid concentrations in the HEC-1B cell line after testosterone treatment

HEC-1B cells exhibited the highest basal expression of HSD7 (figure 6.6) and high basal expression of 5AR1 (figure 6.8) relative to the other cell lines. The enzyme which exhibited a significant change in fold expression after testosterone treatment was HSD8 ($P= 0.005$ at 36 hours and $P= 0.003$ at 72 hours figure 6.13).

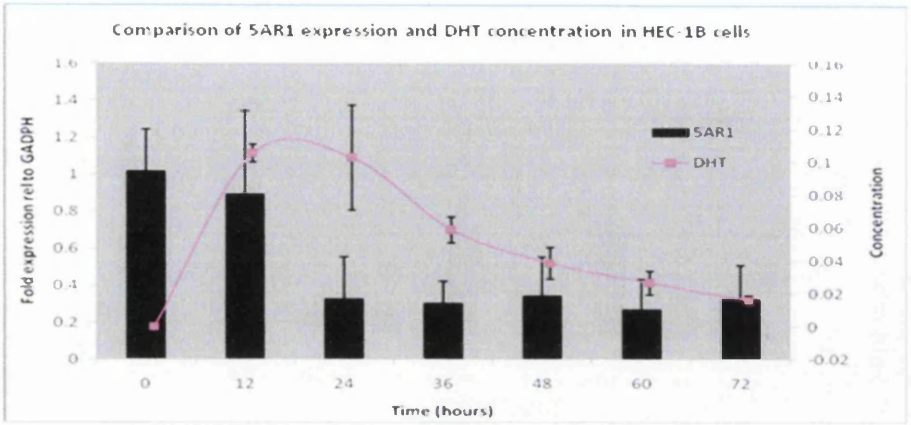

Fig 7.17: Correlations between 5AR1 expression and DHT concentration in HEC-1B cells over 72 hours after addition of a 100nM testosterone media solution. The HEC-1B cell line was grown in specific medium (chapter 2.4) harvested and RNA extracted. Specific primers outlined in table 2.6 were used to establish 5AR1 expression levels through RT-PCR. DHT concentrations were obtained from average values on the LCQ DECA mass spectrometer using an ESI source in positive mode with a C_{18} reversed phase column and an optimised methanol/water 0.1% acetic acid elution system.

5AR1 catalyses the conversion of testosterone to DHT. It was possible to observe a trend between the expression of 5AR1 and concentration of DHT in the HEC-1B cell line (figure 7.17). High expression of 5AR1 in the first 12 hours was correlated to high DHT concentration, after the first 12 hours the expression levels of 5AR1 decreased in correlation with decreasing concentration of DHT this suggests testosterone was converted to DHT by the 5AR1 enzyme in HEC-1B cells.

7.6.5 Correlations between enzyme expression and steroid concentrations in the COV434 cell line after testosterone treatment

The enzymes in COV434 cells which exhibited high basal expression were aromatase, HSD1, HSD8 and 5AR1 (relative to the other cell lines-chapter 6.3). The enzyme which exhibited significant changes in fold expression after testosterone treatment was 5AR1 P= 0.043 (16 hours) P= 0.006 (32 hours) and P= 0.047 (72 hours) as illustrated in figure 6.14.

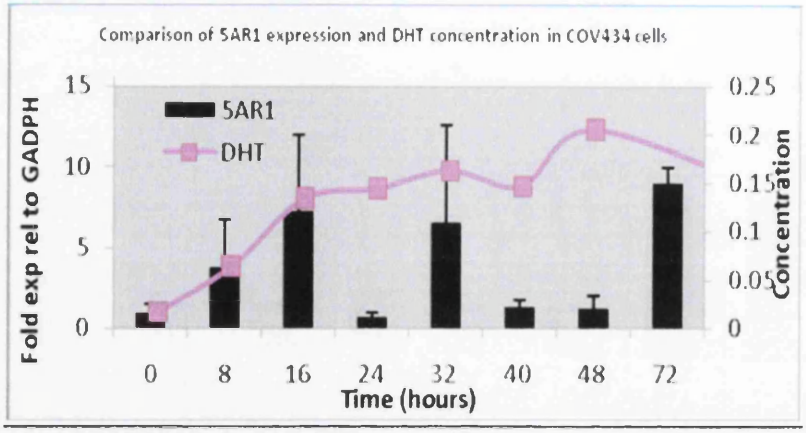

Fig 7.18: Correlation between 5AR1 expression and concentration of DHT in COV434 cells over 72 hours after addition of a 100nM testosterone media solution. The COV434 cell line was grown in specific medium (chapter 2.4) harvested and RNA extracted. Specific primers outlined in table 2.6 were used to establish 5AR1 expression levels through RT-PCR. DHT concentrations were obtained from average values on the LCQ DECA mass spectrometer with an ESI source in positive mode using a C_{18} reversed phase column with an optimised methanol/water 0.1% acetic acid elution system.

5AR1 catalyses the conversion of testosterone to DHT. It was possible to observe a trend between the increasing expression of 5AR1 and increasing concentration of DHT in COV434 cells (figure 7.18) which suggests 5AR1 is converting testosterone to DHT.

7.6.6 Correlations between enzyme expression and steroid concentrations in fertile biopsies following testosterone treatment

In the fertile biopsies the enzymes which exhibited high basal expression were HSD1 and HSD2 (relative to all endometrial disorders except endometriosis). The enzyme 5AR2 exhibited a significant change in expression after testosterone treatment (P= 0.016 at 24 hours) figure 6.37. 5AR2 expression increased at 48 hours which was correlated with a reduction in androstenedione concentration (the reaction precursor) and an increase in androsterone concentration (reaction end product) as illustrated in figure 7.19. High basal expression levels of the oxidative HSDs (HSD2, HSD4 and HSD8) in fertile biopsies was correlated with rapid conversion of testosterone to androstenedione (first 24 hours) with no production of DHT, after this androstenedione was converted into the end products oestrone (and oestradiol) in

correlation with expression of aromatase (at 48 hours) and androsterone in correlation with 5AR2 expression (at 72 hours).

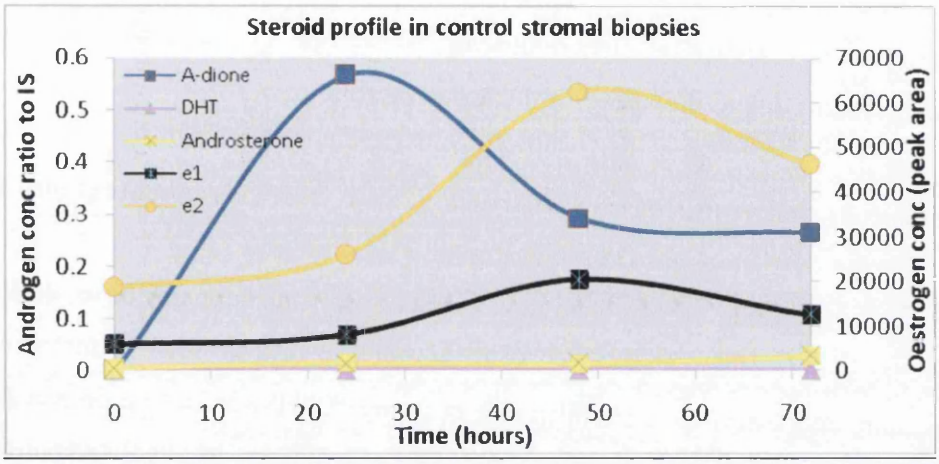

Fig 7.19: Steroid metabolism in stromal biopsies from fertile patients over 72 hours after addition of a 100nM testosterone media solution. Oestrone and oestradiol concentrations were measured as peak areas (right hand axis). Androgen concentration was measured as a ratio to the internal standard (left axis). Results obtained from the average values of four fertile biopsies on the LCQ DECA mass spectrometer using an ESI source in positive mode using either a C_{18} reversed phase column with an optimised methanol/water 0.1% acetic acid elution system (androgens) or a luna phenyl-hexyl column with optimised methanol/water 0.1% formic acid elution system (oestrogens).

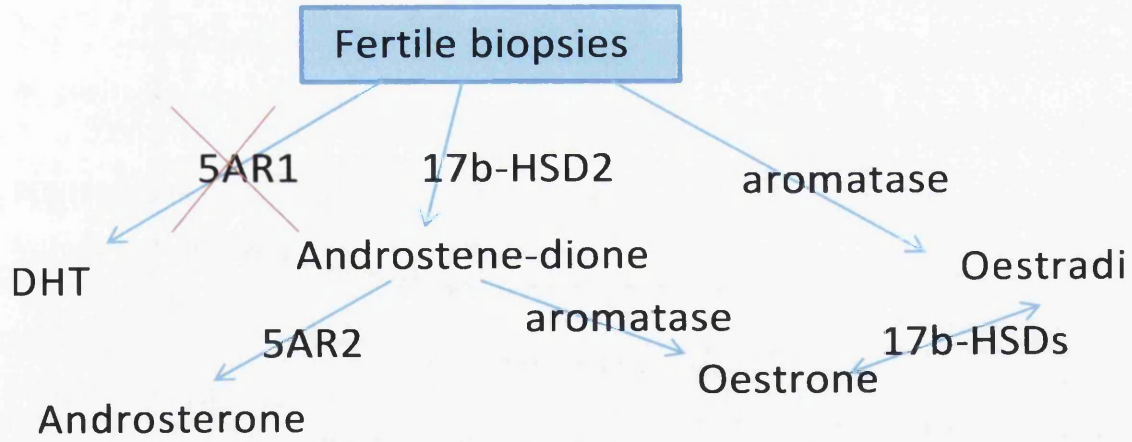

Fig 7.20: Typical metabolism route of testosterone in four fertile biopsies. An arrow with a red cross indicates reaction was not occurring. Enzymes which catalyse each conversion are recorded on each arrow.

The steroid profiles recorded in chapter 5 suggest the majority of oestradiol was produced by the initial conversion of testosterone to androstenedione (which correlates with high expression of HSD2, 4 and 8) followed by conversion to

oestrone (aromatase) and conversion to oestradiol (in correlation to the highly expressed HSD1 enzyme) some oestradiol could also have been produced directly from testosterone through aromatase. There were no correlations between temporal changes in enzyme expression and changes in steroid concentration(s) after testosterone treatment due to the speed of these conversions.

7.6.7 Correlations between enzyme expression and steroid concentrations in unexplained infertility biopsies after testosterone treatment

In comparison to the fertile biopsies the unexplained infertility biopsies have similar enzyme expression (chapter 6.4.5) and steroid profiles for testosterone, androstenedione, androsterone, oestradiol and oestrone (DHT was not be detected at any time). The production of androstenedione was slower in the unexplained infertility biopsies in comparison to fertile biopsies which correlated to lower basal expression of HSD2 and HSD4. The largest change in fold expression relative to time zero in unexplained infertility biopsies was produced with increased expression of 5AR2 at 48 and 72 hours.

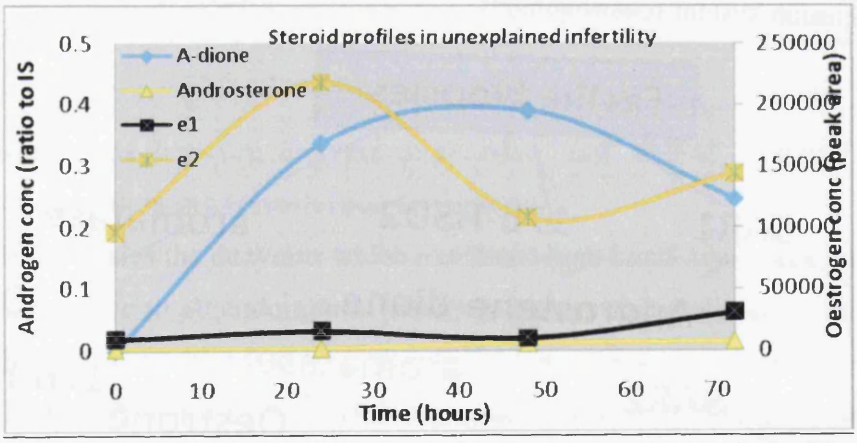

Fig 7.21: Steroid metabolism in stromal cells from unexplained infertility biopsies over 72 hours after addition of a 100nM testosterone media solution. Oestrone and oestradiol concentrations are measured as peak areas (right hand axis). Androgen concentration was measured as a ratio to the internal standard (left axis). Results obtained from the average values of two unexplained infertility biopsies on the LCQ DECA mass spectrometer using an ESI source in positive mode using either a C_{18} reversed phase column with an optimised methanol/water 0.1% acetic acid elution system (androgens) or a luna phenyl-hexyl column with optimised methanol/water 0.1% formic acid elution system (oestrogens).

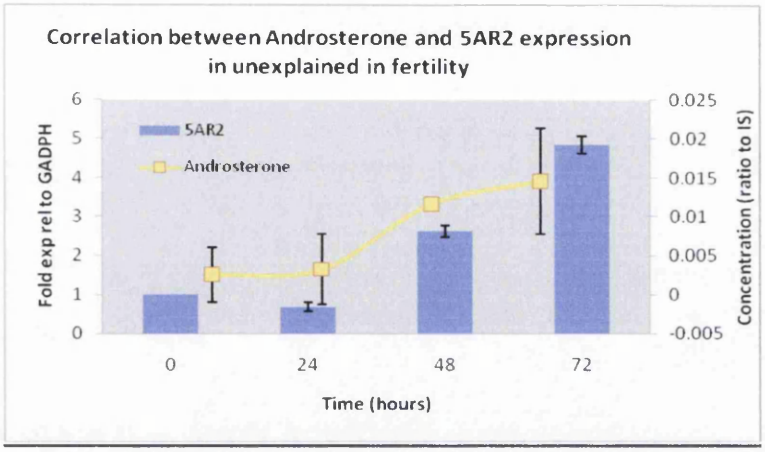

Fig 7.22: Correlation between 5AR2 expression and androsterone concentration in unexplained infertility biopsies over 72 hours after addition of a 100nM testosterone media solution. The unexplained infertility biopsies were grown in specific medium (chapter 2.4) harvested and RNA extracted. Specific primers outlined in table 2.6 were used to establish 5AR2 expression levels through RT-PCR. Androsterone concentrations were obtained from the average values of two experiments on the LCQ DECA mass spectrometer using an ESI source in positive mode with a C_{18} reversed phase column and an optimised methanol/water 0.1% acetic acid elution system.

5AR2 converts the androgen androstenedione to androsterone through the intermediate androstane-dione. It was possible to observe a trend between the increasing expression of 5AR2 and increasing concentration of androsterone in the unexplained infertility biopsies (figure 7.22) suggesting androstenedione was converted to androsterone via 5AR2 (the conversion through the intermediate was also rapid).

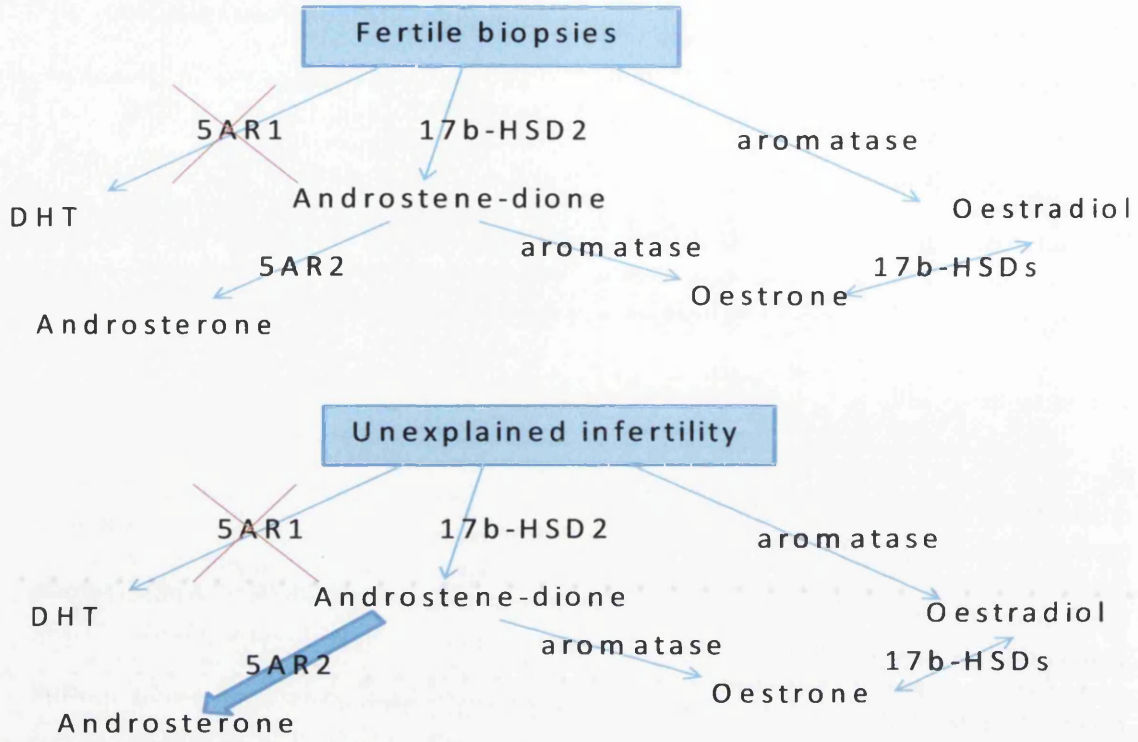

Fig 7.23: Alteration in routes of testosterone metabolism from fertile biopsies to unexplained infertility biopsies. An arrow with a red cross indicates reaction was not occurring, increased arrow size indicates this reaction route was increased (relative to the fertile biopsies). Enzymes which catalyse each conversion are recorded on each arrow.

The metabolism route of testosterone was similar in fertile and unexplained infertility biopsies, as illustrated by figure 7.23. Unexplained infertility biopsies and fertile biopsies produced oestrone and/or oestradiol following testosterone treatment, in correlation with aromatase expression suggesting that aromatase was converting either androstenedione to oestrone and/or testosterone to oestradiol in these biopsies. The similar enzyme expression and steroid profiles again suggested the reason for infertility in these women was not related to steroid metabolism in their endometria.

7.6.8 Correlations between enzyme expression and steroid concentrations in endometriosis biopsies after testosterone treatment

Trends in basal enzyme expression in relation to steroid metabolism were difficult to determine in endometriosis biopsies possibly due to the progression (severity) of the disorder resulting in different levels of enzyme expression as described in chapter 6.4.

The enzymes which exhibited high basal expression relative to the fertile biopsies in the majority of endometriosis biopsies were aromatase, HSD1, HSD5, HSD7, 5AR1(chapter 6.4). Endometriosis biopsies show variations in basal expression of steroid converting enzymes (chapter 6.4), however when investigating temporal changes in enzyme expression after testosterone treatment the endometriosis biopsies were grouped together, this was completed as the basal expression was normalised to one, resulting in only large changes in enzyme expression relative to this being observed. HSD2 exhibited the largest changes in fold expression after testosterone treatment relative to basal expression.

Endometriosis biopsies produced DHT, androstenedione, androsterone, oestradiol and oestrone after testosterone treatment, as described in chapter 5.9. Again the route of synthesis of these steroids was associated with the expression of three specific enzymes, production of androstenedione in correlation with HSD2 expression (HSD2 expression was recorded in half of the endometriosis biopsies figure 6.17), DHT in correlation with 5AR1 expression (recorded in 4 of the 6 biopsies) and production of oestradiol and oestrone associated with aromatase expression. This suggests these enzymes are involved in the utilisation of testosterone in endometria from women with endometriosis.

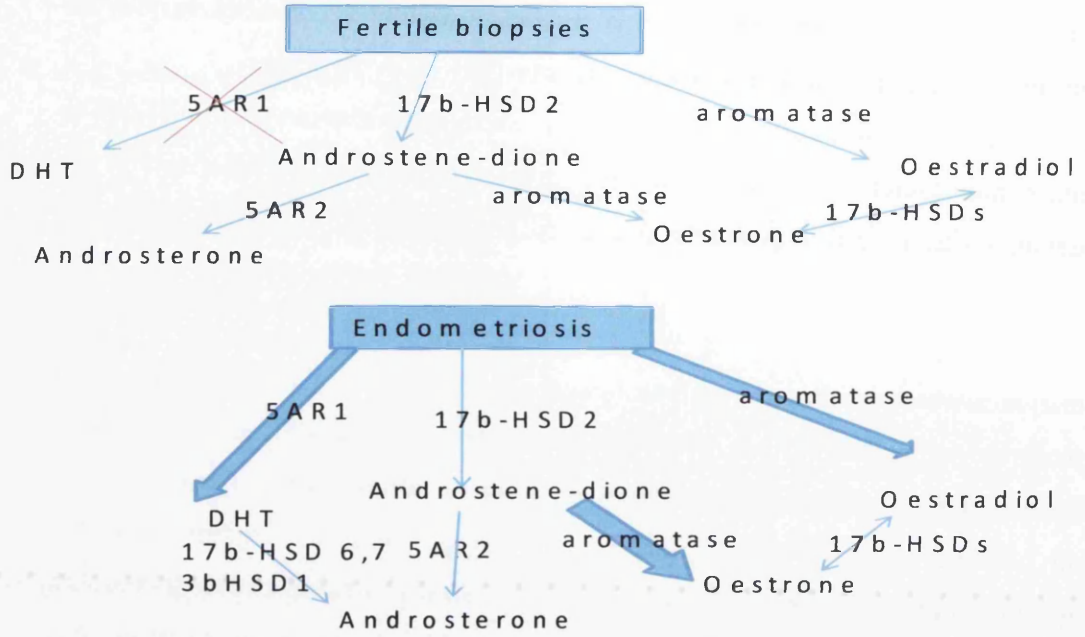

Fig 7.24: Alteration in routes of testosterone metabolism from fertile biopsies to endometriosis biopsies. An arrow with a red cross indicates reaction was not occurring, increased arrow size indicates this reaction route was increased (relative to the fertile biopsies). Enzymes which catalyse each conversion are recorded on each arrow.

There were significant differences in the route of testosterone metabolism in fertile biopsies in comparison to endometriosis biopsies. The presence of androstenedione, DHT, oestradiol and oestrone suggested three active pathways for testosterone metabolism, two of which may cause proliferation and/or progression of endometriosis in these patients due to the production of the potent oestrogen oestradiol or potent androgen DHT, these pathways are outlined in figure 7.24.

The development of endometriosis is characterised by an increase in localised steroid hormones and inflammation. Localised changes in inflammatory responses and steroid production may give rise to increased risk of cancer development in tissues that are steroid dependent such as the endometrium, breast, and ovary. Ness and colleagues described the altered immune function and steroid production in women with endometriosis, they describe a number of growth factors and cytokines which act to promote endometriosis growth and progression.[25] These growth factors can act on specific enzymes to alter expression for example SF-1 has been shown to be up-regulated in endometriosis which stimulates aromatase expression resulting in an

increase in oestrogen concentration. It is possible that a number of steroid converting enzymes are up-regulated due to expression of these growth factors or cytokines in the endometrium of women with endometriosis, such as HSD2, aromatase and 5AR1 (chapter 6.4.1). The role each of these enzymes has on progression of endometriosis requires further investigation with the use of inhibition studies.

The role of 5AR1 and its major product DHT is especially important as there is some disagreement as to its role in endometriosis. Androgens have been used to treat endometriosis possibly via regulation of pituitary gonadotropin expression which reduces oestrogen production. However an increase in some androgens (testosterone and androstenedione) would lead to a higher conversion of androgens to oestrogens.

In these endometriosis biopsies production of oestrogens is a secondary process to production of DHT when testosterone was added. This could be due to the regulation of aromatase conversion by the androgen DHT, or could be due 5AR1 having a higher affinity for testosterone than aromatase (5AR1 and aromatase are in direct competition for the same substrate). To decide which of these hypothesis are correct further experiments are required such as inhibition of 5ARs with specific inhibitors or siRNA, if enzyme affinity was the reason for no production of oestrogens inhibition of 5AR1 and 5AR2 should result in an increase in oestrogen concentrations.

7.6.9 Correlations between enzyme expression and steroid concentrations in endometrial biopsies from patients with PCOS following testosterone treatment

The enzyme which exhibited the highest basal expression relative to the fertile biopsies in the PCOS biopsies was HSD7 (figure 6.29). Large changes in fold expression in PCOS biopsies were observed after testosterone treatment with the enzymes HSD7 and HSD8 (figure 6.40), however there were no observed correlations between changes in steroid concentration and changes in expression of HSD7 or HSD8.

The route of testosterone metabolism in PCOS biopsies was associated with the expression of four enzymes, HSD2, HSD8 (production of androstenedione), 5AR1

(production of DHT) and to a lesser degree aromatase (conversion of androgens to oestrogens). Production of DHT in these biopsies was similar to COV434 cells and androstenedione production was similar to fertile biopsies, demonstrating both sides of the androgen metabolism pathway were active. Testosterone metabolism was altered from fertile to PCOS biopsies as illustrated by figure 7.25, production of the potent androgen DHT and potent oestrogen oestradiol may cause further problems in the endometria of PCOS patients, inclusion of more PCOS biopsies is required to confirm these preliminary observations.

7.6.10 Correlations between enzyme expression and steroid concentrations in an endometrial biopsy from a patient with an ovarian cyst following testosterone treatment

In the ovarian cyst biopsy there was high basal expression of aromatase relative to the fertile biopsies (figure 7.4), however the high concentrations of both oestradiol and oestrone in the cell media at time zero make it impossible to determine any correlations between oestrogen concentration and aromatase expression. There were large changes in the fold expression of HSD5, HSD7, HSD8, 5AR1 and 5AR2 at 48 hours (figure 6.41). These large expression changes in this biopsy at 48 hours may be due to experimental error, due to the very high changes observed for each enzyme. There were some corresponding steroid increases-androstenedione and androsterone concentrations increased at 48 hours and DHT was synthesised at this time, however due to the number of enzymes which exhibited high expression specific correlations were impossible to determine.

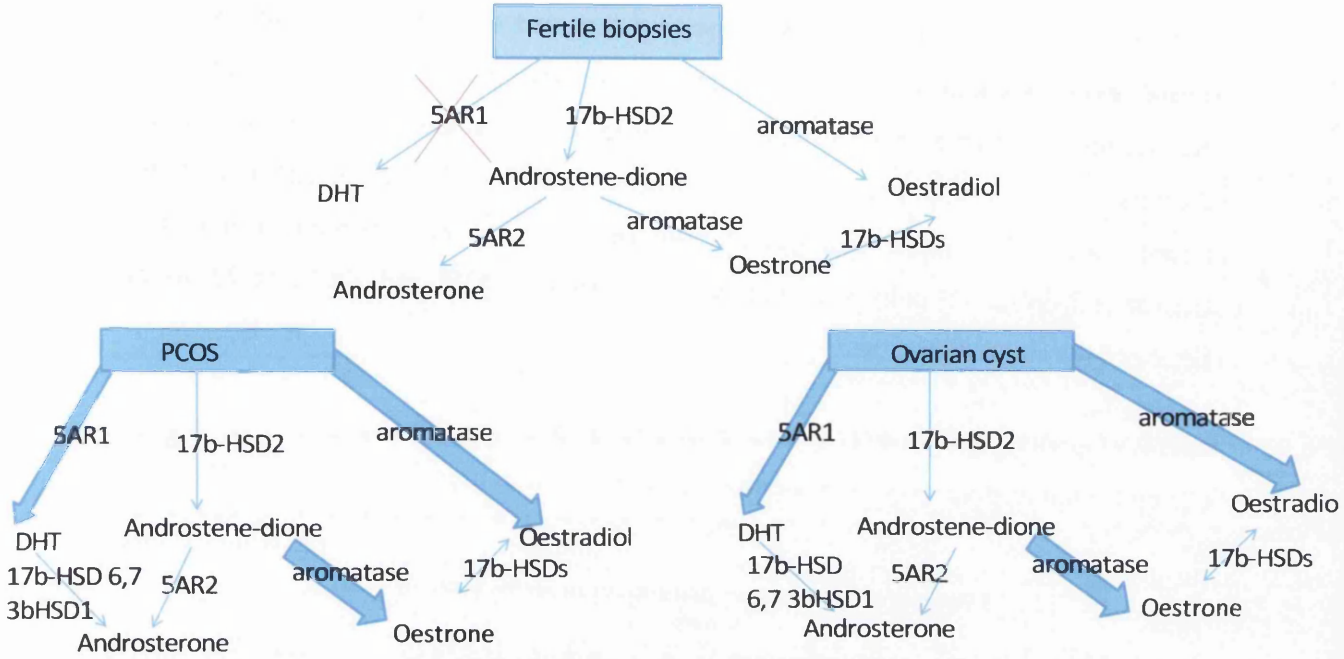

Fig 7.25: Alteration in routes of testosterone metabolism from fertile biopsies to endometrial biopsies from women with PCOS and ovarian cysts. An arrow with a red cross indicates reaction was not occurring, increased arrow size indicates this reaction route was increased (relative to the fertile biopsies). Enzymes which catalyse each conversion are recorded on each arrow.

The ovarian cyst and PCOS biopsies metabolised testosterone through similar pathways. The principal change in testosterone metabolism from fertile to PCOS or ovarian cyst biopsies was the production of DHT as illustrated in figure 7.25. In the ovarian cyst biopsy increased aromatase expression suggested increased oestradiol production, but corresponding steroid information was not available due to the high oestrogens recorded due to FCS.

Both PCOS biopsies exhibited low basal expression of HSD2 and 5AR1 relative to the fertile biopsies. In both PCOS biopsies however aromatase expression was highest followed by 5AR1, and HSD2 exhibited the lowest basal expression (relative to each other), this could explain the production of oestradiol, DHT and androstenedione observed after testosterone treatment.

7.6.11 Correlations between enzyme expression and steroid concentrations in a biopsy from a patient with endometrial hyperplasia after testosterone treatment

The endometrial hyperplasia biopsy was split into stromal and epithelial cells, both cell types produced high basal expression of aromatase relative to the fertile biopsies (figure 7.4). The largest changes in fold expression were observed in both the stromal and epithelial cells with the enzymes HSD5, 5AR1 and 5AR2 at 72 hours (figures 6.42 and 6.43).

7.6.11.1 Epithelial endometrial hyperplasia biopsy

The epithelial hyperplasia biopsy exhibited high basal expression of aromatase.

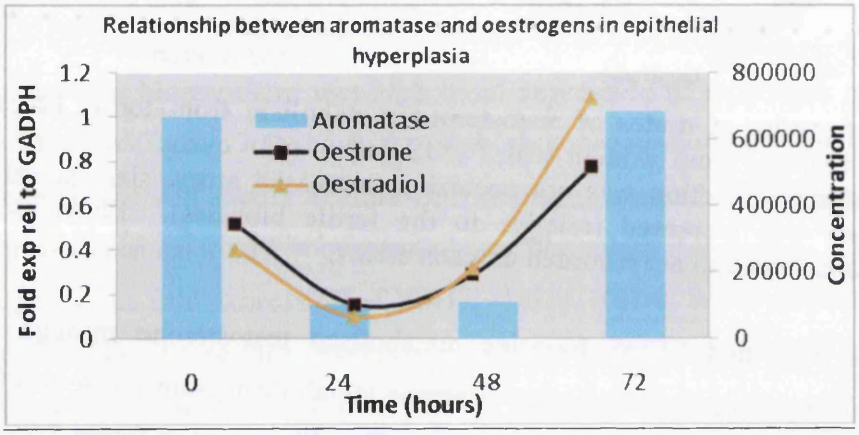

Fig 7.26: Correlation between oestrone and oestradiol concentrations and aromatase expression in an epithelial hyperplasia biopsy over 72 hours after addition of a 100nM testosterone media solution. The epithelial hyperplasia biopsy was grown in specific medium (chapter 2.4) harvested and RNA extracted. Specific primers outlined in table 2.6 were used to establish aromatase expression levels through RT-PCR. Oestrone and oestradiol concentrations were obtained using a luna phenyl-hexyl column with optimised methanol/water 0.1% formic acid elution system on the LCQ DECA mass spectrometer using an ESI source in positive mode.

Aromatase converts testosterone to oestradiol and androstenedione to oestrone. It was possible to observe a trend between increased oestradiol and oestrone concentrations and increasing expression of aromatase in the endometrial epithelial hyperplasia biopsy, suggesting aromatase was converting testosterone to oestradiol and androstenedione to oestrone in this biopsy (figure 7.26).

7.6.11.2 Stromal endometrial hyperplasia biopsy

The stromal cells from a woman with endometrial hyperplasia exhibited high basal expression of 5AR1, HSD7 and aromatase (relative to the fertile biopsies). Largest fold expression changes were observed with the enzymes HSD5, 5AR1 and 5AR2, all 72 hours after testosterone treatment.

The conversion of testosterone to DHT in the stromal biopsy from a woman with atypical endometrial hyperplasia was correlated with expression of 5AR1, and production of oestradiol was correlated with aromatase expression, production of androstenedione was a minor pathway which was correlated with low expression of HSD2, 4 and 8 relative to the fertile biopsies. Androsterone and oestrone were the reaction end products which were produced via a number of pathways illustrated in figure 7.27.

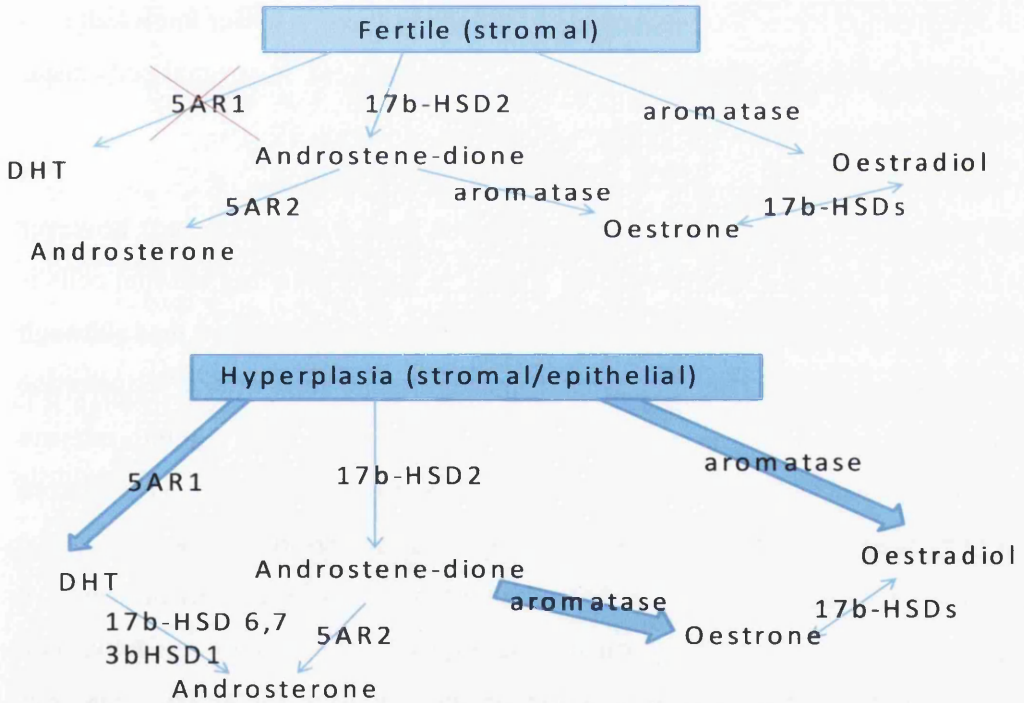

Fig 7.27: Alteration in routes of testosterone metabolism from stromal fertile biopsies to a stromal and epithelial hyperplasia biopsy. An arrow with a red cross indicates reaction was not occurring, increased arrow size indicates this reaction route was increased (relative to the fertile biopsies). Enzymes which catalyse each conversion are recorded on each arrow.

The testosterone metabolism route in epithelial and stromal cells from a hyperplasia biopsy was similar (although concentrations of each steroid and specific enzyme expression values varied). This suggests that to progress from a fertile endometrium to endometrial hyperplasia three changes were required.

1. Increased aromatase expression in correlation with increased oestradiol and/or oestrone concentrations.
2. Production of DHT in correlation with increased 5AR1 expression.
3. Decreased HSD2 expression (linked to bio-accumulation of oestradiol).

These observations only provide preliminary information concerning testosterone utilisation in endometrial hyperplasia, and these interesting findings require confirmation through the inclusion of more biopsies, however the results obtained here reflect previous results described in the literature, for example, increased aromatase expression, decreased HSD2 expression and increased oestradiol concentrations were reported in two recent studies by Ito and Li (and colleagues) in endometrial epithelial hyperplasia biopsies,[26,27] however there is to our knowledge no information concerning the expression of 5AR1 or role of DHT in stromal cells distal to epithelial hyperplasia.

Epithelial cells from endometrial hyperplasia have been widely studied, however information concerning steroid metabolism studies in the surrounding stromal cells is less explored. The results obtained in these experiments demonstrated that although the steroid profiles are similar, the stromal and epithelial cells utilise testosterone through different pathways at specific times in correlation with altered enzyme expression following testosterone treatment. It was probable that *in vivo* altered steroid metabolism in the stromal cells directly affects steroid metabolism in the epithelial cells. Stromal cell interactions with epithelial cells in the endometria have been previously shown to affect steroid metabolism, for example, Cheng and colleagues demonstrated HSD2 expression in endometrial epithelial cells was regulated by factors released from stromal cells.[28] Further developments with co-culture of both epithelial and stromal cells could produce information regarding this relationship.

7.6.12 Correlations between enzyme expression and steroid concentrations in an endometrial biopsy from a patient with an endometrial polyp following testosterone treatment

The endometrial polyp biopsy demonstrated high basal expression of HSD5, 7, 8 and aromatase relative to the fertile biopsies. There were no large increases in fold expression of any enzymes after testosterone treatment of this biopsy (figure 6.44). Rapid metabolism of testosterone to the androgenic end product androsterone (mainly through DHT) and to the oestrogens oestradiol and oestrone occurs 24 hours after testosterone treatment. Prior to testosterone treatment there was high expression of 5AR1 relative to HSD2 (figure 7.4), in correlation with this production of DHT from the precursor testosterone with little conversion to androstenedione was recorded, this was similar to testosterone conversion and enzyme expression in the HEC-1B cell line.

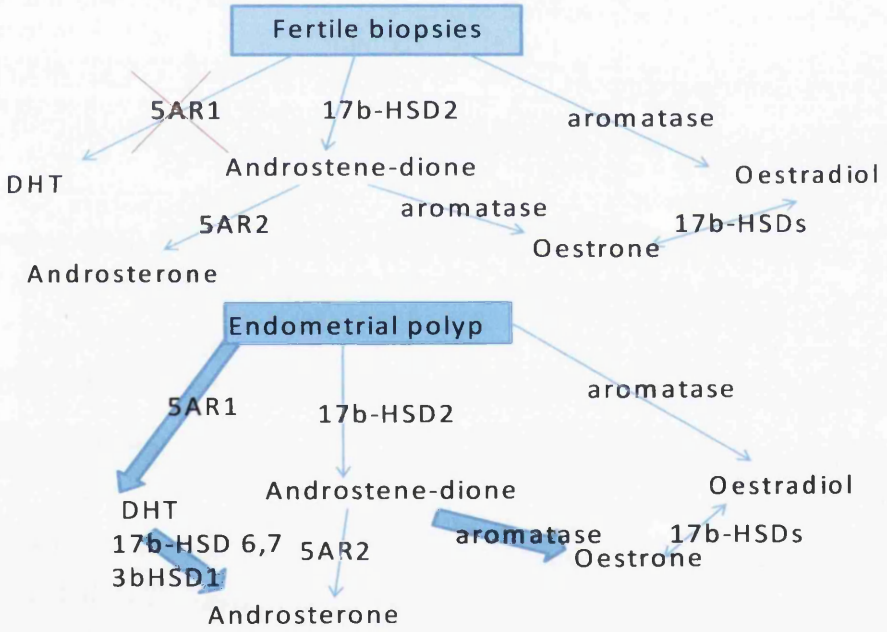

Fig 7.28: Alteration in routes of testosterone metabolism from fertile biopsies to an endometrial polyp biopsy. An arrow with a red cross indicates reaction was not occurring, increased arrow size indicates this reaction route was increased (relative to the fertile biopsies). Enzymes which catalyse each conversion are recorded on each arrow.

Testosterone metabolism was altered from fertile biopsies to the endometrial polyp biopsy as illustrated in figure 7.28. Production of DHT which was not recorded in the fertile biopsies but occurred in the endometrial polyp biopsy. Increased

conversion to the androgenic end product androsterone was observed in the endometrial polyp biopsy which may be linked to increased expression of a number of 17β-HSDs or 3β-HSDs. There was also increased expression of aromatase in the endometrial polyp biopsy (relative to the fertile biopsies) which was correlated with an increase in the conversion of androstenedione to oestrone.

7.7 Summary and discussion of correlations between steroid concentration and enzyme expression in cell lines and endometrial biopsies after testosterone treatment

Relationships between steroid converting enzyme expression and steroid concentrations were observed for most cell lines (except RL95-2) and some biopsies (summarised in table 7.2).

Table 7.2: Correlations between enzyme expression and steroid concentration for the cell lines Ishikawa, RL95-2, HEC-1A, HEC-1B and COV434 and the endometrial biopsies after testosterone treatment.

Cell Line/ Biopsy	Increase in enzyme	Change in steroid concentration
Ishikawa	5AR1 HSD8 Aromatase	Increase in DHT Increase in Androstenedione Increase in Oestradiol
RL95-2	-	-
HEC-1A	HSD5 Aromatase	Increase in Testosterone Decrease in Androstenedione Increase in Oestradiol
HEC-1B	5AR1	Increase in DHT
COV434	5AR1	Increase in DHT
Fertile	-	-
Unexplained Infertility	5AR2	Increase in Androsterone
Endometriosis	5AR1	Increase in DHT
PCOS	-	-
Ovarian Cyst	5AR1	Increase in DHT
Hyperplasia epithelial	Aromatase	Increase in Oestradiol Increase in Oestrone
Hyperplasia stromal	5AR1	Increase in DHT
Endometrial polyp	-	-

Increased expression of the enzyme 5AR1 was correlated with an increase in DHT concentration in three cell lines (Ishikawa, HEC-1B and COV434) and three biopsy

pathologies (endometriosis, ovarian cyst and stromal hyperplasia). Expression of HSD5 was linked to a decrease in androstenedione concentration and an increase in testosterone concentration in HEC-1A cells. Expression of HSD8 was linked to an increase in androstenedione concentration in Ishikawa cells. Increased expression of aromatase was linked to an increase in oestradiol or oestrone concentration in Ishikawa and HEC-1A and epithelial hyperplasia cells. Aromatase expression was also linked to oestradiol production in the fertile and unexplained infertility biopsies, however this only occurred at the start of the experiments as after 24 hours the majority of reaction precursor (testosterone) had been converted to other products.

The number of biopsies available for each endometrial pathology combined with the small number of data points for each biopsy and the longer times between these points makes it difficult to determine correlations between changes in enzyme expression and steroid concentration(s), the inclusion of more biopsies and time points would confirm any relationships.

These results suggest that expression of 5AR1 in endometrial cancer cell lines and biopsies from benign endometrial pathologies was linked to the production of DHT. For treatment of hormone responsive type one endometrial cancer, endometriosis or ovarian cysts 5AR1 inhibition may lead to reduced proliferation due to a reduction in production of this potent androgen.

7.8 Conclusions

Testosterone utilisation in each endometrial cancer cell lines was different. A progression of this work to include clinical biopsies from patients with endometrial cancer would allow determination of the cell lines which utilises testosterone via the most similar route. Some of the cell line produced steroid profiles which were similar to specific biopsy pathologies such as RL95-2 cells and fertile biopsies, (and the endometrial polyp biopsy to the HEC-1B cell line), it may be possible to use these cell lines as representative systems when primary biopsies are not available. The same enzymes were highlighted as important for the route of testosterone utilisation in cell lines and biopsies. These were 5AR1 (which produced DHT), HSD2, 4 and 8 (which produced androstenedione) and to a lesser extent aromatase

(which converted androgens to oestrogens). The roles of 5AR1 and the oxidative HSDs were initially determined based on the relationship between basal expression and the major metabolite(s) following testosterone treatment (chapter 5). The combination of the time course enzyme and steroid studies permitted further investigations into these relationships and supported these initial conclusions as increased expression of 5AR1 (or the oxidative HSDs) resulted in increased reaction product and decreased reaction precursor (observed at specific times) in a number of endometrial cell lines and pathologies.

Production of oestrogens through aromatase occurs in the biopsies from benign endometrial disorders and in Ishikawa, HEC-1A and HEC-1B cells, (although aromatisation was not the major pathway of testosterone metabolism in the cell lines). The use of an aromatase inhibitor would not be viable for treatment of an endometrial disorder which metabolises testosterone in a similar way to the Ishikawa, HEC-1A, and HEC-1B cell lines, as the use of an aromatase inhibitor may result in the production of more androgens (such as DHT) which could lead to an increase in proliferation.

The use of a 5AR1 inhibitor may be required to alter steroid metabolism from DHT production (observed in Ishikawa, HEC-1A HEC-1B, COV434, endometriosis, PCOS, ovarian cyst, endometrial hyperplasia and endometrial polyps) to that of the fertile biopsies (no DHT). These experiments highlight the importance of 5AR1 and a possible role of DHT in proliferation and/or progression of these disorders. This generally ignored area of endometrial steroid metabolism could be more significant than is currently perceived.

In pathologies which converted testosterone to DHT and converted a higher amount of testosterone to oestradiol (or androstenedione to oestrone) compared to the fertile biopsies (endometrial hyperplasia and endometriosis) use of a dual procedure such as inhibition of aromatase in combination with inhibition of 5AR1 may be required. Further experiments are required to determine the optimum procedures for treatment of these conditions.

These experiments have demonstrated the combination of mass spectrometry and enzyme expression data (via QRT-PCR) following steroid treatment to reveal a novel method for determination of steroid and enzyme interactions and possible targets for inhibition. These experiments have also highlighted the importance of studying the wider steroid pathway.

7.9 Discussion

A robust method for the identification of a number of androgens, oestrogens and progestins in endometrial established cell lines and biopsies using LC/MS (LC/MS/MS) was described in this thesis. The optimisation of extractions (SPE) of steroids from cells and cell media was completed and in combination with mass spectrometry this permitted the positive, quantitative analysis of steroids.

The use of cell lines to optimise experimental methods was essential to this work. The cell lines chosen here were used to elucidate testosterone metabolism routes and highlight potential enzyme targets. The application of optimised cell line methods to endometrial biopsies from fertile women and those with endometriosis was vital to further understanding altered steroid metabolism in these conditions. A comparison of testosterone metabolism pathways in fertile biopsies to endometrial cancer cell lines and endometrial disorders was also produced. The investigation of testosterone metabolism in other benign conditions was initiated to determine if the observations recorded in endometriosis were typical of benign endometrial disorders.

Two routes of testosterone metabolism have been highlighted as important these were correlated with expression of specific enzymes;

1. the production of DHT, correlated with 5AR1 expression,
2. the production of androstenedione correlated with expression of HSD2, 4 and/or 8.

The role of aromatase seems less important in the endometrial cell lines than is currently perceived.

Expression of HSD2 was important for the production of androstenedione in fertile biopsies and RL95-2 cells in preference to 5AR1 production of DHT or

aromatisation to oestrogens. Expression of 5AR1 and production of DHT was important in COV434 and HEC-1B cell lines and PCOS and endometrial polyp biopsies. Expression of 5AR1 and HSD2, 4 and 8 were important in the other cell lines and biopsies that metabolise both androstenedione and DHT such as Ishikawa, HEC-1A and endometriosis biopsies.

In these experiments it has been demonstrated that the endometrium has the capacity to metabolise DHT and androstenedione after testosterone treatment in relation to the abundance of specific enzymes. It was also concluded that in situations where high aromatase expression was observed the assumption cannot be made that all testosterone will be converted to oestradiol such as the COV434 cell line. This conclusion could only be reached with the combination of mass spectrometry and QRT-PCR highlighting this invaluable method for determination of a more complete picture of steroid metabolism.

Oestradiol, itself has been shown to activate ER pathway which activates the aromatase promoter SF1.[29] Increased expression of SF1 promotes aromatase expression, therefore the amount of ER expression in the cell line will influence the level of response to oestradiol (only a small amount of oestradiol may be required to cause a response). This together with the availability of transcription factors associated with the ER and aromatase pathway may determine the amount of aromatase expression.

The process of enzyme expression involves a number of steps. Nuclear DNA needs to be transcribed to form mRNA and this in turn has to be translated to form the proteins (the enzymes) which convert the steroids. Each step of this process may require a number of co-factors or compounds for example ATP or NADPH which provide energy for many reactions or more specific co-factors such as 3'-phosphoadenosine-5'-phosphosulphate (which is the cofactor which supplies the sulphate group in the conversion of active steroids to sulphated steroids by steroid sulphotransferase). The availability of these co-factors can inhibit enzyme activity, for example if a specific co-factor is not available the reaction may be slower or may not occur at all. This can lead to disparities between mRNA expression and enzyme

activity, which may be the case for aromatase expression in the COV434 cell line. The relationships between mRNA expression and enzyme activity may be simple as is seen throughout these experiments with 5AR1, where an increase mRNA expression results in an increase in DHT production suggesting all co-factors required are present. Experiments where the protein level of each enzyme is measured, such as western blotting, would determine the link between mRNA expression and protein production for each enzyme (the translation process).

Together a wider understanding of steroid biosynthesis in the endometrium and its disorders has been achieved in this project and therapeutic targets have been revealed.

7.10 Further Work

Correlations between enzyme expression and steroid concentration(s) were determined in the established cell lines and endometrial biopsies, after testosterone treatment providing novel information regarding steroid metabolism. Initial biopsy results were encouraging, the inclusion of more biopsies and experimental time points will permit confirmation of any conclusions.

Further investigations into enzymes highlighted here as important (aromatase, 17β-HSD2, 17β-HSD4, 17β-HSD8, and 5-α reductase 1) and investigations into the roles of DHT, androsterone and androstenedione is required to confirm the importance of these in relation to endometrial disorders. Following this the development of specific inhibitors could be achieved with the aim of altering steroid metabolism in each condition back to the normal route.

mRNA expression does not always equate to enzyme activity, for example some enzymes can be highly expressed at the mRNA level but at the transcription level protein is not produced. siRNA (small interfering RNA) occur naturally, and were initially described as a regulatory mechanism to inhibit viral gene expression by interfering with the translation process. Recently synthetic siRNA has been used to inhibit the expression of specific genes by causing knockdown of mRNA and protein expression[30] (sequence selective inhibitors). Application of siRNA to the

endometrial cell lines and biopsies could be an ideal expansion of this work. For example inhibition of expression of specific enzymes (such as 5AR1 or aromatase) using siRNA or specific enzyme inhibitors such as finasteride would highlight the importance of enzyme competition in relation to specific steroid production. siRNA can also be utilised to knockdown specific enzymes and to determine the activity of each enzyme.[31]

Enzyme activity could be further investigated by determining the rate of production of each steroid over time, this would require inhibition of further reactions of the produced steroid and opposing reactions, for example to determine the activity of the HSD2 mediated conversion of oestradiol to oestrone inhibition of HSD1, 5 and 7 is required (which does the opposite reaction) and inhibition of competing enzymes such as HSD4 and HSD8 would also be required. The substrate oestradiol would then be added at a number of different concentrations and the reaction products recorded after a specific time, this would allow determination of the concentration at which the enzyme reaches saturation (addition of more substrate will not increase the amount of product/unit time). This would also allow us to determine the enzyme activity (conversion rate/unit time, before saturation) and would be an interesting expansion of this work.

The inclusion of more steroid converting enzymes to elucidate further relationships between enzyme expression and steroid metabolism in the wider steroid bio-pathway would be an interesting progression of this work. There has been some work by Purohit and co-workers investigating the role of steroid sulphatase in bio-accumulation of oestrogens in endometrial disorders,[32] further investigation into the role of sulphatase could further illuminate routes of steroid metabolism in these endometrial pathologies, and would be an ideal extension of this methodology.

An ideal expansion of this work would be co-culture experiments, where epithelial and stromal cells are cultured together and interactions between the two cell types can be determined. Interactions between epithelial and stromal cells may be important for the growth and maintenance of both benign and cancerous endometrial

disorders. Cheng and colleagues found that a defect in stromal cells resulted in HSD2 deficiency in the surrounding epithelium resulting in a decrease in the conversion of oestradiol to oestrone.[33] Segawa and colleagues described a link between aromatase expression in stromal cells and poorer survival rates for women with endometrial cancer.[34] This could be due to an increase in the local oestrogen concentration inducing proliferation of the epithelial cells. These studies highlight the importance of the localised environment for progression and maintenance of endometrial disorders, the significance of the stromal-epithelial relationship requires further investigation.

Further work with endometriosis biopsies organised into stages related to progression of the disorder could determine alterations in steroid and enzyme expression profiles through each stage of the condition. This would determine trends in testosterone metabolism and enzyme expression in the four stages of endometriosis, and possibly highlight the ideal time to start treatment(s) with aromatase or 5AR inhibitors.

Further work to investigate the metabolism routes of other abundant circulatory steroids (DHEA, DHEAS, androstenedione, oestrone-sulphate or a combination of all) would also be an ideal expansion of these experiments.

The procedure for analysis of specific steroid metabolism routes developed in this thesis could be directly applied to other steroid responsive tissues such as the brain, adrenal glands, breast or prostate, which would highlight important enzymes and steroids in these areas.

7.11 References Chapter Seven

[1] Baxter FO, Trivic S, Lee IR. J Steroid Biochem Mol Biol **77** (2001) 167-175
[2] Allen NE, Key TJ, Dossus L, Rinaldi S, Cust A, Lukanova A, Peeters PH, Onland-Moret NC, Lahmann PH, Berrino F, Panico S, Larrañaga N, Pera G, Tormo MJ, Sánchez MJ, Quirós JR, Ardanaz E, Tjønneland A, Olsen A, Chang-Claude J, Linseisen J, Schulz M, Boeing H, Lundin E, Palli D, Overvad K, Clavel-Chapelon F, Boutron-Ruault M-C, Bingham S, Khaw K-T, Bueno-de-Mesquita HB, Trichopoulou A, Trichopoulos D, Naska A, Tumino R, Riboli E, Kaaks R. Endocrine-Related Cancer **15** (2008) 485-497
[3] Maliqueo M A, Quezada S, Clementi M, Baccallao K, Anido M, Johnson C, Vega M. Reproductive Biol Endocrinology **2** (2004) 81-91
[4]FDA White Paper. US Food and Drug Administration Health Effects of Androstenedione (2004) http://www.fda.gov/oc/whitepapers/andro.html
[5] Suzuki T, Miki Y, Moriya T, Akahiral J-I, Ishida T, Hirakawa H, Yamaguchi Y, Hayashi S-I and Sasano H. Int J Cancer **120** (2006) 285-291
[6] Suzuki T, Miki Y, Akahira J-I, Moriya T, Ohuchi N, Sasano H. Endocrine J **55** (2008) 455-463
[7] Carruba G, Granata OM, Farruggio R, Cannella S, Bue AL, Leake RE, Pavone-Macaluso M, Castagnetta LAM. Steroids **61** (1996) 41-46
[8] Ito K, Suzuki T, Akahira J-I, Moriya T, Kaneko C, Utsunomiya H, Yaegashi N, Okamura K, Sasano H. Int J. Cancer **99** (2002) 652-657
[9] Apter D. Clincal Endocrinology (Oxf) **12** (1980) 107-120
[10] Scott T, Mercer EI. Concise Encyclopedia Biochemistry and Molecular Biology 2nd Edition (1988) pub Walter de Gruyter 1997 41-42
[11] Suzuki R, Miki Y, Nakamura Y, Moriya T, Ito K, Ojuchi N, Sasano H. Endocrine Related Cancer **12** (2005) 701-720
[12] Simpson ER, Davis SR. Endocrinology **142** (2001) 4589-4594
[13] Hu Y, Ghosh S, Amleh A, Yue W, Lu Y, Katz A Li R. Oncogene **24** (2005) 8343-8348
[14] Havelock JC, Rainey WE, Carr BR. Mol and Cell Endocrinology **228** (2004) 67-78
[15] Thompson MA, Adelson MD, Kaufman LM, Marshall LD, Coble DA. Cancer Research **48** (1988) 6491-6497
[16] George FW, Ojeda SR. Endocrinology **111** (1982) 522-529
[17] Leon L, Bacallao K, Gabler F, Romero C, Valladares L, Vega M. Steroids **73** (2008) 88-95
[18] Berstein LM, Tchernobrovkina AE, Gamajunova VB, Kovalevskij AJ, Vasilyev DA, Chepik OF, Turkevitch EA, Tsyrlina EV, Maximov SJ, Ashrafian LA, Thijssen JHH. J Cancer Res Clin Oncol **129** (2003) 245-249
[19] Maia H, Pimentel K, Silva TMC Freitas LA, Zausner B, Athayde C, Coutinho EM. Gynecol Endocrinology **22** (2006) 219-224
[20] Utsunomiya H, Ito K, Suzuki T, Kitamura T, Kanedko C, Nakata T, Niikura H, Okanura K, Yaegashi N, Sasano H. Clinical Cancer Research **10** (2004) 5850-5856
[21] Kitawaki J, Kado N, Ishihara H, Koshiba H, Kitaoka Y, Honjo H. J Steroid Biochem and Mol Biol **83** (2003) 149-155
[22] Kaku T, Hirakawa T, Sakai K, Amada S, Kobayashi H, Nakano H. Gynecologic Oncology 72 (1999) 51-55
[23] Castagnetta L A M, Montesanti A M, Granata O M, Oliveri G, Sorci C M, Amodio R, Liquori M Carruba G. J Steroid Biochem Mol Biol **55** (1995) 573-579
[24] Castagnetta LA, Granata OM, Taibi G, Lo Casto M, Oliveri G, Carruba G. Journal of Endocrin **150** (1996) Supp73-78
[25] Ness R.B, Modugno F. Euro J Cancer **42** (2006) 691-703
[26] Ito K, Utsunomiya H, Suzuki T, Saitou S, Akahira J-I, Okamura K, Yaegashi N, Sasano H. Mol and Cell Endocrin **248** (2006) 136-140
[27] Li H, Chen X, Qiao J, Inter J of Gyne and Obste **100** (2008) 10-12
[28] Cheng YH, Imir A, Fenkci V, Yilmaz MB, Bulun S E. Am J Ostet Gynecol **196** (2007) 391-398
[29] Bukulmez O, Hardy D.B, Carr B.R, Auchus R.J, Toloubeydokhti T, Word R.A, Mendelson C.R. J Clin Endo Metab **93** (2008) 3471-3477
[30] Forbes K, Desforges M, Garside R, Aplin J.D, Westwood M. Placenta **30** (2009) 124-129
[31] Reischl D, Zimmer A. Nanomedicine, nanotechnology, biology and medicine **5** (2009) 8-20
[32] Purohit A, Fusi L, Brosens J, Woo LWL, Potter BVL, Reed MJ. Hum Reprod **23** (2008) 290-297
[33] Cheng YH, Imir A, Fenkci V, Yilmaz MB, Bulun S E. Am J Ostet Gynecol **196** (2007) 391-398

[34] **Segawa T, Shozu M, Murakami K, Kasai T, Shinohara K, Nomura K, Ohno S, Inoue M. Clin Cancer Research 11 (2005) 2188-2194**

Appendix 1

A1.1: Conferences attended:

BMSS Meeting Edinburgh 2006 Poster presentation. "The capacity of the human endometrium to synthesise steroids: a metabolic (mass spectrometry) and genomic (RT-PCR) approach."

ASMS Denver CO 2008 Poster presentation. "The capacity of the human endometrium to synthesis steroids: a metabolomic (mass spectrometry) and gene expression (RT-PCR) approach"

BMSS Meeting York 2008 Oral presentation "The metabolism of steroids in the human uterus: Steroids biosynthesis from detection to steroid converting enzyme expression."

A1.2: Example of determination of peak area for steroids analysed on the LCQ DECA mass spectrometer.

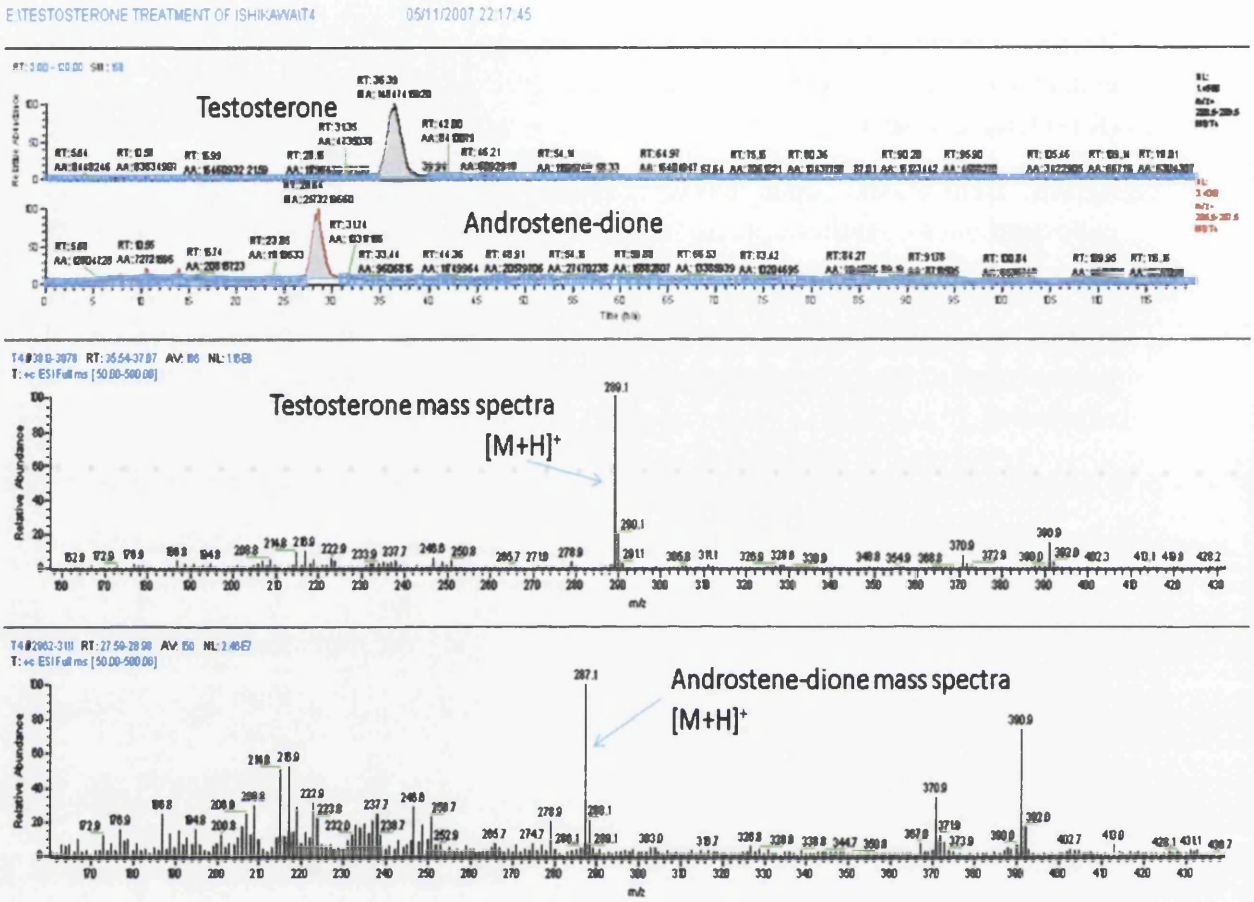

Fig 1: The top chromatograms are selected ion chromatograms for the androgens testosterone and androstenedione 32 hours after testosterone treatment in Ishikawa cells. The grey area on each represents the peak areas used to calculate concentration. The bottom spectra are the corresponding mass spectra for each peak. Testosterone has an m/z ratio of 289 and androstenedione has an m/z ratio of 287, together with specific retention times these two steroids are positively identified in Ishikawa cell media.

A1.3: Example of calculation of RNA expression through RT-qPCR

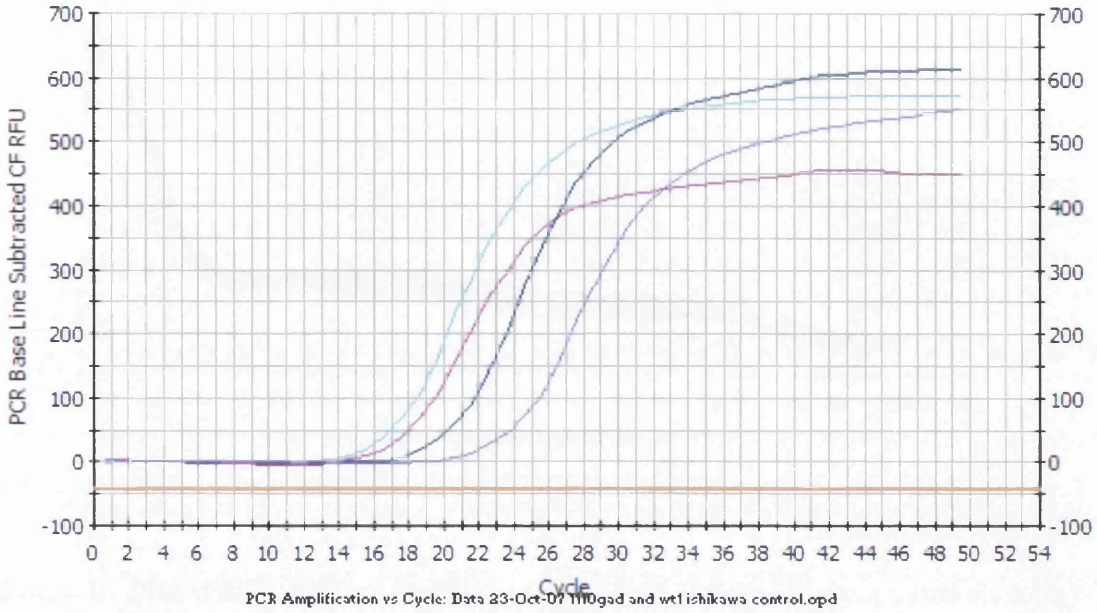

Fig1.2: Example of graph produced by iCycler software fluorescence is plotted against threshold cycle. A Ct value is produced for each cDNA dilution which can be plotted as a calibration graph.

A series of dilutions of the cDNA is produced these are 0.2, 0.1, 0.01 and 0.001ng/μL. The Ct value at which these dilutions fluoresce is plotted against the log of the dilution value, this should produce a linear relationship.

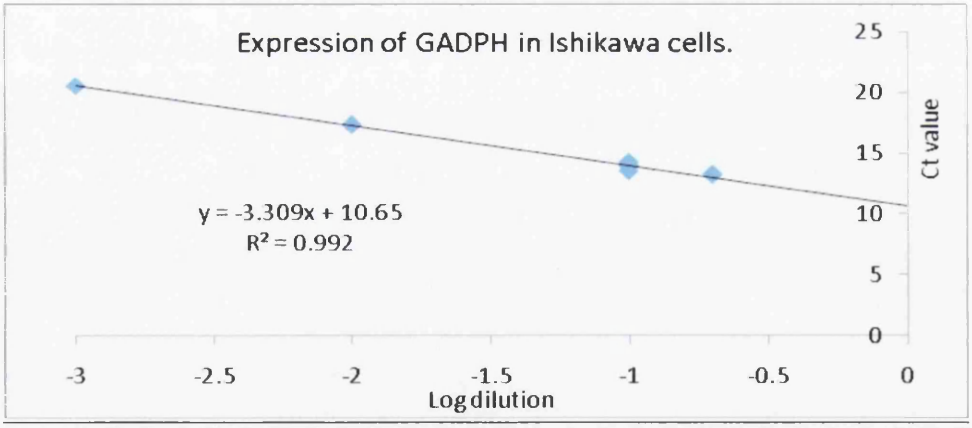

Fig 1.3: Example of a calibration graph cDNA concentration (log of the dilution) is plotted against the Ct value determined from figure 1.2.

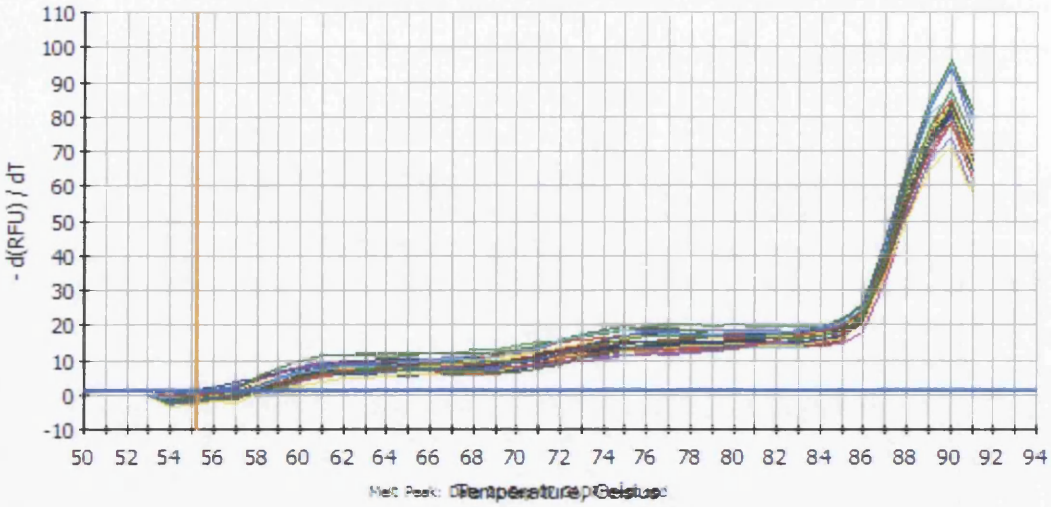

Fig 1.3: Melt curve produced for GADPH bound primers via QRT-PCR using the iCycler apparatus.

The melt curve permits investigation into the efficiency of the primer pair. If a sharp peak is observed with one significant melt temperature (as in figure 1.3) the primers are efficient. The calculation for determination of basal expression and changing expression over time is described in appendix 2.

All calculations in the following appendix were obtained using microsoft excel.

A2.1: Testosterone utilisation by HEC-1B cells comparison of two experiments

Time (hours)	Ratio to IS Experiment 1	Ratio to IS Experiment 2	Average ratio to IS	Standard deviation
0	0.442557	0.51663	0.479594	0.052377
12	0.343473	0.329307	0.33639	0.010017
24	0.168236	0.295431	0.231833	0.08994
36	0.153817	0.156925	0.155371	0.002198
48	0.084758	0.12311	0.103934	0.027119
60	0.060787	0.108798	0.084792	0.033949
72	0.038357	0.080561	0.059459	0.029843

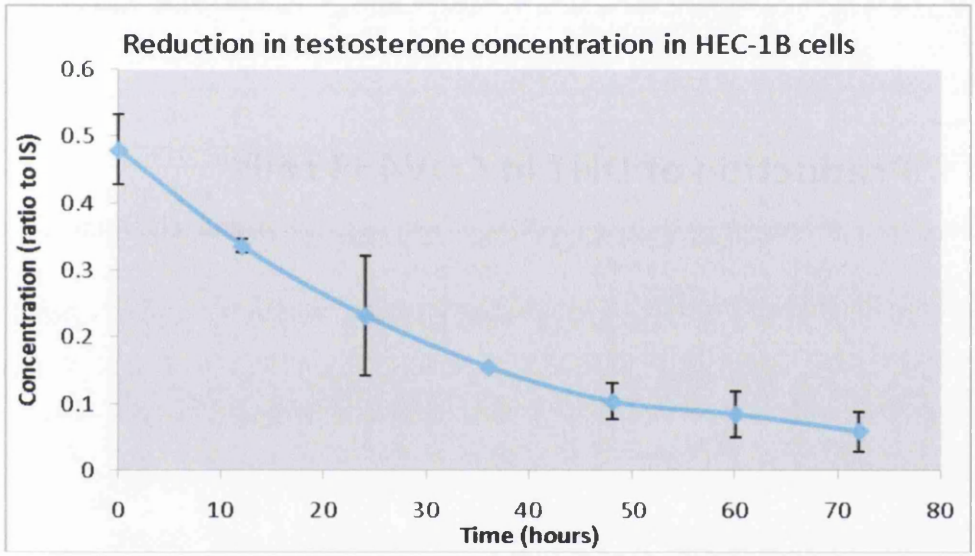

A2.2: Production of DHT by COV434 cells after testosterone treatment

Time (hours)	Ratio to IS Experiment 1	Ratio to IS Experiment 2	Average ratio to IS	Standard deviation
0	0.021651251	0.012582518	0.017116885	0.006413
8	0.055993176	0.070915775	0.063454476	0.010552
16	0.11858888	0.148060457	0.133324668	0.02084
24	0.13901928	0.148060457	0.143539869	0.006393
32	0.106884898	0.218250953	0.162567926	0.078748
40	0.138017765	0.155733183	0.146875474	0.012527
48	0.183376945	0.225850253	0.204613599	0.030033
72	0.1226287	0.123	0.12281435	0.000263

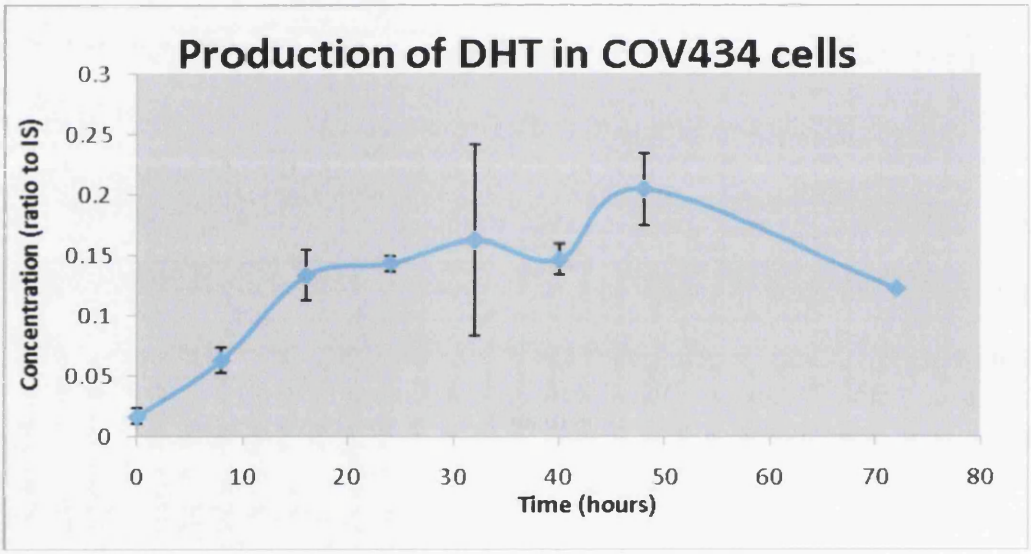

A2.3 DHT Calibration (regression method)

Concentration nM (x10^2)	peak area	IS peak area	Ratio peak area/peak area IS	Avg peak area	SD
0.01	350328368	79600569609	0.004401079		
0.01	396298528	77428211243	0.00511827	0.004763317	0.0003587
0.01	364944579	76498633967	0.004770603		
0.05	1303963919	91742166727	0.014213354		
0.05	1098560739	82796338145	0.013268229	0.013585777	0.0005435
0.05	1114494295	83949637712	0.013275749		
0.1	2102036461	92484929771	0.022728421		
0.1	2174856933	86056742852	0.025272359	0.025386405	0.0027168
0.1	2328829740	82704520200	0.028158434		
0.125	2972522108	86746117983	0.034266918		
0.125	2431413074	84341934616	0.028828045	0.031516106	0.00272
0.125	2522678554	80203797590	0.031453355		
0.25	4446327604	85409331161	0.052059038		
0.25	5128247966	91962507001	0.055764552	0.055304001	0.003041
0.25	4522731725	77859447961	0.058088412		
0.5	9539519374	74033253352	0.128854521		
0.5	9928572704	82358269303	0.12055344	0.122438454	0.0057118
0.5	9329622675	79126693174	0.1179074		
1	20422556051	99249600713	0.205769655		
1	19252172079	93596737889	0.205692768	0.210621846	0.0084709
1	20713241214	93978895271	0.220403114		
5	51596918800	96033163635	0.537282298		
5	50817487048	97858610598	0.519294999	0.514775073	0.0250746
5	45286016413	92847174308	0.487747923		
10	78410498377	98414223515	0.796739491		
10	82379825939	1.0168E+11	0.810189994	0.777134853	0.0460979
10	70490668114	97298955652	0.724475074		
15	1.01982E+11	89873826525	1.134723581		
15	1.06803E+11	90290784558	1.182874825	1.093610618	0.1154482
15	85329742799	88586773045	0.963233447		
20	1.11187E+11	97442449885	1.14105694		
20	1.30985E+11	1.02075E+11	1.283222792	1.166572025	0.1062171
20	1.05826E+11	98403055914	1.075436344		

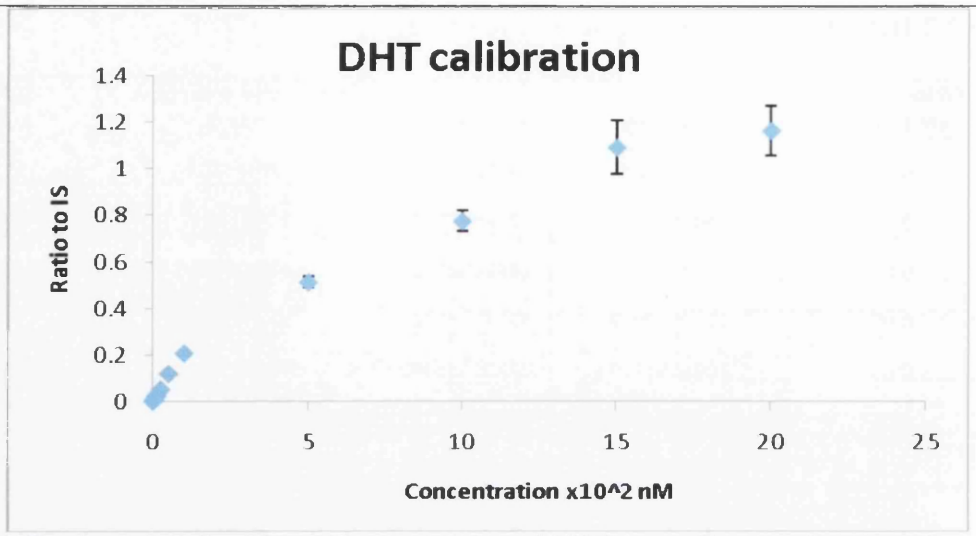

Calibration series is linear from 100 to 1nm solutions of DHT (it is over this range of concentrations that regression statistics are determined).

	Concentration x100 nM	Average ratio	(Xi-avgX)^2	SD
	0.01	0.004763317	0.0001	0.000358651
	0.05	0.013585777	0.0025	0.000543511
	0.1	0.025386405	0.01	0.002716802
	0.125	0.031516106	0.015625	0.002719979
	0.25	0.055304001	0.0625	0.003040957
	0.5	0.122438454	0.25	0.005711814
	1	0.210621846	1	0.008470915
average	0.290714286	0.066230844	1.340725	

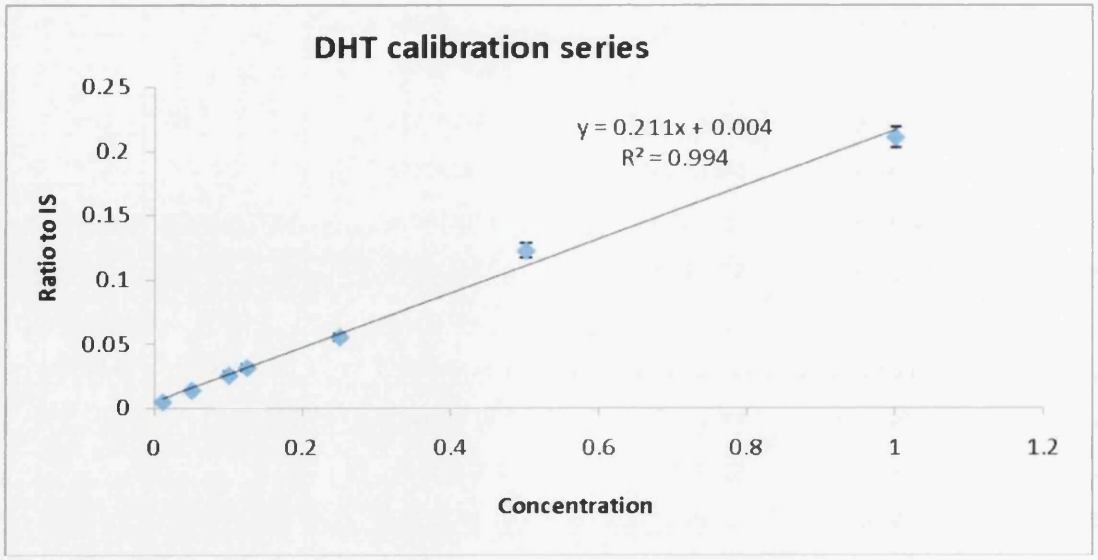

Regression statistics

SUMMARY OUTPUT

Regression Statistics	
Multiple R	0.9972056
R Square	0.9944190
Adjusted R Square	0.9933029
Standard Error	0.0061195
Observations	7

ANOVA

	df	*SS*	*MS*	*F*	*Significance F*
Regression	1	0.033363351	0.033363351	890.91133	7.92E-07
Residual	5	0.000187	3.744E-05		
Total	6	0.033550			

	Coefficients	*Standard Error*	*t Stat*	*P-value*	*Lower 95%*	*Upper 95%*	*Lower 95.0%*	*Upper 95.0%*
Intercept	0.0048793	0.0030942	1.5768857	0.17564	-0.00307	0.01283	-0.003	0.01
X Variable 1	0.2110370	0.0070703	29.848137	7.9E-07	0.192862	0.22921	0.192	0.22

RESIDUAL OUTPUT

Observation	*Predicted Y*	*Residuals*
1	0.00698972	-0.0022264
2	0.01543120	-0.0018454
3	0.02598306	-0.0005966
4	0.03125898	0.00025711
5	0.05763862	-0.0023346
6	0.11039788	0.01204056

Sx/y= 0.006119523

LOD = 0.086992162 pM/μL

= 87nM

A2.4 Androstenedione rate equations combination of two experiments

Time (hours)	Ratio to IS Experiment 1	Ratio to IS Experiment 2	Average ratio to IS	Standard deviation
0	0	0	0	0
12	0.296567775	0.162338439	0.229453107	0.094914474
24	0.112285828	0.092090334	0.102188081	0.014280371
36	0.07172074	0.033867914	0.052794327	0.02676599
48	0.02332918	0.014005284	0.018667232	0.00659299
60	0.014802585	0.009298473	0.012050529	0.003891995
72	0.006823985	0.005113944	0.005968965	0.001209181

Time (hours)	exp1 Ln(C0/C)	exp2 Ln(C0/C)	Average Ln (C0/C)	Standard deviation	Rate of reaction K
0					
12	0	0	0	0	0
24	0.971228119	0.661234882	0.8162315	0.21919832	0.03401
36	1.419495813	1.661536802	1.540516307	0.171148825	0.042792
48	2.542570853	2.544570163	2.543570508	0.001413725	0.052991
60	2.997473945	2.954154643	2.975814294	0.030631372	0.049597
72	3.771832191	3.552033878	3.661933035	0.155420878	0.05086
					average rate of reaction
					0.04605

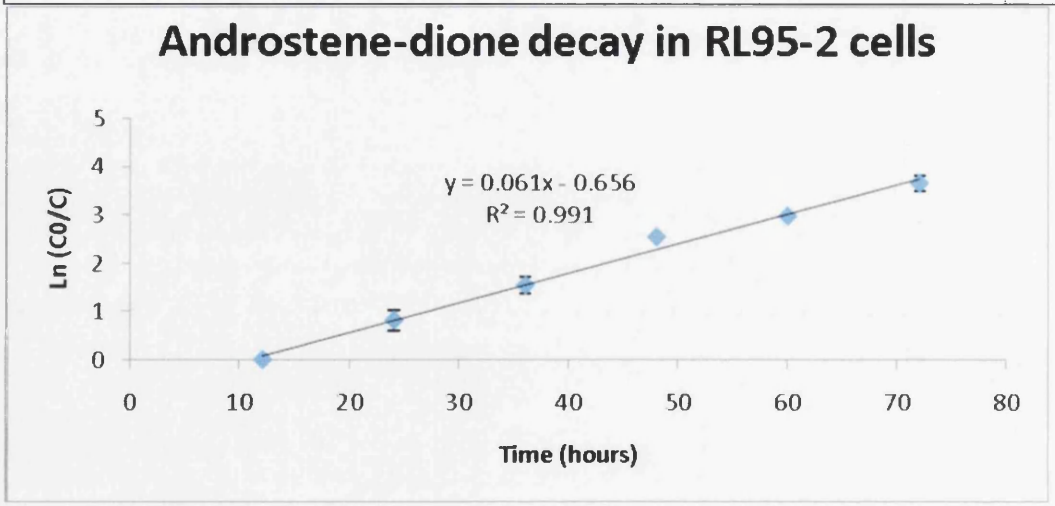

A 2.5: Example calculation to determine basal expression of HSD4 in the established cell lines HEC-1B and RL95-2

From a mixture of RNA from all five cell lines;

RNA dilution	st Q	log dil	Threshold cycle
1/5	0.2	-0.69897	20.1
1/5	0.2	-0.69897	20.3
1/10	0.1	-1	19.5
1/10	0.1	-1	20.9
1/10	0.1	-1	20.8
1/100	0.01	-2	23.4
1/1000	0.001	-3	26.9
1/1000	0.0001	-4	30.2

				calc previously	
				GAPDH	
Avg Threshold cycle		I og Starting quantity	Starting quantity	RF	normalised starting quantity
	20.4	-0.915026373	0.121611215	0.11567	1.051403084

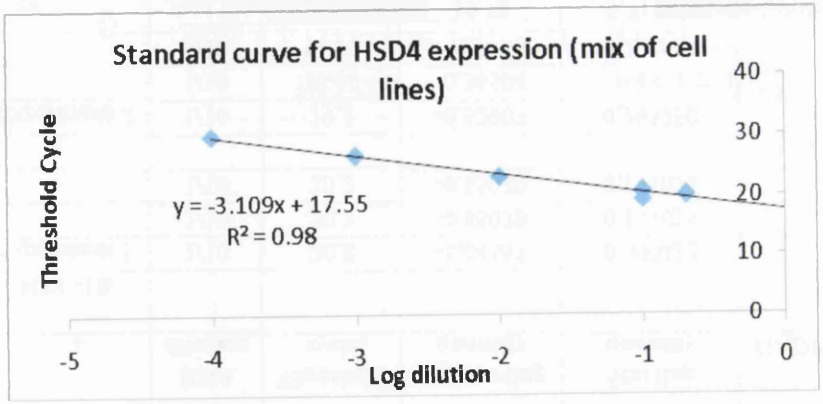

	RNA dilution	Threshold cycle	log Starting quantity	Starting quantity	GADPH SQ	starting quantity normalised to GADPH	Avg fold expression	
HEC-1B					0.107543			**standard deviation**
Experiment 1	1/10	20.8	-1.04367	0.090432		0.840891		
	1/10	20.2	-0.85070	0.141025		1.311341		
	1/10	20.2	-0.85070	0.141025		1.311341		
					0.345822			
Experiment 2	1/10	19.2	-0.52907	0.295750		0.855207	1.0345	0.291
	1/10	18.69	-0.36504	0.4314		1.247673		
	1/10	19.59	-0.65450	0.221559		0.640674		
	Avg Threshold cycle		19.78	-0.715618				
RL95-2					0.173527			
Experiment 1	1/10	21.4	-1.23665	0.057989		0.334178		
	1/10	21	-1.10800	0.077982		0.449396		
	1/10	20.8	-1.04367	0.090432		0.521140		
					0.1093828		0.433	0.0848
Experiment 2	1/10	22	-1.42962	0.037185		0.339955		
	1/10	21.7	-1.33314	0.046436		0.424531		
	1/10	21.4	-1.23665	0.057989		0.530149		
	AvgThreshold cycle		21.38333	-1.231292				

Cell Line	fold expression	Standard deviation
HEC-1B	1.034521749	0.29101687
RL95-2	0.433225354	0.084817169

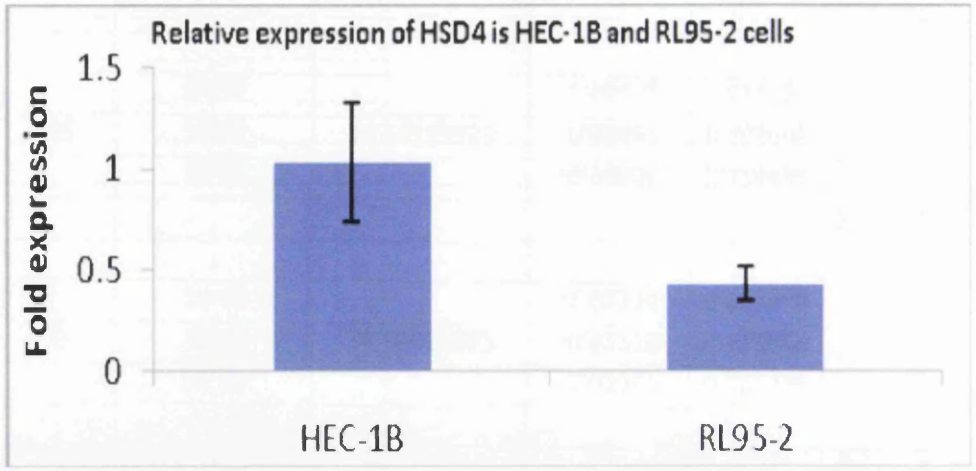

A2.6: Calculation of changing expression of HSD4 in HEC-1A cells following testosterone treatment

Experiment 1

Time (hours)	Threshold cycle	Avg Thershold cycle	log St Q	St Q	Relative factors GADPH	Relative factors starting Q/GADPH	G/avg starting Q (0 hours)	standard deviation	Average Fold expression	Fold exp zer
					1					
	24.47		-1.03387	0.092498		0.092498	0.90586651			
0	24.19	24.35666667	-0.92779	0.118089		0.118089	1.15648733	0.132892252	0.102109707	1
	24.41		-1.01114	0.097468		0.097468	0.95454173			
					5.911765					
	24.13		-0.90506	0.124434		0.021049	0.20613628			
12	24.34	24.24333333	-0.98462	0.103605		0.017525	0.17163147	0.0174779	0.019067144	0.1867
	24.26		-0.95431	0.111094		0.018792	0.18403674			
					6.428073					
	24.46		-1.03008	0.093308		0.014516	0.14215818			
24	24.29	24.40333333	-0.96568	0.108224		0.016836	0.16488287	0.013120109	0.015251297	0.1493
	24.46		-1.03008	0.093308		0.014516	0.14215818			
					2.756792					
	23.9		-0.81793	0.15208		0.055166	0.54025895			
36	24.72	24.17	-1.12858	0.074374		0.026978	0.26420975	0.160760923	0.043589388	0.426
	23.89		-0.81414	0.153413		0.055649	0.54499237			

					2.288737					
	24.64		-1.09827	0.079749		0.034844	0.34124362			
48	24.27	24.51333333	-0.9581	0.110129		0.048118	0.47123474	0.074202393	0.038915144	0.3811
	24.63		-1.09448	0.080448		0.03515	0.34423339			
					1.683692					
	24.34		-0.98462	0.103605		0.061534	0.60263099			
60	24.46	24.38666667	-1.03008	0.093308		0.055419	0.54273775	0.031997853	0.059079804	0.5785
	24.36		-0.9922	0.101813		0.06047	0.59220839			
					2.066101					
	24.67		-1.10964	0.077689		0.037602	0.36825074			
72	24.7	24.7	-1.121	0.075683		0.036631	0.35873873	0.009389426	0.036630707	0.3587
	24.73		-1.13237	0.073728		0.035685	0.34947243			

Results exp1	Fold exp	SD
0	1	0.132892
12	0.186732	0.017478
24	0.149362	0.01312
36	0.426888	0.160761
48	0.381111	0.074202
60	0.578591	0.031998
72	0.358739	0.009389

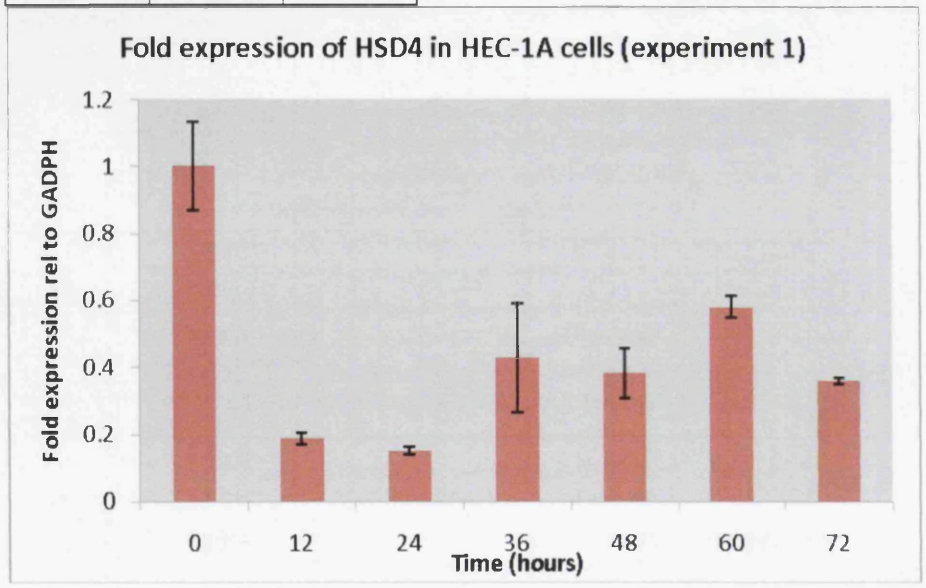

Experiment 2

Time (hours)	Threshold cycle	Avg Thershold cycle	log St Q	St Q	Relative factors GADPH	Relative factors starting Q/GADPH	G/avg starting Q (0 hours)	standard deviation	Average Fold expression	Fold exp rel to zer
					1					
0	24.9		-1.19677	0.063566		0.063566	0.91646413			
	24.7	24.8	-1.121	0.075683		0.075683	1.09115018	0.123521689	0.069360512	1
	24.8		-3.01523	0.000966		0.000966	0.01392061			
					1.349897					
	25.6		-1.46196	0.034517		0.02557	0.36865769			
12	25.5	25.46666667	-1.42408	0.037663		0.027901	0.40226091	0.056523305	0.028724223	0.414129
	25.3		-1.34831	0.044842		0.033219	0.47893534			
					2.459809					
	24.9		-1.19677	0.063566		0.025842	0.37257528			
24	24.4	24.66666667	-1.00735	0.098322		0.039971	0.57628416	0.103398875	0.031675506	0.456679
	24.7		-1.121	0.075683		0.030768	0.44359138			
					1.933911					
	25.9		-1.57562	0.026569		0.013739	0.19807689			
36	25.2	25.46666667	-1.31043	0.04893		0.025301	0.36477536	0.088764307	0.020049908	0.289068
	25.3		-1.34831	0.044842		0.023187	0.33430353			

					1.815165					
	26.3		-1.72716	0.018743		0.010326	0.14887304			
48	26.3	26.26666667	-1.72716	0.018743		0.010326	0.14887304	0.00783453	0.010630569	0.153265
	26.2		-1.68927	0.020452		0.011267	0.16244284			
					1.721428					
	25.4		-1.38619	0.041097		0.023874	0.34419459			
60	25.2	25.26666667	-1.31043	0.04893		0.028424	0.40980107	0.037877923	0.026818163	0.386648
	25.2		-1.31043	0.04893		0.028424	0.40980107			
					0.901714					
	25.3		-1.34831	0.044842		0.04973	0.71698251			
72	25.5	25.4	-1.42408	0.037663		0.041769	0.60219827	0.057410289	0.045576012	0.657088
	25.4		-1.38619	0.041097		0.045576	0.65708875			

Results experiment 2

Results exp1	Fold exp	SD
0	1	0.123522
12	0.414129	0.056523
24	0.456679	0.103399
36	0.289068	0.088764
48	0.153265	0.007835
60	0.386649	0.037878
72	0.657089	0.05741

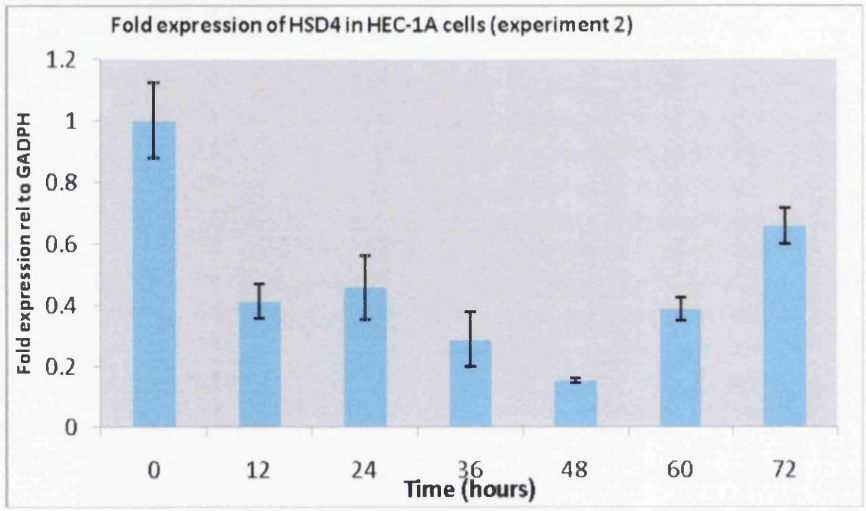

Combination of experiment one and experiment two

Time	Average Fold expression	SD (6)
0	1.004901975	0.112453
12	0.30194307	0.131075
24	0.306941674	0.184399
36	0.374436142	0.142508
48	0.269483444	0.160332
60	0.483562311	0.109351
72	0.508788571	0.168351

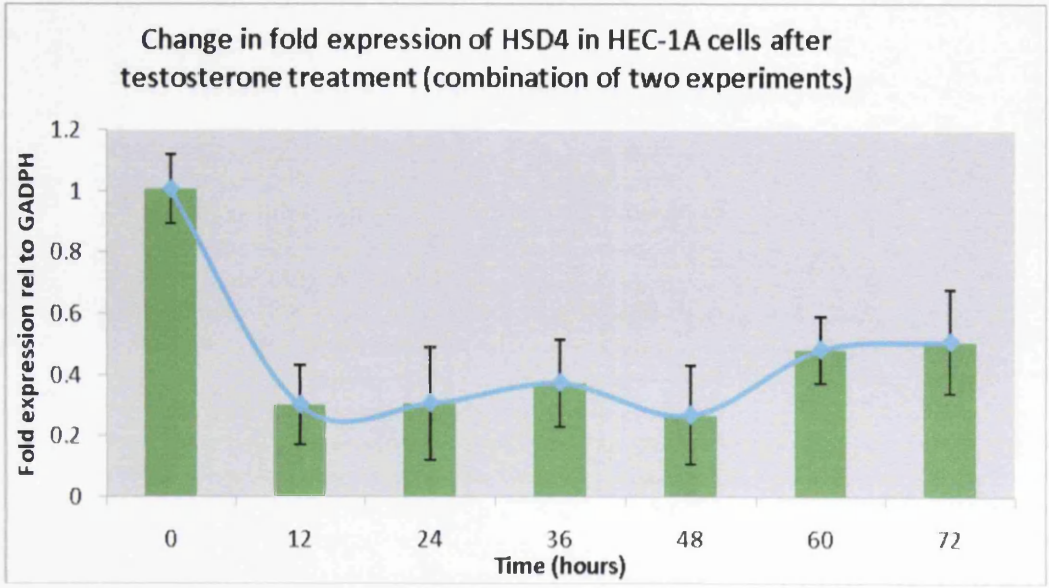

A2.7: Comparison of enzyme expression and steroid concentrations in Ishikawa cells

Time (hours)	DHT (ratio to IS)	Oestradiol (peak area)	SD (DHT)	SD (oestradiol)
0	0.010467	282130	0.003039	358800.1
8	0.021421	109472	0.012522	67320.81
16	0.033937	122088	0.007951	44352.57
24	0.032946	80091	0.018232	16652.36
32	0.049955	74418	0.023269	68112.77
40	0.063157	94625	0.035509	60689.56
48	0.051654	45257.5	0.034942	57859.01
72	0.050774	30466	0.002462	

Enzyme Expression

Avg enzyme fold expression (rel to GADPH)

Time (hours)	5AR1	aromatase	SD (5AR1)	SD (aromatase)
0	1.027254	1.038753	0.249149	0.223022
8	0.546795	0.569716	0.444072	0.381654
16	0.813979	1.168004	0.470783	1.090763
24	0.462599	0.230849	0.32932	0.114007
32	0.538462	0.260196	0.488476	0.230696
40	3.729493	1.186481	3.42008	1.21121
48	1.368435	0.45193	1.262009	0.178774
72	0.179664	0.554878	0.127997	0.506136